EVALUATING STORMWATER POLLUTANT REMOVAL MECHANISMS BY BIORETENTION IN THE CONTEXT OF CLIMATE CHANGE

A Dissertation Presented

by

Amanda Cording

to

The Faculty of the Graduate College

of

The University of Vermont

In Partial Fulfillment of the Requirements
for the Degree of Doctor of Philosophy
Specializing in Plant and Soil Science

May, 2016

Defense Date: March 2, 2016
Dissertation Examination Committee:

Stephanie E. Hurley, D.Des., Advisor
Arne Bomblies, Ph.D., Chairperson
Donald Ross, Ph.D.
Elizabeth Adair, Ph.D.
Cynthia J. Forehand, Ph.D., Dean of the Graduate College

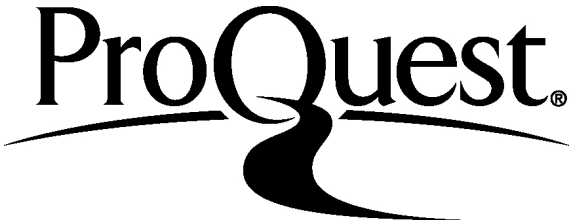

ABSTRACT

Stormwater runoff is one of the leading causes of water quality impairment in the U.S. Bioretention systems are ecologically engineered to treat stormwater pollution and offer exciting opportunities to provide local climate change resiliency by reducing peak runoff rates, and retaining/detaining storm volumes, yet implementation is outpacing our understanding of the underlying physical, biological, and chemical mechanisms involved in pollutant removal. Further, we do not know how performance will be affected by increases in precipitation, which are projected to occur in the northeastern U.S. as a result of climate change, or if these systems could act as a source or sink for greenhouse gas emissions.

This research examines the design, construction, and development of monitoring methods for bioretention research, using the University of Vermont (UVM) Bioretention Laboratory as a case study. In addition, this research evaluates mobilization patterns and pollutant loads from road surfaces during the "first flush" of runoff, or the earlier part of a storm event. Finally, this research analyzes the comparative pollutant removal performance of bioretention systems on a treatment by treatment basis.

At the UVM Bioretention Laboratory, eight lined bioretention cells were constructed with monitoring infrastructure installed at the entrance and at the subterranean effluent. A conventional, sand and compost based, bioretention soil media was compared to a proprietary media engineered to remove phosphorus, called Sorbtive Media™, under simulated increases in precipitation. Two drought tolerant vegetation mixes, native to the northeast, were compared for sediment and nutrient retention. Each treatment was sampled for soil gas emissions to determine if it was a source or a sink.

The monitoring infrastructure designs used in this research allowed for the effective characterization of pollutant mass loads entering and exiting bioretention. Cumulative mass loads from stormwater were found to be highest for total suspended solids, followed by total Kjeldahl nitrogen, nitrate, non-labile phosphorus and soluble reactive phosphorus, in descending order by mass. Total suspended solids, total Kjeldahl nitrogen, and non-labile phosphorus mass were well retained by all bioretention treatments. However, the compost amendment in the conventional soil media was found to release labile nitrogen and phosphorus, far surpassing the mass loads in stormwater. When compared with conventional media, Sorbtive Media™ was highly effective at removing labile phosphorus and was also found to enhance nitrate removal. Systems containing deep-rooted vegetation (*Panicum virgatum*) were found to be particularly effective at retaining both labile and non-labile constituents. Overall, none of the bioretention treatments were found to be a significant source of N_2O and were small sinks for CH_4 in most treatments.

ACKNOWLEDGEMENTS

I would like to express my sincere gratitude to my family, committee, colleagues, and students who helped shape and guide this processes. I would also like to thank the visionary scholars who came before me, whom inspired me to take this path. Without funding from the Lake Champlain Sea Grant, Lintilhac Foundation, VT EPSCoR, and donations of materials, time and expertise from Contech Engineering Solutions, Decagon, Watershed Consulting Associates, and EcoSolutions, none of this would have been possible.

I would specifically like to thank my advisor, Stephanie Hurley, and my committee members (Carol Adair, Don Ross, and Arne Bomblies) for their guidance and support. I would also like to thank (in approximate order of appearance) Alexandra Drizo, Josef Gorres, Eamon Twohig, the bioretention student design team (Chris Brackett, Owen Lapierre, Derek Madsen, John Nummy, and Joannie Stultz), Nancy Hayden, Andres Torizzo, Tony Stout, Dave Whitney and the EcoSolutions construction crew, Tri-Angle Metal Fabricators, Donna Rizzo, Beverly Wemple, Mark with the skill saw, the wonderful people at Teledyne, Dana Allen, Joel Tilley, Scott Merrill, Lindsey Ruhl, Anne-Marie Resnik, Lucas Jackson, Tyler Goeshel, Tom Wippick, Monica Johnson, Chloe Coggins, Matt Gargiulo, Aya Al-Namee, Noah Ahles, Paliza Shrestha, Anna Levine, Katie Bonser, Jackie Guz, Iliansherry Santiago, Luke Perry, and Alan Howard. My everlasting gratitude goes to Simon Cording.

TABLE OF CONTENTS

Page

LIST OF TABLES

Table Page

LIST OF FIGURES

Figure Page

LIST OF EQUATIONS

Equation Page

CHAPTER 1: DISSERTATION OVERVIEW

Stormwater pollution is one of the leading causes of water quality impairment in the U.S., contributing to eutrophication, degradation of freshwater and marine habitat, and loss of income generated from recreational and commercial opportunities (U.S. Environmental Protection Agency 2008). Stormwater treatment systems such as Green Stormwater Infrastructure (GSI) have potential to help prevent further water quality degradation, but the factors contributing to the success of these systems are not well defined. Bioretention systems, in particular, have been shown to be effective at reducing peak stormwater flow rates, retaining and detaining volumes, and removing pollutants such as sediments; however, their removal of labile nutrient fractions has been variable (Lefevre et al. 2015). One critical concern is that the design conditions necessary to treat labile N and P are not necessarily complementary. For instance, anaerobic conditions are necessary for denitrification of nitrate, yet may result in the release of phosphorus previously sorbed to cations in the soil matrix (Groenenberg et al. 2013). Further, anaerobic conditions may result in the release of nitrous oxide and/or methane, which are potent greenhouse gases (Butterbach-Bahl et al. 2013). Research aimed at describing how various bioretention design features influence pollutant removal is limited; research into whether various design features might affect emission or sequestration of greenhouse gases is severely limited.

GSI systems are typically designed to treat a specific portion of the storm event, called a water quality volume (WQv), and require accurate estimates of incoming pollutant loads to measure their effectiveness in reducing pollutant mass. Traditionally,

the first half-inch of runoff has been thought to transport 90% of pollution from impervious surfaces over the course of an event (Bach et al. 2010; Bertrand-Krajewski et al. 1998); however, this "first flush" effect has not been widely validated, and may not be equally exhibited by all pollutant types (e.g., labile and non-labile) (Hathaway et al. 2012). Further, the pollutant speciation and mass loads in stormwater from paved road surfaces is not well documented for different precipitation volumes.

Precipitation in the northeastern U.S. is projected to increase by 10 to 15 percent by the end of the century (Frumhoff et al. 2007; Guilbert et al. 2015). This may influence the pollutant retention capabilities of bioretention systems. However, the resiliency of bioretention performance to increasingly intense rain events with higher volumes has not been tested, yet some assert that bioretention systems and other GSI would be more flexible in the face of climate change than conventional infrastructure (Rosenberg et al. 2010; Waters et al. 2003). Bioretention design features such as soil media and vegetation have been shown to influence pollutant removal and stormwater retention performance (Hsieh and Davis 2006), yet there are very few comparative field studies of these components.

Monitoring bioretention will help improve our understanding of the physical, biological, and chemical mechanisms involved in pollutant removal, and allow us to begin to predict how these mechanisms will respond to changing precipitation patterns due to climate change. Monitoring can provide vital feedback to design engineers, ultimately helping to improve hydrologic and pollutant removal performance, lower costs, and determine long-term effectiveness and maintenance requirements, yet there are

very few bioretention systems that have been monitored in the field. There is currently very little published guidance as to how monitoring infrastructure for bioretention can be integrated into designs, and how it is physically placed during construction (Law et al. 2008).

Eight bioretention systems (or cells) were constructed on either side of a paved roadway at the University of Vermont Bioretention Laboratory, with monitoring equipment installed at each cell's inflow and the outflow to investigate (1) the incoming stormwater pollutant load from various precipitation events, (2) how mobilization and transport characteristics of various pollutants in stormwater compare, (3) how bioretention design features such as soil media influence pollutant load removal, (4) how resilient a conventional soil media would be under increased precipitation conditions, due to climate change (i.e., 20% more precipitation), (5) how resilient a proprietary media design would be under much larger than anticipated increases in precipitation (i.e., 60% more precipitation) conditions, and (6) how various bioretention design features, influence the emission or uptake of greenhouse gases (CH_4, N_2O, and CO_2).

Chapter 2 is a comprehensive literature review containing background information on stormwater, the first flush concept, factors that influence bioretention performance, and factors likely to influence emissions and/or uptake of greenhouse gas emissions in bioretention.

Chapter 3 provides a detailed description of the monitoring infrastructure and sampling methodology used in this research. The goal of chapter 3 is to provide a feasible

monitoring infrastructure design that can be adapted for other locations to monitor bioretention.

Chapter 4 investigates the mobilization and transport of nutrient and sediment mass from a roadway by stormwater, including a critical evaluation of the mass-based first flush from the research site, and a prediction of the total load likely to be delivered from a low to medium traffic paved asphalt road surface, by various precipitation depths. The goal of chapter 4 is to improve our understanding of the factors that influence pollutant mass mobilization, and predictions of stormwater mass loads, of nutrient and sediment pollutants.

Chapter 5 is a comparative evaluation of hydrologic and pollutant removal performance of bioretention systems with different soil media and vegetation treatments. In addition, it includes a description of methods to detect potential greenhouse gas emissions from the soil media within each treatment, and an assessment of the factors likely to influence emissions and/or uptake in bioretention cells. The goals of chapter 5 are to (1) predict how design features influence pollutant removal, (2) assess how the soil media designs presented here would perform under changing precipitation scenarios projected to affect the Northeastern U.S., and (3) evaluate how these design features contribute to GHG emissions or uptake.

CHAPTER 2: COMPREHENSIVE LITERATURE REVIEW

2.1. Stormwater Overview

Urbanization has had a profound effect on local hydrology as a result of increased impervious surfaces (e.g., roads, rooftops, parking lots and driveways), which result in higher stormwater discharge rates than pre-development land surfaces (Booth 1991; Brezonik and Stadelmann 2002; Marsalek et al. 2006). Masterson and Bannerman (1994) showed a > 200% increase in discharge (ft^3s^{-1}) in stream flow after a storm event, from pre to post development. High stormwater velocities mobilize and transport pollutants from impervious surfaces, including cadmium (Cd), chromium (Cr), copper (Cu), lead (Pb), mercury (Hg), zinc (Zn), polychlorinated biphenyls (PCB's), polycyclic aromatic hydrocarbons (PAHs), total phosphorus (TP), non-labile phosphorus (NLP), soluble or dissolved reactive phosphorus (SRP), total nitrogen (TN), organic nitrogen (ON), total keldahl nitrogen ((TKN) contains both NH_3, NH_4^+ and organic nitrogen), nitrite (NO_2^-), nitrate (NO_3^-), total suspended solids (TSS) as well as oil and grease, bacteria and pathogens (National Research Council 2008; U.S. Environmental Protection Agency 1998).

Stormwater pollutants have been shown to degrade the aquatic habitat of receiving water bodies (Booth and Jackson 1997; Galster et al. 2006; Masterson and Bannerman 1994) and significantly contribute to water quality impairment in the Unites States. Although nitrogen is widely recognized as the key nutrient controlling primary production and eutrophication in saltwater ecosystems (Correll 1999; Davis et al. 2006; Zinger et al. 2013), there is increasing discussion regarding the importance of nitrogen in

freshwater systems as well (Pearce et al. 2013; Turner and Rabalais 2013). Thousands of waterbodies are legally required to develop a pollution budget for stormwater associated nutrients, called a total maximum daily load (TMDL) (U.S. Environmental Protection Agency 2008).

The National Pollutant Discharge Elimination System (NPDES) is a program under the umbrella of the Clean Water Act (CWA), and is the primary vehicle through which the federal government regulates the quality of the nation's waters (National Research Council 2008). In 1987, Congress brought stormwater control under the auspices of the NPDES program, and in 1990, the U.S. Environmental Protection Agency (EPA) published the Phase I Stormwater Rules. These rules apply to municipal separate storm sewer systems (MS4s) serving over 100,000 people and for construction sites over 5 acres. In 1999, Phase II Stormwater Rules were issued which expanded the requirements to include construction sites between 1 and 5 acres (National Research Council 2008). These regulations require the use of stormwater control measures (SCMs) or Best Management Practices (BMPs) and limit the concentration of pollution that can be released from a site through a discharge permit. Biological retention, or "bioretention," is a stormwater management technique that is currently being encouraged as a BMP (National Research Council 2008).

2.2. The First Flush Concept

Stormwater practitioners have to select a water quality volume (WQv), or portion of the storm event (e.g., 0.5 inches), to treat with stormwater best management

practices such as detention basins (Sansalone and Cristina 2004) or Green Stormwater Infrastructure (GSI) (e.g., bioretention system, grassed swale) (Law et al. 2008). Traditionally, the first half-inch of runoff has been thought to transport 90% of the total pollution from an impervious surface (Bach et al. 2010; Bertrand-Krajewski et al. 1998). This concept is generally referred to as the first flush (FF) and is described as a disproportionately high concentration and/or mass, of pollutants in the beginning of a storm event with a subsequent rapid decline (Bertrand-Krajewski et al. 1998; Sansalone and Cristina 2004; Stenstrom and Kayhanian 2005). Although it is widely used, the FF concept has not been widely validated for a wide range of pollutant types (e.g., labile and non-labile) and for both concentration and mass (Alias et al. 2014; Hathaway et al. 2012; Soller et al. 2005; Stenstrom and Kayhanian 2005).

When the FF is specifically referring to pollutant concentration, it is called a concentration based first flush (CFF) and when it is referring to mass, it is called a mass based first flush (MFF) (Sansalone and Cristina 2004).The CFF concept is a tenant upon which the regulatory selection of a WQ_v was built (Ringler 2007; Sansalone and Cristina 2004), with the minimum WQv requirements being between 0.5 and 1.0 inches of rainfall (DeBusk and Wynn 2011; Sansalone and Cristina 2004; Stenstrom and Kayhanian 2005; Vermont Agency of Natural Resources 2002a). Although the CFF has been documented for some pollutants (Maestre and Pitt 2004), many studies have found variable results (Soller et al. 2005). The MFF concept has not been widely validated across different watersheds and storm conditions, and may not be equally exhibited by all pollutant types (e.g., labile and non-labile) (Hathaway et al. 2012).

2.2.1. Factors that Influence Mass Mobilization and the First Flush

There are many factors that contribute to the mobilization of mass during a storm event, and accordingly, whether the CFF and/or MFF will be observable. For instance, the watershed area influences the time of concentration (T_c), or the time for the runoff to travel from the most hydrologically remote part of the watershed to the monitoring location (Kang et al. 2008). As pollutant transport time increases, so does the likelihood of mixing, dilution, and the introduction of complicating factors such as changes in land surface composition, friction forces, and abrupt changes in flow direction, which may affect pollutant composition within a storm (Kang et al. 2006). Therefore, smaller watershed sizes have been shown to more reliably present first flush characteristics (Kang et al. 2006; Lee and Bang 2000; Maestre and Pitt 2004).

Rainfall intensity, rainfall depth (Alias et al. 2014) and antecedent dry days (ADD) (Blecken et al. 2009; Brown et al. 2013), have also been shown to influence the distribution of pollutant mass within a storm event, although the relative influence of each is still somewhat unclear. Gupta and Saul (1996) found no correlation between the CFF for TSS and the ADD, however, TSS mass load was found to correlate with ADD, as well as peak rainfall intensity and storm duration. Maestre and Pitt (2004) worked in conjunction with the Center for Watershed Protection to review phase I National Pollutant Discharge Elimination System (NPDES) Municipal Separate Storm Sewer (MS4) data from the national database of 3,700 events in 17 different states. The authors found that the first 30 minutes of runoff had higher concentrations of TKN (NH_3, NH_4^+, organic N) compared to the composite of the storm, but SRP did not shown any CFF

effects. The authors conclude that peak flow rate, rainfall intensity, percent impervious cover, watershed size and land use are factors that influence CFF. Many CFF observations may have been partly due to the dilution effects of increasing stormwater volume during the rising limb of a hydrograph (Deletic 1998; Lee et al. 2002; Maestre and Pitt 2004; Miguntanna et al. 2013).

Stenstrom et al. (2005) found that concentrations and particle sizes decreased as the storm progressed. Larger particles showed more dominant CFF characteristics than smaller particles (Stenstrom and Kayhanian 2005). This could be due to the fact that higher flow rates can move larger particles based on Stokes law, but the larger particles will quickly settle out again when the momentum is reduced (Glysson et al. 2000).

Bach et al. (2010) offered a new method of evaluating CFF by essentially determining what storm volume resulted in a return of pollutant concentrations to low "background" conditions. The authors suggest that using the actual runoff volume needed to remove mass build-up on the road surface, as opposed to a dimensionless ratio that describes the proportion of mass removed by a proportion of volume, would help make studies more comparable, but needed further testing to be widely applied.

Much MFF research has focused on testing various definitions, with variable results (Bertrand-Krajewski et al. 1998; Gupta and Saul 1996; Hathaway et al. 2012; Lee and Bang 2000), and have been inherently difficult to compare across studies (Bach et al. 2010). For instance, Gupta and Saul (1996) broadly defined the FF as the portion of the storm up to the maximum divergence between a plot of cumulative mass and cumulative volume. Bertrand-Krajewski et al. (1998) designated the first flush as 80% or more of the

total pollutant mass that is transported in the first 30% of the runoff volume. Many others have offered variations of the Bertrand-Krajewski et al. (1998) FF definition (Deletic 1998), but according to Hathaway et al. (2012), the MFF is rarely found with these definitions. The definitions are difficult to use from a design standpoint, because the x% of the total storm volume cannot be known *a priori*. The FF volume may also be pollutant specific, thus sizing of tanks or treatment devices would need to be done with a specific pollutant in mind (Bertrand-Krajewski et al. 1998).

Sansalone and Cristina (2004) compared the MFF definitions above in addition to others and found them to be conceptually and mathematically equivalent, with a mass based first flush effect being defined when the M:V ratio is greater than 1.0. The M:V ratio is a dimensionless representation of the cumulative mass divided by the total mass as a function of the cumulative volume, divided by the total volume of a storm event (Bertrand-Krajewski et al. 1998). Sansalone and Cristina (2004) conclude that although a MFF may be present in some storm events, it is not significant enough by any definition, to warrant the development of a water quality volume upon which to base the treatment of a portion of stormwater (Sansalone and Cristina 2004). The authors suggest that instead, research should focus on the factors that affect mass load in order to improve predictions.

Alias et al. (2014) also moved away from using the more traditional definitions of MFF and instead, evaluated the mobilization of TSS, TP and TN mass from a combination of road and roof surfaces across different sections of the runoff hydrograph. The authors found that mass mobilization was highly influenced by increasing volume

and precipitation intensity, given monitored precipitation depths between 0.024 inches and 0.23 inches. The authors did not provide the total mass loads generated per m^2 of drainage area from the site and did not differentiate between labile and non-labile N and P components.

Kang et al. (2006) used the kinematic wave equation to simulate various factors that influence the MFF effect, and predicted that a smaller number of ADDs would produce a lower mass and therefore result in a lower MFF, or the absence of the MFF effect all together. Long ADDs were predicted to result in large initial mass sources and a correspondingly high MFF. Alias et al. (2014) found that rainfall depth and intensity played a more dominant role in runoff characteristics than the length of antecedent dry periods, although the authors did not distinguish between nutrient speciation (e.g., NO_3^- vs TKN), which may have distinct mobilization characteristics (Taylor et al. 2005).

Hathaway et al. (2012) found that the strength of the first flush, measured as the numeric value of the M:V ratio, was as follows, TSS > NH_3 > TKN (NH_3,NH_4^-, organic N) > NO_2-NO_3 > TP > SRP, although the M:V ratios were not greater than 1.0 for all pollutants in most cases. The MFF for TSS was found to be significantly greater than NO_3^- (Hathaway et al. 2012). The MFF for TSS was not significantly different from NH_3 and TKN. Nitrogen displayed a stronger MFF characteristics than phosphorus, with SRP exhibiting the weakest MFF effect, which was virtually nonexistent (Hathaway et al. 2012). Total runoff volume was found to inversely affect the strength of the FF on TSS but was positively correlated with SRP (Hathaway et al. 2012). Interestingly, the two land

use types in this study (impervious and forested) did not have an effect on the strength of the first flush.

It may be more relevant, as suggested by (Bach et al. 2010), to focus on how various influencing factors impact the total mass load that is delivered, and how the mobilization characteristics of different pollutants compare. In order to determine the total mass load that had built up upon the road surface prior to an event, Miguntanna et al. (2013) vacuumed the road surface and used simulated rainfall intensities to generate runoff. The authors found that nitrogen was predominantly present in runoff in a dissolved organic form, which was easily transported by low intensity rainfall events due to its solubility. SRP was found to be the primary species when the runoff particle size was < 75 um, whereas other P species were present when particle sizes were greater than 75 um. The total pollutant mass per m^2 of paved area from a residential area was as follows: TSS (2,250 mg m^2) > TN (37, 190 μg m^{-2}) > TKN (27,110 μg m^{-2}) > TP (9,380 μg m^{-2}), non-labile phosphorus (9,240 μg m^{-2}) > NO_3^- (1,870 μg m^{-2}) > SRP (140 μg m^{-2}).

2.3. Bioretention Design and Performance

Bioretention systems, also known as rain gardens (Davis 2008; Dietz and Clausen 2006; Hunt et al. 2008), biofilters (Zinger et al. 2013), and bioswales (Collins et al. 2010), are composed largely of soil media and vegetation that are intended to remove pollutants while also retaining and detaining stormwater volumes and reducing peak runoff velocities to more closely mimic pre-development hydrology. Bioretention is considered one component of Green Stormwater Infrastructure (GSI), which also falls

under the umbrella of a larger set of goals, referred to as Low Impact Development (LID) (Dietz 2007). In addition to improving water quality, bioretention systems can serve as public amenities, providing improved aesthetics and habitat value (Claytor and Schueler 1996). These systems are rapidly growing in popularity, in both the public and private sectors. Despite being widely promoted, and required in some instances, there are still many unknowns regarding the factors that influence pollutant removal, and the long term viability of these systems.

Some of the many design features that affect the pollutant removal performance of bioretention, and other GSI systems include: residence time (Collins et al. 2010; Hurley and Forman 2011; Kadlec et al. 2010; Rosenquist et al. 2010; Sansalone and Cristina 2004); media depth (Brown and Hunt 2011); vegetation type, root depth, type and architecture (Claassen and Young 2010; Claytor and Schueler 1996; Collins et al. 2010; Davidson et al. 2000; Davis et al. 2009; Kadlec et al. 2010; Lucas and Greenway 2008; Read et al. 2008); organic matter content (Bratieres et al. 2008; DeBusk and Wynn 2011; Fassman et al. 2013; Leytem and Bjorneberg 2009; Thompson et al. 2008); use of mulch (Bratieres et al. 2008; DeBusk et al. 2011; Dietz and Clausen 2006); percent sand, silt, and clay (Liu et al. 2014); chemical characteristics of the soil media (e.g., amount of iron, calcium, and aluminum) (Arias et al. 2001; Groenenberg et al. 2013; Vance et al. 2003); ponding depth, hydraulic conductivity, and infiltration rate (Thompson et al. 2008); and the inclusion of features such as an internal water storage zone (IWS) (Chen et al. 2013; Dietz and Clausen 2006; Hunt et al. 2006; Kim et al. 2003). Proper maintenance and care taken during construction to avoid soil compaction are also critical

factors that will affect the long term performance of bioretention (Brown and Hunt 2011; Dietz and Clausen 2006).

Each of the design features listed above play an important role in the performance of bioretention systems; yet they are not always complementary. For example, phosphorus reduction via sorption can be reversed under reduced conditions (Basta and Dayton 2007), yet prolonged saturation is required for denitrification (Thomson et al. 2012). Understanding the underlying pollutant removal mechanisms of bioretention systems and how design feature influence them is critical to reducing variability in performance.

2.3.1. Depth of Soil Media

Bioretention depth has been shown to positively influence nutrient and sediment removal (Bratieres et al. 2008; Li and Davis 2008, 2009) due to increased overall retention time and settling potential, and reduction in stormwater volume (Brown and Hunt 2011), yet many of the design recommendations for bioretention state that the depth should be "shallow" (Collins et al. 2010; Dietz and Clausen 2005, 2006; Lefevre et al. 2015; Vermont Agency of Natural Resources 2002a). This distinction may have been made to differentiate the systems from conventional detention ponds, which tend to be much deeper than bioretention cells to hold a larger volume (National Research Council 2008) or based on the application of bioretention cells on retrofit sites where a shallow depth would be necessary for reducing confilict with existing utilites and connecting to existing storm drainage infrastructure. The depth of a particular bioretention design is

likely to be site specific, but the term "shallow" may be misleading and discourage investigation into the use of deeper systems where there is potential to do so.

2.3.2. Vegetation

Many stormwater and LID design manuals specify that bioretention systems should be planted (Collins et al. 2010; Davis et al. 2001, 2006; Dietz and Clausen 2005, 2006; Dietz 2007; Hatt et al. 2008; Hunt et al. 2006; Kim et al. 2003), yet few go as far as to specify the pollutant removal benefits that different vegetation types (e.g., ground cover, shrubs, perennials, or trees) might provide (Dietz and Clausen 2005). Vegetation plays a significant role in the removal of labile N and P (Lintern et al. 2011) from the soil pore water stored between precipitation events (Serna et al. 1992), yet nutrient uptake is highly variable and dependent on root architecture, biomass, depth and type (e.g., fibrous vs woody) (Brix 1994, 1997; Le Coustumer et al. 2012; Dietz and Clausen 2006; Read et al. 2008; Tanner 1996). Read et al. (2008) found that pollutant concentration in the effluent from bioretention negatively correlated with root mass for nearly all N and P constituents, with root mass explaining between 20 – 37% of the variability in effluent concentration.

Most plants favor shallower rooting depths (< 1 m) due to lower energy costs for development and maintenance, high short term nutrient contents, close proximity to incoming water, and high oxygen contents (Edwards 1992; Preti et al. 2010; Schenk 2008). However, evidence also suggests that long-term nutrient availabilities (P, Ca^{2+}, K^{+}, and Mg^{2+}) tend to be greater at depth in semi-arid and arid ecosystems (McCulley et al. 2004), which can be homologous to the sand based media often used in bioretention

designs (Houdeshel et al. 2015). Certain plants, such as switchgrass (*Panicum virgatum*) may have adapted deep roots to maximize access to nutrients and moisture (Preti et al. 2010; Schenk 2008). Read et al. (2008) suggests that deep rooted plants may provide important long term performance benefits, however their use in bioretention has not been the specific focus of many previous studies.

Thick-rooted plants have been shown to maintain long term permeability and reduce clogging in bioretention soils (Le Coustumer et al. 2012). By contrast, fine stemmed vegetation such as grasses, sedges and rushes have been shown to be highly efficient at providing above ground filtering capacity (Gagnon et al. 2012). Our current understanding of the role of vegetation in removing labile pollutants in bioretention systems in extremely limited (Lefevre et al. 2015).

2.3.3. Bioretention Soil Media and the Addition of Organic Amendments

It is understood that sediments in stormwater are typically removed through extended detention and physical filtration of fine particles within the bioretention soil media, with removal rates between 70% and 99% being common (Bratieres et al. 2008; Brown and Hunt 2011; Hatt et al. 2008; Hsieh and Davis 2006). Extreme drying conditions have been shown to negatively impact TSS removal performance in soils with higher clay content (Blecken et al. 2009); drying increases the size of macropore channels, which can result in in the release of a portion of the previously removed sediment in the next storm event (Lintern et al. 2011). It is possible that the non-labile fraction of P and N may have similar removal mechanisms as TSS, and would similarly be affected by drying conditions based on their inherently larger particle sizes

(Chen et al. 2013; Claytor and Schueler 1996; Davis 2007; Zinger et al. 2013); however, the sand-dominated bioretention soil media used in this research was not likely to exhibit extreme shifts in macropore size due to drying. The distinctive removal mechanisms of the different fractions of N and P are not well characterized within exisitng bioretention studies, and warrant further research.

2.3.4. Organic Amendments in Bioretention Soil Media

The engineered soil media used in bioretention designs varies, and includes both native soil removed during construction (Dietz 2007) as well as imported material, when native infiltration rates are not optimal. Imported sand based media designs are common, with the addition of an organic amendment usually recommended (Bratieres et al. 2008; DeBusk and Wynn 2011; Michigan Department of Environmental Quality 2008; Thompson et al. 2008; Vermont Agency of Natural Resources 2002a; Washington State University Pierce County Extension 2012). Organic matter (e.g., compost, mulch) provides nutrients to plant communities, moisture retention, cation exchange capacity and fosters microbial growth (Kim et al. 2003; Lintern et al. 2011). Soil organic matter (OM) is a grouped measure, containing both partially decomposed organic compounds and soil humus. It is largely a measure of soil carbon, and can range from less than 1% in coarse sandy soils to greater than 5% in fertile grassland soils (Brady and Weil 2008).

Thompson et al. (2008) found that the addition of compost in bioretention increased saturated hydraulic conductivity, aggregate stability, water holding capacity, and decreased bulk density. Mulch is also often included in bioretention designs to retain moisture and subdue weed growth, as one would in a traditional landscaping setting

(Davis et al. 2001, 2006; Dietz and Clausen 2005, 2006; Dietz 2007; Hunt et al. 2006). Mulch, and other organic amendments, have also been shown to be highly effective at removing metals from stormwater (Hsieh and Davis 2006; Muthanna et al. 2007). There is concern within the literature that the benefits provided by organic amendments may be undone by their potential to release nutrients (Lefevre et al. 2015), however the specific mass loads from organic amendments and their relative contribution to the performance of bioretention has not been the specific focus of many previous research studies. The following section reviews the nutrient retention and export associated with bioretention soil media.

2.3.5. N and P Cycling in Soils

Soils and organic amendments (e.g., compost, mulch) contain two major nutrient pools: (1) insoluble particulate organic and inorganic N and P (non-labile) and (2) dissolved organic and inorganic N and P (labile), which are in soil solution. The organic portion of the pool in traditional soils is variable, usually ranging from 20 to 80% (Schachtman et al. 1998). SRP, NO_2^-, NO_3^-, NH_3, and NH_4^+ are inorganic labile nutrients that can be transported from the soil profile during a storm event (Schachtman et al. 1998). Labile nutrients removed from within the soil media are replaced by decomposition and mineralization (Basta and Dayton 2007) and may not be well retained by bioretention systems (Blecken et al. 2010; Clark and Pitt 2009; Dietz and Clausen 2005; Hsieh and Davis 2003, 2006; Hunt et al. 2006; Lucas and Greenway 2011).

Organic nitrogen is broken down by mineralization, releasing the ammonium ion (NH_4^+) in a highly temperature and moisture dependent microbially mediated process

(Serna et al. 1992). Removal occurs via plant uptake and sorption reactions with negatively-charged organic matter and clay particles in the soil matrix (Arias et al. 2001; Brix et al. 2001; Komlos and Traver 2012; Lucas and Greenway 2011). Plant uptake rates have been shown to increase up to external NH_4^+ concentrations of 240 mg/L (Serna et al. 1992). In some plants, NH_4^+ is absorbed by plant roots at a higher rate than NO_3^-, and results in a decrease in surrounding pH (Serna et al. 1992).

In aerobic conditions, microbes oxidize ammonium to nitrite (NO_2^-) and nitrate (NO_3^-) during the second step of nitrification (Conrad 1996), which produces H^+ and decreases pH. Ammonium is therefore thought to be short lived, having a turnover time of approximately 24 hours in most soils (Jones et al. 2005). Nitrate (NO_3^-) is a monovalent, negatively charged ion that is rapidly transported through the soil matrix by water, making it difficult to remove through adsorption and plant uptake. The rate of NO_3^- diffusion in soil is thought to be approximately five times higher than NH_4^+ (Serna et al. 1992). Any uptake that does occur is likely being pulled from the nitrate stored in the soil matrix as soil pore water between storm events. Nitrate uptake rates by plant roots have been shown to increase until external nitrate levels of 120 mg/L, and result in an increase in pH around plant roots (Serna et al. 1992).

Denitrification is thought to be the primary nitrate removal mechanism in bioretention systems (Bratieres et al. 2008; Davis et al. 2006; Kim et al. 2003; Lucas and Greenway 2008). Biotic denitrification is a microbially-mediated conversion of nitrate to nitrogen gas and requires oxygen contents of less than 0.5 mg L^{-1} (Rönner and Sörensson

1985). The stepwise denitrification process is as follows, with the oxidation states of N shown in parenthesis.

$$NO_3^- [+5] \rightarrow NO_2^- [+3] \rightarrow NO [+2] \rightarrow N_2O [+1] \rightarrow N_2 [0]$$

Abiotic denitrification of NO_3^- may also occur in the presence of inorganic ions (Fe^{2+}, Cu^{2+}, Mn^{2+}) in the soil matrix, in a process called chemodenitrification (Butterbach-Bahl et al. 2013; Luther et al. 1997), although this process is not well understood. Prolonged periods of saturation and low oxygen content are typically needed for denitrification, but if incomplete, the process can release nitrous oxide (N_2O), which is a long-lived greenhouse gas (144 years) that is currently the most important natural cause of stratospheric ozone depletion (Bond-Lamberty and Thomson 2010; Butterbach-Bahl et al. 2013; Del Grosso and Parton 2012). It is, therefore, vitally important that the transport and removal mechanisms of nitrogen in bioretention cells are well understood.

Although soil phosphorus content may range anywhere from 500 to 2,000 mg/L, bioavailable phosphorus (orthophosphate) may be only a few mg/L because much of it forms insoluble complexes with soil cations (Vance et al. 2003). To compensate for P complexation, the roots of many plants exude citric and malic acids into the rhizosphere. The exudates allow for the chelation of Al^{3+}, Fe^{3+}, and Ca^{2+}, that subsequently releases insoluble phosphorus (Horst et al. 2001; Plaxton and Podestá 2006). This newly released P can then be taken up by plants. SRP is also generated during decomposition and mineralization of organic matter (Sinsabaugh et al. 2005).

2.3.6. CEC and pH

Cation exchange capacity (CEC) is a measure of the capacity of the soil to hold cations , and are available to replenish nutrients as they are taken up in the water-soluble phase, or adsorbed by plant roots directly through active transport (Sonon et al. 2014). CEC is most directly influenced by the amount of calcium (Ca^{2+}), magnesium (Mg^{2+}), sodium (Na^{+}), and potassium (K^{+}) ions present in a soil (Sonon et al. 2014), which are often related to percent organic matter. These ions are also referred to as base cations, for they outcompete the hydronium ion (H^{+}) for binding sites on negatively charged clay particles and organic matter complexes, thereby increasing the pH in the surrounding soil solution (Brady and Weil 2008).

Divalent cations (i.e., Ca^{2+}, Mg^{2+}) share similar properties in both the soil water phase, and when adsorbed to cation exchange sites, however, Ca^{2+} is preferentially adsorbed and more strongly held when compared to Mg^{2+} (Sonon et al. 2014). Divalent cations are more strongly held to negatively charged soil particles than monovalent cations (i.e., K^{+}, Na^{+}) (Sonon et al. 2014). Soils with low CEC values are less resilient to leaching effects and the pH is more likely to decrease over time (Sonon et al. 2014). A sandy soil has the lowest CEC, typically between 1 – 5 $cmol_c\ kg^{-1}$ (Sonon et al. 2014), as shown in Table 1.

Table 1. Soil textures and CEC (Sonon et al. 2014).

Soil Texture	CEC ($cmol_c\ kg^{-1}$)
Sand	1-5
Fine Sandy Loam	5-10
Loam	5-15
Clay Loam	15-30
Clay	> 30

The leaching of cations from soil solution during precipitation events, and the removal via plant uptake can decrease soil pH (Brady and Weil 2008). As cations are removed from soil, the empty negatively charged binding sites become occupied by H^+ and Al^{3+}. A large decrease in pH can iron solubility, which could result in the dissolution of previously unavailable ferric (Fe^{3+}) oxyhydroxides and any associated phosphorus (Jones 1998).

2.3.7. Inconsistent Labile N and P Removal in Bioretention

As outlined in the latest review of bioretention performance by Lefevre et al. (2015), labile nitrogen and phosphorus removal reported to date has been extremely variable, ranging from -630% to 98% for nitrate and from -78% to 98% for SRP (Bratieres et al. 2008; Dietz and Clausen 2005; Geosyntec Consultants and Wright Water Engineers 2012; Hatt et al. 2008; Hunt et al. 2006; Li and Davis 2009). Geosyntec Consultants and Wright Water Engineers (2012) conducted a comprehensive review of the International Stormwater BMP Database and found a net export of labile P from bioretention overall, with median effluent concentrations of 130 μg L^{-1}. The variability of labile N and P removal has been thought to be related to the soil media (Lefevre et al. 2015), but the relative contribution of the labile N and P from the soil media has not been the explicit focus of many research efforts.

Bratieres et al. (2008) found SRP concentration reduction of greater than 83% in sandy loam filter media, and sandy loam with 10% vermiculite and 10% perlite, but media with10% leaf compost and 10 % mulch resulted in a net export of SRP, of greater than 78%. Debusk et al. (2011) found that leaf compost contained 900 mg kg^{-1} of TP and

13,500 mg kg^{-1} of TN. Potting soil had 400 mg kg^{-1} of TP and 2,270 mg kg^{-1} of TN, and topsoil had 200 mg mg^{-1} of TP and 594 mg kg^{-1} of TN. Mulch contained 335 mg $kg^{-1}$of TP and 1,800 mg kg^{-1} of TN. All of the above were thought to contribute some portion of their labile nutrient content, resulting in the export of nutrients from the system; however, the relative contribution was not explicitly studied. Hunt et al. (2007) concluded that if the bioretention soil media was low in available phosphorus, then it would be unlikely to export phosphorus in the future.

Despite the potential for labile N and P to be released from organic amendments used in bioretention media, the dominant concerns regarding plant establishment and metals removal have prevailed, thus, organic amendments, such as compost and mulch are, still being broadly recommended by many government agencies and stormwater professionals for use in bioretention cells (Bratieres et al. 2008; Brown and Hunt 2011; Busnardo et al. 1992; Clark and Pitt 2009; Claytor and Schueler 1996; Davis et al. 2009; DeBusk and Wynn 2011; Dietz and Clausen 2005; Eger 2012; Hunt et al. 2006; Kim et al. 2003; Lintern et al. 2011; Paus et al. 2013; Stander and Borst 2010; Thompson et al. 2008). The relative contribution of labile N and P from organic amendments to the effluent from bioretention cells is largely untested.

2.3.8. Soil Media Designed to Remove Labile P

New research is being conducted to specifically engineer soil media to remove phosphorus within bioretention and other stormwater management applications through selective inclusion of different cations within the soil, as well as the chemical engineering

of new proprietary media (e.g. Sorbtive Media ™, Blue Pro®). A review of phosphorus sorption mechanisms is provided in the following section.

Labile phosphorus (i.e., SRP) can be removed from solution through precipitation and sorption reactions (also called fixation, surface complexation, ion exchange and ligand exchange), which vary in their bonding strength and relative stability, depending on mineral structure and pH (Figure 1.) (Sollins et al. 1988).

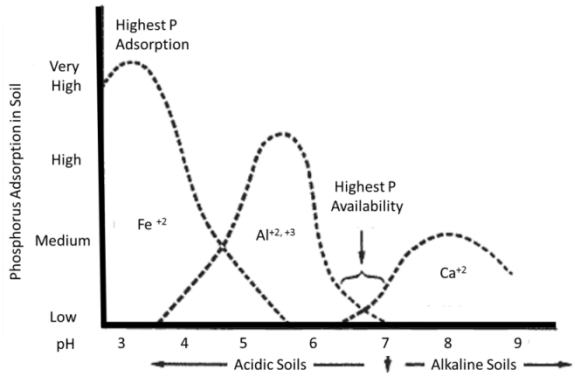

Figure 1. Phosphorus adsorption in soils with increasing pH (Michigan State University Extension).

In alkaline conditions, phosphorus reacts with calcium and becomes insoluble, precipitating from solution (Sollins et al. 1988). In more acidic conditions, iron (Fe) and aluminum (Al) are thought to be the main drivers of phosphorus sorption (Arias et al. 2001; Gerritse 1993). Sorption can occur through the formation of outer sphere (adsorption) or inner sphere (absorption) complexes (Sollins et al. 1988; Weng et al. 2012). Outer sphere complexes result from the formation of positive or negative charges on the particle surface, which attract the opposite charge. Aluminosilicate clays and sesquioxides (oxides, hydroxides and oxyhydroxides) of Fe and Al provide the majority of the surface adsorption potentials. These charges form as a result of the protonation

(addition of an H^+) and deprotonation (removal of H^+) of hydroxyl groups (OH^-) (Essington 2004).

Inner sphere complexes can form when a functional group (e.g., hydroxyl) on the particle surface is replaced by an ion complex, resulting in the formation of a covalent bond (Essington 2004; Sollins et al. 1988). Inner sphere complexes are stronger than outer sphere due to a lack of water molecules separating the ion from the soil surface charge. Inner sphere phosphorus sorption occurs when surface hydroxyls are replaced by phosphate and form covalent bonds with Al, Fe, or Si (Sollins et al. 1988; Weng et al. 2012).

Researchers have begun to apply these concepts in bioretention, in order to maximize phosphorus retention by the soil media. For example, Chardon et al. (2005) tested the phosphorus sorption capacities of iron-coated sand, a byproduct of the drinking water industry in the Netherlands. The authors found that the material had an average P removal efficiency of 94%. Stoner et al. (2012) found that the controlling factors in P removal were dependent on the dominant mineral association. For instance, with retention times of 0.5 to 10 minutes, inflow P concentrations and retention times were the most important factors in materials dominated by calcium, and chemical precipitation was the primary removal mechanism. In Fe and Al dominated systems, retention time did not play as large a role in P removal as metal content and incoming P concentration, where ligand exchange was the primary P removal mechanism (Stoner et al. 2012).

2.3.9. Phosphorus Desorption

Although metal sorption seems promising for removing labile P, doubts are often raised regarding its longevity if the conditions become anaerobic. In an anaerobic environment, oxygen depletion forces the microbial communities to utilize electron acceptors preferentially, in the following order: $O_2 > NO_3^- > Mn^{4+} > Fe^{3+} > SO_4^{2-}$ (Spivakov et al. 1999). This produces the reduced version of the species, which includes N_2 (and other reduced forms of N), Mn^{3+}, Fe^{2+}, and S^{2-} or H_2S. The reduced form of ferric iron (Fe^{3+}), is ferrous iron (Fe^{2+}), which is soluble and can release phosphorus previously bound to it (Spivakov et al. 1999). There is some uncertainty regarding whether phosphorus that is released from iron complexes during reduced conditions will be transported from the soil, effectively being lost from the system. For instance, P that is released from Fe^{3+} in soil may remain suspended in the adjacent pore water, loosely held by attraction, to be sorbed again when aerobic conditions return (Young and Ross 2001). This would not be the case, however, if gravitational or fluid forces became dominant, as may be the case in bioretention. Some mineral phosphorus associations also help protect against desorption. For instance, the presence of manganese oxide has been shown to prevent the reductive dissolution of phosphorus bound to ferric iron oxide (Groenenberg et al. 2013).

Anaerobic conditions, and potential phosphorus desorption, are most likely to occur in bioretention designs which include an internal water storage (IWS) zone, for enhanced nitrogen removal via denitrification. Phosphorus removal data from these systems has been variable (Passeport et al. 2009), with enhanced P removal being shown

in some cases. For instance, Hunt et al. (2006) found SRP concentrations from designs with IWS zones (520 μg L^{-1}) were lower than from designs without an IWS zone (2,200 μg L^{-1}). Dietz and Clausen (2006) showed some of the lowest outflow TP concentrations reported (39 μg L^{-1} to 43 μg L^{-1}), in a system designed with an IWS zone. It is unclear if phosphorus desorption in bioretention is related to the inclusion of an IWS zone and warrants future research. The use of an IWS zone for nitrogen removal will be discussed in the following section.

2.3.10. Nitrogen Removal with an Internal Water Storage Zone (IWS)

Nitrogen transformation dynamics are complex, with nitrification and denitrification occurring simultaneously within aerobic and anaerobic microsites throughout a soil aggregate (Vilain et al. 2014). Nitrate is often exported from bioretention, with the soil media thought to be a contributor (Davis et al. 2001, 2006; Hunt et al. 2006). In an attempt to increase nitrate removal, IWS zones have been trialed to promote denitrification (Chen et al. 2013; Dietz and Clausen 2006; Hunt et al. 2006; Kim et al. 2003). The results have been somewhat successful, although the necessary conditions for optimal denitrification (e.g., labile carbon content, saturation duration, optimal electron donors) in bioretention are still not fully understood.

2.3.11. Volumetric Water Content (VWC)

Volumetric water content (VWC) is a measure of the fraction of the total volume of soil that is occupied by water (m^3 m^{-3}), and is often expressed as a percent (Mengel and Kirkby 2001). The ambient VWC of a soil varies depending on the soil's

water holding capacity. The plant available water is the difference between the permanent wilting point and field capacity (Mengel and Kirkby 2001), as shown in Figure 2.

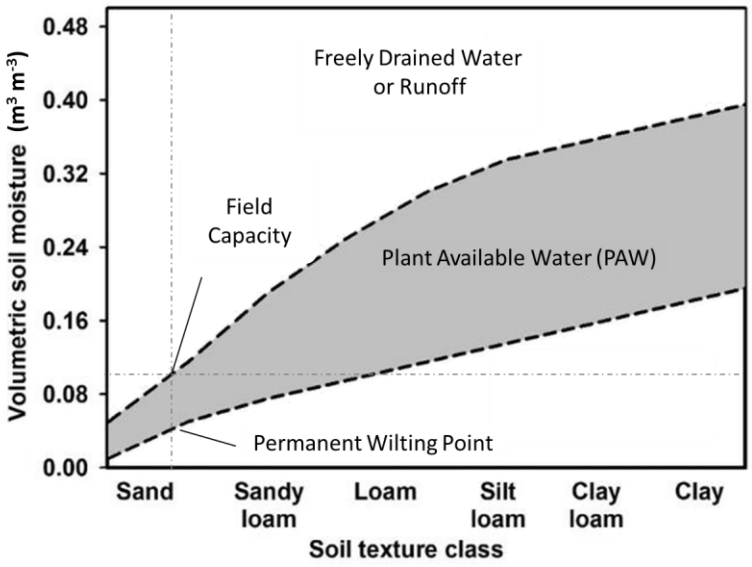

Figure 2. Volumetric soil moisture content by soil textural class, modified from Zotarelli et al. (2010).

Soils with a higher silt, clay, and organic matter content will have higher plant available water and ambient VWC (Brady and Weil 2008; Zotarelli et al. 2010). As the VWC increases, the soil and pore fluid interface undergoes a host of dynamic exchanges. Ionic material that is loosely bound to the soil matrix becomes part of the soil pore water, and ions can be transferred between the pore water and the soil matrix (Mengel and Kirkby 2001).

Plant roots are able to remove nutrients held in pore water, with the remaining water requiring more energy to extract (Mengel and Kirkby 2001). Vertical migration of water through the soil profile occurs when water content is above field capacity and gravity overcomes the soil matric potential. This downward movement of water can transport ionic material in pore water to lower layers of the soil profile (Mengel and

Kirkby 2001). Sandy soils are known to have low plant available water with field capacity relating to a VWC of between 5% - 10% (Zotarelli et al. 2010) (Figure 2).

2.3.12. Electrical Conductivity (EC)

Electrical conductivity (EC) is comprised of two primary components: (1) the exchangeable cations (Ca^{2+}, Mg^{+}, K^{+}) from the solid soil particles themselves and (2) the ions present in a soil solution (Heiniger et al. 2003). Bioretention soil receives inputs of nutrients from rain water, mineralization of existing organic matter, and stormwater. Rain water typically has an EC of between 5 x 10^{-4} dS m^{-1} and 0.003 dS m^{-1} (Essington 2004). The EC of stormwater varies widely, depending on the amount of dissolved solutes present (Kayhanian et al. 2007). Soil EC is naturally highly variable. The University of Georgia Extension rates soil EC from 0 – 0.15 dS m^{-1} as low enough to cause plants to exhibit signs of nutritional deficiency. Soil EC greater than 4 dS m^{-1} is considered slightly saline by the USDA and can reduce vegetative growth and microbial decomposition, respiration and nitrification (USDA Natural Resources Conservation Service 2011). The Washington State University Extension Low Impact Development Manual (2005) recommends a maximum EC of 5 dS m^{-1} for bioretention soil media (Washington State University Pierce County Extension 2012).

2.4. Climate Change in the Northeastern U.S.

Temperatures in the northeastern U.S. are predicted to rise between 2.5 ^{o}F (1.4 ^{o}C) and 4 ^{o}F (2 ^{o}C) in the winter, and between 1.5 ^{o}F (0.83 ^{o}C) and 3.5 ^{o}F (1.9 ^{o}C) in the summer, regardless of future changes in greenhouse gas emissions (Frumhoff et al. 2007;

Guilbert et al. 2015). Hot summer conditions are expected to arrive earlier and last longer. The number of days with temperatures greater than 100 ^{o}F are projected to increase, and the length of winter is projected to decrease (Frumhoff et al. 2007). These scenarios have the potential to change pest and crop dynamics, and increase water temperatures, which would impact nutrient cycling, and threaten important economic industries such as agriculture, fisheries and tourism among many others (Frumhoff et al. 2007).

In the northeastern U.S., precipitation has increased by 5 to 10 percent since 1900 (Frumhoff et al. 2007; Guilbert et al. 2015). This trend is predicted to continue under both high and low emission scenarios, with an increase in annual precipitation of 10 to 15 percent (~ 10.2 cm per year) by the end of the century (Frumhoff et al. 2007; Gillian et al. 2014). Precipitation intensity is also projected to increase in the northeast (Guilbert et al. 2015) and globally, due to increased atmospheric water vapor from the warming oceans (Gillian et al. 2014). The effects of these changes are not easy to predict on a local scale. Changes in precipitation and temperature are likely to generally affect nitrous oxide (N_2O) and methane (CH_4) emissions (Castellano et al. 2010; Connor et al. 2010; U.S. Climate Change Science Program and the Subcommittee on Global Change Research 2008). Both precipitation and temperature impact soil nitrogen cycling (mineralization, biological fixation, nitrification, denitrification, ammonia volatilization and nitrate leaching) as well as the growth rate of plants, which directly affects nitrogen demand (Del Grosso and Parton 2012). Increased precipitation is likely to enhance nitrification and denitrification rates, which release N_2O, while also increasing nitrogen

uptake via plants (Del Grosso and Parton 2012), which would in turn, limit the nitrate substrate available for microbial processes (Del Grosso and Parton 2012). The relative dominance of either process is uncertain.

In the stormwater community, there is considerable interest in determining how to maximize the denitrification of nitrate to nitrogen gas. In bioretention systems, the soil media is selected to meet a number of criteria. Although denitrification of nitrate is often listed as a goal, the soil conditions in-situ (aerobic) do not always encourage complete denitrification (Davis et al. 2001, 2006; Hunt et al. 2006) but instead, may encourage nitrification; both processes have the potential to release nitrous oxide (Butterbach-Bahl et al. 2013; Thomson et al. 2012). More research is needed to determine the scale of nitrous oxide emissions possible from bioretention systems, and which conditions are best suited to promote efficient nitrogen transformation (e.g., carbon and nitrate content, saturation duration).

2.4.1. Nitrous Oxide (N_2O)

Nitrous oxide (N_2O) is a long-lived trace gas, with an atmospheric lifespan of 144 years (Bond-Lamberty and Thomson 2010), with an average mixing ratio of 322.5 parts per billion by volume (ppbv) in 2009 (Butterbach-Bahl et al. 2013), and a 100-year warming potential 298 times that of carbon dioxide (Butterbach-Bahl et al. 2013; Dalal et al. 2003; Del Grosso and Parton 2012; Thomson et al. 2012). Concentrations have increased by 19 % since pre-industrial history, with an average increase of 0.77 parts per billion per volume per year (ppbv/yr) from 2000-2009. N_2O contributes 6.24 % to the overall global radiative forcing, and is currently the most important natural cause of the

depletion of stratospheric ozone (Butterbach-Bahl et al. 2013; Del Grosso and Parton 2012; Portmann et al. 2012; Ravishankara et al. 2009; Thomson et al. 2012).

It is well known that microbial activity in soils is a major contributor of N_2O to the atmosphere. It is produced during both nitrification and denitrification, with the latter also being a sink for N_2O (Conrad 1996; Schlesinger 2013; Zhuang et al. 2012). The seminal work of Nommik (1956) outlined the main environmental factors that control N_2O production, building the case for microbiological production of N_2O and N_2. The main processes which drive nitrogen reactions are nitrogen fixation (nitrogen gas to ammonia), nitrification (ammonia to nitrate), dissimilatory nitrate reduction to ammonia or nitrate ammonification (nitrate to ammonia), anaerobic ammonia oxidation or anammox, and denitrification (nitrate to nitrogen gas) (Conrad 1996). N_2O can be reduced back to N_2 by some DNRA (dissimilatory reduction of nitrate to ammonia) bacteria or in the stepwise denitrification process (Conrad 1996).

2.4.1.1. Nitrous Oxide Emissions

Roughly 62% of N_2O emissions globally can be traced back to natural and agricultural soils through bacterial denitrification and oxidation of ammonia (Smith et al. 2012; Thomson et al. 2012). Zhuang et al. (2012) developed a large-scale global inventory of N_2O emissions from natural systems alone, and found large spatial and seasonal variability in emissions due to soil type, climate and vegetation. The authors estimate that non-agricultural global soil N_2O sources produce 3.37 Tg of N per year, with a major source coming from tropical warm and moist soils. High latitude ecosystems were estimated to contribute less than 0.10 Tg N per year (Zhuang et al. 2012).

According to the hole-in-the-pipe model first presented by Firestone and Davidson in 1989, both nitrification and denitrification processes are enhanced by the availability of nitrogen in the soil (Verchot et al. 1999), which is heavily influenced by the nutrient inputs via fertilization and by the growth of nitrogen fixing vegetation (Del Grosso and Parton 2012). Agricultural emissions from nitrogen-based fertilizers and manure management are between 4.3–5.8 Tg N_2O-N/yr, whereas emissions from natural soils are between 6-7 Tg N_2O-N/year, with combined soil and agricultural emissions accounting for about 56 – 70%% of the global N_2O emissions (Schlesinger 2013).

Recent analyses suggests that 3 to 5 percent of the nitrogen from agricultural land is converted to N_2O annually, which is possibly responsible for the increase in N_2O mixing ratio from 270 ppbv in 1860 to 315 ppbv in 2000 (Del Grosso and Parton 2012; Smith et al. 2012). Sources of reactive nitrogen in agricultural systems include the addition of synthetic fertilizers, the biological fixation of nitrogen, and mineralized organic nitrogen when organic matter is broken down during cultivation (Thomson et al. 2012). Processes such as volatilization, leaching and erosion can also trigger N_2O emissions without direct N applications (Butterbach-Bahl et al. 2013).

Soil water content is also a key influencing factor in N_2O emissions, for water can result in displacement of gases previously trapped in the soil matrix, create localized anoxic conditions which encourage denitrification, or effectively block gas from escaping through various soil macropores if they are filled with water (Davidson et al. 2000). Water filled pore space (WFPS) for many soils at field capacity is about 60%, where micropores are filled with water and macropores are filled with air (Castellano et al.

2010). This dynamic hybrid-condition allows both oxidative and reductive processes to take place. When WFPS is between roughly 50% and 60%, N_2O emissions are thought to predominantly be the result of nitrification, whereas when WFPS is greater than 60%, N_2O emissions are thought to begin to occur predominantly as a result of denitrification (Bouwman 1998; Davidson et al. 2000).

N_2O emissions measured from soils in different land use settings have been variable. For instance, native grasslands and wheat fields have been shown to have N_2O emissions of less than 4 $\mu g\ m^{-2}\ h^{-1}$ with peaks of 15 $\mu g\ m^{-2}\ h^{-1}$ and 19 $\mu g\ m^{-2}\ h^{-1}$ during winter measurements due to freeze and thaw events (Kaye et al. 2004). Lawns have shown N_2O emissions less than 10 $\mu g\ m^{-2}\ h^{-1}$ with peaks of greater than 60 after fertilization (Livesley et al. 2010). In one of the few studies that quantified emissions of N_2O in bioretention cells, Grover el al. (2013) found that the soil media in bioretention cells was a source of N_2O overall, with average emissions over the course of one year between of 13.8 $\mu g\ m^{-2}\ h^{-1}$ and 65.6 $\mu g\ m^{-2}\ h^{-1}$. The soil media profile included sandy loam, 80% sandy loam with10% compost, and 10% hardwood mulch and contained a 0.2 m (0.656 ft) internal water storage zone (Grover et al. 2013)

Soil depth is another factor in nitrification and denitrification due to the greater availability of carbon in topsoil (Conrad 1996; Senbayram et al. 2012; Vilain et al. 2014). For instance, Vilain et al. (2014) found that nitrous oxide emissions via denitrification were significantly greater in topsoils (10 – 30 cm) as opposed to subsoils (90-110 cm). Plants also release low molecular weight organic compounds into the soil via their root systems which denitrifiers and nitrate ammonifiers (bacteria that sequentially reduce

nitrate to ammonium) are thought to compete for (Mengis et al. 1997; Thomson et al. 2012). This helps explain why nitrous oxide rates are often positively correlated with soluble organic carbon content (Del Grosso and Parton 2012).

2.4.1.2. Nitrous Oxide Uptake

Although most soils act as a net source of N_2O emissions, uptake or consumption has also been observed (Butterbach-Bahl et al. 2013; Chapuis-Lardy et al. 2007; Conrad 1996; Schlesinger 2013). The term "uptake" describes both the flux of a gas from the atmosphere to the soil, as well as the transformation of one gas to another (i.e., N_2O reduction to N_2 via reduction) (Chapuis-Lardy et al. 2007). N_2O uptake is thought to occur predominantly as a result of denitrification, where heterotrophic bacteria utilize nitrogen oxides as an energy source, and terminal electron acceptor (Chapuis-Lardy et al. 2007; Conrad 1996; Schlesinger 2013). The main sink for N_2O is commonly referred to as N_2OR or nitrous oxide reductase. N_2OR is an enzyme found in denitrifying bacteria and reduces nitrous oxide to nitrogen gas. This enzyme uses copper (Cu) clusters as a catalyst (Thomson et al. 2012). This enzymatic activity is fragile and can be stunted or interrupted by even brief exposures to oxygen and decreases in pH, which likely affects the assembly of N_2OR (Thomson et al. 2012).

Above 80% WFPS, N_2O consumption is predicted to occur via denitrification, with N_2 being the main end product (Bouwman 1998), although field measurements frequently diverge from this model, making it difficult to generalize (Adviento-Borbe et al. 2010; Chapuis-Lardy et al. 2007). For instance, when WFPS was consistently < 60%, Adviento-Borbe et al. (2010) found negative N_2O fluxes in agricultural maize plots. N_2O

consumption typically ranges from 0.01 μg m^{-2} h^{-1} to 10 μg m^{-2} h^{-1} (Adviento-Borbe et al. 2010; Syakila and Kroeze 2011). Abiotic nitrate reduction via chemodenitrification may also be involved in the net consumption of N_2O but these processes are not well understood (Chapuis-Lardy et al. 2007; Schlesinger 2013). There are many factors that are still unknown with regard to the controlling factors on N_2O consumption in soils; consumption has been reported under variable conditions, making it difficult to generalize regarding the particular conditions which lead to N_2O uptake (Chapuis-Lardy et al. 2007).

2.4.2. Methane (CH_4)

Methane is the second most important greenhouse gas (Connor et al. 2010) after carbon dioxide and has caused roughly 20% of the human-induced increase in radiative forcing since 1750 (Kirschke et al. 2013; Nisbet et al. 2014). In the early 2000's methane concentrations seemed to be stabilizing, which was possibly linked to a decrease in, or stabilization of fossil fuel and microbial emissions (Kirschke et al. 2013). After a near decade of no-growth, methane concentrations increased by 8.3 +/- 0.6 ppb from 2007 to 2008, with the largest increase occurring in the tropics (Nisbet et al. 2014). High temperatures in the artic, increased precipitation in the tropics (Dlugokencky et al. 2009), increased emissions from wetlands spurred by high temperatures in northern high latitudes in 2007, and fossil fuel burning, (Kirschke et al. 2013) have been listed as possible causes, but relative contributions are uncertain.

In 2010, methane concentrations reached 1,799 ± 2 ppb (Kirschke et al. 2013). The recent increase in methane emissions spurred important questions about global

causes, but in-situ monitoring is very limited. The sources and sinks for methane are complex, vary with latitude (Nisbet et al. 2014), and depend on soil organic matter content, temperature, soil moisture and populations of methanotrophic and methanogenic soil microorganisms (Harriss et al. 1982; Nesbit and Breitenbeck 1992; Steudler et al. 1989). With a relatively short lifetime of 10 years in the atmosphere, there are opportunities to make a meaningful impact in reducing CH_4 emissions. By developing a better understanding of the conditions that results in emissions and/or uptake of CH_4 from bioretention, and the size of those fluxes, we can reduce emissions in the future.

2.4.2.1. Methane Emissions

Methanogens, or methane producing bacteria, and methanotrophs, or methane using bacteria, are ubiquitous in soil (Nesbit and Breitenbeck 1992). Methanogenic bacteria form methane as the major product of their metabolism. They are strict anaerobes and obtain energy from H_2 and CO_2, formate (HCO_2^-), acetate ($C_3H_2O_3^-$), methanol (CH_3OH), trimethylamine ($N(CH_3)_3$), dimethylsulfide ($(CH_3)_2S$) and some small alcohols (Nesbit and Breitenbeck 1992; Whitman et al. 2006). Methanogenic bacteria prefer temperatures of more than 35 °C (95 ^{o} F) whereas methanotrophs prefer cooler temperatures (Higgins et al. 1981). When incubation temperatures were increased to 40°C (104 ^{o}F), Nesbit and Breitenbeck (1992) found that methane uptake was substantially reduced in both cultivated and non-cultivated soils.

Roughly 60% of global methane emissions are anthropogenic, with the remaining 40% coming from natural sources (Kirschke et al. 2013; Nisbet et al. 2014; Rhoderick and Dorko 2004; Steudler et al. 1989). Estimates of CH_4 emissions vary

widely. Some broad sources of CH_4 include wetlands, natural gas, thawing permafrost, and disturbance of methane hydrates (Nisbet et al. 2014). Methane emissions can be grouped into three categories: thermogenic, pyrogenic, and biogenic (Kirschke et al. 2013). Thermogenic sources include geologic pools of methane which become vented to the surface during coal, oil and natural gas exploration and extraction. Pyrogenic sources include the incomplete combustion of biomass in wildfires, fossil fuels and biomass production (Kirschke et al. 2013). Biogenic sources of methane include methanogens which require anaerobic conditions. Examples of places that encounter such conditions are wetlands, rice paddies, dams, and digestive systems, organic wastes such as manure, sewage and landfills (Kirschke et al. 2013).

2.4.2.2. Methane Uptake

The primary global sink for atmospheric CH_4 is oxidation by hydroxyl radicals (OH), mostly in the troposphere, which accounts for around 90% of the global CH_4 sink (Kirschke et al. 2013). In an aerobic environment, certain soil bacteria can also use atmospheric methane as an energy source, making them an important global sink (Kaye et al. 2004). Current research suggests that methanotrophic bacteria in aerated soils account for approximately 4% of the global methane sink (Kirschke et al. 2013), although CH_4 uptake values from field studies vary widely (Harriss et al. 1982; Higgins et al. 1981; Keller et al. 1986; Steudler et al. 1989). In aerobic soils, methane uptake between 25 to 45 $\mu g\ m^{-2}\ h^{-1}$ has been shown in grasslands, with highs of 55 $\mu g\ m^{-2}\ h^{-1}$ during soil drying conditions (Kaye et al. 2004). When the water table drops enough to expose soils which had been previously saturated, methane consumption rates in wetland soils have

been shown to be as high as 100 μg CH_4 m^{-2} hr^{-1} (Le Mer and Roger 2001). The highest consumption rates of methane in soils are thought to be where methanogenesis was recently producing higher concentrations than the atmosphere (Le Mer and Roger 2001), such as in recently drained or intermittently flooded soils (Nesbit and Breitenbeck 1992).

Methanotrophs are sensitive to water stress (i.e., saturation) and are thought to be more successful at soil depths where moisture levels are more stable. Consumption often occurs between the A and B horizons (Conrad 1996). Nesbit and Breitenbeck (1992) found that adjusting soil water contents between 25% of pore volume (860-1260 kPa) and 75% (30-74 kPa) did not significantly affect the rate of CH_4 consumption by methanotrophs, however, increasing soil water to 100% of pore volume, reduced initial activity by an average of 56%. The predominance of CH_4 consumption at a greater soil depth may also be linked to the higher concentrations of NH_4^+ in surface soil layers, which can serve as an inhibitor of CH_4 oxidation (Nesbit and Breitenbeck 1992).

In bioretention cells, Grover et al. (2013) found both a sandy loam, and 80% sandy loam with10% compost and 10% hardwood mulch to usually be a sink for CH_4, with average uptake rates of between 4.2 μg m^{-2} h^{-1} and16.4 μg m^{-2} h^{-1}. Large peaks in CH_4 emissions were observed on occasion (~200 μg m^{-2} h^{-1}) (Grover et al. 2013).

2.4.3. Carbon Dioxide (CO_2)

Soil organisms and plant roots release CO_2 during microbial and root respiration (Mith et al. 2003). Soil respiration is thought to emit between 10 and 15 times more CO_2 than the burning of fossil fuels (Mith et al. 2003), and is the second largest terrestrial carbon flux (Bond-Lamberty and Thomson 2010). Soils store at least twice the amount of

CO_2 that is in the atmosphere, which makes them an important global sink (Bond-Lamberty and Thomson 2010).

Global circulation models (GCMs) have indicated that rising temperatures as a result of climate change may accelerate the decomposition of soil carbon through microbial respiration, however there is also evidence that respiration may be independent of mean annual temperatures (Giardina and Ryan 2000). Soil moisture, which enhances decomposition and mineralization (Brady and Weil 2008; Davis and Cornwell 1998; Van Meeteren et al. 2007), and vegetative productivity may also influence soil respiration (Bond-Lamberty and Thomson 2010). There is high spatial and temporal variability in soil respiration, and research that investigates the influencing factors in local soil conditions can ultimately help refine global models.

Smart and Peñuelas (2005) found that a spike in CO_2 emissions from soils occurred after a simulated precipitation event, resulting from the displacement of soil pore gases by water. CO_2 levels returned to pre-precipitation levels approximately 4 hours later. The authors also suggested that fine rooted vegetation may have alloted more belowground carbon via rhizodeposition than larger woody roots, providing more substrate for respiration and higher CO_2 emissions (Smart and Peñuelas 2005). Adviento-Borbe et al. (2010) found that CO_2 soil emissions ranged from 11 to 1015 mg CO_2 m^{-2} h ^{1} in agricultural experiments. Qiu et al. (2005) investigated the role of leaf litter decomposition on microbial respiration, and found that leaf litter and increased temperature increased CO_2 emissions, with CO_2 emissions ranging from 175 to 365 mg m^{-2} h^{-1}.

2.5. Research Goals and Hypotheses

The broad goals of this research are to (1) provide a feasible monitoring infrastructure design that can be adapted for other locations to monitor stormwater and bioretention performance; (2) better understand the factors controlling build-up and wash-off of stormwater pollutants from small paved road watersheds, and to predict the mass load of various constituents, as a function of precipitation depth; (3) predict how certain design features (i.e., vegetation and soil media) influence pollutant removal in bioretention systems; (4) assess how the soil media types presented here would perform under changing precipitation scenarios projected to affect the Northeastern U.S.; and (5) evaluate how these design features contribute to GHG emissions or uptake. The broad hypotheses in this research are as follows:

1) Labile pollutant constituents will exhibit a higher MFF effect than non-labile constituents.
2) A bioretention vegetation palette with numerous species and variable root depths will remove more nutrients and sediment than one with fewer species and deep roots.
3) Bioretention soil media that includes reactive cations will remove more labile P than a conventional sand-based bioretention soil mixture.
4) Increased precipitation and runoff will decrease nutrient and sediment retention by bioretention.
5) Increased precipitation and runoff will increase the production of N_2O and CH_4, and decrease the production of CO_2 within bioretention cells.

CHAPTER 3: MONITORING METHODS AND DESIGNS FOR EVALUATING BIORETENTION PERFORMANCE

Amanda. L. Cording

Keywords: Stormwater, Bioretention, Monitoring Methods, Construction, Hydrograph

Abstract

Bioretention systems provide exciting opportunities to remove harmful pollutants from stormwater, but there are still many unknowns regarding their strengths and limitations. Monitoring can provide vital feedback to design engineers, ultimately helping to improve hydrologic and pollutant removal performance, lower costs, and determine long-term effectiveness and maintenance requirements, yet there are very few bioretention systems that have been monitored in the field. The goal of this research is to reduce the barriers to monitoring bioretention, by providing a detailed account of the inflow and outflow monitoring system infrastructure installed at the University of Vermont Bioretention Laboratory, which can be adapted to achieve monitoring goals in other settings. Ninety-degree v-notch and compound weirs equipped with differential pressure transducer probes were used, in the inflow and outflow, respectively, to relate water height to flow rate for eight bioretention cells. This allowed for the conversion of pollutant concentration to mass for each water sample. Monitoring was time-based, with discrete samples taken in rapid succession to span the inflow and outflow hydrographs. This ultimately allowed for the calculation of pollutant mass removal on an equal volume basis.

3.1. Introduction

Stormwater runoff contributes to eutrophication (U.S. Environmental Protection Agency 2008), which is the most prevalent global water quality impairment (The United Nations 2015). The cost of freshwater eutrophication in the U.S. is estimated at $2.2 billion per year (Dodds et al. 2009). Biological retention, or "bioretention," is a stormwater management technique that is currently being encouraged as a Best

Management Practice (BMP) by federal regulators, as a part of the National Pollution Discharge Elimination System (NPDES) program (National Research Council 2008). The NPDES program is under the umbrella of the Clean Water Act (CWA) and is the primary vehicle through which the federal government regulates the quality of the nation's waterbodies (National Research Council 2008). Despite being widely promoted, and required in some instances, there are still many unknowns regarding the strengths, limitations, and resiliency of bioretention systems (Lefevre et al. 2015; Mangangka et al. 2014).

Bioretention systems, also known as rain gardens (Davis 2008; Dietz and Clausen 2006; Hunt et al. 2008), biofilters (Zinger et al. 2013), and bioswales (Collins et al. 2010), are largely composed of soil media and vegetation that are intended to remove stormwater pollutants while also retaining and detaining stormwater volumes and reducing peak runoff velocities to more closely mimic pre-development hydrology (Lefevre et al. 2015). Bioretention systems are one type of physical practice listed within the broader category of alternative stormwater infrastructure termed Green Stormwater Infrastructure (GSI) (Nylen and Kiparsky 2015; Palmer 2012) or Water Sensitive Urban Design (WSUD) (Alias et al. 2014; Blecken et al. 2009; Taylor and Wong 2002; Wong 2006) which falls under the broader alternative approach to traditional land development called Low Impact Development (LID) (Brown and Hunt 2011; Dietz 2007).

Inside and outside the regulatory sphere, these techniques are becoming increasingly popular, with residents and developers expressing an interest in these aesthetically pleasing, eco-friendly alternatives to traditional stormwater treatment

systems (Collins et al. 2010; Henderson et al. 2007; Stone 2013). The presence of bioretention systems in a landscape also provides an opportunity to engage the community in a dialogue about water resources and natural water filtering processes, while improving habitat, and encouraging the use of native and pollinator friendly plants (Hurley and Forman 2011).

However, the installation of these systems is outpacing the research regarding the comparative effectiveness of specific design features in achieving the goals of bioretention (Law et al. 2008), which include (a) reduced stormwater volume, (b) reduced and attenuated peak flow rate, (c) reduction in targeted pollutants, (d) improved aesthetics and, (e) environmental sustainability (Davis et al. 2009). Of the limited number of bioretention systems that have been monitored, many have shown inconsistent performance (Davis et al. 2009; Dietz 2007; Geosyntec Consultants and Wright Water Engineers 2012; Lefevre et al. 2015).

Some of the many design features that affect the pollutant removal performance of bioretention and other GSI systems include: residence time (Collins et al. 2010; Hurley and Forman 2011; Kadlec et al. 2010; Rosenquist et al. 2010);media depth (Brown and Hunt 2011); vegetation type, root depth, and root architecture (Claassen and Young 2010; Claytor and Schueler 1996; Collins et al. 2010; Davidson et al. 2000; Davis et al. 2009; Kadlec et al. 2010; Lucas and Greenway 2008; Read et al. 2008); organic matter content (Bratieres et al. 2008; DeBusk and Wynn 2011; Fassman et al. 2013; Leytem and Bjorneberg 2009; Thompson et al. 2008); use of mulch (Bratieres et al. 2008; DeBusk et al. 2011; Dietz and Clausen 2006); percent sand, silt, and clay (Liu et al. 2014); chemical

characteristics of the soil media (e.g., amount of iron, calcium, and aluminum) (Arias et al. 2001; Groenenberg et al. 2013; Vance et al. 2003); ponding depth, hydraulic conductivity, infiltration rate (Thompson et al. 2008); and the inclusion of features such as internal water storage zones (IWS) (Chen et al. 2013; Dietz and Clausen 2006; Hunt et al. 2006; Kim et al. 2003). Operation and maintenance and care taken during construction to avoid soil compaction are also critical factors that will affect the long term performance of these systems (Brown and Hunt 2011; Dietz and Clausen 2006).

Monitoring can provide vital feedback to design engineers, ultimately helping to improve performance, lower costs, and determine long-term effectiveness and maintenance requirements of these systems (Lenth et al. 2008). There are very few detailed examples of bioretention monitoring infrastructure, and virtually no guidelines as to how the infrastructure can be incorporated into project designs and placed during bioretention construction, or what considerations are important in developing sampling regimes (Geosyntec Consultants and Wright Water Engineers 2013; Law et al. 2008).

The goal of this chapter is to describe a clear and effective bioretention monitoring approach that is incorporated from project outset. The availability of this information can help reduce the barriers to project monitoring and foster improvements in future bioretention designs. Bioretention monitoring infrastructure used at the University of Vermont (UVM) Bioretention Laboratory, including design considerations and steps taken to install the equipment during construction, will be described. Further, the sampling regime and automated sampling equipment used to capture runoff from small

paved road watersheds, in the context of our research goals, is outlined in detail, to provide a reference for future monitoring projects.

3.2. Site Description

In 2012, the University of Vermont Bioretention Laboratory was constructed on the UVM campus, in Burlington, VT. The research site consists of eight small paved road sub-watersheds (or drainage areas) with areas ranging from 320 ft^2 (29.729 m^2) to 1,293 ft^2 (120.12 m^2). The road is one of the main thoroughfares for bus and vehicular traffic entering and exiting the UVM campus. Sub-watershed boundaries were delineated from the crown of the road to a granite curb at a 45-degree angle, culminating for each bioretention cell at a point that corresponds with a trapezoidal curb-cut into which runoff flows. For each cell, stormwater is directed from the road surface, through the cub-cut, and along a narrow conveyance strip, ranging from 3.72 m^2 to 19.20 m^2, lined with a rubber EPDM membrane, and covered with stone (with diameters ranging from approximately two to four inches (5.08 cm to 10.16 cm)) prior to entering the bioretention cell inflow monitoring equipment.

The eight bioretention cells are rectangular, equally-sized, parallel to the road, and have dimensions of 4 ft. (121.92 cm) wide x 10 ft. (304.80 cm) long x 3 ft. (914.40 cm) deep with approximately 6 inches (15.24 cm) of ponding depth. The cell bottom and sides are lined with a EPDM impermeable rubber liner, and contain an underdrain at one end, which ultimately connects back to the existing storm sewer network. Each of the bioretention cells has monitoring infrastructure at the entrance (inflow) and exit

(outflow), which will be described in further sections. The layout of a typical cell is shown in Figure 3. The bioretention cells used in this research contained two soil profile designs, as shown in Figure 4.

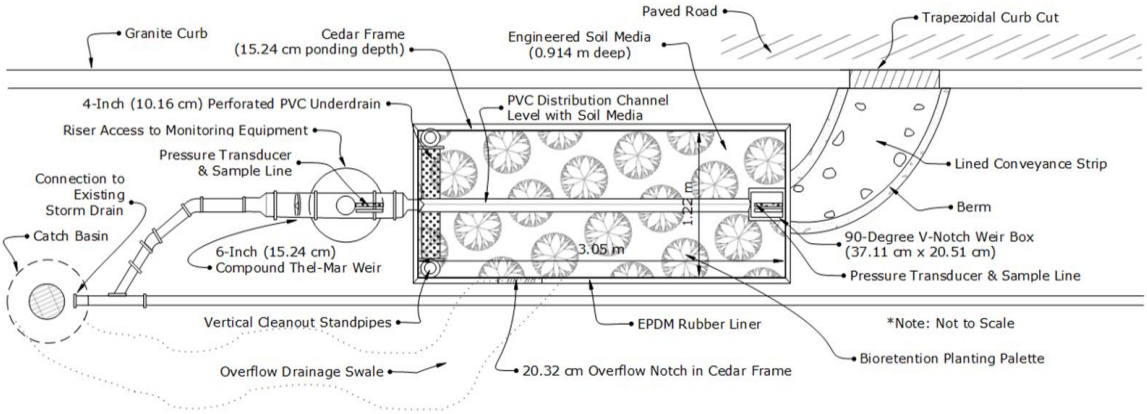

Figure 3. Layout view of a typical bioretention cell at the UVM Bioretention Laboratory.

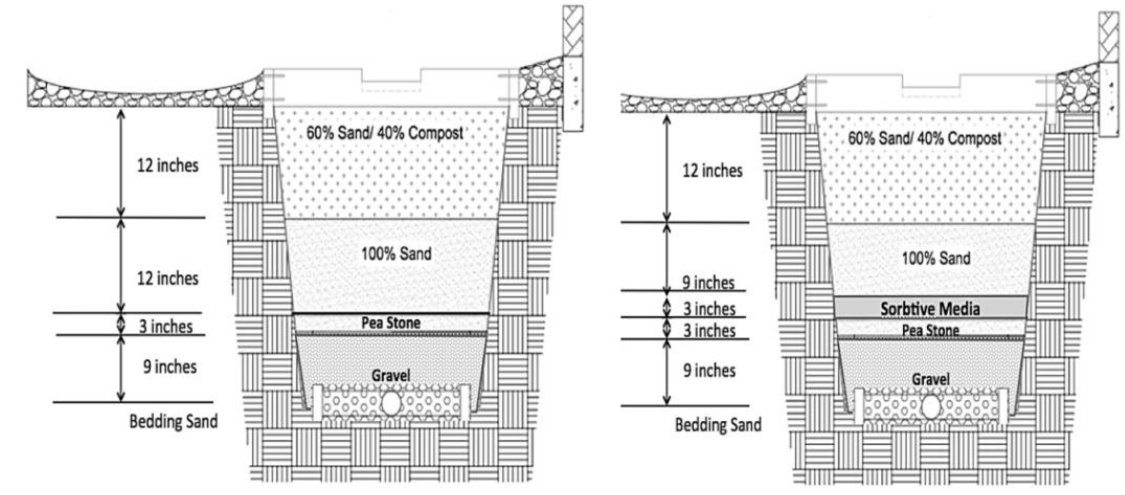

Figure 4. Bioretention Profiles: Conventional Media (left), Sorbtive Media™ (right). Image Credit: J. Schultz, C. Brackett, J. Nummy, O. Lapierre.

3.3. Monitoring Bioretention

The design objectives for the monitoring infrastructure and sampling protocol used in this research were aimed at characterizing stormwater mass loads from small paved road watersheds, at multiple points during the inflow and outflow hydrograph. A hydrograph is a plot of flow rate (Q), or the changing velocity of water, over time (Hornberger et al. 1998). Flow rate is required for the conversion of concentration-based measurements to mass or load (U.S. Environmental Protection Agency 1997), and is particularly useful in numerically describing the erosive and pollutant transport potential of stormwater (Bertrand-Krajewski et al. 1998). Water with increasing velocities can transport increasing particle sizes based on Stokes Law, affecting the proportion of dissolved and particulate pollutants in a given sample (Glysson et al. 2000).

Flow rate is determined by measuring the height of water upstream of a hydraulic control structure, such as a flume (Davis 2007; Hunt et al. 2006) or weir (Hathaway et al. 2012; Hunt et al. 2006; Komlos and Traver 2012; Wemple et al. 2007), that produces a crest of falling water in front of it. The height of water behind the control device can be measured with a pressure transducer (DeBusk and Wynn 2011; Dietz and Clausen 2005; Hunt 2003; Kosmerl 2012) or a bubble flow meter (Davis 2007). The height measurements are used to calculate flow rate using height to discharge tables or equations (U.S. Bureau of Reclamation 2001).

3.3.1. Inflow Monitoring Infrastructure

The incoming stormwater from each sub-watershed on the research site was directed into a small wooden box, constructed of weather resistant cedar boards, equipped

with a 90-degree v-notch weir, hereinafter referred to as a "weir box." A 90-degree v-notch weir is recommended for small flows, with a thickness of between 0.762 mm to 2.03 mm at the notch, to prevent water from clinging to the weir (U.S. Bureau of Reclamation 2001). Weir plates are typically attached to an inflow collection device, which can be made of any material that is non-permeable, long-lasting and largely chemically inert. Concrete is often used for large channels (U.S. Bureau of Reclamation 2001). The weir plates in this research were attached the aforementioned wooden weir box; they were constructed of 0.0625 inch (1.59 mm) thick stainless steel (Tri-Angle Metal Fabricators, Milton, VT). The cedar was easy to work with and provided a simple, cost effective alternative to concrete. The stainless steel weir plates were fitted into a narrow vertical groove cut in the weir box. All seams and points of contact were filled with waterproofing silicone and tested for water tightness throughout each monitoring season. These small devices (Figure 5) were designed to break incoming stormwater into incremental segments that could be sampled in rapid sequence to detect any changes in pollutant mass load over the course of the storm hydrograph.

The average weir box dimensions (n = 8) are 37.11 cm long and 20.51 cm wide (B) (Figure 5-6). The average height to the bottom of the v-notch (P) is 5.58 cm. The height from the v-notch to the max height (H) is 7.62 cm. Maximum capacity is reached (H+P) at 13.20 cm. Approximately 4.25 L (0.150 ft^3 or 0.00425 m^3) are stored beyond the low-point of the notch and 10.05 L (0.3548 ft^3 or 0.01005 m^3) can be held at maximum capacity. Any level over this height was considered an overflow event. The dimensions of each individual weir box are listed in Table 29, in the Appendix.

Figure 5. 90-degree thin plate v-notch weirs (foreground)

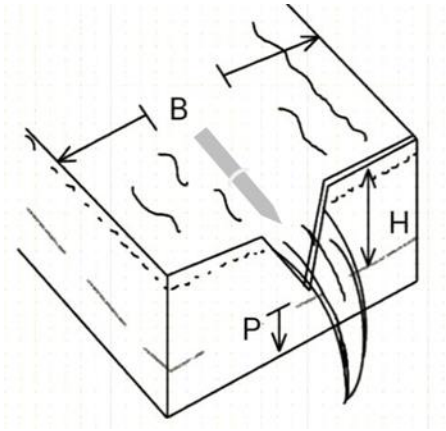

Figure 6. Weir box dimensions reference showing pressure transducer probe (not to scale).

The American Society for Testing and Materials (ASTM) recommendations (D5242) for 90-degree v-notch weirs were used to determine the weir dimensions, with modifications being made where necessary, to achieve the monitoring goals of this study. The ASTM weir guidelines were developed for large pipes and channels, such as streams or wastewater conveyance systems, which transmit water with discharges between 0.05 and 4 cfs (0.001 m^3 to 0.1 m^3) (U.S. Bureau of Reclamation 2001). By contrast, the peak flow rates and runoff volumes expected from the small drainage areas on the UVM research site constrained the weir box sizing, but were ideal for detecting small changes

in stormwater quality. In the following section, some of the key design considerations for the inflow weir boxes will be discussed in further detail.

3.3.1.1. Design Considerations

The water that flows over the notch, in a v-notch weir, needs to pitch freely for a given distance (P), in order to create an air filled nappe under the flow (U.S. Bureau of Reclamation 2001). The minimum recommended distance for (P), is 3.6 inches (9.14 cm) (Figure 6). In this research, (P) on the box itself was 5.58 cm, yet the total distance the water had to freefall was 12.08 cm, due to the presence of a distribution trench under the crest of the falling water.

In order to evenly distribute water longitudinally across the bioretention cells, and avoid scouring effects that are commonly observed at the entrance to bioretention cells (Claytor and Schueler 1996), a distribution channel was inserted immediately below the weir boxes (Figure 3). This was built by cutting a PVC rain gutter in half lengthwise, drilling perforations within it and, placing it in the top of the soil media such that the gutter's side walls were level with the top surface. The depth of the distribution channel was 6.50 cm.

The height of the water inside the inflow weir box was measured with a Teledyne™ ISCO 720 differential pressure transducer, which was compatible with the Teledyne 6700 series automated samplers used in this study. The pressure transducer accurately measures water levels between 0.1 ft (3.048 cm) and 10.0 ft of (304.8 cm), when temperatures are between 32 ^{o}F and 120 ^{o}F, with a minimum sensitivity of 0.01 ft (0.3048 cm) (Teledyne ISCO 2012). The automated sampling equipment was

programmed to begin only when the water height reached a minimum of 0.21 ft (6.50 cm) above the bottom of the weir box, in order to avoid any potential under or over estimations of flow rate (Harmel et al. 2002). This threshold was equivalent to 0.03 ft (0.914 cm) from the v-notch, which is the location from which the pressure transducer measures the baseline water height (Harmel et al. 2002).

3.3.1.2. Developing a Rating Curve

The height of water behind the weir is often related to discharge, or flow rate, using height to discharge tables, or a version of the Kindsvater-Shen equation (Kulin and Compton, 1975) (Equation 1).

$$Q = 4.28\, C \tan\left(\frac{\Theta}{2}\right)(h + K)^{\frac{5}{2}} \quad (1)$$

Where,
Q is the discharge or flow rate over the weir (cfs)
C is the effective discharge coefficient
Θ is the notch angle
h is the head over the notch in the weir (ft)
k is the head correction factor (ft)

The empirical constants used to determine flow rate in Equation 1 (i.e., C and K) were developed for large volumes and are highly influenced by the weir geometry. In this research, each weir was, therefore, individually rated, or evaluated, to determine the appropriate discharge equation (U.S. Bureau of Reclamation 2001). In studies where storm flows are expected to be large and weir geometry is in accordance with standard ASTM weir guidelines, this step may not be necessary.

A rating curve, or stage-to-discharge graph, was developed manually for each weir by taking simultaneous water level and volumetric measurements over time, in the

lab (U.S. Bureau of Reclamation 2001). The pressure transducer probe and sample line were placed in the weir box to keep the displacement factor equal to what would be experienced in the field. The weir box was filled with water until it overflowed, then allowed to stabilize, forming a meniscus at the bottom of the notch (Davis and Cornwell 1998). The water level was recorded as 0.00 ft in the autosampler software, to establish a baseline from which the pressure transducer would measure height (Harmel et al. 2003). The inflow flow rate was gradually increased until the water reached and maintained a specified height above the notch. A minimum of five timed volumetric measurements were taken at five different water heights, spanning the low and high flow thresholds on the weir. The average of the five measurements at each water height was used to determine the discharge at that height. This process was repeated for each of the eight weirs. Equation 2 was used to determine the values of the weir coefficient (C) and (n). The logarithmic form of this equation (Log (Q) = *n** log (H) + log (C)) has the linear form of Y = mx + b, which allowed the values of (C) and (n) to be obtained by plotting the value of (Q) and (H) on a log-log plot.

$$Q=CH^n \tag{2}$$

Where,
Q is the flow rate over the weir (ft^3s^{-1})
C is the coefficient of discharge, or weir coefficient
H is the depth of water (head) behind the weir (ft)
n is an empirical exponent (dimensionless)

The equation of the line provided the values for n (slope) and C (y-intercept). The rules of log were employed to convert log (C) to C. The discharge equations for the eight weirs are shown in Table 28, in the Appendix.

3.3.2. Sampling the Inflow Hydrograph

The goal in any water quality monitoring program is to collect samples that encompass the spatial and temporal variability of the site conditions (Harmel et al. 2003). When designing bioretention systems for the purpose of monitoring, the overall research questions, bioretention drainage configuration, final reportable units (e.g., concentration or mass), hydraulic conductivity, specific yield of the bioretention soil media, local rules and regulations, budgetary and logistical constraints, and proximity to underground utilities are important considerations (Law et al. 2008).

There are many different methods to sample stormwater, with time-based and flow-based sampling being the two most commonly used (Harmel et al. 2003). Time-based sampling is most appropriate for research in small watersheds, where land cover is fairly homogeneous (Harmel et al. 2003; Sansalone and Cristina 2004). Such conditions will produce a hydrograph that can be sampled with equally spaced samples over its rising limb, peak, and falling limb in an ideal storm (Alias et al. 2014; Harmel et al. 2003). Alternatively, flow-based sampling allows for samples to be taken after a specified volume of water has passed (Law et al. 2008) and is more robust to changing precipitation intensities over time, and when site conditions are likely to alter flow rates, such as those which contain irregular surfaces, diverse land use, or when drainage areas are larger in size (Harmel et al. 2003).

In this research, discrete, time-based samples were collected at multiple locations throughout the runoff hydrograph, from small, paved, road sub-watersheds. The timing of inflow samples was based on estimates of peak inflow discharge rates for the

eight watersheds, which were determined using the time of concentration, rainfall intensity duration frequency (IDF), curves and the rational method, which are described in the following sections. These values were then used to determine the length of time required to take representative samples at multiple intervals throughout an idealized hydrograph. The sub-watersheds in this study were modeled as homogeneous paved road surfaces, using a runoff coefficient for paved asphalt.

3.3.2.1. Time of Concentration

The Time of Concentration (T_c) estimates how long it will take a drop of water to travel from the most hydrologically remote part of the watershed, to the monitoring location, using the runoff coefficient, total distance, and slope as the main variables, as shown in Equation 3 (Kang et al. 2008; King et al. 2005). The distance from the farthest corner of the largest watershed to the monitoring device, in this research was approximately 104 ft (31.7 m). A runoff coefficient of 0.95 for impervious asphalt (Allen Burton and Pitt 2002) and a slope value of 0.01 ft/ft were used to approximate the time of concentration. The time of concentrations from the smallest to largest watersheds ranged from 4.73 minutes to 8.27 minutes. The Tc value was then used to determine the approximate rainfall intensity, using a rainfall IDF curve, and the rational method.

$$Tc = \frac{G\ (1.1 - C)L^{0.5}}{(100\ S)^{1/3}} \quad (3)$$

Where,
T_c is the time of concentration (min)
G is equal to 1.8 (FAA method, constant)
C is the runoff coefficient using the rational method (dimensionless)
L is the longest distance from the fixed location within the watershed (ft)
S is the slope of the watershed (ft ft^{-1}or m m^{-1})

3.3.2.2. Estimating Peak Discharge with Intensity Duration Frequency (IDF) Curves

Rainfall IDF curves depict the relationship between precipitation intensity and duration, given a selected frequency of return for a specific climatic region (Claytor and Schueler 1996; Davis and Cornwell 1998). In this research, a rainfall IDF curve for Chittenden County, Vermont was used (Figure 7), with a 1-year recurrence interval, from 5 minutes to 120 minutes (Northeast Regional Climate Center Precipitation Data). The rainfall intensities, which corresponded with the time of concentrations from each sub-watershed, ranged from approximately 3.32 in hr^{-1} (2.34 x 10^{-5} m s^{-1}) to 2.57 in hr^{-1} (1.81 x 10^{-5} m s^{-1}). The rainfall intensity for each watershed was used to estimate peak discharge with the rational method, as shown in Equation 4.

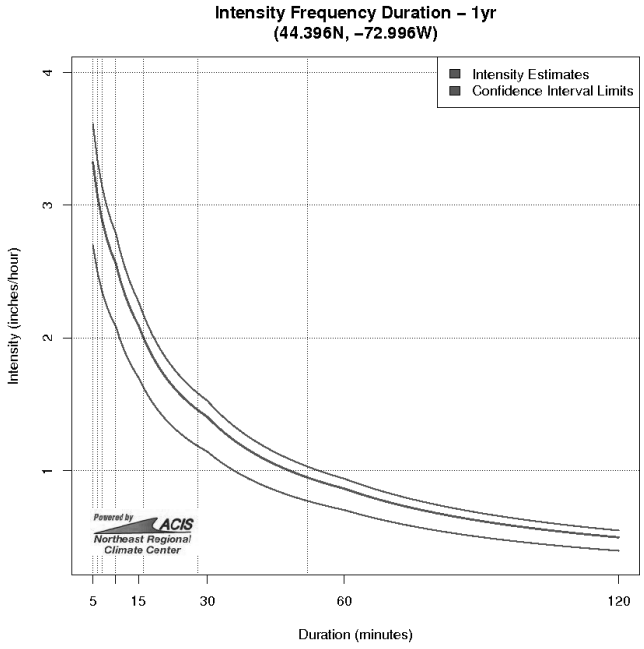

Figure 7. Rainfall Frequency Intensity Duration Curve for Chittenden County, VT.

$$Q = C_f * C_i * A \quad (4)$$

Where,
Q is the peak discharge ($ft^3 s^{-1}$ or $m^3 s^{-1}$)
C_f is the runoff coefficient (dimensionless)
C_i is the rainfall intensity ($ft\ s^{-1}$ or $m\ s^{-1}$)
A is the drainage area (ft^2 or m^2)

The rational method is most appropriate for small watersheds, which are highly impervious (Natural Resources Conservation Service 1986). The assumptions of the rational method are as follows: (a) peak flow rate is a direct function of the drainage area and average rainfall intensity during the time of concentration, (b) rainfall is uniformly distributed over the paved road sub-watersheds, (c) rainfall intensity remains constant during the time of concentration, and (d) the runoff coefficient is constant and consistent throughout the sub-watersheds (Natural Resources Conservation Service 1986).

The peak flow rate occurs when the total watershed area is contributing runoff (Davis and Cornwell 1998). The peak flow rate values were used to estimate the total length of time needed to sample a specific rainfall depth (Equation 5).

$$Time = \frac{watershed\ area\ x\ rainfall\ depth}{peak\ flow\ rate} \quad (5)$$

The rainfall depth selected was 0.90 inches (0.0229 m), which is a common water quality volume to be treated with stormwater best management practices (Vermont Agency of Natural Resources 2002b).

3.3.2.3. Monitoring Duration for the Inflow Hydrograph

The time for the peak flow rate to reach the monitoring equipment in the eight sub-watersheds on this research site were between approximately 17 and 21 minutes. A

multiplier of two was applied to the time, in order to account for the falling limb of the hydrograph (Table 30, Appendix). A larger multiplier may be warranted if the assumptions used to determine the peak flow rate cannot be fully met.

The Teledyne ISCO 6700 series automated samplers can hold a maximum of twenty four 1-L bottles. To encompass the inflow hydrograph, the inflow samples from each cell were taken every two minutes for 48 minutes (n = 24), when inflow flow rates were consistently above the minimum sampling threshold of 0.21 ft (6.50 cm). If the inflow flow rate dropped below the minimum threshold, sampling stopped, and resumed if levels rose again, until all 24 bottles were filled. An example inflow hydrograph from the site is shown in Figure 8.

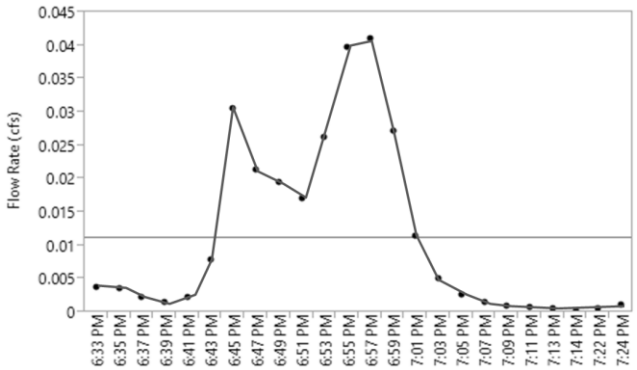

Figure 8. Example inflow hydrograph, showing samples (n=24) taken from watershed 6, 7/3/14.

3.3.3. Outflow Monitoring Infrastructure

Outflow monitoring from bioretention can be difficult, given the subterranean infrastructure requirements of sampling from systems that contain under drains. A few of the systems which can be used to monitor the subsurface of bioretention cells include observation wells or piezometers with pressure transducers (DeBusk and Wynn 2011; Kosmerl 2012), lysimeters (Komlos and Traver 2012), collection chambers with a pump

(Dietz and Clausen 2005), and in-pipe weir systems combined with pressure transducers or bubble flow meters (Davis 2007; DeBusk and Wynn 2011; Roseen et al. 2009).

Although infiltration is often a goal in bioretention projects, in this research, the native subsoil material was non-homogeneous construction fill with a thick clay layer underneath. Shallow depth to groundwater was also a concern. Given these site constraints, and our interest in developing water and nutrient budgets, the cells were enveloped with EPDM rubber liners, which enclosed the bottom and sides of the cells, and the lower horizon of the bioretention cells were equipped with underdrains, which flowed into our outflow monitoring sampling systems and ultimately connected to the existing storm drainage network. A profile view of the outflow monitoring infrastructure is shown in Figure 9.

At the outflow of each bioretention cell, a Thel-Mar™ compound weir was installed at one end of a 6-inch diameter PVC pipe and connected to a 6-inch PVC tee-pipe, which allowed access to the pressure transducer and sample line. A reducer pipe was used to create a shallow sidewall, behind which water pooled enough to take a sample. The 4-inch pipe from the monitoring section was connected to the perforated underdrain at the far end of each cell. In this configuration, the depth of standing water at the weir notch inside the outflow horizontal monitoring pipe was approximately 1.60 inches (4.064 cm), holding a volume of 1.54 L. The sampling tube diameter was 0.550 inches (1.40 cm).

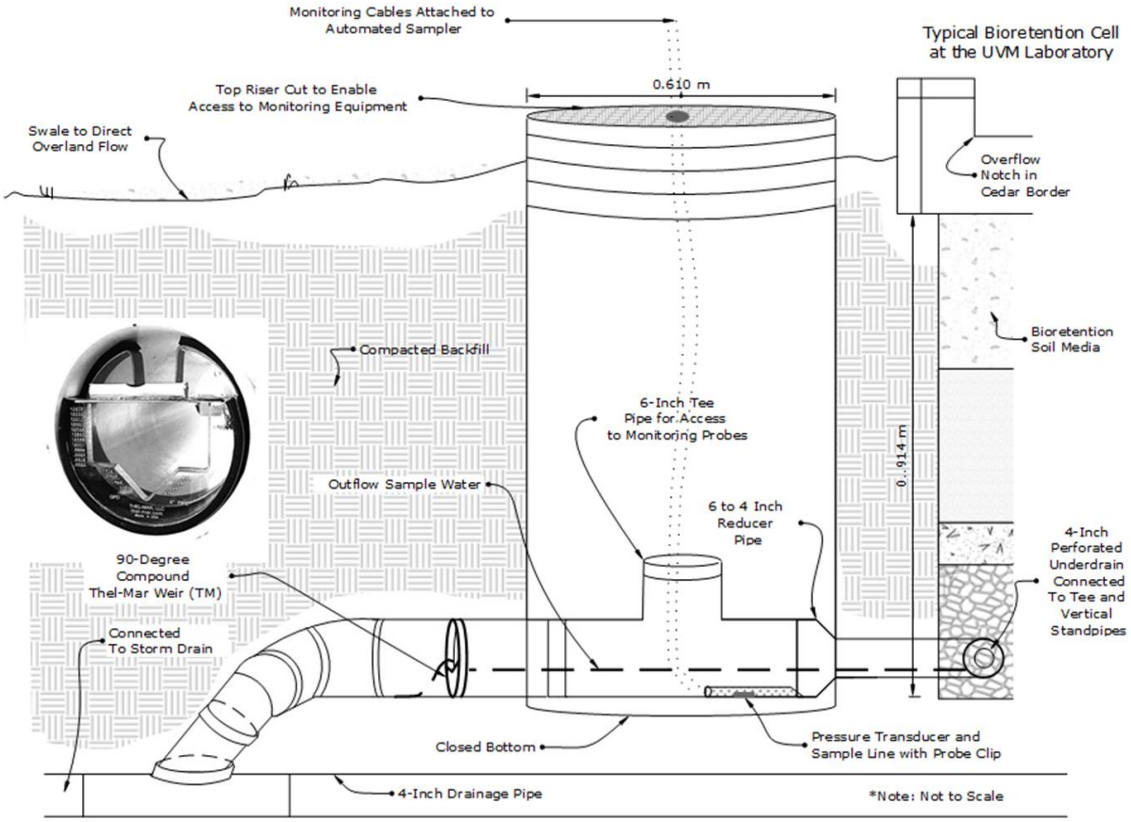

Figure 9. Outflow sampling design profile.

The type of strainer that is typically used over the ISCO autosampler suction tube was too big to fit in the outflow sampling area, but was not warranted, for large sediment was not present in the outflow water from the bioretention cells. The monitoring infrastructure was accessed via the 24-inch (0.61-meter) cylindrical riser, which allowed for access to the outflow so that the suction tube and pressure transducer to be clipped into place at the bottom of the sample area in order to ensure the consistent accuracy of head measurements during high flow rates. The probe clip in this design is located on the bottom of the t-pipe, back just far enough that it required an individual to enter the sump area, in order to clip the probe and suction line into place, to ensure that water height

measurements were taken at a minimum of 3-4 times the maximum expected height of water above the weir notch (U.S. Bureau of Reclamation 2001). Other designs might be able to eliminate the need to manually install the probe by using a long tool, if the probe clip could be placed directly underneath the access manhole cover.

This outflow bioretention monitoring infrastructure accurately captured flow rates between 0.0001 cfs and 0.0170 cfs (0.0028 L s^{-1} and 0.4814 L s^{-1}). This range adequately encompassed the outflow flow rates experienced in the field in most cases, with low flows being more difficult to capture than high flows. The outflow weir equation was developed from the table of level to discharge values provided by the Thel-Mar company (Equation 6).

$$Q=3.416646 * H^{2.5515} \quad (6)$$

Where,
Q is the flow rate (ft^3 s^{-1})
H is the height or level of water behind the weir (ft)

3.3.4. Sampling the Outflow Hydrograph

Sampling the effluent from bioretention requires a number of considerations. For instance, reduction of stormwater volume by bioretention has been shown to be as high as 90% (DeBusk and Wynn 2011; Hunt et al. 2008), which can limit the number and volume of outflow samples collected. DeBusk and Wynn (2011) collected outflow samples from a perforated underdrain, above a clay layer installed to decrease groundwater infiltration, and, of the 28 storm events (DeBusk and Wynn 2011), only five outflow samples could be collected. In bioretention systems designed to infiltrate into surrounding soils, outflow volumes will be affected by the internal soil water holding

capacity, and the characteristics of the surrounding soil media (e.g., water holding capacity and hydraulic conductivity) (DeBusk and Wynn 2011; Dietz 2007; Michigan Department of Environmental Quality 2008). For instance, Brown and Hunt (2011) found approximately 39% of runoff exfiltrated from loamy-sand soils at a depth of 2.95 ft (0.90 m).

In lined bioretention systems that do not have any infiltration to surrounding soils or to groundwater, the total volume exiting the system is largely a function of the storm volume and the internal water holding capacity of the soil media. Vegetated bioretention systems can also result in reduced volume in the soil matrix between storm events due to evapotranspiration (DeBusk and Wynn 2011).

3.3.4.1. Estimating Hydraulic Conductivity

The lined bioretention cells in this research did not have any infiltration to groundwater or surrounding soils. The outflow sampling regime was time-based, and estimated using the mean vertical and horizontal hydraulic conductivity of the bioretention cell, (Freeze and Cherry 1979; Hornberger et al. 1998), using Equation 7.

$$K_z = \frac{D}{\sum_{i=1}^{n} \frac{d_i}{k_i}} \quad (7)$$

Where,
K_z is the equivalent hydraulic conductivity for the layered system (ft s^{-1} or m s^{-1})
D is the total cumulative depth of the layers (ft or m)
d_i is the depth of a given layer (ft or m)
k_i is the hydraulic conductivity of a given layer (ft s^{-1} or m s^{-1})

Equation 7 assumes that flow is vertical, and directed from low to high conductivities in an unsaturated media. In systems that are transversely isotropic, having regions of lower hydraulic conductivity or relative impermeability (e.g., a liner or clay layer), horizontal flow along the X-plane may ensue (Freeze and Cherry 1979). In which case, the horizontal hydraulic conductivity of the media at that location will need to be considered (Equation 8).

$$K_x = \sum_{i=1}^{n} \frac{K_i d_i}{d} \quad (8)$$

Where,
K_x is the horizontal hydraulic conductivity (ft s^{-1} or m s^{-1})
d_i is the depth of a given layer (ft or m)
K_i is the hydraulic conductivity of a given layer (ft s^{-1} or m s^{-1})
d is the horizontal distance of the given layer (m)

In the bioretention cells used at the UVM Laboratory, the mean vertical hydraulic conductivity was estimated to be approximately 3.64 x 10^{-4} m s^{-1} (131.04 cm hr^{-1} or 51.59 in hr^{-1}). This estimation is similar to the infiltration rates found by Thompson et al. (2008) for sand and compost mixes (150 to 178 cm hr^{-1}), but is much higher than the minimum recommended rate of 2.54 cm hr^{-1} (Davis et al. 2009; Washington State University Pierce County Extension 2012). A table containing the estimated hydraulic conductivity of each soil media layer in the bioretention cells in this research is listed in Table 2. The influence of vegetation on hydraulic conductivity was not considered in this model and the proprietary media (i.e., Sorbtive Media™), which was used in two of the cells, was modeled as medium sand.

Table 2. Estimating the vertical hydraulic conductivity of the UVM bioretention cells

Bioretention Media	Depth (m)	Hydraulic Conductivity (m/s)	d_i/k_i
Sand and Compost 60:40 Mixture	0.3048	1.50E-04	2.03E+03
Medium Sand	0.3048	6.90E-04	4.42E+02
Pea Gravel	0.0762	6.40E-03	1.19E+01
Gravel	0.2286	9.14E-03	2.50E+01
			Total d_i/k_i = 2.51E+03
			Total Depth = 0.9144 m
			K_z (m/s) = 3.64E-04

3.3.4.2. Monitoring Duration for the Outflow Hydrograph

The total time needed to monitor the outflow hydrograph was calculated as the sum of the time to travel the vertical distance within the bioretention cell media and the time to travel horizontally across the liner, from the most remote point in the bioretention cell to the outflow monitoring equipment, as shown in Equation 9. The total time necessary to monitor the runoff from a 0.9-inch storm event was found to be approximately 90 minutes, which included the time for runoff to travel across the paved road surface.

$$T = \frac{A_w D}{K_z A_{BR(z)}} + \frac{A_w D}{K_x A_{BR(X)}} \quad (9)$$

Where,
T is the time for the outflow peak to reach monitoring equipment (s)
A_w is the watershed area (m^2)
D is the selected rainfall depth (m)
K_z is the cumulative vertical hydraulic conductivity (m s^{-1})
K_x is the horizontal hydraulic conductivity (m s^{-1})
A_{BR} (z) is the vertical cross-sectional area along the Y-plane (m^2)
A_{BR} (x) is the vertical cross-sectional area of the layer directly above the flow impeding layer along the X-plane (m^2)

The automated sampling program was set to take samples every 4 minutes for 96 minutes, producing 24 samples. An example of the outflow hydrograph is shown in Figure 10. Actual sample number varied based on the characteristics of the storm event, with smaller storms producing fewer samples.

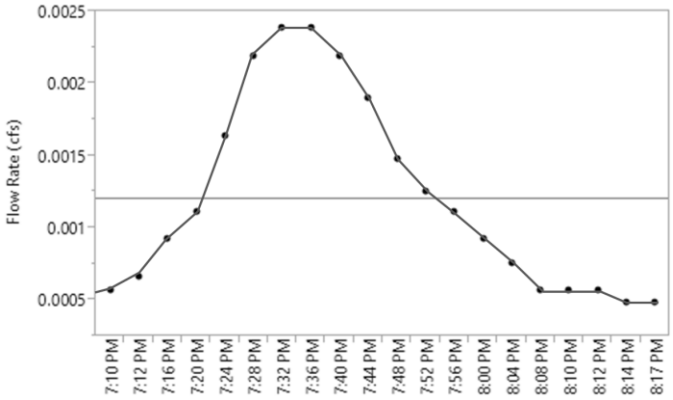

Figure 10. Example Outflow Hydrograph, Watershed 8, 7/28/14

3.3.5. Normalizing Baseline Sampling Conditions

In order to accurately determine the initial concentration of water being sampled in the early part of a storm event, the antecedent conditions inside the monitoring infrastructure needed to be normalized prior to an event. Organic debris, nutrients, and sediment were removed from the monitoring infrastructure as close to the time before a storm event as possible. The inflow and outflow weirs were filled to the v-notch and allowed to stabilize, so that the automated sampler could be programmed to read this level as zero. This set the baseline for the pressure transducer.

The standing water in the inflow weir boxes prior to an event, after the weir boxes had been cleaned, was approximately 4.25 L, minus that which was displaced by the pressure transducer and suction probe. The volume was increased to 4.95 L prior to

being triggered for sampling, of which approximately 14% (0.696 L) was new stormwater. After an ISCO is triggered, it begins a process of purging the suction lines with water from the sample area to remove any water the sample lines that might remain from a previous event. The time it takes for the machine to register that it has been triggered, take the water in, purge the lines, and release it back out again is approximately one minute (Harmel et al. 2003). Meanwhile, stormwater moves through the weir box, further mixing and displacing the water used to clean the system. Water moving at an average inflow flow rate of 0.1 L s^{-1} would replace the 4.95 L of water in the weir box in 49.5 seconds. Flow rate and sample measurements are taken together, one minute increments after the sampler is triggered. Because the time from when the equipment is triggered to when the first water sample is taken, is greater than the time to replace the water used to clean the weir box, its influence was deemed insignificant. The progressively increasing flow rate in the rising limb of the hydrograph, and corresponding volume moving through the monitoring system were also likely to dwarf any dilution effects from the weir-rinse water.

3.4. Bioretention Construction Steps and Considerations

Unlike the cases in which a bioretention system is retrofitted for the purpose of monitoring after it has already been installed, the UVM Bioretention Laboratory was specifically constructed to facilitate intensive monitoring of various parameters. Construction of this project was completed by an engineering and construction company (EcoSolutions, LLC.) with specialized experience in bioretention construction; however,

this will not likely always be possible. The specific steps that were critical to the successful installation of the bioretention cells are described in detail herein.

3.4.1. Excavation

Prior to construction, the bioretention cell corners, catch basins, and drainage lines were laid out on the project site with spray paint and stakes and all underground utilities (both private and public) were noted. Not all public utility location services identify private lines and the cost and danger of coming into contact with underground infrastructure during construction can be very high, therefore it is important to carefully check as-built drawings for any utility lines that may not have been marked by dig-safe or other utility organizations.

Construction began by digging the drainage trench and area around the catch basin with a mini-excavator. This machine ensured the accuracy of width and depth cuts due to its smaller bucket size. The drain trench was laser-leveled to ensure proper drainage slope and topped with a thin layer of bedding sand on which the pipe would be laid. A hole was drilled in the existing catch basin, which was connected to 4-inch PVC drainage pipe laid in sections, back to the location of the bioretention cells. The majority of the trench was backfilled with material previously removed during excavation, while the end of the drainage pipe remained uncovered until the bioretention cell was excavated and its underdrain could be attached to the monitoring equipment.

Site-specific conditions such as soil type, previous land use, and close proximity to utilities will heavily influence the time and cost needed for excavation. The underlying material at this site consisted of clay and disaggregated construction fill, which was not

noted on as-built plans, and took much longer than expected to dig through. During excavation, depth measurements were taken every few minutes to ensure excavation was consistent with designs and that underlying utilities were not in jeopardy.

3.4.2. Installation of Outflow Monitoring Equipment

The bioretention cell area and adjacent outflow monitoring area were excavated as one large rectangle. The monitoring infrastructure was pre-assembled on-site, and consisted of a vertical two-foot diameter sump, approximately 6 feet tall, with cut-outs at the bottom to fit over the monitoring piping configuration (Figure 4). The bottom of the sump was capped and all connections between the sump and monitoring configuration were sealed for water tightness. Once the bioretention cell and outlet monitoring area had been excavated, the pre-assembled monitoring equipment was gently lowered into the cavity. The Thel-Mar™ weir was then fitted inside the end of a six-inch pipe protruding horizontally from the sump and final adjustments were made using the bubble level located at the top of the weir. Further disturbances to the monitoring equipment were carefully avoided.

3.4.2.1. Installation of Liner and Drainage Infrastructure

Geotextile fabric was placed upon the bare soil, with a rubber liner on top. The geotextile provided a protective barrier between the liner and the bare soil, but did not affect water movement within the cell. For each bioretention cell, a cedar frame was assembled onsite and was fitted along the upper cell perimeter. The frame functioned to ensure that the length and width dimensions remained accurate and comparable between cells, while also providing a solid platform to which the rubber liner could be secured and

an outside barrier against flow from adjacent grassed areas, which were explicitly excluded in this research. Two notches were cut into the cedar frame. One was at the position of the overflow swale to allow any overflow water to enter the existing storm drain network. The other was at the entrance to the bioretention cell, where the inflow monitoring equipment would ultimate be attached.

A hole just smaller in diameter than the four-inch outlet pipe, was cut in the liner and geotextile near the bottom of the cell. The material was stretched over the four-inch pipe that protruded into the bioretention cell. A rubber coupling was used to seal the rubber liner to the monitoring pipe. The perforated underdrain drainage configuration was pre-assembled above ground and consisted of two vertical PVC cleanout pipes, which were connected via elbow pipes to a horizontal four-inch perforated PVC drainage pipe with pre-drilled 3/8-inch diameter holes. The cleanout pipes were tall enough to protrude from the finished top surface, and would allow maintenance on the perforated pipe area, should it ever become clogged. The U-shaped drainage structure was lowered into the cell at the downstream end of each bioretention cell. The perforated underdrain pipe was coupled to the four-inch pipe, which ultimately tied to the monitoring equipment. Although this drainage design did not specifically include an internal water storage (IWS) zone, the perforated underdrain was approximately two inches (5.08 cm) higher than the bottom of the cell, in order to connect it to the outflow monitoring equipment.

3.4.2.2. Layering the Bioretention Soil Media

The designed depths of each layer of bioretention soil media were measured from the bottom of the cells and marked on the aforementioned vertical cleanout pipes.

Gravel (~1.5 inches in diameter), pea gravel (or pea stone, 1/8 inch – 3/8 inch diameter), sand, and a sand/compost mixture were added in subsequent layers, with care taken to avoid compaction (Figure 6). Approximately six inches of ponding depth was maintained above the final soil layer, between the top of the soil media and the overflow notch in the cedar frame. Mulch was not used in this bioretention design to avoid potential release of labile N and P.

3.4.3. Grading from the Curb Cut to the Inflow Sampling Area

Once the cells were installed, the grading was completed from the trapezoidal curb cut to the cell opening and from the overflow notch to the storm drain. Geotextile fabric and rubber liner were laid down from the curb cut to the notch in the cedar to create an impermeable pathway to the monitoring equipment. Two to four-inch stone was laid upon the impermeable layer within the conveyance strip to hold the fabrics in place. Berms were constructed from the curb cut to the eight-inch opening in the cedar frame on either side of the entrance swale, where the inflow water would ultimately enter the monitoring equipment. This ensured that no stormwater was lost on its way to the inflow weir box.

3.4.4. Installation of Inflow Monitoring Equipment and Vegetation

Construction of the eight bioretention cells was complete in November of 2012. The total snow accumulation during the winter of 2012-2013 was approximately 86.5 inches (NOAA, Precipitation Frequency Data Server). The media experienced some compaction due to the weight of the snow; however, the high hydraulic conductivity of the sand media prevented any significant reduction in drainage capacity. In soil media

designs with more silt and clay, compaction can damage macropores, reducing hydraulic conductivity (Thompson et al. 2008) and should be carefully avoided. Freeze and thaw cycles did not shift the media inside the cells themselves due to the high sand content, but did alter the surrounding soil media, which needed to be re-graded in some places the following spring.

In May of 2013, the inflow weir boxes were placed inside the bioretention cells and screwed to the interior of each cedar frame, such that the top of the weir boxes were level with the bottom of the frame entrance notches. The rubber liner, which ran from the curb cut across the conveyance strip, was extended to cover the area where the weir box and cedar frame met, with a waterproof rubber patch. At the beginning of each sampling season, weir boxes were leveled and silicone was reapplied to ensure water tightness and accuracy of flow measurements. The narrow perforated distribution channel was placed inside the cell, in a shallow trench, starting at the edge of the weir box (Figure 3), such that the top most part of the channel was level with the soil media.

Vegetation was planted in May of 2013 and watered for three weeks during the initial establishment phase. Plant selection was based on height, rooting habit, bloom time, color, diversity, pollen supply, robustness to drought and flood conditions, and salt tolerance. Water quality monitoring began in June of 2013. Information regarding the comparative water quality performance of the soil media and plants used in this research can be found in Chapter 5.

3.5. Conclusions

Monitoring can provide critical information regarding the effectiveness of bioretention systems, how key design features influence the pollutant removal mechanisms, and how those features are likely to change over time. The inflow and outflow bioretention monitoring infrastructure in this research was specifically designed to allow for a detailed characterization of mass based bioretention pollutant removal performance, and can be adapted to achieve various stormwater sampling goals. The time-based sampling method proved to be effective at capturing the inflow and outflow hydrographs from this research site. The equipment allowed for the conversion of concentration to mass for any sample, and comparison of the inflow and outflow mass loads. The care taken during construction resulted in the proper installation of the monitoring equipment and overall functionality of the cells.

REFERENCES

Alias, N., Liu, A., Egodawatta, P., and Goonetilleke, A. (2014). "Sectional analysis of the pollutant wash-off process based on runoff hydrograph." *Journal of Environmental Management*, 134, 63–9.

Allen Burton, G., and Pitt, R. (2002). *Stormwater effects handbook: a toolbox for watershed managers, scientists, and engineers*. Lewis Publishers, Boca Raton.

Arias, C., Del Bubba, M., and Brix, H. (2001). "Phosphorus removal by sands for use as media in subsurface flow constructed reed beds." *Water Research*, 35(5), 1159–68.

Bertrand-Krajewski, J.-L., Chebbo, C., and Saget, A. (1998). "Distribution of pollutant mass vs volume in stormwater discharges and the first flush phenomenon." *Water Resources*, 32(8), 2341–2356.

Blecken, G.-T., Zinger, Y., Deletić, A., Fletcher, T., and Viklander, M. (2009). "Influence of intermittent wetting and drying conditions on heavy metal removal by stormwater biofilters." *Water Research*, 43(18), 4590–8.

Bratieres, K., Fletcher, T., Deletic, A., and Zinger, Y. (2008). "Nutrient and sediment removal by stormwater biofilters: a large-scale design optimisation study." *Water Research*, 42(14), 3930–40.

Brown, R. A., and Hunt, W. F. (2011). "Impacts of media depth on effluent water quality and hydrologic performance of undersized bioretention cells." *Journal of Irrigation and Drainage Engineering*, 137(March), 132–143.

Chen, X., Peltier, E., Sturm, B. S. M., and Young, C. B. (2013). "Nitrogen removal and nitrifying and denitrifying bacteria quantification in a stormwater bioretention system." *Water Research*, 47(4), 1691–700.

Claassen, V., and Young, T. (2010). *Model guided specification for using compost and mulch to promote establishment of vegetation and improvement in stormwater quality*.

Claytor, R. A., and Schueler, T. R. (1996). *Design of stormwater filtering systems*. Ellicott City.

Collins, K. A., Lawrence, T. J., Stander, E. K., Jontos, R. J., Kaushal, S. S., Newcomer, T. A., Grimm, N. B., and Cole Ekberg, M. L. (2010). "Opportunities and challenges for managing nitrogen in urban stormwater: A review and synthesis." *Ecological Engineering*, 36(11), 1507–1519.

Davidson, E., Keller, M., Erickson, H., Verchot, L., and Veldkamp, E. (2000). "Testing a conceptual model of soil emissions of nitrous and nitric oxides." *BioScience*, 50(8), 667–680.

Davis, A. P. (2007). "Field performance of bioretention: water quality." *Environmental Engineering Science*, 24(8), 1048–1064.

Davis, A. P. (2008). "Field performance of bioretention: hydrology impacts." *Journal of Hydrologic Engineering*, 13(2), 90–95.

Davis, A. P., Hunt, W. F., Traver, R. G., and Clar, M. (2009). "Bioretention technology: Overview of current practices and future needs." *Journal of Environmental Engineering*, 135(3), 109–117.

Davis, M., and Cornwell, D. (1998). *Inroduction to environmental engineering*. McGraw-Hill, Boston.

DeBusk, K., Hunt, W., and Line, D. (2011). "Bioretention outflow: does it mimic nonurban watershed interflow?" *Journal of Hydrologic Engineering*, 16(March), 274–279.

DeBusk, K., and Wynn, T. (2011). "Storm-water bioretention for runoff quality and quantity mitigation." *Journal of Environmental Engineering*, 137(September), 800–808.

Dietz, M. (2007). "Low impact development practices: a review of current research and recommendations for future directions." *Water, Air, and Soil Pollution*, 186(1-4), 351–363.

Dietz, M., and Clausen, J. (2005). "A field evaluation of rain garden flow and pollutant treatment." *Water, Air, and Soil Pollution*, 167(1-4), 123–138.

Dietz, M. E., and Clausen, J. C. (2006). "Saturation to improve pollutant retention in a rain garden." *Environmental Science & Technology*, 40(4), 1335–40.

Dodds, W. K., Bouska, W. W., Eitzmann, J. L., Pilger, T. J., Pitts, K. L., Riley, A. J., Schloesser, J. T., and Thornbrugh, D. J. (2009). "Eutrophication of U.S. freshwaters: analysis of potential economic damages." *Environmental Science & Technology*, 43(1), 12–19.

Fassman, E., Simcock, R., and Wang, S. (2013). *Media specification for stormwater bioretention devices*.

Freeze, A. R., and Cherry, J. A. (1979). *Groundwater*. Prentice-Hall International, Englewood Cliffs, NJ.

Geosyntec Consultants, and Wright Water Engineers. (2012). *International Stormwater Best Management Practices (BMP) Database Pollutant Category Summary Statistical Addendum: TSS, Bacteria,*

Nutrients, and Metals.
Geosyntec Consultants, and Wright Water Engineers. (2013). *Advanced analysis: influence of design parameters on performance*.
Glysson, G. D., Gray, J. R., and Conge, L. M. (2000). *Adjustment of total suspended solids data for use in sediment studies*. *Building Partnerships*, American Society of Civil Engineers, Reston, VA.
Groenenberg, J. E., Chardon, W. J., and Koopmans, G. F. (2013). "Reducing phosphorus loading of surface water using iron-coated sand." *Journal of Environment Quality*, 42(1), 250.
Harmel, D., King, K., Wolfe, J., and Torbert, A. (2002). "Minimum flow considerations for automated storm sampling on small watersheds." *The Texas Journal of Science*, 54(2), 177–178.
Harmel, R. D., King, K. W., and Slade, R. M. (2003). "Automated storm water sampling on small watersheds." *Applied Engineering in Agriculture*, 19(6), 667–674.
Hathaway, J. M., Tucker, R. S., Spooner, J. M., and Hunt, W. F. (2012). "A traditional analysis of the first flush effects for nutrients in stormwater runoff from two small urban catchments." *Water, Air, and Soil Pollution*, 223(9), 5903–5915.
Henderson, C., Greenway, M., and Phillips, I. (2007). "Removal of dissolved nitrogen, phosphorus and carbon from stormwater by biofiltration mesocosms." *Water Science & Technology*, 55(4), 183.
Hornberger, G., Raffensperger, J., Wiberg, P., and Eschleman, K. (1998). *Elements of physical hydrology*. The Johns Hopkins University Press, Baltimore.
Hunt, W. F. (2003). "Pollutant removal evaluation and hydraulic characterization for bioretention stormwater treatment devices." *Doctoral Dissertation*, Pennsylvania State University.
Hunt, W. F., Jarrett, A. R., Smith, J. T., and Sharkey, L. J. (2006). "Evaluating bioretention hydrology and nutrient removal at three field sites in North Carolina." *Journal of Irrigation and Drainage Engineering*, 132(6), 600–608.
Hunt, W. F., Smith, J. T., Jadlocki, S. J., Hathaway, J. M., and Eubanks, P. R. (2008). "Pollutant removal and peak flow mitigation by a bioretention cell in urban Charlotte, N.C." *Journal of Environmental Engineering*, 134(5), 403–408.
Hurley, S. E., and Forman, R. T. T. (2011). "Stormwater ponds and biofilters for large urban sites: Modeled arrangements that achieve the phosphorus reduction target for Boston's Charles River, USA." *Ecological Engineering*, 37(6), 850–863.
Kadlec, R. H., Cuvellier, C., and Stober, T. (2010). "Performance of the Columbia, Missouri, treatment wetland." *Ecological Engineering*, Elsevier B.V., 36(5), 672–684.
Kang, J.-H., Kayhanian, M., and Stenstrom, M. K. (2008). "Predicting the existence of stormwater first flush from the time of concentration." *Water Research*, 42(1-2), 220–8.
Kim, H., Seagren, E. A., Davis, A. P., and Davis, P. (2003). "Engineered bioretention for removal of nitrate from stormwater runoff." *Water Environment Federation*, 75(4), 355–367.
King, K. W., Harmel, R. D., and Fausey, N. R. (2005). "Development and sensitivity of a method to select time- and flow-paced storm event sampling intervals for headwater streams." *Journal of Soil and Water Conservation*, 60(6), 323–331.
Komlos, J., and Traver, R. G. (2012). "Long-term orthophosphate removal in a field-scale storm-water bioinfiltration rain garden." *Journal of Environmental Engineering*, 138(October), 991–998.
Kosmerl, P. (2012). "Water balance of right of way retrofit gardens." Ohio State University.
Law, N. L., Fraley-McNeal, L., Cappiella, K., and Pitt, R. (2008). *Monitoring to demonstrate environmental results: guidance to develop local stormwater monitoring studies using six example study designs*. Ellicott City.
Lefevre, G. H., Paus, K. H., Natarajan, P., Gulliver, J. S., Novak, P. J., and Hozalski, R. M. (2015). "Review of dissolved pollutants in urban storm water and their removal and fate in bioretention cells." *Journal of Environmental Engineering*, 141.
Lenth, J., Rheaume, A., and Tackett, T. (2008). "Lessons learned from monitoring bioretention swales in west Seattle's high point neighborhood." *Low Impact Development for Urban Ecosystem and Habitat Protection*.
Leytem, A., and Bjorneberg, D. (2009). "Changes in soil test phosphorus and phosphorus in runoff from calcareous soils recieve manure compost, and fertilizer application with and without alum." *Soil Science*, 174.

Liu, J., Sample, D., Owen, J., Li, J., and Evanylo, G. (2014). "Assessment of selected bioretention blends for nutrient retention using mesocosm experiments." *Journal of Environment Quality*.
Lucas, W. C., and Greenway, M. (2008). "Nutrient retention in vegetated and nonvegetated bioretention mesocosms." *Journal of Irrigation and Drainage Engineering*, 134(5), 613–623.
Mangangka, I. R., Liu, A., Egodawatta, P., and Goonetilleke, A. (2014). "Performance characterisation of a stormwater treatment bioretention basin." *Journal of Environmental Management*, Elsevier Ltd, 150C, 173–178.
Michigan Department of Environmental Quality. (2008). *Low Impact Development Manual for Michigan: A Design Guide for Implementers and Reviewers*.
National Research Council. (2008). *Urban Stormwater Management in the United States*.
Natural Resources Conservation Service. (1986). *Urban Hydrology for Small Watersheds TR-55*. *Urban Hydrology for Small Watersheds TR-55*.
Nylen, N. G., and Kiparsky, M. (2015). *Accelerating cost-effective green stormwater infrastructure: learning from local implementation*.
Palmer, E. T. (2012). "Nitrate and phosphate removal through an optimized bioretention system." *Masters Thesis*, Washington State University.
Read, J., Wevill, T., Fletcher, T., and Deletic, A. (2008). "Variation among plant species in pollutant removal from stormwater in biofiltration systems." *Water Research*, 42(4-5), 893–902.
Roseen, R., Ballestero, T., Houle, J., Avellaneda, P., Briggs, J., Fowler, G., and Wildey, R. (2009). "Seasonal performance variations for storm-water management systems in cold climate conditions." *Journal of Environmental Engineering*, 135(March).
Rosenquist, S. E., Hession, W. C., Eick, M. J., and Vaughan, D. H. (2010). "Variability in adsorptive phosphorus removal by structural stormwater best management practices." *Ecological Engineering*, Elsevier B.V., 36(5), 664–671.
Sansalone, J. J., and Cristina, C. M. (2004). "First flush concepts for suspended and dissolved solids in small impervious watersheds." *Journal of Environmental Engineering*, 130(November), 1301–1314.
Stone, R. M. (2013). "Evaluation and optimization of bioretention design for nitrogen and phosphorus removal." *Masters Thesis*, University of New Hampshire.
Taylor, A., and Wong, T. (2002). *Non-structural stormwater quality best management practices - a literature review of their value and life-cycle costs*.
Teledyne ISCO. (2012). *720 Submerged Probe Flow Module*.
The United Nations. (2015). *World Water Development Report*.
Thompson, A. M., Paul, A. C., and Balster, N. J. (2008). "Physical and hydraulic properties of engineered soil media for bioretention basins." *American Society of Agricultural and Biological Engineers*, 51(2), 499–514.
U.S. Bureau of Reclamation. (2001). *Water Measurement Manual*. U.S. Government Printing Office, Washington, D.C.
U.S. Environmental Protection Agency. (1997). "Load Estimation Techniques." *National Management Measures to Control Nonpoint Pollution from Agriculture*, 225–242.
U.S. Environmental Protection Agency. (2008). *TMDLs to Stormwater Permits Handbook*.
Vance, C. P., Uhde-Stone, C., and Allan, D. L. (2003). "Phosphorus acquisition and use: critical adaptations by plants for securing a nonrenewable resource." *New Phytologist*, 157(3), 423–447.
Vermont Agency of Natural Resources. (2002). *The Vermont Stormwater Management Manual Volume II – Technical Guidance*.
Washington State University Pierce County Extension. (2012). *Low Impact Development Technical Guidance Manual for Puget Sound*.
Wemple, B., Shanley, J., Denner, J., Ross, D., and Mills, K. (2007). "Hydrology and water quality in two mountain basins of the northeastern US : assessing baseline conditions and effects of ski area development." *Hydrologic Processes*, 21, 1639–1650.
Wong, T. H. F. (2006). "An Overview of Water Sensitive Urban Design Practices in Australia." 1(1).
Zinger, Y., Blecken, G.-T., Fletcher, T. D., Viklander, M., and Deletić, A. (2013). "Optimising nitrogen removal in existing stormwater biofilters: Benefits and tradeoffs of a retrofitted saturated zone." *Ecological Engineering*, 51, 75–82.

CHAPTER 4: INVESTIGATING POLLUTANT MASS MOBILIZATION AND SPECIATION DURING THE STORMWATER FIRST FLUSH

Amanda L. Cording

Keywords: stormwater, mass based first flush, pollutant load, nitrogen, phosphorus, nutrients, TSS, precipitation intensity, flow rate.

Abstract

The mobilization of sediments and nutrient constituents in stormwater from the paved road surface was investigated over the course of 19 storm events to critically evaluate the occurrence of the mass-based first flush and factors that influence total pollutant loads. Mass loads were found to be highly positively correlated with storm intensity and total precipitation volume, with N and P constituent species having distinct mobilization patterns. The total cumulative mass load in stormwater was found to be highest for total suspended solids, followed by total Kjeldahl nitrogen, nitrate, non-labile phosphorus and soluble reactive phosphorus. Mass loads per m^2 of paved road are predicted with linear regression as a function of precipitation depth. The results from this site clearly dispute the commonly held assumption that 90% of the pollution will be mobilized by 0.5 inches of precipitation, within a 0.9-inch storm event. The dominance of non-labile pollutant constituents in stormwater is encouraging, for this pollutant fraction is known to be effectively removed by green stormwater infrastructure techniques, such as bioretention.

4.1. Achieving Water Quality Targets by Treating the First Flush

The first half-inch of runoff has been thought to transport 90% of the total pollution over the course of an event (Bach et al. 2010; Bertrand-Krajewski et al. 1998). This concept is generally referred to as the "first flush" (Bertrand-Krajewski et al. 1998; Sansalone and Cristina 2004; Stenstrom and Kayhanian 2005). Although there are many variations on the definition, the first flush (FF) concept has been heavily utilized by

stormwater practitioners, who have to recommend/require a water quality volume (WQv), or portion of the storm event (e.g., 0.5 inches), to treat with stormwater best management practices. Minimum WQv requirements typically range between 0.5 and 1.0 inch of rainfall (DeBusk and Wynn 2011; Sansalone and Cristina 2004; Stenstrom and Kayhanian 2005; Vermont Agency of Natural Resources 2002a). However, the actual pollutant mass loads from a 0.5-inch or 1.0-inch storm event are not well predicted, and results from FF investigations have been highly variable, with changing definitions making it difficult to compare results between studies (Alias et al. 2014; Bach et al. 2010; Gupta and Saul 1996; Hathaway et al. 2012).

According to Sansalone and Cristina (2004), the FF concept should be broken into a concentration-based first flush (CFF) and a mass-based first flush (MFF). The CFF is broadly defined by an initially high concentration in the early portion of the storm event with a subsequent rapid decline. The MFF is defined as a disproportionately high mass delivery in relation to total flow volume (Sansalone and Cristina 2004). The distinction between concentration and mass measurements is particularly important, for they have different policy implications (Sansalone and Cristina 2004). The stormwater discharge from a site may be regulated by either a discharge permit, or a total maximum daily load (TMDL) limit. Discharge permits are based on limiting the runoff concentration from a site (Sansalone and Cristina 2004), whereas a TMDL limits the total mass from a site (U.S. Environmental Protection Agency 1998). A TMDL is a pollution budget for waters that have been deemed impaired under the Clean Water Act (U.S. Environmental Protection Agency 2008).

The CFF has been found for various pollutant constituents, and is largely due to the dilution effects of increasing stormwater volume during the rising limb of the storm hydrograph (Deletic 1998; Lee et al. 2002; Maestre and Pitt 2004; Miguntanna et al. 2013). Dilution may be helpful in some contexts, but it does not alter the total pollutant mass delivered to a receiving water (Smith et al. 1999). The MFF concept has not been widely validated across different storm conditions, and may not be equally exhibited by all pollutant types (e.g., labile and non-labile) (Hathaway et al. 2012).

The factors that influence the mobilization and transport of sediment and nutrient mass in various forms of chemical speciation (e.g., non-labile P vs. labile P) are not well characterized (Sansalone and Cristina 2004). Further, predicting the pollutant mass loads associated with a range of storm events will help us better understand how those loads are related to the responses of aquatic environments (e.g., eutrophication) (Charbeneau and Barrett 1998; Kang et al. 2008) and can be used to evaluate BMP performance on a mass basis. Both concentration and mass values are valid in certain settings, and both are susceptible to the factors that contribute to the variability of build-up and wash-off process, which will be discussed below.

4.2. Factors Contributing to First Flush Variability

According to the build-up/wash-off model, available pollutant load is thought to follow a dynamic equilibrium, where pollutant mass accumulates upon an impervious surface prior to a storm event, and a portion of it is mobilized during a precipitation event (Francey 2010; Herngren 2005; Vaze and Chiew 2003a).

4.2.1. Build-Up

Some factors that influence the build-up of pollutant mass include land-cover, land-use, traffic, the number of days since the last rain event, also known as the antecedent dry period, or antecedent dry days (ADD) (Alias et al. 2014; Kayhanian et al. 2007; Lee et al. 2002); and the amount of rainfall that fell during the most recent event, or antecedent precipitation conditions (APC) (Blecken et al. 2009; Brown et al. 2013; Deletic 1998). Air temperature also plays a role in localized decomposition and mineralization rates (Dillon and Chanton 2005), which may increase pollutant availability. Although antecedent conditions are likely to influence the available pollutant load, in stormwater models often hold this value constant (Vaze and Chiew 2003b).

4.2.2. Wash-Off

Each precipitation event is thought to have a specific capacity to mobilize and transport pollutants (Charbeneau and Barrett 1998; Egodawatta et al. 2007; Vaze and Chiew 2003a). Pollutant mobilization dynamics are still under investigation, and it is unclear how pollutants in various stages of decomposition (e.g., labile and non-labile pollutants) are likely to differ in their mobilization and transport patterns. Some of the factors that influence pollutant mobilization and transport from an impervious surface include the detachment of surface pollutants by the kinetic energy supplied by a falling raindrop, the rainfall intensity, and the resulting shear stress supplied by runoff (Egodawatta et al. 2007; Vaze and Chiew 2003a).

Stormwater velocity influences the dissolved and particulate fractions of pollution in a given sample, with increasing velocities transporting increased particle

sizes based on Stokes Law (Glysson et al. 2000). Runoff velocity is variable throughout a storm, however, and its relative influence on the total mass load of different pollutant types has not been well characterized. Overall, the total pollutant mass load from stormwater runoff has not been easily predicted, and the relative strength of influencing factors on different pollutant types is not well known (Brezonik and Stadelmann 2002; Charbeneau and Barrett 1998; LeBoutillier et al. 2000).

4.2.3. Pollutant Speciation

Pollutant wash-off is typically modeled with an exponential equation, in which assumptions include that nutrients (N and P) are grouped together and modeled as one would model a particle (Charbeneau and Barrett 1998; Egodawatta et al. 2007; Kang et al. 2006; Miguntanna et al. 2013). Yet the local aquatic environment may respond very differently to influxes of nitrogen and phosphorus (Havens et al. 2003; Turner and Rabalais 2013). Further, grouped measures such as total phosphorus (TP) and total nitrogen (TN) are often used in stormwater analysis, but these measures contain both labile and non-labile constituents, which are likely to have different short-term and long-term impacts on receiving waters, with labile constituents being more immediately available to phytoplankton (Paerl 2006). The two constituent forms may also have different removal mechanisms in GSI (Henderson et al. 2007; Lefevre et al. 2015).

By understanding the dominant mechanisms governing the build-up and wash-off of stormwater pollutants in various forms of speciation, researchers and practitioners will be better able to predict pollutant loads and improve pollutant removal designs, models, and regulations (Charbeneau and Barrett 1998; Vaze and Chiew 2003a).

4.3. Research Objectives

The broad goals of this research are to better understand the factors controlling build-up and wash-off of stormwater pollutants from small paved road watersheds, and to predict the mass load of various constituents, as a function of precipitation depth. Specifically, this research addresses the following research questions:

1) What is the composition and total mass load of stormwater runoff from a low to medium traffic, paved road surface?
2) Is there consistent evidence for a mass based first flush (MFF)? Is it equally displayed by all constituents?
3) What portion of pollutant mass is mobilized by various precipitation depths?
4) How do hydrologic and environmental factors differ in their relative contribution to nutrient and sediment mass delivered during a storm event?

4.4. Site Description

In 2012, the University of Vermont Bioretention Laboratory was constructed on the University of Vermont (UVM) campus, in Burlington, VT. The research site consists of eight small paved road sub-watersheds with areas ranging from 320 ft^2 (29.729 m^2) to 1,293 ft^2 (120.12 m^2). The road is one of the main thoroughfares for bus and vehicular traffic entering and exiting the UVM campus. Sub-watershed boundaries were delineated from the crown of the road to a granite curb at a 45-degree angle, leading into a trapezoidal curb cut. Stormwater is directed from the road surface, through the cub-cut,

and across a narrow conveyance strip, ranging from 3.72 m^2 to 19.20 m^2, which was lined with a rubber EPDM membrane and covered with 2 to 4 inch stone.

4.5. Materials and Methods

4.5.1. Stormwater Monitoring Infrastructure and Equipment

Runoff was captured in a monitoring device, called a "weir box" prior to entering a bioretention cell (see Chapter 3). Each weir box was sized to allow stormwater to be sampled in rapid, sequential segments, and is equipped with a 90-degree v-notch weir, which was selected for optimal measurement of small changes in volume (U.S. Bureau of Reclamation 2001). This maximized the detection of incremental changes in runoff quality throughout an event. The dimensions of the weir boxes were based on U.S. Bureau of Reclamation (2001) recommendations, and are described in detail in Chapter 3.

The height or level of the stormwater in each weir box was measured with a Teledyne™ 720 differential pressure transducer, which took continuous measurements throughout each storm event, in one-minute intervals. The pressure transducers were clipped to the base of the weir box to ensure accurate measurements in high flow events and are equipped with a venting system that compensates for changes in atmospheric pressure. It records level from 0.03 ft (0.9144 cm) to 5.0 ft (1.524 m) (+/- 0.243 cm), with an operating temperature of 32 to 120^o F. Automated sample collection was conducted by Teledyne™ ISCO 6700 series automated samplers, which can hold a maximum of twenty-four 1-L bottles.

4.5.2. Sampling Considerations

The size of the research drainage area and sampling regime have been shown to influence the detectability of a FF event (Maestre and Pitt 2004), and were carefully considered in this research. The watershed area influences the time of concentration (T_c) or the time for the runoff to travel from the most hydrologically remote part of the watershed to the monitoring location (Kang et al. 2008). As pollutant transport time increases, so does the likelihood of mixing, dilution, and the introduction of complicating factors such as changes in land surface composition, friction forces, and abrupt changes in flow direction, which may affect pollutant composition within a storm (Kang et al. 2006). Therefore, smaller watershed sizes (< 10 m^2) have been previously shown to more reliably represent first flush characteristics (Kang et al. 2006; Lee and Bang 2000; Maestre and Pitt 2004). Sansalone and Cristina (2004) recommend that if the goal is to detect a CFF, the sampling design should target the early portion of the event, whereas if mass characterization is the target, measurements should be based on the hydrograph shape, with more samples leading to greater accuracy.

4.5.3. Water Quality Sampling

The eight small paved road sub-watersheds in this study provided an ideal setting in which to investigate the first flush. The runoff sampling design was based on the length of time required to take successive samples throughout an idealized hydrograph. The time of concentration, rainfall intensity duration curves, and the rational method were used to estimate peak flow rates for each sub-watershed. Details regarding the sampling methods can be found in Chapter 3. Teledyne ISCO 6700 series automated

sampling equipment took 900-ml runoff samples every two minutes for 48 minutes (n = 24) when inflow flow rates were consistently above a minimum water level threshold of 0.21 ft (6.50 cm) from the bottom of the weir box. Rapid sequential flow rate measurements were taken every minute, as suggested by Vaze and Chiew (2003a), and allowed for the conversion of concentration to mass load for any given sample. Stormwater levels were converted to flow rates using discharge equations developed for each of the eight weirs.

4.5.4. Water Quality Analysis

Each sample was analyzed for total phosphorus (TP), soluble reactive phosphorus (SRP), total nitrogen (TN), nitrate (NO_3^-), and total suspended solids (TSS). All stormwater samples were filtered with a Fisherbrand 0.45 μm nylon syringe filter prior to analyzing for dissolved inorganic nutrients according to standard methods (APHA 1992) and read by a Lachat™ automated colorimeter (Flow Injection Analysis, QuikChem 8000, Hach Company, Loveland, CO). Total phosphorus (TP) and total nitrogen (TN) concentrations were determined using potassium persulfate digestions on unfiltered samples. Potassium persulfate was prepared fresh for each digestion (APHA, 1995). Quality control samples for both TN and TP were prepared using para-Nitrophenylphosphate (para-NPP). A blank, standard and QC were included each time samples were run. SRP (dissolved ortho-phosphate) and TP (persulfate digested o-PO_4^{3-} were analyzed using the Lachat QuickChem Method 10-115-01-1-Q. NO_3^- and TN were analyzed using the Lachat QuickChem Method 10-107-04-1-B. TSS was measured according to standard methods (APHA 2011).

In order to investigate nutrient speciation in stormwater, TN and TP were mathematically separated into the approximate equivalent of total Kjeldahl nitrogen (TKN) and non-labile phosphorus (NLP), respectively. NLP was determined by subtracting the SRP from TP for each sample, and includes both the particulate and dissolved fraction of organic P. Dissolved organic phosphorus is predominantly non-labile, requiring bacterial decomposition (mineralization) to become ortho-phosphate (SRP), which is labile (Spivakov et al. 1999). TN is defined as the sum of organic nitrogen, nitrate, nitrite, ammonia and ammonium. TKN is traditionally defined as the portion of nitrogen measured using the Kjeldahl method. It is a grouped measure, which includes NH_3, NH_4^+ (labile, sometimes referred to as "free ammonia" or "ammonia"), and organic nitrogen (both labile and non-labile). The Kjeldahl method requires the use of toxic chemicals and poses hazardous disposal issues (Patton and Kryskalla 2003), therefore this research used an alternative method used by the Hach Company® for determining the equivalent portion of nitrogen to TKN in a sample, by using a persulfate digestion to determine total nitrogen, then subtracting the nitrate and nitrite components to determine TKN (Antonio and Walker 2011).

4.5.5. Data Analysis

A total of 463 samples were taken over the course of 19 storm events dispersed over two sampling seasons (July to November 2013 and June to October 2014). In order to compare the different nutrient constituents within a sample (e.g., TKN and NO_3^-), samples that did not have enough water to measure both TP and TN were discarded. On some occasions, more than one of the eight watersheds was sampled during the same

event. This was not possible during every event due to a lack of equipment. Each storm event that was sampled at one of the eight watershed locations is called a 'watershed event'. Nutrient data were collected from all watershed events (n = 35). Total suspended solids were collected from all events except one (n = 34). The number of samples taken during each event varied, depending on the characteristics of the storm. The sample number for each watershed event is listed in Table 32, in the Appendix.

4.5.6. Calculating Pollutant Mass Load and Concentration

The pollutant load was defined as the amount of mass (typically µg or mg) transported by a given volume of stormwater, in a given amount of time (U.S. Environmental Protection Agency 1997). Numeric integration was used to estimate the area under the flow rate and concentration functions, which provide volume and mass values, respectively. Equation 10 shows how numeric integration can be employed in a generalized function.

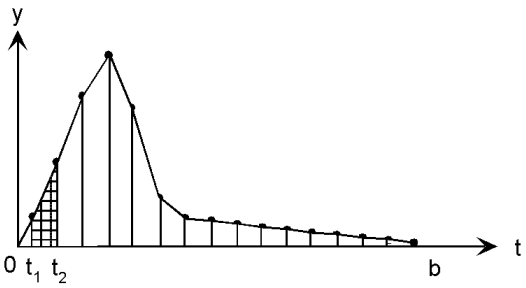

$$Area = (t_2 - t_1)\left[\frac{f(t_1) + f(t_2)}{2}\right] \quad (10)$$

The accuracy of this method increases with an increased number of samples in any given length of time (Stenstrom and Kayhanian 2005); therefore, numerous discrete samples were taken in short time increments throughout the hydrograph in a method similar to Alias et al. (2014). The total mass load was determined using Equation 11. Precipitation

depth was determined by dividing the cumulative stormwater volume by the individual contributing drainage area, which included the area of the lined conveyance strips.

$$Mass\ Load = \int_{t0}^{tn} C(t)dt\ Q(t)\ dt \tag{11}$$

Where,
C (t) is the concentration as a function of time (mg L^{-1})
Q (t) is the flow rate as a function of time (L s^{-1})

4.5.7. Partial Event Mean Concentration

The Event Mean Concentration (EMC) is often used to represent the average stormwater concentration over the course of an event, and is defined as the total cumulative pollutant mass divided by the total cumulative volume (Stenstrom and Kayhanian 2005). Volume and mass measurements used in the EMC are typically determined using flow-weighted composite sampling of an entire storm event. Composite sampling provides an adequate average representation of concentration, but does not provide any temporal information regarding the overall distribution of mass over the course of an event (Stenstrom and Kayhanian 2005).

In the partial event mean concentration (PEMC), the average concentration can be calculated for any sampled portion of the hydrograph (Lee et al. 2002; Stenstrom and Kayhanian 2005), as shown in Equation 12. The limits of the numerical integration run from the initiation of runoff (t_0) to the time at which sampling stops (t_n). When the entire event is sampled, the PEMC and EMC are equal.

$$PEMC = \int_{t_0}^{t_n} \frac{c(t)q(t)dt}{q(t)dt} = \frac{\sum_{t_o}^{t_n} m(t)}{\sum_{t_o}^{t_n} v(t)} \quad (12)$$

Where,
t_0 is the time at which the sample is collected in a storm event
t_n is the time the sampling has stopped
c is the sample concentration as a function of time (mg L^{-1})
q is the flow rate as a function of time (L s^{-1})
m is the pollutant mass delivered during a specific portion of the storm event (µg or mg)
v is the volume delivered during a specific portion of the storm event (L)

4.5.8. Mass Based First Flush

The M:V ratio is often used to portray the relative distribution of pollutant mass within a storm event, as a function of total measured runoff volume (Bach et al. 2010; Hathaway et al. 2012; Maestre and Pitt 2004). Any value over 1.0 represents a higher delivery of mass per volume of stormwater, and is considered a mass-based first flush effect (Sansalone and Cristina 2004). The M:V ratio is calculated by dividing the ratio of cumulative sample mass at time *t*, to the total cumulative mass (m), by the ratio of sample cumulative volume at time *t*, to total cumulative volume (v), as shown in Equation 13. The maximum cumulative mass load of each pollutant constituent and maximum volume measured from the site were used in order to compare the MFF effect between different storm events. The maximum mass delivered (M) for each constituent is listed in Table 9. The maximum volume measured (V) was generated from a 0.928 inch precipitation event.

$$M{:}V = \frac{\frac{\sum \int_0^{t1} C(t)Q(t)dt}{m}}{\frac{\sum \int_0^{t1} Q(t)dt}{v}} \quad (13)$$

Where,
M:V is the mass mobilized per unit of volume
C (t) is the concentration as a function of time (mg L^{-1})
Q (t) is the flow rate as a function of time (L s^{-1})
m is the maximum mass delivered (constant) (µg or mg)
v is the maximum measured (constant) runoff volume

4.5.9. Investigating the Role of Flow Rate on Mass Mobilization

In order to evaluate the strength of precipitation intensity on the mobilization of mass, the M:Q ratio was developed. The M:Q ratio is mathematically similar to the M:V ratio, and depicts the amount of mass mobilized by different flow rates. The relative strength of flow rate is measured by the ratio of sample flow rate at time *t* to the maximum event peak flow rate measured, as shown in Equation 14. The highest sampled flow rate was 2.55 L/s (0.090 cfs).

$$M{:}Q = \frac{\frac{\sum \int_0^{t1} C(t)Q(t)dt}{m}}{\frac{q(t)}{q}} \quad (14)$$

Where,
M:Q is the mass mobilized per unit of total flow rate
C (t) is the concentration as a function of time (mg L^{-1})
Q (t) is the flow rate as a function of time (L s^{-1})
m is the maximum mass delivered (constant) (µg or mg)
q (t) is the flow rate at time t (L s^{-1})
q is the peak flow rate measured (constant) (2.55 L s^{-1})

4.5.10. Statistical Analysis

All statistical analysis was conducted with JMP Pro 11.2. Normality of distributions was evaluated using the Kolmogorov-Smirnov test. Where normality could not be met, non-parametric methods were used. A non-parametric version of the paired t-test (Wilcoxon signed rank) was used to compare differences between paired repeated measures data. Spearman's rho is a non-parametric correlation method, and was used to evaluate multivariate correlations due to its strength with data that may have a non-linear characteristic, does not require normality, and is robust against the presence of outliers (Dytham 2003). Linear regression coefficents were used to estimate the magintude of change in cumualtive mass load deliverd and percent mass removed from the road surface, as a function of increasing precipitation. The probability level of $p \leq 0.05$ was accepted as significant in all tests.

4.6. Results and Discussion

4.6.1. Antecedent Environmental and Hydrologic Characteristics

Nineteen storm events were monitored across the eight sub-watersheds, for a total of 35 watershed events. The total sampled stormwater volume ranged from 13 L to 898 L, which corresponded to between 0.004 inches (0.01 cm) and 0.928 inches (2.36 cm) of precipitation in the corresponding watersheds from which those samples were taken. The event peak flow rate ranged from 0.014 Ls^{-1} to 2.55 L s^{-1}, excluding overflow events. The antecedent dry days (ADD) prior to an event ranged from 0 to 11. The antecedent precipitation condition (APC) in the prior event, ranged from 0.01 inches

(0.03 cm) to 1.61 inches (4.09 cm). The maximum daily air temperature ranged from 59 ^{o}F (15 ^{o}C) to 89 ^{o}F (31.7 ^{o}C). The antecedent conditions for each watershed event are provided in Table 31 in the Appendix.

4.6.2. Mobilization of Mass by Volume

Results indicate that some storm events exhibited a MFF effect for one or more constituents, as shown in Figure 11, however, the average M:V ratio (n = 35, n = 34 for TSS) was less than 1.0 for all N and P constituents and TSS (Table 3).

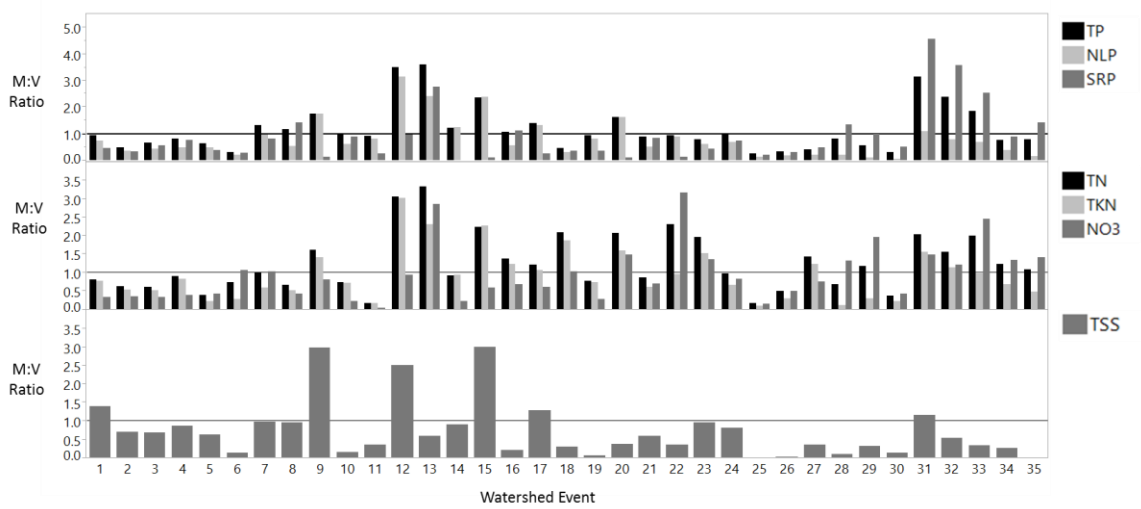

Figure 11. Average M:V ratio per watershed event. Values greater than 1.0 display a first flush.

Table 3. Summary statistics for the M:V ratios

Constituent	Measurement	Mean	Std Dev	Std Error	Upper 95% Mean	Lower 95% Mean	Number of Watershed Events Sampled
NLP	M:V	0.80	0.71	0.12	1.05	0.56	35
SRP	M:V	0.90	1.01	0.17	1.24	0.55	35
TKN	M:V	0.93	0.68	0.12	1.16	0.70	35
NO_3^-	M:V	0.95	0.75	0.13	0.69	0.69	35
TSS	M:V	0.74	0.76	0.13	1.00	0.47	34

There were no significant differences in the MFF found between constituents. Flow rate, APC, and maximum daily air temperature may have influenced the MFF of some constituents. For instance, spearman's rho results indicate that the peak flow rate per watershed event (n = 34) was found to positively correlate with the MFF for TSS (r_s = 0.57, p = 0.0005). The APC was found to negatively correlate with the MFF for SRP (r_s = -0.35, p = 0.0381) and NO_3^- (r_s = -0.40, p = 0.0175). The rainfall from a previous event would have removed some of the SRP and NO_3^-, resulting in a lower available mass at the start of the subsequent event, which weakens the MFF effect (Kang et al. 2006). The maximum daily temperature was found to positively correlate with the MFF for NLP (r_s = 0.37, p = 0.0276), TKN (r_s = 0.48, p = 0.0034) and TSS (r_s = 0.52, p = 0.0018). Temperature may have resulted in higher decomposition rates and resulting mass values, which would have strengthened the MFF effect.

Hathaway et al. (2012) also found M:V ratios less than 1.0 from storm sewer outflows with rainfall depths between of 0.79 inches and 0.90 inches. The authors found the overall strength of the MFF, although less than 1.0, to be significantly higher for TSS than for NO_3^-, and that nitrogen generally displayed a stronger MFF characteristics than phosphorus, with SRP exhibiting the weakest MFF effect (Hathaway et al. 2012). In this research, nitrogen also tended to display a higher MFF effect, but was not significantly higher than P constituents.

4.6.3. Mobilization of Mass by Flow Rate

The overall influence of flow rate on the mobilization of mass, as measured with the M:Q ratio was found to be variable, but greater than 1.0 for all constituents (Table 4).

Table 4. Summary statistics for the M:Q ratios

Constituent	Measurement	Mean	Std Dev	Std Error	Upper 95% Mean	Lower 95% Mean	Number of Watershed Events Sampled
NLP	M:Q	4.87	11.93	2.02	8.97	0.77	35
SRP	M:Q	5.80	11.00	1.86	9.57	2.02	35
TKN	M:Q	5.82	12.09	2.04	9.97	1.66	35
NO_3^-	M:Q	4.82	5.56	0.94	6.73	2.92	35
TSS	M:Q	4.84	12.83	2.20	9.32	0.37	34

There were no statistically significant differences in the M:Q ratios found between the various pollutant constituents. The average M:V and M:Q ratios from each of the 35 watershed events were compared using Wilcoxon Signed Rank. Results indicate that flow rate had a larger influence than volume on the mobilization of both labile and non-labile pollutant mass (Table 5).

Table 5. Wilcoxon signed rank comparison of the average M:V and M:Q ratios for each watershed event (n = 35).

Variable	By Variable	S	p > |S|
TP M:Q	TP M:V	217.5	<0.0001
NLP M:Q	NLP M:V	202.5	0.0002
SRP M:Q	SRP M:V	232.5	<0.0001
TN M:Q	TN M:V	209.5	<0.0001
TKN M:Q	TKN M:V	204.5	0.0001
NO3 M:Q	NO3 M:V	205.5	0.0001
TSS M:Q	TSS M:V	179.5	0.0012

These results agreed with the findings of Egodawatta et al. (2007) and Alias et al. (2014), and have important implications with regard to climate change and stormwater policy. Projected increases in precipitation intensity (Frumhoff et al. 2007; Guilbert et al. 2015)

could result in higher pollutant loads from impervious surfaces. Both precipitation volume and intensity are important considerations in the mobilization of mass and ultimately the selection of a WQv to be treated by stormwater control measures. These factors will be discussed below.

4.6.4. Pollutant Mobilization Factors and Speciation

The total cumulative pollutant mass from an event (n = 35) was found to be highly correlated with both precipitation depth and the event peak flow rate for all constituents (Table 6).

Table 6. Spearman's rho non-parametric correlations between cumulative mass, cumulative volume, and flow rate, with n = 35 for all constituents, except TSS where n = 34.

Variable	By Variable	Spearman ρ	Prob > |ρ|
TP	Precipitation	0.86	<0.0001
TP	Flow Rate	0.83	<0.0001
NLP	Precipitation	0.79	<0.0001
NLP	Flow Rate	0.84	<0.0001
SRP	Precipitation	0.79	<0.0001
SRP	Flow Rate	0.71	<0.0001
TN	Precipitation	0.89	<0.0001
TN	Flow Rate	0.76	<0.0001
TKN	Precipitation	0.87	<0.0001
TKN	Flow Rate	0.80	<0.0001
NO3	Precipitation	0.84	<0.0001
NO3	Flow Rate	0.57	<0.0001
TSS	Precipitation	0.81	<0.0001
TSS	Flow Rate	0.86	<0.0001

Slightly higher correlations were found between flow rate and non-labile pollutant fractions (i.e., NLP and TSS), as compared to labile constituents (i.e., SRP and NO_3^-), which were more highly correlated with volume. Non-labile constituents have larger mass, therefore a greater force would be necessary for transport, whereas labile constituents are highly soluble, thereby more easily transported by volume, regardless of

the rate of flow. Cumulative TKN mass was found to be more highly correlated with volume than flow rate overall, which may reflect its labile components (e.g., NH_4^+), however in other instances, it displayed more particulate characteristics. TKN is a grouped measure, which contains both labile and non-labile components, and is thus inherently more complex.

4.6.5. Antecedent Conditions

When the entire event was considered (n = 35), Spearman's rho results indicate that neither the antecedent conditions (i.e., ADD, APC), nor the maximum daily air temperature played a significant role in the pollutant mass load delivered. This is similar to the findings of others (Alias et al. 2014; Egodawatta et al. 2007). However, if one considers only the initial part of each storm (the first 0.1 inches of rainfall), the influences of antecedent and environmental factors were more prevalent than if one examines the same factors throughout the entire storm. For instance, when the individual samples from the first 0.1 inches of precipitation across the 35 events were isolated (n = 228, n = 207 for TSS), the number of antecedent dry days were found to weakly positively correlate with increasing mass load for NLP ($r_s = 0.24$, $p = 0.0002$), TKN ($r_s = 0.28$, $p<0.0001$), NO_3^- ($r_s = 0.21$, $p = 0.0014$), and TSS ($r_s = 0.22$, $p = 0.0016$). Interestingly, the ADD did not correlate with SRP. This may indicate that the build-up of SRP on the road surface may not be as strongly influenced by temporal processes. The APC weakly positively correlated with NLP ($r_s = 0.35$, $p <0.0001$), TKN ($r_s = 0.22$, $p = 0.0011$), and weakly negatively correlated with NO_3^- ($r_s = -0.18$, $p = 0.0065$). There were no correlations between APC and SRP or TSS.

The positive correlations between APC and NLP/TKN are particularly interesting, in that they may indicate that in the beginning of a storm event, the wash-off factor from the previous event is less dominant than the build-up factor between events for those constituents. The build-up factor in this case is moisture, which is known to be enhance decomposition and mineralization (Brady and Weil 2008; Davis and Cornwell 1998; Van Meeteren et al. 2007). Conversely, the negative correlation between NO_3^- mass and APC in beginning of a storm may be related to the easily transportable nature of the monovalent anion during previous events (Sollins, Homann, and B. Caldwell 1996).

Maximum daily air temperature was found to weakly positively correlate with increasing SRP mass ($r_s = 0.15$, $p = 0.0226$), TKN ($r_s = 0.20$, $p = 0.0020$), and moderately correlated with TSS ($r_s = 0.28$, $p<0.0001$) and NO_3^- ($r_s = 0.39$, $p<0.0001$) mass. This may be indicative of decomposition and mineralization processes. There was no correlation between temperature and NLP.

4.6.6. Total Mass Load of Stormwater Constituents

The total mass loads of N and P constituents (n = 35) are shown in Figure 12. Some of the factors that contributed to outliers in Figure 12 will be discussed in further sections.

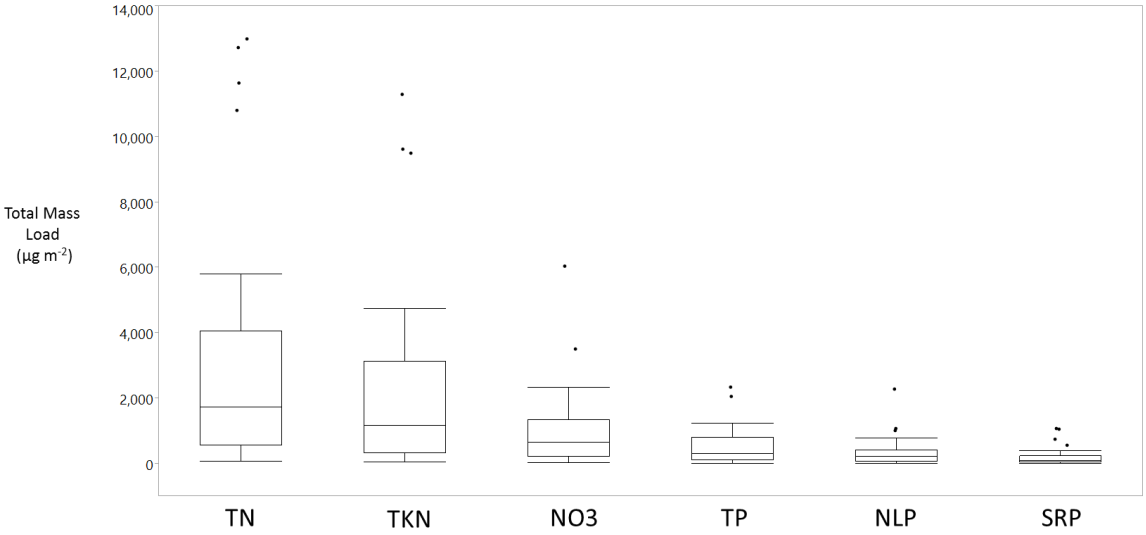

Figure 12. Box plot of cumulative stormwater mass load delivered across all watershed event (n = 35) for each nutrient constituent.

Wilcoxon signed rank results (n = 35) indicate that the cumulative TKN mass load in stormwater runoff was significantly higher than nitrate ($z = 226.50$, $p < 0.0001$), NLP ($z = 291.5$, $p < 0.0001$), and SRP ($z=297.5$, $p < 0.0001$). Nitrate mass was significantly higher than SRP ($z = 297.50$, $p < 0.0001$) and NLP ($z = 208.5$, $p < 0.0001$). Non-labile P mass was significantly higher than SRP mass ($z = 145.5$, $p = 0.0106$). Results from Spearman's rho tests (n = 35) indicate that the mobilization of TSS mass highly correlated with NLP mass ($r_s = 0.9037$, $p<0.0001$) and TKN ($r_s = 0.8671$, $p<0.0001$), but only moderately correlated with SRP ($r_s = 0.6058$, $p = 0.0001$) and NO_3^- ($r_s = 0.6128$, $p = 0.0001$).

The strong correlation between TSS and TKN is interesting, in that it suggests that TKN may have been composed of a large portion of organic N, which is different than what has been found by others (Miguntanna et al. 2013). On average (n = 35) the cumulative TN mass was composed of 63% (± 19) TKN and 37% (± 20%) NO_3^-. Total

phosphorus was composed of 63% (± 24%) NLP and 38% (± 24%) SRP. The dominance of TKN and NLP in the relative composition of TN and TP, respectively, is generally in agreement with results found by others (Maestre and Pitt 2004; Miguntanna et al. 2013; Stenstrom and Kayhanian 2005; Taylor et al. 2005). These results have encouraging implications for the magnitude of pollutant removal that is possible with GSI, which has been found to be proficient at removing large particulate fractions of pollutants (Bratieres et al. 2008; Lucas and Greenway 2008). The dominance of NLP in stormwater runoff is important to consider, for it may result in a lag between the time a storm event discharges mass to a receiving water body and the time that the non-labile P is mineralized and becomes bioavailable.

4.6.7. Predicting Total Mass Load as a Function of Precipitation

The load graph shown in Figure 13 displays the mobilization patterns of the stormwater constituents from the 35 watershed events, across a unified precipitation gradient, with TSS shown on the right vertical axis. All constituents were significantly associated with precipitation ($p<0.0001$), with linear regression coefficients and equations presented in Table 7. Conditions that influence the partitioning of labile and non-labile constituents in stormwater will be discussed in further sections.

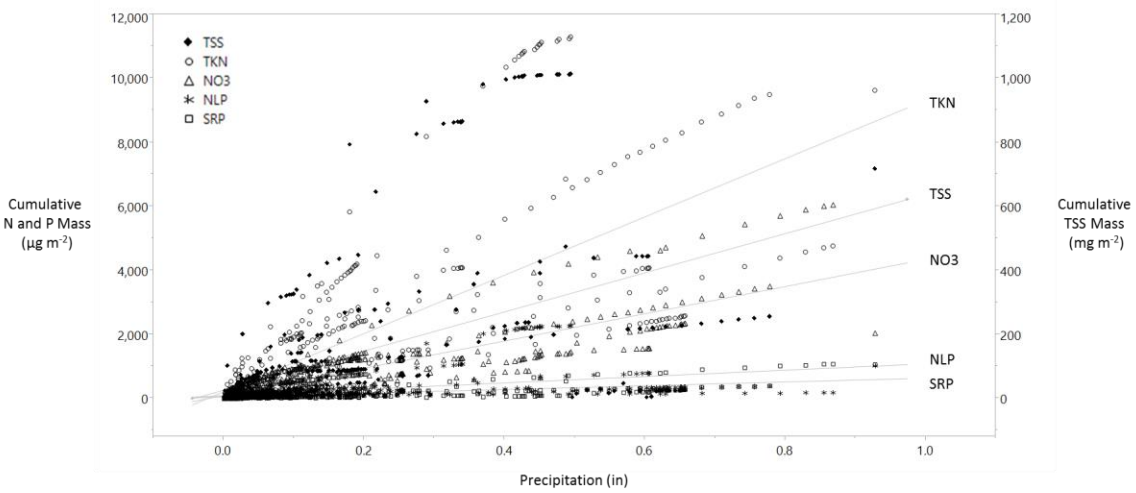

Figure 13. Cumulative TKN, NO_3^- , NLP, SRP and TSS mass per m^2 of drainage area by precipitation depth (n = 463, n = 410 for TSS) shown with the best fit line for each constituent.

Table 7. Linear regression parameters for the total cumulative mass load per m^2 of paved surface with increasing precipitation in units of inches (n = 463, n = 410 for TSS).

Parameter	unit	Linear Fit	R^2	Regression Coefficient	Standard Error	T Ratio	Prob > |t|
TP	µg m^{-2}	106.75+1,565*X	0.42	1,565	86	18.29	<0.0001
NLP	µg m^{-2}	75.03+994*X	0.21	994	89	11.21	<0.0001
SRP	µg m^{-2}	30.76+589*X	0.35	589	37	15.72	<0.0001
TN	µg m^{-2}	271.89+13,355*X	0.70	13,355	404	33.07	<0.0001
TKN	µg m^{-2}	193.75+9,106*X	0.53	9,106	401	22.70	<0.0001
NO_3^-	µg m^{-2}	79.05+4,256*X	0.72	4,256	123	34.59	<0.0001
TSS	mg m^{-2}	24.38+611*X	0.24	611	54	11.37	<0.0001

4.6.8. Conditions That Contribute to High Mass Loads

The maximum cumulative mass of all constituents mobilized across the watershed events (n = 35) are listed in Table 8. Interestingly, the peak in mass loads for the various constituents (e.g., labile and non-labile) did not occur during the same event, and seem to be driven by different processes. In the following section, two storm events are described in detail to investigate factors that contributed to the delivery of high mass loads.

4.6.8.1. Case Studies: Maximum Cumulative Mass Conditions

The highest cumulative TKN, NLP, and TSS mass values were delivered by Watershed Event 15 (n = 20, TSS n = 18), shown in Figure 14.

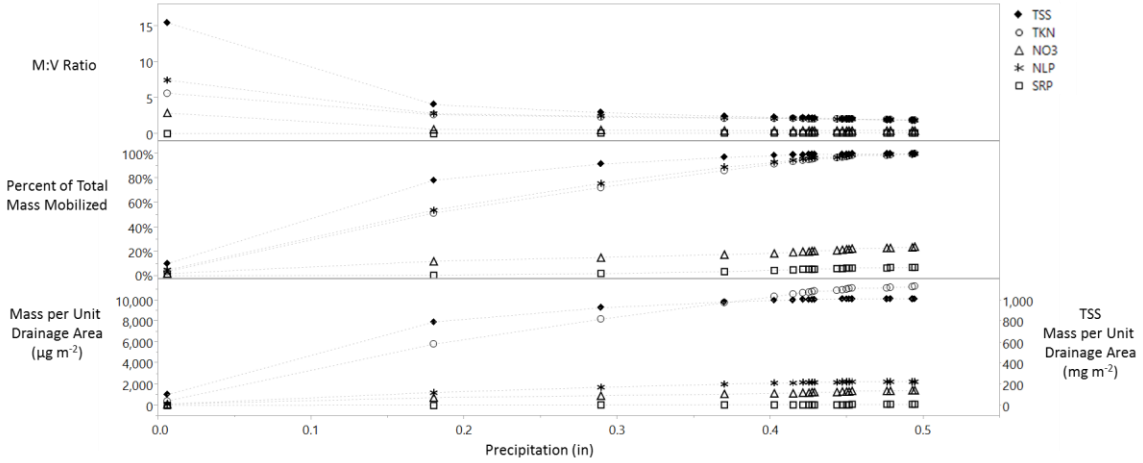

Figure 14. Watershed Event 15 (6/3/14, Cell 6): The M:V ratio (top), percent of total mass mobilized by the storm event (middle) and cumulative mass per m^2 of drainage area (bottom) (n = 20, TSS n = 18). This event delivered the highest cumulative TKN, NLP and TSS.

Watershed Event 15 can be characterized as having a high volume and high peak flow rate (both greater than the upper 95% mean for all events), with a relatively long duration of approximately 4 hours. The total precipitation depth measured during this event was 0.49 inches (1.2 cm), with a peak flow rate of 1.28 L s^{-1}, which was higher than the upper 95% mean of peak flow rates measured. The ADD was three days and the APC was 0.40 inches (1.0 cm) of rainfall. The peak daily temperature was 89 ^{o}F (32 ^{o}C). In this event, the high flow rate, combined with a high volume, likely maintained the momentum needed to transport TSS and NLP. The fact that TKN also had a peak mass load during this event, points to the non-labile characteristics of the grouped measure, which were dominant in this case.

The highest cumulative SRP and NO_3^- mass values were delivered by Watershed Event 35 (n = 22), shown in Figure 15. TSS was not measured during this storm event.

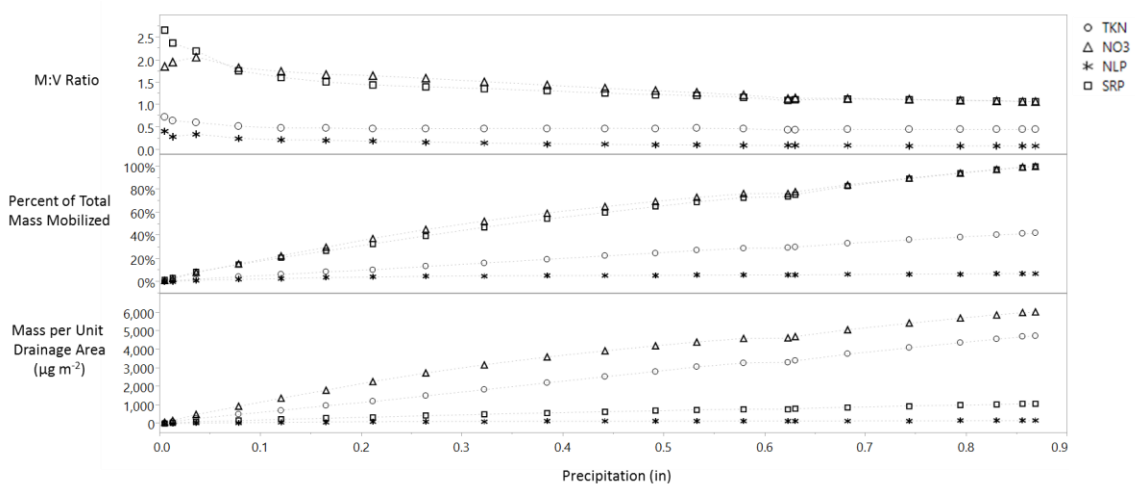

Figure 15. Watershed Event 35 (10/4/14, Cell 7): The M:V ratio (top), percent of total mass mobilized by the storm event (middle) and cumulative mass per m^2 of drainage area (bottom) (n = 22). This event delivered the highest cumulative SRP and NO_3^- mass loads.

Watershed Event 35 can be characterized as having a high volume and medium peak flow rate, with a two-part duration. The first precipitation duration lasted 28 minutes and delivered 0.58 inches (1.5 cm). There was a 52 minutes break, before the second precipitation duration, which lasted 13 minutes and delivered 0.25 inches (0.64 cm). The peak flow rate during this event was 0.4476 L s^{-1}, which was just above the lower 95% mean for peak flow rates measured. The ADD was the highest measured, at 11 days, with a low APC of 0.02 inches (0.05 cm). The maximum temperature on this day was 59 ^oF (15 ^oC). The cumulative SRP and NO_3^- mass loads may have been influenced by the wetting and rewetting sequence of the storm event, which has been shown to increase the availability of labile constituents (Peñuelas et al. 2013). It may have also been influenced by seasonal effects (Lee et al. 2004). For instance, Watershed Event 35 took place in

October, when there is an abundance of organic material available in areas adjacent to the road, which may be easily transported via wind onto the road surface. Brown et al. (2013) also found elevated concentrations of labile and non-labile P and N in runoff as a result of seasonal pollen and leaf litter deposition.

4.6.9. Comparing Pollutant Mass Build-Up Values from the Literature

There is inherent spatial and temporal variability in build-up conditions, which are influenced by land use; however, mass loads from different land use types, on a small per area basis, are needed as reference points to help predict the total mass loads from a larger drainage area. The cumulative mass build-up on a paved road found in this study were generally higher but comparable to results found by Brezonik and Stadelmann (2002), and lower than results found by Miguntanna et al. (2013) (Tables 8-9).

Table 8. Comparative literature review of initially available (build-up) mass loads per m^2 of drainage area for nutrient and sediment constituents from stormwater runoff.

Author	TP	NLP	SRP	TN	TKN	NO3	TSS
	$\mu g\ m^{-2}$	$\mu g\ m^{-2}$	$\mu g\ m^{-2}$	$\mu g\ m^{-2}$	$\mu g\ m^{-2}$	$\mu g\ m^{-2}$	$mg\ m^{-2}$
Brezonik and Stadelmann (2002), presenting results from mixed land uses	1,900	990	910	10,300	9,600	2,000	743
Miguntanna et al. (2013), presenting results from residential land use	9,380	9,240	140	37,190	27,110	1,870	2,250

Table 9. Build-up of mass per m^2 of paved road surface prior to an event.

	TP	NLP	SRP	TN	TKN	NO3	TSS
	$\mu g\ m^{-2}$	$\mu g\ m^{-2}$	$\mu g\ m^{-2}$	$\mu g\ m^{-2}$	$\mu g\ m^{-2}$	$\mu g\ m^{-2}$	$mg\ m^{-2}$
Max	2,334	2,260	1,064	12,979	11,286	6,039	1,011
Mean	529.52	337.29	193.85	3,170.51	2,254.24	925.60	170.05
Std Dev	549.62	438.49	269.62	3,660.52	2,839.25	1,168.77	249.76
Std Err	92.90	74.12	45.57	618.74	479.92	197.56	42.83
N	35	35	35	35	35	35	34

Brezonik and Stadelmann (2002) compiled runoff data from an urban and suburban database. Land use included paved surfaces as well as sites with natural features. Precipitation depths ranged from 0.001 inches to 0.91 inches. Precipitation intensity ranged from 0.01 in hr^{-1} to 1.8 in hr^{-1} (Brezonik and Stadelmann 2002). Miguntanna et al. (2013) vacuumed 3 m^2 paved road plots and used a precipitation simulator to generate different intensities. The storm durations were 40 minutes, with rainfall intensities from 0.79 in hr^{-1} to 5.31 in hr^{-1}.

4.6.10. Predicting the Percentage of Mass Removed as a Function of Precipitation

Using the maximum mass loads found in this study, the percent mass removed for each constituent across a precipitation gradient are shown in Figure 16. Linear regression was found to be significant for each constituent, as shown in Table 10.

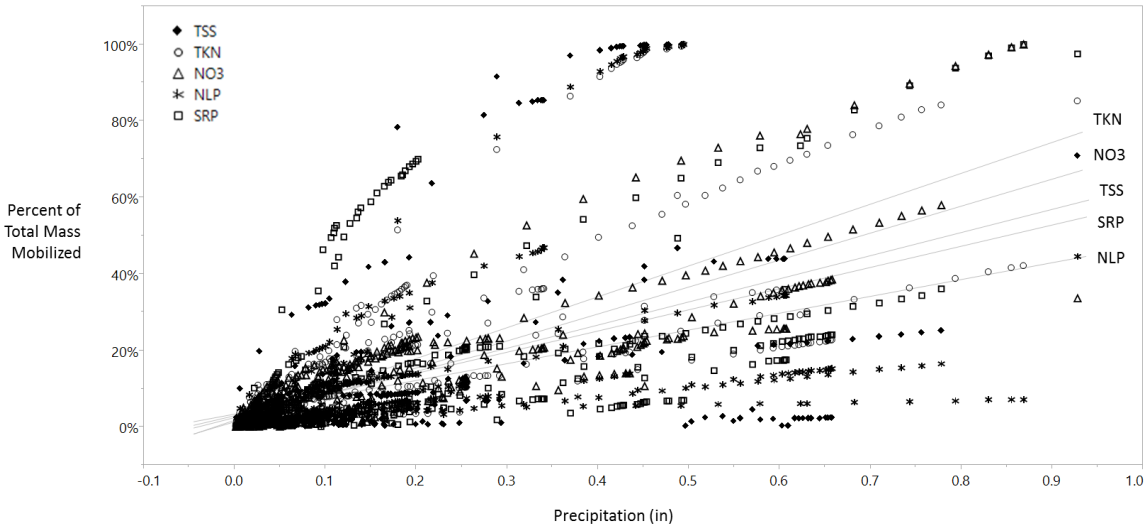

Figure 16. Percent TKN, NO_3^-, NLP, SRP and TSS mass removed by increasing precipitation (n = 463, n = 410 for TSS) shown with the best fit line for each constituent.

Table 10. Linear regression parameters for the percent of total mass removed from the paved road surface as a function of precipitation, using the maximum mass build-up from this site.

Parameter	Linear Fit	R^2	Regression Coefficient	Standard Error	T Ratio	Prob > |t|
TP	0.0457 + 0.6705*X	0.42	0.6705	0.0367	18.29	<0.0001
NLP	0.0334+0.4399*X	0.21	0.4399	0.0393	11.21	<0.0001
SRP	0.0289+0.5540*X	0.35	0.5540	0.0352	15.72	<0.0001
TN	0.0209+1.0290*X	0.70	1.0290	0.0311	33.07	<0.0001
TKN	0.0172+0.8068*x	0.53	0.8068	0.0355	22.70	<0.0001
NO_3^-	0.0131+0.7047*X	0.72	0.7047	0.0204	34.59	<0.0001
TSS	0.0241+0.6047*X	0.24	0.6047	0.0534	11.37	<0.0001

In this linear model, 0.5 inches of precipitation is predicted to remove approximately 38% of TP, 25% of NLP, 31% SRP, 54% of TN, 42% of TKN, and 37% of NO_3^- mass. These results clearly dispute the commonly held assumption that 90% of the pollution will be mobilized by 0.5 inches of precipitation (Bach et al. 2010; Bertrand-Krajewski et al. 1998).

4.6.11. Stormwater Partial Event Mean Concentration (PEMC)

The PEMC across the watershed events was variable, as can be seen in Figures 17 a, b, and c. The average pollutant concentrations across the monitored precipitation depths in this study (PEMC) (Table 11) were on the low side overall, when compared to "full" EMC values from the literature (Table 12). TP, NLP, and SRP concentrations were similar to Hunt et al. (2006). TN and TKN constituents were slightly lower than EMC values reported in the national stormwater data compiled by Geosyntec Consultants and Wright Water Engineers (2012), but NO_3^- concentrations were higher than Davis (2007). TSS values were slightly lower than Davis (2007).

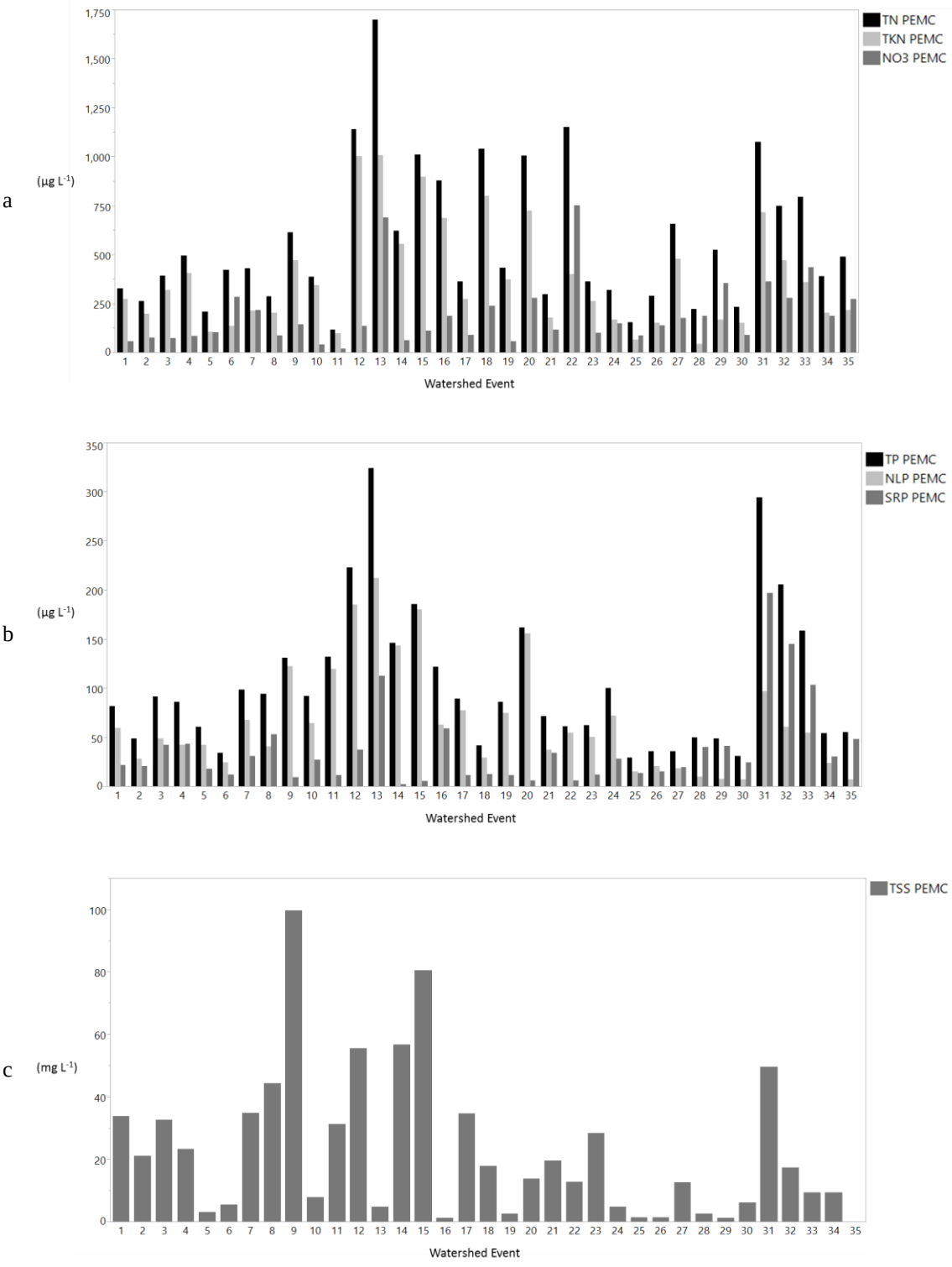

Figure 17 a, b, and c. Inflow TN, TKN, NO3 (a), TP, IP, SRP (b) and TSS (c) partial event mean concentration for each watershed event.

Table 11. Summary statistics for the partial event mean concentration (PEMC) from 2013 to 2014.

PEMC							
	TP	NLP	SRP	TN	TKN	NO3	TSS
	$\mu g\ L^{-1}$	$\mu g\ L^{-1}$	$\mu g\ L^{-1}$	$\mu g\ L^{-1}$	$\mu g\ L^{-1}$	$\mu g\ L^{-1}$	$mg\ L^{-1}$
Mean	104.33	66.82	37.99	570.18	380.22	195.53	23.07
Std Dev	73.00	54.21	42.76	361.17	267.64	165.80	23.61
Std Err	12.34	9.16	7.23	61.05	45.24	28.03	4.05
Upper 95% Mean	129.41	85.44	52.68	694.25	472.15	252.49	31.30
Lower 95% Mean	79.26	48.19	23.30	446.11	288.28	138.57	14.83
Number of watershed events	35	35	35	35	35	35	34

Table 12. Comparative literature review of inflow EMC results, in ascending order by TP concentration. NLP was derived from TP-SRP.

Author	TP	NLP	SRP	TN	TKN	NO3	TSS	Avg Rainfall Depth	Notes
	µg/L	µg/L	µg/L	µg/L	µg/L	µg/L	(mg/L)	(in)	
Dietz and Clausen (2005)	19	-	-	1,200	700	500	-	-	Roof runoff
Alias et al. (2014)	74	-	-	1,170	-	-	40.54	0.099	Average of all sites
Hunt et al. (2006)	105	52	53	1,310	880	420	-	1.49	Average of all sites
Geosyntec Consultants and Wright Water Engineers (2012)	110	100	10	1,250	940	260	37.5	-	Median bioretention
Passeport et al. (2009)	137	80	57	1,662	1,106	419	-	-	Average Inflow
Hathaway et al. (2012)	195	135	60	-	1,510	360	91.35	0.831	Average of all sites
Geosyntec Consultants and Wright Water Engineers (2008)	250	160	90	940	1,800	590	52.15	-	Average Inflow
Bratieres et al. (2008)	427	300	127	2,210	-	790	160	-	Laboratory Synthetic stormwater
Brezonik and Stadelmann (2002)	580	380	200	3,080	2,620	530	184	0.9055 (Max)	Average of all sites
Alias et al. (2014)	743	-	-	1,167	-	-	40.54	0.0993	Average of all events
Davis (2007)	1,200	-	-	-	-	133	37.17	-	Average of all events
Lee and Bang (2000)	6,670	2,878	3,792	-	12,417	620	172	-	Average of all sites

4.7. Conclusions

The composition of stormwater from the small, paved, low to medium traffic roadway drainage arewas that were analyzed in our study was found to be dominated by TKN, NO_3^-, NLP, and SRP in descending order. Stormwater was found to contain approximately six times more TN mass than TP, with the majority of TN being comprised of TKN, and the majority of TP being comprised of NLP. The overall dominance of non-labile constituents in stormwater is encouraging as green stormwater infrastructure techniques have been shown to be effective at removing this fraction of stormwater pollutants.

Precipitation intensity (measured as flow rate) and volume were both highly correlated with mass for all constituents, and precipitation intensity was found to have a stronger influence on pollutant mobilization than volume, although it was not typically sustained throughout the storm events monitored. This has important implications, as larger pollutant mass loads could be generated by projected increases in precipiation intensity as a result of climate change.

Pollutant contituents were found to have distinct mobilization patterns, with NLP, TKN, and TSS being more closely correlated with flow rate, while SRP and NO_3^- were more closely correlated with volume. TSS mass mobilization was highly correlated with NLP and less so with SRP and NO_3^-, indicating that NLP may be able to be accurately modelled as a particle, but labile constituents (i.e., SRP and NO_3^-) should be seperately considered. TKN exhibited both labile and non-labile characteristics, as a grouped measure. A small portion of the mass build-up on the road surface was

influenced by the number of antecedent dry days, antecedent precipitation conditions, and temperature; however, their influence appears to be limited to the beginning of a storm event, and did not have a significant influence on the total mass load measured over a longer duration of an event.

The total mass upon the road surface in this study may not have been completely mobilized, and may have been lower than loads found elsewhere, yet it is clear, that pollutant mass was not entirely depleted from the paved road surface during the majority of storm events. A mass-based first flush was seen for some constituents during some storm events, however, the MFF was not observed for labile N and P constituents or TSS overall, and the strength of the MFF was not significantly different between pollutant constituents.

More research is needed to estimate the precipitation volume that would be required to remove total mass build-up of different forms of pollution (e.g., labile and non-labile) from the road surface, and from other land use types. Based on this research, the FF concept may not be an adequate method for determining a WQv to treat pollutant mass from a paved road surface.

REFERENCES

Alias, N., Liu, A., Egodawatta, P., and Goonetilleke, A. (2014). "Sectional analysis of the pollutant wash-off process based on runoff hydrograph." *Journal of Environmental Management*, 134, 63–9.

Antonio, A., and Walker, D. (2011). *Total Kjeldahl Nitrogen: Simplified with s-TKN ™*.

APHA. (1992). *Standard Methods for the Examination of Water and Wastewater*. American Public Health Association, Washington, D.C.

APHA. (2011). *Standard Methods for the Examination of Water and Wastewater*. American Public Health Association, Washington, D.C.

Bach, P. M., McCarthy, D. T., and Deletic, A. (2010). "Redefining the stormwater first flush phenomenon." *Water Research*, 44(8), 2487–98.

Bertrand-Krajewski, J.-L., Chebbo, C., and Saget, A. (1998). "Distribution of pollutant mass vs volume in stormwater discharges and the first flush phenomenon." *Water Resources*, 32(8), 2341–2356.

Blecken, G.-T., Zinger, Y., Deletić, A., Fletcher, T., and Viklander, M. (2009). "Influence of intermittent wetting and drying conditions on heavy metal removal by stormwater biofilters." *Water Research*, 43(18), 4590–8.

Brady, N. C., and Weil, R. R. (2008). *The nature and properties of soils*. Prentice Hall, Upper Saddle River.

Bratieres, K., Fletcher, T., Deletic, A., and Zinger, Y. (2008). "Nutrient and sediment removal by stormwater biofilters: a large-scale design optimisation study." *Water Research*, 42(14), 3930–40.

Brezonik, P. L., and Stadelmann, T. H. (2002). "Analysis and predictive models of stormwater runoff volumes, loads, and pollutant concentrations from watersheds in the Twin Cities metropolitan area, Minnesota, USA." *Water Research*, 36(7), 1743–57.

Brown, R. A., Birgand, F., and Hunt, W. F. (2013). "Analysis of consecutive events for nutrient and sediment treatment in field-monitored bioretention cells." *Water, Air, and Soil Pollution*, 224(6), 1581.

Charbeneau, R. J., and Barrett, M. E. (1998). "Evaluation of methods for estimating stormwater pollutant loads." *Water Environment Research*, 70(7), 1295–1302.

Davis, A. P. (2007). "Field performance of bioretention: water quality." *Environmental Engineering Science*, 24(8), 1048–1064.

Davis, M., and Cornwell, D. (1998). *Inroduction to environmental engineering*. McGraw-Hill, Boston.

DeBusk, K., and Wynn, T. (2011). "Storm-water bioretention for runoff quality and quantity mitigation." *Journal of Environmental Engineering*, 137(September), 800–808.

Deletic, A. (1998). "The first flush load of urban surface runoff." *Water Research*, 32(8), 2462–2470.

Dietz, M., and Clausen, J. (2005). "A field evaluation of rain garden flow and pollutant treatment." *Water, Air, and Soil Pollution*, 167(1-4), 123–138.

Dillon, K. S., and Chanton, J. P. (2005). "Nutrient transformations between rainfall and stormwater runoff in an urbanized coastal environment: Sarasota Bay, Florida." *Limnology and Oceanography*, 50(1), 62–69.

Dytham, C. (2003). *Choosing and using statistics: A biologist's guide*. Blackwell Publishing, Malden, MA.

Egodawatta, P., Thomas, E., and Goonetilleke, A. (2007). "Mathematical interpretation of pollutant wash-off from urban road surfaces using simulated rainfall." *Water Research*, 41(13), 3025–31.

Francey, M. (2010). "Characterising Urban Pollutant Loads." *Masters Thesis*, Monash University.

Frumhoff, P., Mccarthy, J. J., Melillo, J. M., Moser, S. C., and Wuebbles, D. J. (2007). *Confronting climate change in the U.S. northeast*. *Northeast Climate Impacts Assessment*.

Geosyntec Consultants, and Wright Water Engineers. (2008). *Overview of Performance by BMP Category and Common Pollutant Type*. *International Stormwater Best Management Practices (BMP) Database*.

Geosyntec Consultants, and Wright Water Engineers. (2012). *International Stormwater Best Management Practices (BMP) Database Pollutant Category Summary Statistical Addendum: TSS, Bacteria, Nutrients, and Metals*.

Glysson, G. D., Gray, J. R., and Conge, L. M. (2000). *Adjustment of total suspended solids data for use in sediment studies*. *Building Partnerships*, American Society of Civil Engineers, Reston, VA.

Guilbert, J., Betts, A., Rizzo, D., Beckage, B., and Bomblies, A. (2015). "Characterization of increased persistence and intensity of precipitation in the northeastern United States." *Geophysical Research Letters*, 1888–1893.
Gupta, K., and Saul, A. (1996). "Specific relationships for the first flush load in combined sewer flows." *Water Resources*, 1354(95), 1244–1252.
Hathaway, J. M., Tucker, R. S., Spooner, J. M., and Hunt, W. F. (2012). "A traditional analysis of the first flush effects for nutrients in stormwater runoff from two small urban catchments." *Water, Air, and Soil Pollution*, 223(9), 5903–5915.
Havens, K. E., James, R. T., East, T. L., and Smith, V. H. (2003). "N:P ratios, light limitation, and cyanobacterial dominance in a subtropical lake impacted by non-point source nutrient pollution." *Environmental Pollution*, 122(3), 379–90.
Henderson, C., Greenway, M., and Phillips, I. (2007). "Removal of dissolved nitrogen, phosphorus and carbon from stormwater by biofiltration mesocosms." *Water Science & Technology*, 55(4), 183.
Herngren, L. F. (2005). "Build-up and wash-off process kinetics of PAHs and heavy metals on paved surfaces using simulated rainfall." *Masters Thesis*, Queensland University of Technology.
Hunt, W. F., Jarrett, A. R., Smith, J. T., and Sharkey, L. J. (2006). "Evaluating bioretention hydrology and nutrient removal at three field sites in North Carolina." *Journal of Irrigation and Drainage Engineering*, 132(6), 600–608.
Kang, J.-H., Kayhanian, M., and Stenstrom, M. K. (2006). "Implications of a kinematic wave model for first flush treatment design." *Water Research*, 40(20), 3820–30.
Kang, J.-H., Kayhanian, M., and Stenstrom, M. K. (2008). "Predicting the existence of stormwater first flush from the time of concentration." *Water Research*, 42(1-2), 220–8.
Kayhanian, M., Suverkropp, C., Ruby, a., and Tsay, K. (2007). "Characterization and prediction of highway runoff constituent event mean concentration." *Journal of Environmental Management*, 85, 279–295.
LeBoutillier, D. W., Kells, J. a., and Putz, G. J. (2000). "Prediction of pollutant load in stormwater runoff from an urban residential area." *Canadian Water Resources Journal*, 25(April 2015), 343–359.
Lee, H., Lau, S.-L., Kayhanian, M., and Stenstrom, M. K. (2004). "Seasonal first flush phenomenon of urban stormwater discharges." *Water Research*, 38(19), 4153–63.
Lee, J. H., and Bang, K. W. (2000). "Characterization of urban stormwater runoff." *Water Resources*, 34(6), 1773–1780.
Lee, J. H., Bang, K. W., Ketchum, L. H., Choe, J. S., and Yu, M. J. (2002). "First flush analysis of urban storm runoff." *The Science of the Total Environment*, 293(1-3), 163–75.
Lefevre, G. H., Paus, K. H., Natarajan, P., Gulliver, J. S., Novak, P. J., and Hozalski, R. M. (2015). "Review of dissolved pollutants in urban storm water and their removal and fate in bioretention cells." *Journal of Environmental Engineering*, 141.
Lucas, W. C., and Greenway, M. (2008). "Nutrient retention in vegetated and nonvegetated bioretention mesocosms." *Journal of Irrigation and Drainage Engineering*, 134(5), 613–623.
Maestre, A., and Pitt, R. (2004). *Nonparametric Statistical Tests Comparing First Flush and Composite Samples from the National Stormwater Quality Database*. *Stormwater and Urban Water Systems Modeling*.
Van Meeteren, M. M., Tietema, A., and Westerveld, J. W. (2007). "Regulation of microbial carbon, nitrogen, and phosphorus transformations by temperature and moisture during decomposition of Calluna vulgaris litter." *Biology and Fertility of Soils*, 44, 103–112.
Miguntanna, N. P., Liu, A., Egodawatta, P., and Goonetilleke, A. (2013). "Characterizing nutrients wash-off for effective urban stormwater treatment design." *Journal of Environmental Management*, 120, 61–7.
Paerl, H. W. (2006). "Assessing and managing nutrient-enhanced eutrophication in estuarine and coastal waters : Interactive effects of human and climatic perturbations." *Ecological Engineering*, 26, 40–54.
Passeport, E., Hunt, W. F., Line, D. E., Smith, R. A., and Brown, R. A. (2009). "Field study of the ability of two grassed bioretention cells to reduce storm-water runoff pollution." *Journal of Irrigation and Drainage Engineering*, 135(August), 505–510.
Patton, C., and Kryskalla, J. (2003). *Methods of Analysis by the U.S. Geological Survey National Water*

Quality Laboratory - Evaluation of alkaline persulfate digestion as an alternative to kjeldahl digestion for determination of total and dissolved nitrogen and phosphorous in water. *U.S. Geological Survey Water-Resouces Investigations Report 03-4174*.

Peñuelas, J., Poulter, B., Sardans, J., Ciais, P., van der Velde, M., Bopp, L., Boucher, O., Godderis, Y., Hinsinger, P., Llusia, J., Nardin, E., Vicca, S., Obersteiner, M., and Janssens, I. (2013). "Human-induced nitrogen-phosphorus imbalances alter natural and managed ecosystems across the globe." *Nature Communications*, 4, 2934.

Roy-Poirier, A. (2009). "Bioretention for phosphorus removal: Modelling stormwater quality improvements." *Masters Thesis*, Queen's University, Canada.

Sansalone, J. J., and Cristina, C. M. (2004). "First flush concepts for suspended and dissolved solids in small impervious watersheds." *Journal of Environmental Engineering*, 130(November), 1301–1314.

Smith, V. H., Tilman, G. D., and Nekola, J. C. (1999). "Eutrophication: impacts of excess nutrient inputs on freshwater, marine, and terrestrial ecosystems." *Environmental Pollution*, 100(1-3), 179–96.

Sollins, P., Homann, P., and Caldwell, B. (1996). "Stabilization and destabilization of soil organic matter: mechanisms and controls." *Geoderma*, 74(1-2), 65–105.

Spivakov, B. Y., Maryutina, T. a., and Muntau, H. (1999). "Phosphorus speciation in water and sediments." *Pure and Applied Chemistry*, 71(11), 2161–2176.

Stenstrom, M., and Kayhanian, M. (2005). *First flush phenomenon characterization*. Sacramento.

Taylor, G. D., Fletcher, T. D., Wong, T. H. F., Breen, P. F., and Duncan, H. P. (2005). "Nitrogen composition in urban runoff-implications for stormwater management." *Water Research*, 39(10), 1982–9.

Turner, R., and Rabalais, N. (2013). "Nitrogen and phosphorus phytoplankton growth limitation in the northern Gulf of Mexico." *Aquatic Microbial Ecology*, 68(2), 159–169.

U.S. Bureau of Reclamation. (2001). *Water Measurement Manual*. U.S. Government Printing Office, Washington, D.C.

U.S. Environmental Protection Agency. (1997). "Load Estimation Techniques." *National Management Measures to Control Nonpoint Pollution from Agriculture*, 225–242.

U.S. Environmental Protection Agency. (1998). *Report of the Federal Advisory Committee on the Total Maximum Daily Load (TMDL) Program*.

U.S. Environmental Protection Agency. (2008). *TMDLs to Stormwater Permits Handbook*.

Vaze, J., and Chiew, F. (2003a). "Study of pollutant washoff from small impervious experimental plots." *Water Resources Research*, 39(6).

Vaze, J., and Chiew, F. (2003b). "Comparative evaluation of urban storm water quality models." *Water Resources Research*, 39(10), 1–10.

Vermont Agency of Natural Resources. (2002). *The Vermont Stormwater Management Manual Volume I - Stormwater Treatment Standards*.

CHAPTER 5: EVALUATING CRITICAL BIORETENTION DESIGN FEATURES IN THE CONTEXT OF CLIMATE CHANGE

Amanda L. Cording

Keywords: *Bioretention, climate change, labile nutrients, phosphorus sorption, denitrification, plant uptake*

Abstract

Bioretention is a stormwater management tool that is becoming increasingly popular in both the private and public sectors, yet there are many unanswered questions regarding the factors that contribute to performance variability, and resiliency in the face of projected increases in precipitation due to climate change in the northeastern U.S. It is also unclear if bioretention systems, like wetlands, will be a source of greenhouse gas emissions. This research evaluated how critical design factors, such as soil media and vegetation, influenced hydrologic performance (i.e., reduction in peak flow rate and volume) and the removal of total suspended solids and nutrients (N and P species), and greenhouse gas (GHG; nitrous oxide, methane and carbon dioxide) emissions, from stormwater under ambient and increased water inputs (i.e., rainfall plus runoff). A conventional, sand and compost based, bioretention soil media was compared to a proprietary media designed to remove phosphorus, Sorbtive Media™. Two vegetation mixes were also compared for sediment and nutrient retention.

Non-labile phosphorus, total suspended solids, and total Kjeldahl nitrogen mass were well retained by all treatments, including under simulated increases in precipitation. However, the compost amendment in the conventional soil media was found to release labile nitrogen and phosphorus, far surpassing the mass loads in incoming stormwater. When compared with conventional media, Sorbtive Media™ was highly effective at removing labile phosphorus and was also found to enhance nitrate removal. Deep rooted systems containing *Panicum virgatum* (Switchgrass) were found to be particularly effective at removing both labile and non-labile constituents. Overall, none of the bioretention treatments were found to be a significant source of N_2O and were small sinks for CH_4 in most treatments. Overall, this research shows that bioretention cells are an important tool in increasing local climate change resiliency, with regards to increases in precipitation in the northeastern U.S., and that the selection of vegetation and soil media highly influences the overall removal of labile nutrients.

5.1. Introduction

5.1.1. Stormwater and Climate Change

In the northeastern United States, precipitation has increased by 5-10 percent since 1900 (Frumhoff et al. 2007). This trend is predicted to continue under both high and low greenhouse gas (GHG) emission scenarios (Frumhoff et al. 2007; Guilbert et al. 2015). Changes in precipitation due to climate change are likely to have a direct impact on stormwater volumes and velocities in the urban landscape, which have already been severely altered by impervious surfaces (e.g., roads, rooftops, parking lots and driveways). Masterson and Bannerman (1994) have shown > 200% increases in stream flow rates after a storm event, from pre to post development (Masterson and Bannerman 1994). High stormwater velocities mobilize and transport pollutants e such as non-labile phosphorus (NLP), soluble reactive phosphorus (SRP), organic nitrogen (ON), total Kjeldahl nitrogen (TKN), nitrite (NO_2^-), nitrate (NO_3^-), total suspended solids (TSS), cadmium (Cd), chromium (Cr), copper (Cu), lead (Pb), mercury (Hg), zinc (Zn), polychlorinated biphenyls (PCB's), polycyclic aromatic hydrocarbons (PAHs), as well as long chain hydrocarbons (oil/grease), bacteria, and pathogens from impervious surfaces (National Research Council 2008; U.S. Environmental Protection Agency 1998). Thousands of waterbodies in the United States are already categorized as "impaired" and have been required to develop a pollution budget, called a total maximum daily load (TMDL) (U.S. Environmental Protection Agency 2008). Increased precipitation due to climate change may exacerbate already challenging water quality impairment problems in some regions.

Bioretention systems, also known as rain gardens (Davis 2008; Dietz and Clausen 2006; Hunt et al. 2008), biofilters (Zinger et al. 2013), and bioswales (Collins et al. 2010), are composed largely of soil media and vegetation that are intended to remove stormwater pollutants while also retaining and detaining stormwater volumes and reducing peak runoff velocities to more closely mimic pre-development hydrology. Bioretention systems are one type of physical practice listed within the broader category of alternative stormwater infrastructure termed Green Stormwater Infrastructure (GSI) (Nylen and Kiparsky 2015; Palmer 2012) or Water Sensitive Urban Design (WSUD) (Alias et al. 2014; Blecken et al. 2009; Taylor and Wong 2002; Wong 2006), which falls under the broader alternative approach to traditional land development called Low Impact Development (LID) (Brown and Hunt 2011; Dietz 2007). In addition to improving water quality, bioretention systems can serve as a public amenity, providing improved aesthetics and habitat value to pollinators and other wildlife (U.S. Environmental Protection Agency 2015).

These systems are rapidly growing in popularity, in both the public and private sectors, and are encouraged by stormwater regulators as a Best Management Practice (BMP) under the National Pollutant Discharge Elimination System (NPDES) (National Research Council 2008). The NPDES program is under the umbrella of the Clean Water Act (CWA) and is the primary vehicle through which the federal government regulates the quality of the nation's waterbodies (National Research Council 2008). Despite being widely promoted, and required in some instances, there are still many unknowns regarding the strengths, limitations, and resiliency of bioretention systems.

5.1.2. Bioretention Design Features and Performance Review

Some of the many design features that affect the pollutant removal performance of bioretention, and other GSI systems, include: residence time (Collins et al. 2010; Hurley and Forman 2011; Kadlec et al. 2010; Rosenquist et al. 2010; Sansalone and Cristina 2004); media depth (Brown and Hunt 2011); vegetation type, root depth, type and architecture (Claassen and Young 2010; Claytor and Schueler 1996; Collins et al. 2010; Davidson et al. 2000; Davis et al. 2009; Kadlec et al. 2010; Lucas and Greenway 2008; Read et al. 2008); organic matter content (Bratieres et al. 2008; DeBusk and Wynn 2011; Fassman et al. 2013; Leytem and Bjorneberg 2009; Thompson et al. 2008); use of mulch (Bratieres et al. 2008; DeBusk et al. 2011; Dietz and Clausen 2006); percent sand, silt and clay (Liu et al. 2014); chemical characteristics of the soil media (e.g., amount of iron, calcium, and aluminum) (Arias et al. 2001; Groenenberg et al. 2013; Vance et al. 2003); ponding depth, hydraulic conductivity and infiltration rate (Thompson et al. 2008); and the inclusion of features such as an internal water storage zone (IWS) (Chen et al. 2013; Dietz and Clausen 2006; Hunt et al. 2006; Kim et al. 2003). Proper maintenance and care taken during construction to avoid soil compaction are also critical factors that will affect the long term performance of bioretention (Brown and Hunt 2011; Dietz and Clausen 2006).

Each of the design features listed above plays an important role in the performance of bioretention systems, yet they are not always complementary. For example, phosphorus reduction via sorption can be reversed under reduced conditions

(Basta and Dayton 2007), yet prolonged saturation is required for denitrification (Thomson et al. 2012). A critical review of select design features is provided below.

5.1.2.1 Particulate Pollutant Removal Mechanisms

It is understood that sediments or total suspended solids (TSS) in stormwater are typically removed through extended detention and physical filtration of fine particles within the bioretention soil media; removal rates between 70% and 99% are common (Bratieres et al. 2008; Brown and Hunt 2011; Hatt et al. 2008; Hsieh and Davis 2006). Extreme drying conditions have been shown to negatively impact TSS removal performance in soils with higher clay content (Blecken et al. 2009),or as drying increases the size of macropore channels, which may release previously removed sediment in the next storm event (Lintern et al. 2011). It is possible that the non-labile fractions of N and P may have similar removal mechanisms as TSS, based on their inherently larger particle sizes (Chen et al. 2013; Claytor and Schueler 1996; Davis 2007; Zinger et al. 2013), although the sand-dominated bioretention soil media used in this research is not likely to exhibit extreme shifts in macropore size due to drying. The distinctive removal mechanisms of the different fractions of N and P are not well characterized within bioretention (Brown et al. 2013; Lefevre et al. 2015).

5.1.2.2 The Role of Vegetation in Pollutant Removal

Many stormwater and LID design manuals specify that bioretention systems should be planted (Collins et al. 2010; Davis et al. 2001, 2006; Dietz and Clausen 2005, 2006; Dietz 2007; Hatt et al. 2008; Hunt et al. 2006; Kim et al. 2003), yet few go as far as to specify the pollutant removal benefits that different vegetation types (e.g., ground

cover, shrubs, perennials, or trees) might provide (Dietz and Clausen 2005). Vegetation plays a significant role in the removal of labile N and P (Lintern et al. 2011) from the soil pore water stored between precipitation events (Serna et al. 1992); yet nutrient uptake is highly variable and dependent on root architecture, biomass, depth and type (e.g., fibrous vs woody) (Brix 1994, 1997; Le Coustumer et al. 2012; Dietz and Clausen 2006; Read et al. 2008; Tanner 1996).

Read et al. (2008) found that pollutant concentration in the effluent from bioretention negatively correlated with root mass for nearly all N and P constituents, with root mass explaining 20 – 37% of the variation in effluent concentration. The authors suggest that deep rooted plants may provide important long term performance benefits to bioretention systems. Most plants favor shallow rooting depths due to lower energy costs for development and maintenance, short-term access to nutrients, close proximity to incoming water, and high oxygen content in upper soil horizons (Edwards 1992; Preti et al. 2010; Schenk 2008). However, evidence also suggests that long-term nutrient availabilities (P, Ca^{2+}, K^{+}, and Mg^{2+}) tend to be greater at depth in semi-arid and arid ecosystems (McCulley et al. 2004), which may be homologous to the sand-based systems commonly used in bioretention (Houdeshel et al. 2015). Certain plants, such as switchgrass (*Panicum virgatum*), may have adapted deep roots to adjust to this type of environment (Preti et al. 2010; Schenk 2008).

Thick-rooted plants have been shown to help maintain long-term soil permeability and reduce clogging of bioretention systems (Le Coustumer et al. 2012). By contrast, fine-stemmed vegetation such as grasses, sedges, and rushes have been shown to

be highly efficient at providing above-ground filtering capacity (Gagnon et al. 2012). Our current understanding of the role of vegetation in removing labile pollutants in bioretention systems in extremely limited (Lefevre et al. 2015), and warrants further investigation.

5.1.2.3. Bioretention Soil Media and the Addition of Organic Amendments

The engineered soil media used in bioretention designs varies, and may include native soil removed during construction (Dietz 2007) and/or imported material, such as in the cases when native soil infiltration rates are not optimal. Use of imported sand based media is common and the addition of an organic amendment is often recommended (Bratieres et al. 2008; DeBusk and Wynn 2011; Michigan Department of Environmental Quality 2008; Thompson et al. 2008; Vermont Agency of Natural Resources 2002a; Washington State University Pierce County Extension 2012).

Organic matter (e.g., compost, mulch) provides nutrients to plants during the establishment phase, soil moisture retention, cation exchange capacity and fosters microbial growth (Kim et al. 2003; Lintern et al. 2011). Thompson et al. (2008) found that the addition of compost in bioretention increased saturated hydraulic conductivity, aggregate stability, and water holding capacity, and decreased bulk density. Mulch is often included in the surface of bioretention designs to retain moisture and subdue weed growth, as one would use mulch in a traditional landscaping setting (Davis et al. 2001, 2006; Dietz and Clausen 2005, 2006; Dietz 2007; Hunt et al. 2006). While mulch and other organic amendments have been shown to be highly effective at removing metals (Hsieh and Davis 2006; Muthanna et al. 2007; Seelsaen et al. 2006), there is concern that

the benefits provided by organic amendments may be undone by their potential to release nutrients (Hunt et al. 2006; Lefevre et al. 2015). The following section reviews the nutrient retention and export associated with bioretention soil media.

5.1.2.4. Inconsistent Labile N and P Removal in Bioretention

Soils and organic amendments contain two major nutrient pools: 1) insoluble particulate organic and inorganic N and P (non-labile) and 2) dissolved organic and inorganic N and P (labile), which are in soil solution. The organic portion of the pool in traditional soils is variable, usually ranging from 20% to 80% (Schachtman et al. 1998). SRP, NO_3^-, and NH_4^+ are examples of inorganic labile nutrients that can be leached from the soil profile during a storm event (Schachtman et al. 1998). Total Kjeldahl nitrogen is a grouped measure, and contains both labile (NH_3, NH_4^+) and non-labile (organic nitrogen) components, making it more complex. Labile nutrients removed within the bioretention soil media by vegetative uptake or absorption within the soil itself (i.e., water holding capacity of the soil) may be replaced by the decomposition and mineralization of any organic matter present within the soil (Basta and Dayton 2007). If plant uptake and water retention process are les dominant than decomposition and mineralization, labile forms of N and P may not be well retained by bioretention systems (Blecken et al. 2010; Clark and Pitt 2009; Dietz and Clausen 2005; Hsieh and Davis 2003, 2006; Hunt et al. 2006; Lucas and Greenway 2011).

As outlined in the latest review of bioretention performance by Lefevre et al. (2015), labile nitrogen and phosphorus removals reported to date have been extremely variable, ranging from -630% to 98% for nitrate and from -78% to 98% for SRP

(Bratieres et al. 2008; Dietz and Clausen 2005; Geosyntec Consultants and Wright Water Engineers 2012; Hatt et al. 2008; Hunt et al. 2006; Li and Davis 2009). Geosyntec Consultants and Wright Water Engineers (2012) conducted a comprehensive review of the International Stormwater BMP Database and found a net export of labile P from bioretention overall. Bratieres et al. (2008) found SRP removal rates of greater than 83% in all media, except that with 10% leaf compost and mulch, which resulted in a net export of SRP, which was greater than 78%.

Nutrient export from bioretention systems may be attributable to soils and/or amendments; these components may be deliberately included in bioretention designs or inadvertently imported to the systems, such as within potting mixes used in containers of plant material. Debusk et al. (2011) found that leaf compost contained 900 mg kg^{-1} of TP and 13,500 mg kg^{-1} of TN, potting soil had 400 mg kg^{-1} of TP and 2,270 mg kg^{-1} of TN, and mulch contained 335 mg $kg^{-1}$of TP and 1,800 mg kg^{-1} of TN. Topsoil had the lowest N and P, with 200 mg kg^{-1} of TP and 594 mg kg^{-1} of TN (Debusk et al. 2011). Herrera Environmental Consultants (2012) found that the bioretention soil mixture used in the City of Redmond, WA contained approximately 660 mg kg^{-1} of TP. All of the above were considered to contribute some N and P to the effluent of the bioretention systems.

Despite these results, there is a dominant, relevant concern that limiting the organic matter in bioretention soils would be detrimental to vegetation establishment, and potentially lessen metals removal performance. Organic amendments, such as compost and mulch are, thus, still being broadly recommended and used in bioretention cells

(Brown and Hunt 2011; Thompson et al. 2008; Vermont Agency of Natural Resources 2002a; Washington State University Pierce County Extension 2012).

Hunt et al. (2007) concluded that if the bioretention soil media was low in available phosphorus (naturally or by design), then it would be unlikely to export phosphorus in the future. New research is being conducted to specifically engineer soil media to remove phosphorus within bioretention and other stormwater management applications through selective inclusion of different metals and textures within the soil, as well as the chemical engineering of new proprietary media (e.g. Sorbtive Media ™, Blue Pro®). A review of phosphorus sorption mechanisms is provided below.

5.1.2.5. Soil Media Designed to Remove Labile P

Labile phosphorus can be removed from solution through precipitation and sorption reactions (also called fixation, surface complexation, ion exchange and ligand exchange), which vary in their bonding strength and relative stability, depending on mineral structure and pH (Sollins et al. 1988). In alkaline conditions, phosphorus reacts with calcium, becomes insoluble, and precipitates from solution (Sollins et al. 1988). In more acidic conditions, iron (Fe) and aluminum (Al) are thought to be the main drivers of phosphorus sorption (Arias et al. 2001; Gerritse 1993; Weng et al. 2012). A few factors that can change soil pH include exudation of citric and malic acids (Horst et al. 2001; Plaxton and Podestá 2006), the release of H^+ during NH_4^+ uptake or nitrification, and the removal of base cations (Ca^{2+}, Mg^{2+}, K^+) by plants (Serna et al. 1992).

Sorption can occur through the formation of outer sphere (adsorption) or inner sphere (absorption) complexes (Sollins et al. 1988; Weng et al. 2012). Outer sphere

complexes result from the formation of positive or negative charges on the particle surface, which attract the opposite charge. Aluminosilicate clays and sesquioxides (oxides, hydroxides and oxyhydroxides) of Fe and Al provide the majority of the surface adsorption potentials (Sollins, Homann, and B. A. Caldwell 1996). Outer sphere adsorption is electrostatic, highly pH-dependent, and easily reversible. Inner sphere complexes can form when a functional group (e.g., hydroxyl) on the particle surface is replaced by an ion complex, resulting in the formation of a covalent bond (Essington 2004; Sollins et al. 1988). Inner sphere complexes are stronger than outer sphere due to a lack of water molecules separating the ion from the soil surface charge. Inner sphere phosphorus sorption occurs when surface hydroxyls are replaced by phosphate and form covalent bonds with Al, Fe, or Si (Sollins et al. 1988; Weng et al. 2012).

Researchers have begun to apply these concepts in bioretention, to develop media that maximizes phosphorus retention. A list of the Ca, Al, and Fe contents of various media that have been trialed for P sorption are presented in Table 13.

Table 13. Soil Fe, Al, Ca, and SRP content in bioretention media targeting phosphorus removal.

Reference	Media	Composition	Ca (mg/kg)	Fe (mg/kg)	Al (mg/kg)	SRP (mg/kg)	TP Removal (%)
Liu et al. (2014)	TerraSolve	15% coir and peat mix, 9% shredded hardwood mulch, 12% aluminum-based water treatment residuals (WTRs), 58% sand	-	1,979	7,541	196	90– 99
	Biofilter	25% saprolite, 20% papermill sludge compost, 50% sand	-	10,107	4,124	179	54 – 96
	Virginia Institute of Technology Mixture	3% wastewater treatment residuals, 15% saprolite, 25% yard waste compost (YWC), 57% sand	-	6,613	3,367	138	58 – 95
Stoner et al. (2012)	Industrial Byproducts	Geothite, gypsum, calcite, quartz, portlandite	90 – 6,500	600 – 40,000	60 – 58,000	-	10 – 60
Arias et al. (2001)	Denmark Sands	Quartz sand	600	1,210	320	40	-
Chardon et al. (2005)	Iron-coated Sand	Iron-coated sand	6,100	198,000	620	3,400	94

For instance, Chardon et al. (2005) tested the phosphorus sorption capacities of iron-coated sand, a byproduct of the drinking water industry in the Netherlands. The authors found that the material had an average P removal efficiency of 94%. Stoner et al. (2012) found that the controlling factors in P removal were dependent on the dominant mineral association. For instance, in systems dominated by calcium, when the primary P removal mechanism was chemical precipitation, the inflow P concentration and total retention time (between0.5 and 10 minutes), were the most important factors. In systems dominated by Fe and Al, where ligand exchange was the primary P-removal mechanism , retention time did not play as large a role in removal as incoming P concentrations and total Fe and Al content (Stoner et al. 2012).

5.1.2.6. Nutrients Dynamics within an Internal Water Storage Zone (IWS)

Although metal sorption seems promising for removing labile P, doubts are often raised regarding its longevity if the conditions become anaerobic. In an anaerobic environment, oxygen depletion forces the microbial communities to utilize electron acceptors preferentially, in the following order: $O_2 > NO_3^- > Mn^{6+} > Fe^{3+} > SO_4^{2-}$ (Spivakov et al. 1999). This produces the reduced version of the species, which includes N_2 (and other reduced forms of N), Mn^{2+}, Fe^{2+}, and S^{2-} or H_2S. The reduced form of ferric iron (Fe^{3+}), is ferrous iron (Fe^{2+}), which is soluble and can release phosphorus previously bound to it (Spivakov et al. 1999). Anaerobic conditions are most likely to occur in bioretention designs which include an internal water storage (IWS) zone for enhanced nitrogen removal via denitrification, yet phosphorus removal data from these systems have been variable (Passeport et al. 2009), with enhanced phosphorus removal only in some cases. For instance, Hunt et al. (2006) found SRP concentrations from designs with IWS zones (520 µg L^{-1}) were lower than from designs without an IWS zone (2,200 µg L^{-1}). Dietz and Clausen (2006) showed some of the lowest outflow TP concentrations reported (39 µg L^{-1} to 43 µg L^{-1}), in a system designed with an IWS zone. It is unclear what conditions will lead to phosphorus desorption in bioretention, and this warrants future research.

Although nitrogen is widely recognized as the key nutrient controlling primary production and eutrophication in saltwater systems (Correll 1999; Davis et al. 2006; Zinger et al. 2013), there is increasing discussion regarding the importance of nitrogen in freshwater systems as well (Turner and Rabalais 2013). Nitrogen transformation

dynamics are complex, with nitrification and denitrification occurring simultaneously within aerobic and anaerobic microsites throughout a soil aggregate, respectively (Vilain et al. 2014). Nitrate is often exported from bioretention cells, with soil media likely being a significant contributor (Davis et al. 2001, 2006; Hunt et al. 2006). In an attempt to increase nitrate removal, IWS zones have been trialed to promote denitrification (Chen et al. 2013; Dietz and Clausen 2006; Hunt et al. 2006; Kim et al. 2003). The results have been somewhat successful, although the necessary conditions for optimal denitrification (e.g., labile carbon content, saturation duration, optimal electron donors) in bioretention are still not fully understood. A summary of conditions influencing nitrate removal in bioretention is provided in Table 14.

Table 14. Nitrate removal from bioretention designs with an internal water storage (IWS) zone.

Reference	Inflow ($\mu g\ L^{-1}$)	Outflow ($\mu g\ L^{-1}$)	Estimated Retention Time (hrs)	Drainage Configuration	Soil Media	Infiltration ($cm\ hr^{-1}$)
Kim et al. (2003)	2,300	1,400 3,760	15 – 20	Elevated underdrain	1) sawdust 2) wheat straw 3) woodchips	4
Hunt et al (2006)	340	280 - 300	4 - 22	Elevated underdrain	Sandy loam and sand	7.62 – 38.1
Dietz and Clausen (2006)	900	300 - 400	17	Elevated underdrain	Native loamy sand	3.5
Lucas and Greenway (2008)	880	40	1) 1 2) 1 3) 12-18	Elevated underdrain	1) pea gravel 2) sand 3) loam	18 18 2.0 – 4.5

5.1.3. Bioretention Designs and Greenhouse Gas (GHG) Emissions

5.1.3.1. Carbon Dioxide (CO_2)

Soil respiration is the sum total of CO_2 released by root respiration and the decomposition of root exudates and organic matter by heterotrophs (Mith et al. 2003;

Rochette and Hutchinson 2005). Soil respiration is thought to emit between 10 and 15 times more CO_2 than the burning of fossil fuels (Mith et al. 2003), and is the second largest terrestrial carbon flux (Bond-Lamberty and Thomson 2010). Soils store at least twice the amount of CO_2 than is in the atmosphere, which makes them an important global sink (Bond-Lamberty and Thomson 2010).

Global circulation models show that rising temperatures resulting from climate change may accelerate decomposition of soil carbon through microbial respiration (Giardina and Ryan 2000), however the amount is unclear. There is high spatial and temporal variability in soil respiration; thus research that gathers CO_2 soil emissions data from a wide variety of local soil conditions will ultimately help refine global models. Some of the broad factors that contribute to the variability in CO_2 emissions from soils include temperature (e.g., Q_{10} factor), moisture, and the productivity of vegetation (Bond-Lamberty and Thomson 2010).

Smart and Peñuelas (2005) found that a spike in CO_2 emissions from soils occurred after a simulated precipitation event, resulting from the displacement of soil pore gases by water. CO_2 returned to pre-precipitation levels approximately 4 hours after the event (Smart and Peñuelas 2005). The authors suggested that fine rooted vegetation may have alloted more belowground carbon via rhizodeposition than larger woody roots, providing more substrate for respiration and higher CO_2 emissions.

5.1.3.2. Nitrous Oxide (N_2O)

Soil microbial nitrification and denitrification both contribute nitrous oxide (N_2O) to the atmosphere, with the latter also being a sink for N_2O in some cases

(Bouwman 1998; Chapuis-Lardy et al. 2007; Conrad 1996; Zhuang et al. 2012). N_2O is a long-lived trace gas, with an atmospheric lifespan of 144 years (Bond-Lamberty and Thomson 2010), and a 100-year warming potential that is 298 times higher than carbon dioxide (Butterbach-Bahl et al. 2013; Dalal et al. 2003; Del Grosso and Parton 2012; Thomson et al. 2012). N_2O contributes approximately 6% to the overall global radiative forcing, or ability to influence the energy balance in the atmosphere, and is currently the most important natural cause of stratospheric ozone depletion (Butterbach-Bahl et al. 2013; Del Grosso and Parton 2012; Portmann et al. 2012; Ravishankara et al. 2009; Thomson et al. 2012).

Both nitrification and denitrification processes are enhanced by the availability of nitrogen and carbon in the soil (Del Grosso and Parton 2012); maximum production of N_2O is most prevelant in the surface soil, where the majority of the microbial biomass is located (Nesbit and Breitenbeck 1992). Vilain et al. (2014) found that N_2O emissions via denitrification were significantly greater in topsoils (10 – 30 cm) as opposed to subsoils (90-110 cm), with ranges of 26 to 250 ng g^{-1} hr^{-1} N_2O-N and 1.5 to 31 ng g^{-1} hr^{-1} N_2O-N in topsoil and subsoils, respectively.

Soil water content is also a key influencing factor in N_2O emissions, for water can result in displacement of gases previously trapped in the soil matrix, create localized anoxic conditions that encourage denitrification, or effectively block gas from escaping through soil macropores if they are filled with water (Davidson et al. 2000).
WFPS for many soils at field capacity is about 60%, where micropores are filled with water and macropores are filled with air (Castellano et al. 2010). This dynamic hybrid-

condition allows both oxidative and reductive processes to take place. When WFPS is between roughly 50% and 60%, N_2O emissions are thought to predominantly be the result of nitrification, whereas when WFPS is greater than 60%, N_2O emissions are thought to begin to occur predominantly as a result of denitrification (Bouwman 1998; Davidson et al. 2000), although field measurements frequently diverge from this model, making it difficult to generalize (Chapuis-Lardy et al. 2007).

Although most soils act as a net source of N_2O emissions, uptake or consumption has also been observed (Butterbach-Bahl et al. 2013; Chapuis-Lardy et al. 2007; Conrad 1996; Schlesinger 2013). The term "uptake" describes both the flux of a gas from the atmosphere to the soil, as well as the transformation of one gas to another (i.e., N_2O reduction to N_2 via reduction) (Chapuis-Lardy et al. 2007). N_2O uptake is thought to occur in soils with low available NO_3^-, predominantly as a result of denitrification, where heterotrophic bacteria utilize nitrogen oxides as an energy source and terminal electron acceptor (Chapuis-Lardy et al. 2007; Conrad 1996; Schlesinger 2013). Above 80% WFPS, N_2O consumption is predicted to occur via denitrification, with N_2 being the main end product (Bouwman 1998). Abiotic reactions between N_2O and the soil minerals (Fe^{2+}, Cu^{2+}) may also be involved in the net consumption of N_2O as a result of chemodenitrification, but these processes are not well understood (Chapuis-Lardy et al. 2007). There are many factors that are still unknown with regards to the controlling factors on N_2O consumption in soils; consumption has been reported under variable conditions, making it difficult to generalize regarding the particular conditions which lead to N_2O uptake (Chapuis-Lardy et al. 2007).

In bioretention cells, some N_2O uptake and/or emissions is expected to occur in the soil surface layers (Conrad 1996; Vilain et al. 2014); however, it is also possible that dissolved organic carbon and the nitrate produced during nitrification will infiltrate into the soil profile with precipitation (Conrad 1996). Accumulation of these compounds may be encouraged in designs that include an IWS or an impermeable liner, which may result in denitrification. Conversely, predominantly sand-based bioretention media may maintain aerobic conditions and encourage nitrification. The resulting positive or negative N_2O flux in conditions within bioretention cells has not been well characterized to date.

5.1.3.3. Methane (CH_4)

Methane (CH_4) has caused roughly 20% of the human-induced increase in radiative forcing since 1750 (Kirschke et al. 2013; Nisbet et al. 2014). After nearly a decade of stable levels, global atmospheric methane concentrations increased by 8.3 +/- 0.6 ppb from 2007 to 2008 (Nisbet et al. 2014), reaching 1,799 ± 2 ppb in 2010 (Kirschke et al. 2013). High temperatures in the arctic, increased precipitation in the tropics, fossil fuel burning, and increased emissions from wetlands have been listed as possible causes (Dlugokencky et al. 2009; Kirschke et al. 2013). Methane production in soils occurs via the microbial decomposition of organic compounds under prolonged anaerobic conditions (Higgins et al. 1981; Kirschke et al. 2013; Le Mer and Roger 2001), with emissions typically lower than 10 mg CH_4 m^{-2} hr^{-1} (Le Mer and Roger 2001). CH_4 production occurs only after O_2, NO_3^-, Fe (III), Mn (IV) and SO_4^{2-} have been reduced (Mith et al. 2003).

In an aerobic environment, certain soil bacteria can use atmospheric methane as an energy source, making them an important global CH_4 sink (Kaye et al. 2004). Methane consumption rates are thought to be highest in soils where methanogenesis was recently producing higher concentrations than the atmosphere (Le Mer and Roger 2001). Nesbit and Breitenbeck (1992) suggest that recently drained or intermittently flooded soils are likely to display the greatest CH_4 uptake. Several early field studies have demonstrated that well-aerated soils can serve as sinks for atmospheric CH_4 (Harriss et al. 1982; Higgins et al. 1981; Keller et al. 1986; Steudler et al. 1989), although actual values vary widely. There is little research to date on CH_4 emissions from bioretention, or how these emissions are affected by different soil media, vegetation, or increases in precipitation.

5.1.3.4. Increased Precipitation and Greenhouse Gas Emissions

Changes in precipitation due to climate change will directly impact soil moisture, which is one of the main factors controlling whether soils are a source or a sink for N_2O and CH_4. Some of the many other factors include temperature, soil nitrogen, and soil carbon content (Castellano et al. 2010; Connor et al. 2010; U.S. Climate Change Science Program and the Subcommittee on Global Change Research 2008). As bioretention and other stormwater mitigation strategies are introduced into the landscape, it is important to understand their role as a source or sink for GHGs, and to predict how current designs will respond to increases in stormwater volume that are likely to occur in the northeast due to climate change. Further, by investigating the gas component of nutrient and carbon cycles, we can deepen our understanding of the internal dynamics of the cells themselves. This research will attempt to provide information regarding the soil

gas dynamics (CO_2, N_2O, and CH_4) within bioretention cells under various conditions throughout the majority of the growing season.

5.2. Methods

5.2.1. Research Goals and Hypotheses

The broad goals of this research are to improve our collective understanding of fundamental bioretention pollutant removal mechanisms and to clarify how various design features and environmental conditions affect them. Specifically, the objectives of this research are to 1) compare the influence of (a) vegetation, (b) soil media, and (c) increased precipitation, on the retention of nutrients, sediment, and soil greenhouse gas flux (CO_2, N_2O, CH_4) on performance of small bioretention systems. The specific hypotheses are as follows:

1) The vegetation palette with numerous species with variable root depths is predicted to remove more nutrients and sediment than one with fewer species and deep roots.
2) The soil media that includes reactive cations (Sorbtive Media™) is predicted to remove more labile P than a conventional soil media.
3) Increased precipitation and runoff is predicted to decrease nutrient and sediment retention in bioretention and increase the production of N_2O and CH_4. CO_2 emissions are predicted to decrease with increased precipitation and volume.

5.2.2. Site Context

The University of Vermont (UVM) Bioretention Laboratory was constructed on the UVM campus located in Burlington, Vermont, in November of 2012. Burlington receives approximately 37 inches (0.940 m) of rainfall, and 81 inches of snowfall (2.06 m) a year (NOAA, National Weather Service). There are eight bioretention cells on the study site, which capture road runoff from an area of approximately 5,002 ft^2 (464.7 m^2) or 0.115 acres. Data from seven of the bioretention cells are reported here. The drainage areas of the paved road sub-watersheds range from 320 ft^2 to 1,293 ft^2 (29.73 m^2 to 120.12 m^2), and were delineated from the crown of the road, at a 45-degree angle to a granite curb, which ends at a trapezoidal curb cut at the entrance of each bioretention cell. Stormwater is directed from the road surface, through the curb-cut, and across a narrow conveyance strip, ranging from 3.72 m^2 to 19.20 m^2, which was lined with rubber EPDM membrane and covered with 2 to 4-inch stone prior to entering the bioretention cell inflow monitoring equipment. The road is one of the main thoroughfares for bus and automobile traffic entering the UVM campus. A list of the bioretention design parameters is provided in Table 15.

Table 15. Site specifications for the University of Vermont Bioretention Laboratory

Construction Completion Date	November 2012
Sampling Date Range	June - November 2013 & May - October 2014
Total Drainage Area Range Including Conveyance	34.7 m^2 – 136.8 m^2
Cell Dimensions	Rectangular: 10 ft (3.048 m) x 4 ft (1.219 m)
Media Depth	3 feet (0.9144 m)
Bioretention Cell Surface Area	40 ft^2 (3.72 m^2)
Cell Surface Area to Drainage Area Ratio	3 – 11%
Sorbtive Media ™ Depth (in two cells)	3 inches (0.0762 m)
Bioretention Ponding Depth	6 inches (15.24 cm)

The eight bioretention cells are rectangular, equally sized, parallel to the road, and have dimensions of 4 ft (1.2192 m) wide x 10 ft (3.048 m) long x 3 ft (0.9144 m) deep with approximately 6 inches (15.24 cm) of ponding depth. The layout of a typical cell, displaying the location of the monitoring equipment, is shown in Figure 18.

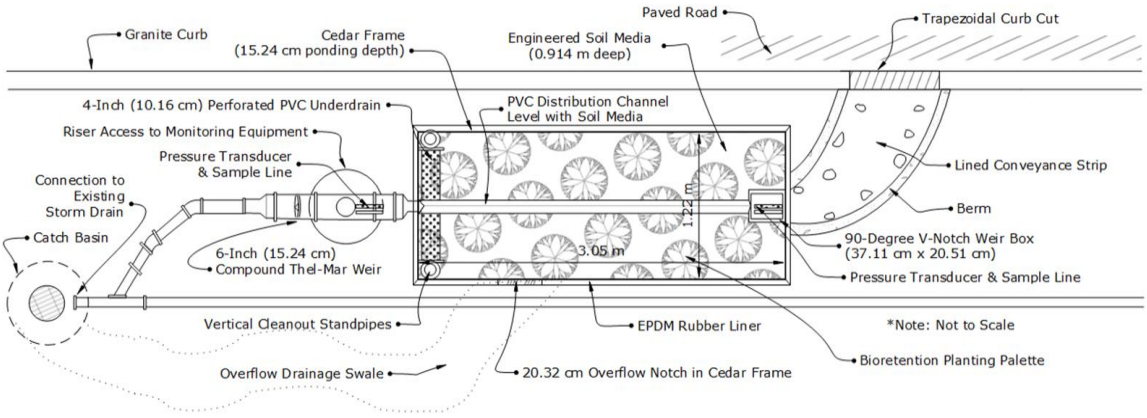

Figure 18. Layout view of a typical bioretention cell at the UVM Bioretention Laboratory.

The cells are fully enveloped by an EPDM impermeable rubber liner, and contain an underdrain at one end, which ultimately connects back to the existing storm sewer network. Each of the bioretention cells has specially designed monitoring infrastructure at the entrance (inflow) and exit (outflow), which will be described in future sections.

5.2.3. Bioretention Design Overview

The section profiles of the two media designs used in this study are shown in Figure 19. The top 12 inches (0.3048 m) of each bioretention cell is composed of 60% sand and 40% compost, by volume, as recommended by Washington State University Pierce County Extension (2012) and the Vermont Agency of Natural Resources (2002).

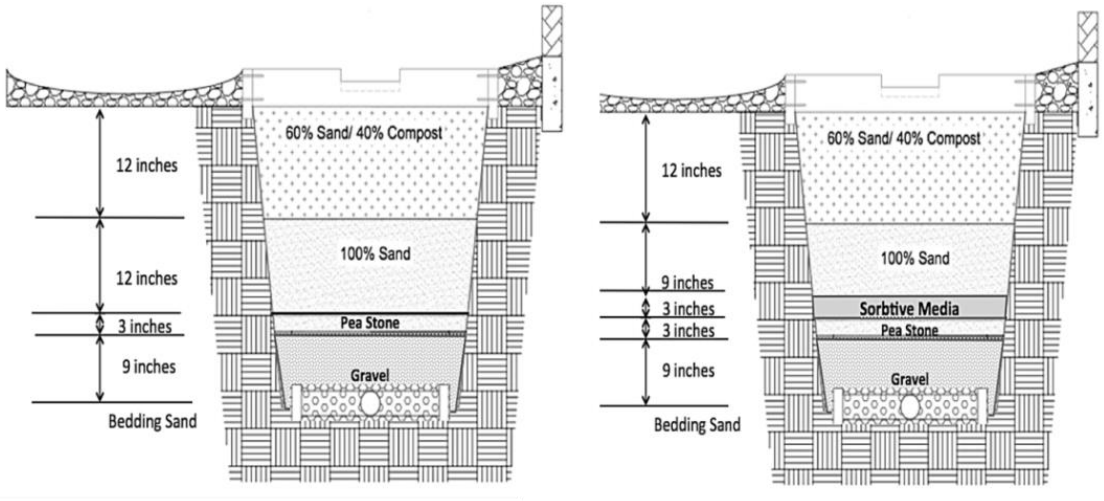

Figure 19. Bioretention Profiles: Conventional Media (CM) (left), Sorbtive Media™ (SM) (right). Image Credit: J. Schultz, C. Brackett, J. Nummy, O. Lapierre.

The total volume of the sand/compost mixture within each cell is 1.13 m^3 and was created onsite prior to field installation. The bulk density of the original bioretention 60:40 sand/compost mix was 1.37 g cm^{-3}, which is typical for a sand to sandy loam mixture **(**1.2 g cm^{-3} – 1.7 g cm^{-3}) (Brady and Weil 2008). The two soil treatments in this research were conventional media (CM) and Sorbtive Media™ (SM) (Figure 19; see also section 5.2.4.2 of this chapter). In the conventional media (CM) cell shown on the left in Figure 19, the soil profile included 12 inches (0.3048 m) of locally sourced 'bedding sand' above 3 inches (0.0762 m) of pea gravel (size: 1/8 inch – 3/8 inch) and 9 inches (0.9906 m) of washed stone, or gravel (size: 1.5 inch). In the Sorbtive Media™ (SM) cell (Figure 19), the 12 inches of bedding sand in the CM cells are substituted with 9 inches (0.9906 m) of bedding sand and 3 inches of Sorbtive Media™; above and below this 12-inch layer, the profiles of the SM and CM cells are identical.

Although groundwater recharge is often a goal in bioretention projects, in this research, the native subsurface soils contained non-homogeneous construction fill with a

thick clay layer underneath. Shallow depth to groundwater was also a concern; therefore, each cell is enveloped in a rubber liner.

Underground utilities (i.e., water, steam, electrical) were between two and four feet (0.61 m and 1.2 m) below ground-level, and affected the final placement of the cells within the narrow grassed areas parallel to the road. The distances from the curb cuts to the entrance of each bioretention cell are not equal. The areas of the conveyance strips (Figure 18) are listed in Table 27 in the Appendix. The ratio of surface area to drainage area across all cells is between 3% and 11%; the upper end of this range is higher than Debusk and Wynn (2011) but close to the typical recommended range of 5% to 7% (Hunt et al. 2006). The bioretention cells did not specifically include an IWS zone; however, the underdrain was approximately 2 inches (5.08 cm) higher than the bottom of the cells, which was a necessary to connect the underdrain to the outflow monitoring structure during construction. The porosity of gravel is typically between 25% and 40%, therefore between approximately 47 L and 76 L could be stored in the bottom of the cells between events (Chapter 3).

5.2.4. Experimental Design and Overview of Treatments

To enable the monitoring of multiple treatments at once, with a small number of subjects, a semi-factorial paired watershed treatment design was selected. A plan view of the experimental design is shown in Figure 20, Table 16.

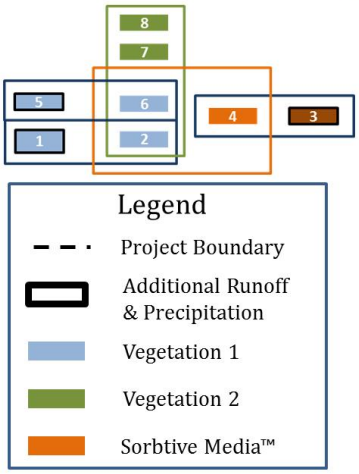

Bioretention Cells	Paired Treatment	Abbreviation
1 and 2	Conventional Media + 20% vs. Conventional Media	CM20 vs. CM
(2 & 6) and (7 & 8)	Vegetation 1 vs. Vegetation 2	V1 vs. V2
(2 & 6) and 4	Conventional Media vs. Sorbtive Media ™	CM vs. SM
3 and 4	Sorbtive Media™ + Climate 60% vs. Sorbtive Media™	SM60 vs. SM

Figure 20, Table 16. Study design layout showing bioretention cells grouped by treatment.

5.2.4.1. Vegetation Treatments, V1 and V2

Two planting designs were selected to compare pollutant retention. The plant species and layout are shown in Figure 21. The majority of the cells (1 through 6) were planted with vegetation palette 1 (V1), consisting of seven species, and contained fifteen plants per cell. The remaining cells (7 & 8) were planted with vegetation palette 2 (V2), consisting of two species, and contained nine plants per cell. The planting layout was designed to achieve approximately equal percent cover when plants were fully grown. The two planting palettes were selected based on height, rooting habit, bloom time, color, diversity, pollen production, robustness to both drought and flood conditions, and salt

tolerance. The bioretention cells were planted in May 2013 and watered during the initial establishment phase for three weeks.

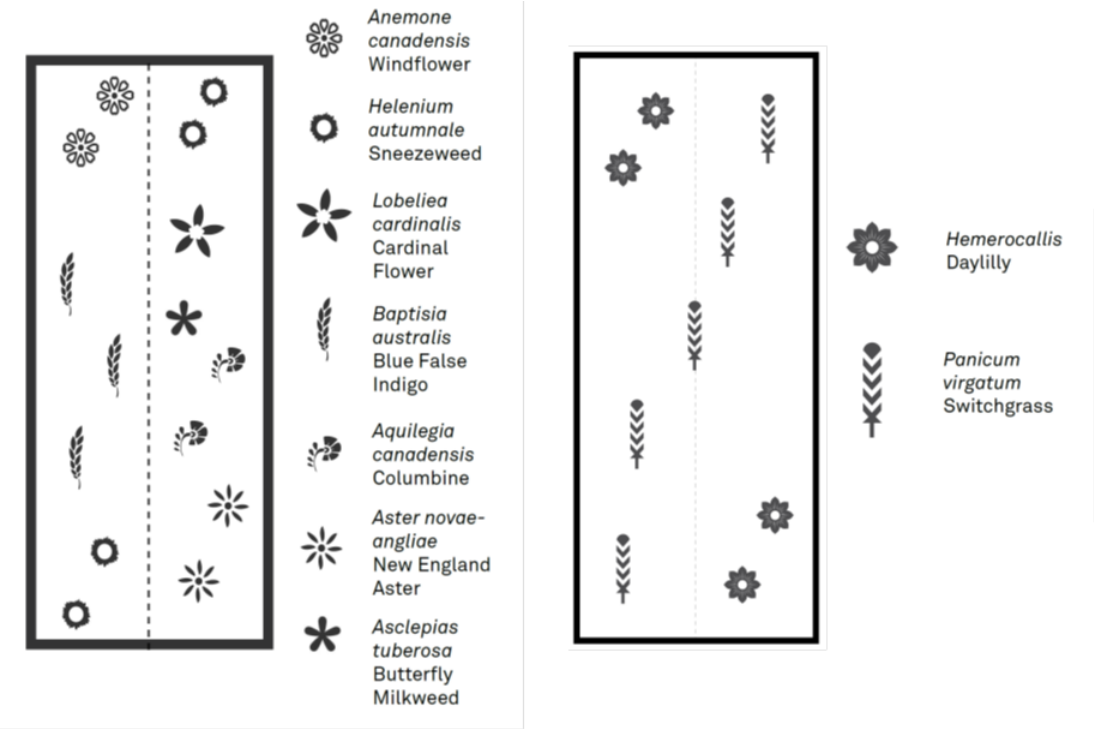

Figure 21. Planting Configuration: Vegetation Palette 1 (Left) and Vegetation Palette 2 (Right) (Diagram created by S. Hurley and A. Zeitz, unpublished).

Water quality monitoring began in June of 2013. At the end of the first growing season, all of the vegetation, except the switchgrass, was cut back to heights between 1 and 4 inches tall depending on species, to prevent the decomposition and re-release of nutrient and metals back into the system (Lantzke et al. 1998). Switchgrass plants in V2 provided aesthetic value during winter, and were cut back prior to the start of the growing season in April of 2014. The vegetation palette with numerous species and variable root depths (V1) was predicted to remove more nutrients and sediment than the one with fewer species but deep roots (V2).

5.2.4.2. Soil Media Treatments, CM and SM

Two soil media designs were selected to compare pollutant retention via physical, chemical, and biological mechanisms (Hogan and Walbridge 2007). Each bioretention cell contained either a conventional soil media (CM) or a chemically-engineered media called Sorbtive Media™ (SM). The sorbtive media product is produced by Contech Inc, and is defined as "an oxide-coated, high surface area, reactive engineered media that performs adsorption, surface complexation, and filtration of stormwater for total phosphorus removal" (Imbrium Systems 2012). Sorbtive media was incorporated into two of the eight cells (cells 3 and 4) on the research site, as a 3-inch thick layer, 21 inches (53.34 cm) below the surface of the cell (Figure 19). For analytical purposes, results from replicate CM cells (2 and 6) were averaged and compared with SM cell 4.The SM was expected to remove more labile P than the CM, due to its highly reactive oxide-coated surface.

5.2.4.3. Precipitation Treatments, CM20 and SM60

To evaluate the influence of increased precipitation on both CM and SM designs, additional precipitation and runoff were added to one cell within each of the CM and SM groups, by a specified amount (i.e., 20% or 60%), while the other cell was unaltered (i.e., ambient conditions). Precipitation was added with a simulation device called a rain pan (Figure 22). Runoff was effectively "added" by the fact that the size of the drainage area of the paired treatment was proportionately larger than the drainage area of the control (in other words, the drainage areas were 20% or 60% different for identically sized bioretention cells, depending on the treatment.

Figure 22. Rain pan on treatment SM60 with new vegetation.

In the first precipitation treatment, cell 2 (CM) was paired with cell 1 (CM20). CM20 received approximately 20% more precipitation via an attached rain pan and has a drainage area that is approximately 20% larger than CM (Fig 19, Table 15), which added 20% more runoff. In the second precipitation treatment, cell 4 (SM) was paired with cell 3 (SM60). SM60 received approximately 60% more precipitation than cell 4, via an attached rain pan and has a drainage area that is approximately 60% larger than the SM cell, which added 60% more runoff (Fig 20, Table 16).

The surface area of the rain pans were calculated by multiplying the difference in the size of the paired watersheds by the bioretention cell surface area (e.g., cells 3 & 4 are 60.8 % different in size: $0.608 \times 40ft^2 = 24.32ft^2$ of rain pan surface area for the rain pan on cell 3; see also Figure 20). The two rain pans were constructed of corrugated clear, non-reactive acrylic roofing material.

Precipitation was distributed across the cell surface via two PVC pipes with a 2-inch diameter (5.08 cm) which ran the length of the cell, and had 5/16-inch (0.79 cm) holes drilled on the underside. Additional precipitation and runoff was expected to

negatively influence nutrient and sediment retention and increase N_2O and CH_4 emissions due to the potential formation of anaerobic microsites within the soil profile.

5.2.5. Monitoring Equipment

Inflow runoff was captured in a monitoring device, called a "weir box" prior to entering each of the eight bioretention cells. Each weir box is equipped with a 90-degree v-notch weir and sized to allow stormwater to be sampled in small, sequential segments as it moved through the monitoring system. This maximized the detection of incremental changes in runoff quality throughout an event. The dimensions of the weir boxes were based on U.S. Bureau of Reclamation (2001) recommendations, and are described in detail in Chapter 3. The cells are equipped with an underdrain, which is connected to the storm drain network. A Thel-Mar™ compound weir was installed in a 6-inch diameter drainage pipe at the outflow of each bioretention cells (Figure 9, Chapter 3). Design details for the outflow monitoring equipment are described in Cording, (Chapter 3).

The height, or level, of the stormwater in both the inflow and outflow monitoring systems was measured with Teledyne™ 720 differential pressure transducers. Inflow level was converted to flow rate using discharge equations developed for each of the eight weirs. Outflow discharge equations for the in-pipe weirs were provided by Thel-Mar, LLC. The pressure transducer is equipped with a venting system, which compensates for changes in atmospheric pressure and records level from 0.03 ft (0.9144 cm) to 5.0 ft (1.524 m) (+/- 0.243 cm), and has an operating temperature between 32 ^{o}F and 120 ^{o}F. The inflow and outflow pressure transducers were clipped to the base of the inflow weir box and outflow monitoring chamber to ensure accurate measurements in

high flow events. The pressure transducers took continuous water level measurements throughout each storm event, in one minute intervals.

5.2.6. Inflow and Outflow Sample Timing

Automated sample collection was conducted by the Teledyne ISCO™ 6700 series, which can hold a maximum of twenty four 1-L bottles. The inflow and outflow sampling regimes were designed to capture samples at multiple locations throughout the inflow and outflow runoff hydrographs, and mass retention was compared on an equal volume basis. The number and timing of inflow samples targeting the inflow hydrograph and were based on estimates of peak flow rates for each road sub-watershed, which were determined using the time of concentration, rainfall intensity duration curves, and the rational method (Cording, Chapter 3; King et al. 2005).

For each storm and bioretention cell monitored, discrete samples were taken at the entrance of each cell every two minutes for up to 48 minutes (n = 24) when inflow flow rates were consistently above a minimum threshold of 0.21 ft (6.50 cm) from the bottom of the weir box. If the inflow flow rate dropped below the minimum threshold, sampling stopped, and resumed again if levels rose again, until all 24 bottles were filled. Outflow sampling was also time-based and targeted the outflow hydrograph based on the mean vertical and horizontal hydraulic conductivity of the cell (Chapter 3). For each storm and bioretention cell monitored, discrete outflow samples were taken every four minutes for up to 96 minutes (n = 24), when outflow flow rates were consistently above the minimum sampling threshold of 0.03 ft (0.91 cm) above the v-notch in the Thel-Mar™ weir. If the outflow flow rate dropped below the minimum threshold, sampling

stopped, and resumed again if levels rose again, until all 24 bottles were filled. The total number of sample bottles collected and the total sampling time at both the inflow and outflow varied and depended on the nature of the storm.

5.2.7. Water Quality Analysis

Each sample was analyzed for total phosphorus (TP), soluble reactive phosphorus (SRP), total nitrogen (TN), nitrate (NO_3^-), and total suspended solids (TSS). All stormwater samples were filtered with a Fisherbrand 0.45 μm nylon syringe filter prior to analyzing for dissolved inorganic nutrients according to standard methods (APHA 1992) and read by a Lachat™ automated colorimeter (Flow Injection Analysis, QuikChem 8000, Hach Company, Loveland, CO). Total phosphorus (TP) and total nitrogen (TN) concentrations were determined using potassium persulfate digestions on unfiltered samples. Potassium persulfate was prepared fresh for each digestion (APHA, 1995). Quality control samples for both TN and TP were prepared using para-Nitrophenylphosphate (para-NPP). A blank, standard and QC were included each time samples were run. SRP (dissolved ortho-phosphate) and TP (persulfate digested o-PO_4^{3-} were analyzed using the Lachat QuickChem Method 10-115-01-1-Q. NO_3^- and TN were analyzed using the Lachat QuickChem Method 10-107-04-1-B. TSS was measured according to standard methods (APHA 2011).

In order to investigate nutrient speciation in stormwater, TN and TP were mathematically separated into the approximate equivalent of total Kjeldahl nitrogen (TKN) and non-labile phosphorus (NLP), respectively. NLP was determined by subtracting the SRP from TP for each sample, and includes both the particulate and

dissolved fraction of organic P. Dissolved organic phosphorus is predominantly non-labile, requiring bacterial decomposition (mineralization) to become ortho-phosphate (SRP), which is labile (Spivakov et al. 1999). TN is defined as the sum of organic nitrogen, nitrate, nitrite, ammonia and ammonium. TKN is traditionally defined as the portion of nitrogen measured using the Kjeldahl method. It is a grouped measure, which includes NH_3, NH_4^+ (labile, sometimes referred to as "free ammonia" or "ammonia"), and organic nitrogen (both labile and non-labile). The Kjeldahl method requires the use of toxic chemicals and poses hazardous disposal issues (Patton and Kryskalla 2003), therefore this research used an alternative method used by the Hach Company® for determining the equivalent portion of nitrogen to TKN in a sample, by using a persulfate digestion to determine total nitrogen, then subtracting the nitrate and nitrite components to determine TKN (Antonio and Walker 2011).

5.2.8. Soil Analysis: SRP, Inorganic N, and Bulk Density

One of the goals of this study was to determine the nutrient load coming from the bioretention media itself, and how that load may have changed over time. A sample of the sand/compost mixture used in the top twelve inches of the bioretention cells was collected prior to being placed in the cells during construction in November 2012, and was analyzed for SRP, inorganic N, extractable metals, CEC, OM, and pH. Separately, after installation of the bioretention cells, three soil subsamples of the compost mixture were collected from the top 10 cm of each cell seven times from June 2013 to October 2014 and analyzed as described above. Inorganic nitrogen and bulk density measurements were taken on a weekly to bi-weekly basis during season II (n = 13). Bulk

density was measured in December 2013 prior to snowfall and from May 2013 to September 2013 (n = 10) by calculating the total change in mass per volume of a cylindrical soil core container (g cm^{-3}). To determine inorganic N and SRP content, soils were dried at 45°C, ground to pass a 2-mm sieve, and extracted with 2M KCl and Modified Morgan's solution, respectively (Northeast Regional Coordinating Committee on Soil Testing 2009). Extracts were read by a Lachat™ automated colorimeter. Macro and micronutrients were analyzed using inductively coupled plasma spectroscopy (ICP-OES). Organic matter content was determined using the loss on ignition method at 375^{o}C. The pH and effective CEC were determined by the University of Maine Analytical Laboratory using methods from the Northeast Regional Coordinating Committee on Soil Testing (2009).

5.2.9. VWC, EC, and Temperature of Soil Media

Two Decagon 5TE probes measured volumetric water content (VWC), electric conductivity (EC), and temperature every five minutes, from July 2013 through October 2014, at 5-cm and 61-cm depths in cell 1 (CM20), cell 2 (CM), and cells 7 & 8 (V2). The probe at the 61-cm depth in cell 2 (CM) had an equipment malfunction and did not produce useable data. The probe determines VWC, by measuring the dielectric constant of the media using frequency domain technology (Decagon Devices 2015). The sensor uses a 70-MHz frequency, which minimizes salinity and textural effects. VWC has an accuracy of +/- 1 (ε_a) from 1 to 40, +/- 15% from 40 to 80 VWC (Decagon Devices 2015). The EC probe measures the combined electrical conductivity of the soil and water in a porous soil substrate with a stainless steel electrode array. EC is expressed as dS m^{-1}

(equal to ms cm^{-1}) and has a range from 0 to 23 dS m^{-1} and an accuracy of +/- 10% from 0 to 7 dS m^{-1}. Soil temperature was measured with a thermistor and had a range from -40 to 60^{o}C with an accuracy of +/- 1 ^{o}C (Decagon Devices 2015).

5.2.10. Calculating Pollutant Mass and Concentration

The pollutant load was defined as the amount of mass (typically µg or mg) transported by a given volume of stormwater, in a given amount of time (U.S. Environmental Protection Agency 1997). Numeric integration was used to estimate the area under the flow rate and concentration functions over time (Davis and Cornwell 1998; U.S. Environmental Protection Agency 1997). The accuracy of this method increases with the number of samples taken over time (Stenstrom and Kayhanian 2005). Rapid discrete samples were taken throughout the inflow and outflow hydrographs, typically up to 48 minutes and 96 minutes, respectively (see Section 5.2.6). The total mass load was determined using Equation 15.

$$Mass\ Load = \int_{t0}^{tn} C(t)dt\ Q(t)\ dt \qquad (15)$$

Where,
C (t) is the concentration as a function of time (mg L^{-1})
Q (t) is the flow rate as a function of time (L s^{-1})

The Event Mean Concentration (EMC) is often used to represent the average stormwater concentration over the course of an event, and is defined as the total cumulative pollutant mass divided by the total cumulative volume generated during a storm event (Stenstrom and Kayhanian 2005). Volume and mass measurements used in the EMC are typically determined using flow-weighted composite sampling. Composite

sampling provides an adequate average representation of concentration (Stenstrom and Kayhanian 2005), but does not provide any temporal information regarding the distribution of mass during an event.

Alternatively, in the partial event mean concentration (PEMC), the average concentration can be calculated for any sampled portion of the hydrograph (Stenstrom and Kayhanian 2005), as shown in Equation 164, and was selected for use in this study. The limits of the numerical integration run from the initiation of runoff (0) to the time at which sampling stops (t) (Stenstrom and Kayhanian 2005). When the entire event is sampled, the PEMC and EMC are equal.

$$\text{PEMC} = \int_{t_0}^{t_n} \frac{c(t)q(t)dt}{q(t)dt} = \frac{\sum_{t_o}^{t_n} m(t)}{\sum_{t_o}^{t_n} v(t)} \quad (16)$$

Where,
t_0 is the time at which the sample is collected in a storm event
t_n is the time the sampling has stopped
c is the sample concentration as a function of time (mg L^{-1})
q is the flow rate as a function of time (L s^{-1})
m is the pollutant mass delivered during a specific portion of the storm event (µg or mg)
v is the volume delivered during a specific portion of the storm event (L)

5.2.11. Evaluating Hydrologic Performance

Continuous water level measurements collected in one-minute increments throughout the entire storm duration were used to assess hydrologic performance. The maximum inflow and outflow flow rate and cumulative volumes (excluding any flood events) were compared in each cell, with replicates being averaged within each treatment. Flood events were defined as events within which flow rate measurements were over the

maximum measureable threshold for the inflow weirs (3.4 L s^{-1}). Data from that event were not included in flow rate and cumulative volume reduction calculations. Outflow peak flow rates were well below the measurement threshold of 1.98 L s^{-1}.

5.2.12. Evaluating Pollutant Removal Within and Between Treatments

Because volume reduction is a dominant driver in pollutant retention, to isolate other potential pollutant removal mechanisms, mass loads were compared on an equal volume basis, comparing inflow to outflow (within a treatment) and comparing between treatments, as recommended by Geosyntec Consultants and Wright Water Engineers (2013). The stormwater volume that was compared for the inflow and outflow of cells and across all events was 120 liters. Lucas and Greenway (2008) used similar outflow volumes (98 L – 127 L) in bioretention column studies. The inflow and outflow samples within the 120-L volume were broken into six 20-L segments. Each 20-L increment contained the cumulative mass values from each storm event and each cell for both the inflow and the outflow. The total number of samples per 20-L segment are listed in Table 33 in the Appendix.

The average of the inflow cumulative mass across all cells and storm events within each of the six 20-L segments was taken to represent the mass in stormwater delivered by that portion of volume, up to 120-L. The average of the outflow cumulative mass for each treatment was similarly used. The six inflow cumulative mass values across the total 120-L volume (e.g., 20-L, 40-L, 60-L, etc.) were then compared to the six outflow mass values, across the 120-L volume. The six outflow mass values across the 120-L were also compared between treatments. The 120-L spanned the outflow

hydrograph, as shown in Figure 23. This method allowed for the comparison of inflow and outflow mass values within a treatment, and between treatments, which were not necessarily from the same storm event, but were equally weighted and related by volume.

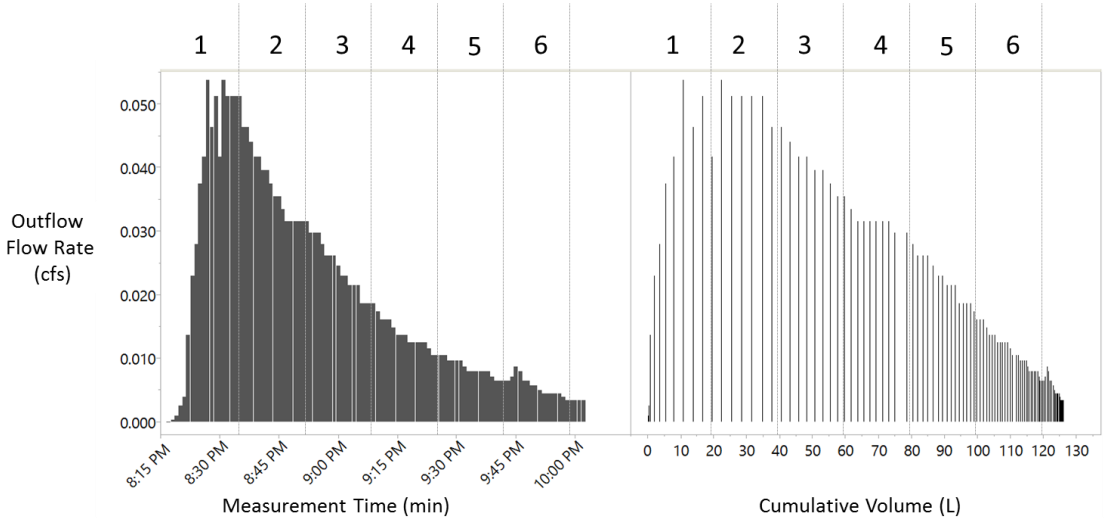

Figure 23. Example of sampling segments overlaid on the outflow flow rate hydrograph (left) and flow rate per cumulative volume (right) across 120-L

Simultaneous sampling within and between treatments was not always possible due to limited equipment. Percent mass removal from inflow to outflow was calculated using the average cumulative inflow and outflow mass loads from each of the six hydrograph segments. The average of the six incremental percent removal values is representative of the percent mass removal from the entire 120-L volume.

5.2.13. Greenhouse Gas Sample Collection and Analysis Methods

Soil gas emissions were collected within each cell from fixed anchors, in homogeneous soil conditions (Corbella and Puigagut 2013), excluding vegetation, using the closed chamber method (Hutchinson and Livingston 1993; Kutzbach et al. 2007; Rochette et al. 1997). Anchor and chamber were constructed to specifications in Parkin

and Venterea (2010). Cells with Sorbtive Media™ contained two anchors; all others contained three anchors. Anchors were weeded a minimum of 24 hours prior to any sampling event. Disturbance was minimized in all other circumstances. Samples were collected weekly to bi-weekly, as practicable, from July to October 2014 (n = 11) to capture the gas flux during the majority of the growing season. Headspace gas samples (10 mL) within static chambers were taken at 0, 15, 30, and 45 minute intervals using syringes and injected into evacuated 10 mL vials. Soil temperatures were recorded in each of the cells at a depth of 15 cm. Humidity inside the chambers was minimized with short deployment times. Temporal and temperature variability was minimized by sampling at either 10 AM or 3 PM, and by using insulated PVC pipes and reflective mylar tape, as recommended by Parkin and Venterea (2010). Pressure disturbances were minimized by using a vent tube inside the chamber (Parkin and Venterea 2010).

Gas samples were analyzed within 24 hours for N_2O, CH_4, and CO_2 concentrations at the UVM Plant and Soil Science Department, on the Shimadzu GC-17A (Columbia, MD, USA) greenhouse gas analyzer with AOC-5000 autosampler. An electron capture detector (ECD) was used to measure N_2O and a flame ionization detector (FID) was used to measure CH_4 and CO_2. Water vapor was removed from samples via a 1.0-m Poropak- Q column and a 2.0-m Hayesep D column was used for sample separation, with nitrogen (N_2) as the carrier gas. The gas chromatography (GC) oven, injection, and FID temperatures were maintained at 60°C, 150°C, and 250°C, respectively.

As a precaution, samples from individual anchors were run in sequence (e.g., Anchor 1: t_0, t_{15}, t_{30}, $t_{45;}$ Anchor 2: t_0, t_{15}, t_{30}, t_{45}) rather than segregating samples by time, to account for any GC drift, as recommended by Parkin and Venterea (2010). Flux rates were calculated with Equation 17.

$$f = \frac{V}{A} \text{ x } \frac{dC}{dt} \tag{17}$$

Where,
f = gas flux, expressed as a mass $m^{-2}\, h^{-1}$
V = the volume of the chamber, including the anchor or collar volume
A = the soil surface area covered by the chamber
$\frac{dC}{dt}$ = the change in gas concentration over the sampling period

The gas flux equation assumes a linear increase in concentration in the chamber; therefore, the rate of change is the slope of the best-fit regression line of gas concentration over time. Each series of flux measurements was evaluated for linearity ($p \leq 0.05$) and points outside of the confidence boundary were discarded. Values showing a downward or upward drift at the end of the time step were discarded to avoid an under or over estimation of the total flux, as recommended by Rochette and Hutchinson (2005).

5.2.14. Statistical Analysis

All statistical analysis was conducted with JMP Pro 11.2. Normality of distributions was evaluated using the Kolmogorow-Smirnov test. Where normality could not be met, non-parametric methods were used. Levene's test was used to assess equality of variance. Where variances were not equal, a non-parametric version of the paired t-test (Wilcoxon signed rank) was used to compare differences between paired repeated measures data. Spearman's rho is a non-parametric correlation method, and was used to

evaluate multivariate correlations due to its strength with data which may have a non-linear characteristic, does not require normality, and is robust against the presence of outliers (Dytham 2003). A paired t-test was used to compare differences between paired data when normality was assumed. The average soil characteristics from seasons I and II (n = 7) were compared within each treatment to the original sand-compost mixture (collected pre-installation) using Dunnett's control (Allen Burton and Pitt 2002). Linear regression coefficents were used to estimate the outflow mass load from each treatment as a function of cumulative volume. The probability level of $p \leq 0.05$ was accepted as significant in all tests.

5.3. Results

5.3.1. Hydrologic Bioretention Performance

Paired t-test results indicate that the flow rate and runoff volume were significantly reduced from inflow to outflow in all bioretention treatments (Tables 17 - 19). Reductions in peak flow rate ranged from 48% to 100% across all treatments. Volume reductions were ranged from 16% to 100%. Reductions inversely correlated with the size of the storm event: Spearman's rho results indicate that as the size of the precipitation event (n = 50) increased, there was a decrease in percent volume reduction (r_s = -0.3206, p = 0.0232) and peak flow rate reduction (r_s= -0.3870, p = 0.0055).

Table 17. Inflow and outflow peak flow rate by treatment, where n is the number of storm events.

Treatment	n	Inflow Flow Rate				Outflow Flow Rate				Peak Flow Rate Reduction			
		L s^{-1}				L s^{-1}				%			
		Min	Mean	±	Max	Min	Mean	±	Max	Min	Mean	±	Max
V1/CM (cells 2 & 6)	14	0.014	0.984	0.882	3.337	2.14E-06	0.049	0.055	0.154	71.1	94.2	7.6	100.0
V2	16	0.002	0.642	0.865	3.541	1.26 E-05	0.044	0.069	0.258	47.7	90.3	13.6	100.0
CM (cell 2 only)	1	1.040	-	-	1.040	2.14E-06	-	-	2.14E-06	100.0	100.0	-	100.0
CM20	7	0.069	0.460	0.509	1.436	0.001	0.059	0.064	0.190	56.8	80.9	16.2	99.5
SM	3	0.131	0.669	0.788	1.573	0.017	0.063	0.071	0.144	52.6	77.1	23.3	98.9
SM60	6	0.023	0.765	0.667	1.597	7.36 E-5	0.049	0.059	0.144	89.9	95.5	3.8	99.7

Table 18. Inflow and outflow cumulative volume reduction by treatment, where n is the number of storm events.

Treatment	n	Inflow Cumulative Volume				Outflow Cumulative Volume				Volume Reduction			
		L				L				%			
		Min	Mean	±	Max	Min	Mean	±	Max	Min	Mean	±	Max
V1/CM (cells 2 & 6)	14	59	1050	1069	3582	-	199	259	779	70.0	86.3	12.2	100.0
V2	16	6	729	849	2611	0.02	138	170	546	31.5	79.7	24.7	99.6
CM (cell 2 only)	1	63	-	-	63	0.0001	0.00	-	-	100.0	100.0	-	100.0
CM20	7	49	450	297	907	0.71	161	140	345	41.6	70.8	19.1	98.5
SM	3	29	185	173	370	1.96	22	23	47	39.1	69.5	30.2	99.5
SM60	6	6	343	333	902	0.33	80	106	266	16.1	78.0	31.1	99.0

Table 19. Comparing inflow and outflow flow rate (Q) and cumulative volume (Vol) with a paired t-test, where n is the number of storm events.

Treatment	Inflow	Outflow	n	df	Mean Diff	Standard Error	t-ratio	p-value (one-sided)
V1/CM (cells 2 & 6)	Q	Q	14	13	0.9352	0.2333	4.01	0.0007
	Vol	Vol	14	13	851.43	230.44	3.69	0.0013
V2	Q	Q	16	15	0.5984	0.0202	2.96	0.0048
	Vol	Vol	16	15	590.93	196.64	3.01	0.0044
CM20	Q	Q	7	6	0.4004	0.1727	2.32	0.0298
	Vol	Vol	7	6	289.25	70.77	4.09	0.0032
SM60	Q	Q	6	5	0.7160	0.2519	2.84	0.0181
	Vol	Vol	6	5	263.10	122.31	2.15	0.0421

The vertical hydraulic conductivity (K_z) of the CM cells was estimated to be 131.04 cm hr^{-1} (51.59 in hr^{-1}), based on the individual conductivities of each bioretention media layer (Chapter 3). The hydraulic conductivity of the Sorbtive Media™ is 73.15 cm hr^{-1} (28.80 in hr^{-1}) (Imbrium Systems, personal communication, December 13, 2015), resulting in a K_z of approximately 118.44 cm hr^{-1} (46.63 in hr^{-1}) in the SM cells.

5.3.2. Inflow to Outflow: Pollutant Removal within Each Treatment

The average NLP, SRP, TKN and NO_3^- mass loads from each 20-L increment of inflow and outflow stormwater volume up to 120 liters are shown in Figure 24. The inflow mass is normalized by watershed area and includes data from the eight bioretention cells.

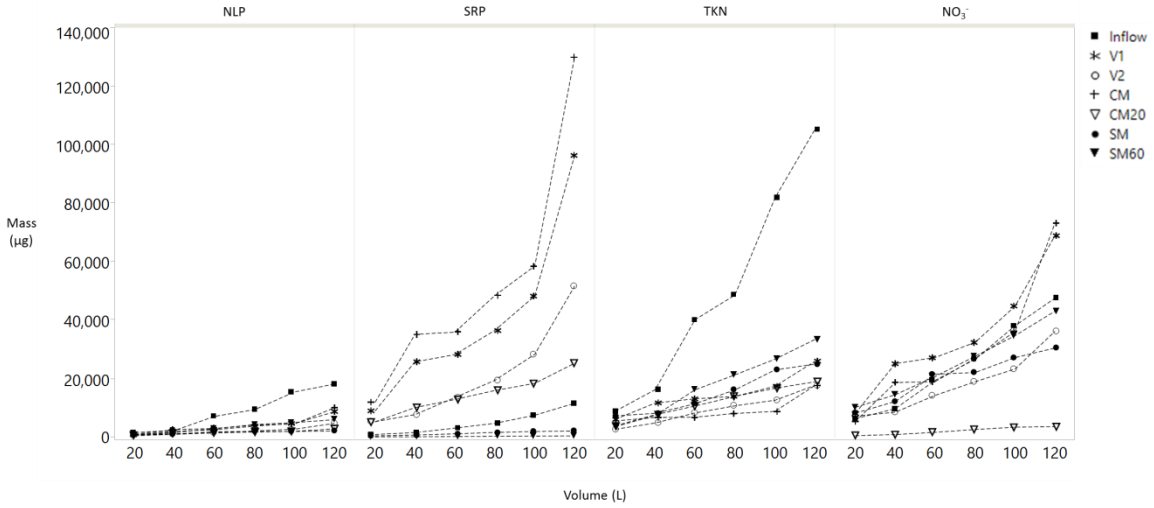

Figure 24. Average inflow and outflow cumulative mass per cumulative volume by treatment (120-L). CM contains data from cell 2 only.

Paired t-test results (Table 20) comparing inflow to outflow mass across the 120-L volume indicate that the NLP mass was significantly reduced, from inflow to outflow in all treatments. The percent NLP mass removal (Table 20) ranged from 42% (CM, cell 2

only) to 74% (V2). The SRP mass load was significantly increased from inflow to outflow in all treatments, except those containing Sorbtive Media (i.e., SM and SM60). The percent SRP mass removal ranged from -1,180% (CM, cell 2 only) to 94% (SM60). The TKN mass was also significantly reduced, from inflow to outflow, in all treatments. The percent TKN mass removal ranged from 59% (V1 and SM) and 78% (V2). The outflow nitrate mass load from V1 was significantly higher than the inflow (-52%). Nitrate significantly decreased from inflow to outflow in V2 (19%) and CM20 (91%). There was no significant difference between nitrate mass from inflow to outflow in CM (cell 2 only), SM or SM60. The TSS mass (not shown) was found to be significantly reduced from inflow to outflow in all treatments. The percent TSS mass reduction ranged from 66% (CM, cell 2 only) to 93% (CM20). The outflow cumulative mass from each treatment was found increase with cumulative volume, and was well predicted by linear regression, as shown in Table 21.

Table 20. Paired t-test comparing inflow and outflow mass on an equal volume basis (120 L), where n = 6 (df = 5) and percent mass removal and standard deviation (±) also shown.

Group	Mass	Level	- Level	Score Mean Diff	Std Err Dif	t-ratio	One sided p-value	Percent Removal (%)	±
V1	TP	In	Out	-30,753	9,728	-3.16	0.0125*	-285.0	1.74
	NLP	In	Out	5,266	1,761	2.99	0.0152*	51.8	0.195
	SRP	In	Out	-35,807	10,743	-3.33	0.0104*	-868.8	3.56
	TN	In	Out	26,214	11,513	2.28	0.0359*	21.8	0.326
	TKN	In	Out	35,474	12,724	2.79	0.0193*	58.5	0.228
	NO3	In	Out	-9,820	2,939	-3.34	0.0103*	-52.0	0.529
	TSS	In	Out	3,420	1,043	3.28	0.0110*	78.5	0.088
V2	TP	In	Out	-9,517	3,793	-2.51	0.0269*	-83.2	0.416
	NLP	In	Out	6,931	2,188	3.17	0.0124*	73.7	0.087
	SRP	In	Out	-16,109	5,379	-2.99	0.0151*	-359.7	0.731
	TN	In	Out	46,373	14,688	3.16	0.0126*	57.7	0.126
	TKN	In	Out	40,701	13,091	3.11	0.0133*	77.5	0.063
	NO3	In	Out	6,552	2,438	2.69	0.0217*	19.3	0.185
	TSS	In	Out	3,727	1,056	3.53	0.0084*	89.3	0.0186
CM	TP	In	Out	-43,602	14,216	3.07	0.0139*	-404.7	2.490
	NLP	In	Out	4,800	1,761	2.73	0.0207*	42.3	0.288
	SRP	In	Out	-4,888	48,462	-3.22	0.0118*	-1,179.7	5.117
	TN	In	Out	36,251	11,687	3.10	0.0134*	43.0	0.2089
	TKN	In	Out	41,220	13,740	3.00	0.0150*	72.5	0.199
	NO3	In	Out	-5,266	4,398	1.20	0.8576	-20.8	0.4250
	TSS	In	Out	2,994	984	3.04	0.0143*	65.8	0.1505
CM20	TP	In	Out	-2,879	1,290	-2.23	0.0380*	-65.2	0.8151
	NLP	In	Out	7,359	2,481	2.97	0.0157*	73.2	0.1614
	SRP	In	Out	-9,750	1,291	-7.55	0.0003*	-308.0	1.75
	TN	In	Out	59,146	18,282	3.24	0.0115*	77.3	0.070
	TKN	In	Out	38,203	13,049	2.93	0.0164*	69.3	0.122
	NO3	In	Out	22,531	6,054	3.72	0.0068*	91.3	0.0082
	TSS	In	Out	3,939	1,135	3.47	0.0089*	93.3	0.0320
SM	TP	In	Out	10,720	3,685	2.91	0.0167*	71.8	0.147
	NLP	In	Out	7,368	2,579	2.86	0.0178*	71.2	0.187
	SRP	In	Out	3,578	1,399	2.56	0.0254*	65.7	0.109
	TN	In	Out	39,633	15,646	2.53	0.0262*	39.8	0.262
	TKN	In	Out	35,002	12,250	2.86	0.0178*	59.2	0.221
	NO3	In	Out	4,339	3,325	1.30	0.1244	2.7	0.284
	TSS	In	Out	3,867	1,106	3.50	0.0087*	91.0	0.0477
SM60	TP	In	Out	9,791	3,284	2.98	0.0154*	68.8	0.082
	NLP	In	Out	5,586	1,970	2.84	0.0182*	55.0	0.136
	SRP	In	Out	4,650	1,601	2.90	0.0168*	93.8	0.020
	TN	In	Out	29,845	11,404	2.62	0.0236*	31.8	0.164
	TKN	In	Out	32,074	10,783	2.99	0.0153*	60.8	0.0567
	NO3	In	Out	-524	1,530	0.343	0.6271	-17.3	0.3056
	TSS	In	Out	3,662	1,082	3.39	0.0098*	84.3	0.074

Table 21. Linear regression of the cumulative outflow mass with cumulative volume to 120 L (n=6). Units of mass are in µg, except TSS (mg). CM is cell 2 only.

Treatment	Parameter	Linear Fit	R^2	Regression Coefficient	Standard Error	T Ratio	Prob > |t|
V1	TP	-11,724 + 798X	0.83	798	183	4.36	0.0120
	NLP	-1,148 + 70X	0.88	70	13	5.53	0.0052
	SRP	-10,631 + 733X	0.82	733	169	4.33	0.0124
	TN	1629 + 646X	0.90	646	106	6.12	0.0036
	TKN	2974 + 167X	0.89	167	29	5.78	0.0044
	NO_3^-	-2380 + 526X	0.91	526	86	6.30	0.0032
	TSS	123 + 8.70X	0.89	8.70	1.5	5.78	0.0044
V2	TP	-9,488 + 463X	0.87	463	85	5.17	0.0066
	NLP	-630 + 39X	0.91	39	6	6.31	0.0032
	SRP	-8,976 + 428X	0.87	428	83	5.15	0.0068
	TN	-2,030 + 411X	0.94	411	50	8.16	0.0012
	TKN	-633 + 144X	0.98	144	9.9	14.50	0.0001
	NO_3^-	-1,327 + 277X	0.93	277	39	7.10	0.0021
	TSS	-107 + 7.62	0.98	7.62	0.58	13.15	0.0002
CM	TP	-14,909 + 1,027X	0.78	1,027	275	3.74	0.0202
	NLP	-1,010 + 74X	0.80	74	19	4.00	0.0161
	SRP	-14,010 + 962X	0.78	962	254	3.78	0.0194
	TN	-8,759 + 651X	0.79	651	169	3.86	0.0181
	TKN	2,126 + 97X	0.68	97	33	2.91	0.0435
	NO_3^-	-10,084 + 571X	0.82	571	133	4.31	0.0126
	TSS	249 + 12.98X	0.82	12.98	3.03	4.30	0.0127
CM20	TP	2,113 + 202X	0.97	202	17	11.67	0.0003
	NLP	298 + 19X	0.95	19	2	9.14	0.0008
	SRP	1,815 + 183X	0.97	183	15	12.02	0.0003
	TN	1,132 + 183X	0.99	183	7	24.71	<0.0001
	TKN	1,392 + 151X	0.99	151	6	25.22	<0.0001
	NO_3^-	-291 + 34X	0.97	34	3	11.95	0.0003
	TSS	39 + 2.48X	0.98	2.48	0.19	13.36	0.0002
SM	TP	688 + 28X	0.95	28	3	8.51	0.0010
	NLP	742 + 13X	0.84	13	3	4.60	0.0100
	SRP	50 + 18X	0.99	18	1	16.99	<0.0001
	TN	8,431 + 357X	0.98	357	25	14.37	0.0001
	TKN	1,373 + 197X	0.95	197	21	9.19	0.0008
	NO_3^-	4,587 + 224X	0.96	224	24	9.33	0.0007
	TSS	-11.53 + 4.24X	0.86	4.24	0.87	4.88	0.0081
SM60	TP	-284 + 56X	0.99	56	3	19.43	<0.0001
	NLP	-337 + 54X	0.99	54	3	21.38	<0.0001
	SRP	-7.13 + 3.51X	0.99	3.51	0.19	18.47	<0.0001
	TN	-1,177 + 635X	1.00	635	22	28.50	<0.0001
	TKN	-3,122 + 303X	0.99	303	13	23.73	<0.0001
	NO_3^-	1,944 + 332X	0.99	332	16	21.01	<0.0001
	TSS	78.8 + 5.82X	0.99	5.82	0.24	24.63	<0.0001

5.3.3. Comparing Cumulative Outflow Mass Loads between Treatments

Paired t-test results comparing outflow mass between treatments (Table 22, Figure 25) indicate that the outflow mass from V2 was significantly lower than V1 for all constituents. The outflow mass from SM was significantly lower than CM for all constituents, except TKN and NLP, which were not statistically different between treatments. Outflow mass from CM20 was significantly lower than CM for all constituents except TKN. Outflow SRP mass from SM60 was significantly lower than SM. NLP and TSS mass from SM60 were significantly higher than SM.

Table 22. Cumulative outflow mass compared between treatments using a paired t-test. When CM and SM are compared, CM contains averaged data from replicate cells 2 &6. When CM is compared with CM20, CM contains data from cell 2 only.

Parameter	Level	- Level	df	Mean Diff	Std Err	t	Prob > |t|	Lower CL	Upper CL
TP	V2	V1	5	-21,236	6,037	-3.50	0.0170	-36,753	-5,718
	CM	SM	5	41,473	13,046	3.18	0.0246	7,938	75,009
	CM20	CM	5	-40,723	14,880	-2.74	0.0410	-78,974	-2,472
	SM60	SM	5	929	419	2.22	NS	-148	2,007
NLP	V2	V1	5	-1,665	518	-3.22	0.0236	-2,996	-334
	CM	SM	5	2,102	973	2.16	NS	-400	4,604
	CM20	CM	5	-2,559	985	-2.60	0.0484	-5,091	-27
	SM60	SM	5	1,782	629	2.83	0.0365	166	3,397
SRP	V2	V1	5	-19,697	5,534	-3.56	0.0162	-33,923	-5,471
	CM	SM	5	39,384	12,101	3.25	0.0226	8,277	70,492
	CM20	CM	5	-38,714	13,987	-2.77	0.0395	-74,668	-2,760
	SM60	SM	5	-1,072	224	-4.79	0.0049	-1,647	-496
TN	V2	V1	5	-20,159	4,383	-4.60	0.0058	-31,426	-8,893
	CM	SM	5	13,420	5,771	2.33	NS	-1,415	28,254
	CM20	CM	5	-22,894	8,942	-2.56	NS	-45,881	92
	SM60	SM	5	9,789	4,332	2.26	NS	-1,347	20,924
TKN	V2	V1	5	-5,228	799	-6.54	0.0013	-7,283	-3,173
	CM	SM	5	-472	1,324	-0.36	NS	-3,874	2,931
	CM20	CM	5	3,017	1,433	2.10	NS	-668	6,701
	SM60	SM	5	2,928	1,794	1.63	NS	-1,684	7,539
NO_3^-	V2	V1	5	-16,372	4,292	-3.81	0.0124	-27,405	-5,338
	CM	SM	5	14,159	5,455	2.60	0.0485	138	28,180
	CM20	CM	5	-27,796	9,179	-3.03	0.0291	-51,391	-4,202
	SM60	SM	5	4,864	1,952	2.49	NS	-153	9,880
TSS	V2	V1	5	-307	57	-5.40	0.0029	-453	-161
	CM	SM	5	447	98	4.56	0.0061	195	699
	CM20	CM	5	-945	183	-5.15	0.0036	-1,417	-474
	SM60	SM	5	201	36	5.60	0.0025	109	292

a

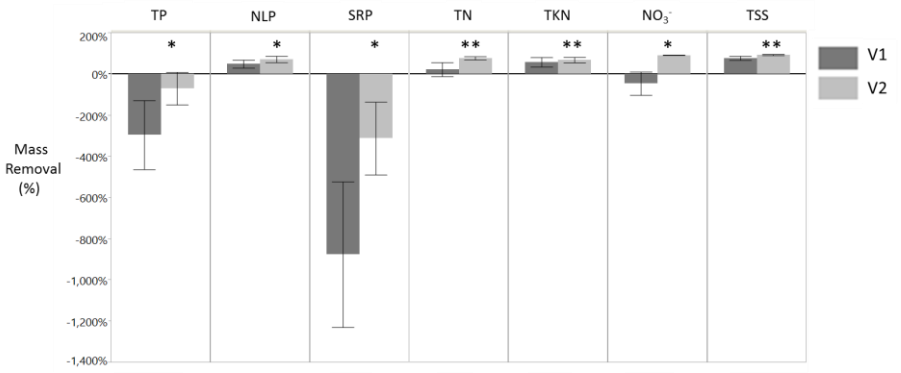

b

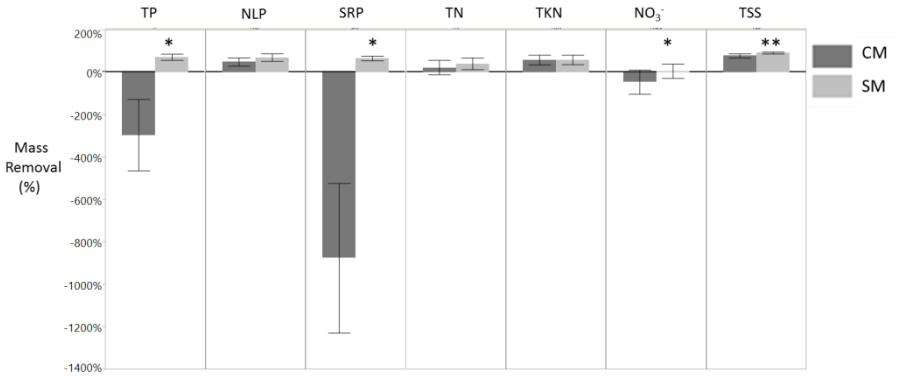

c

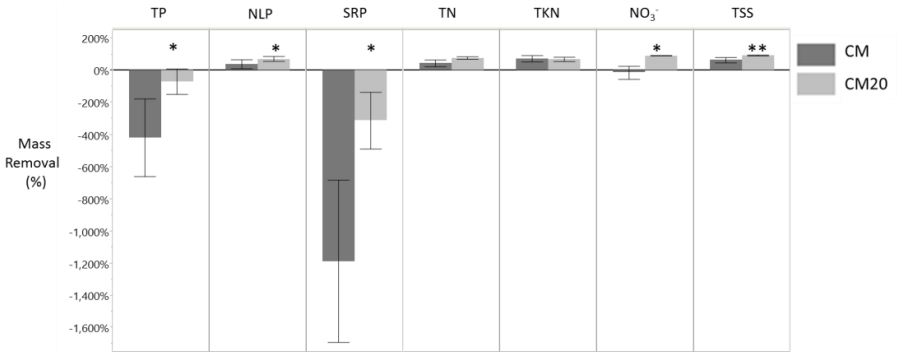

d

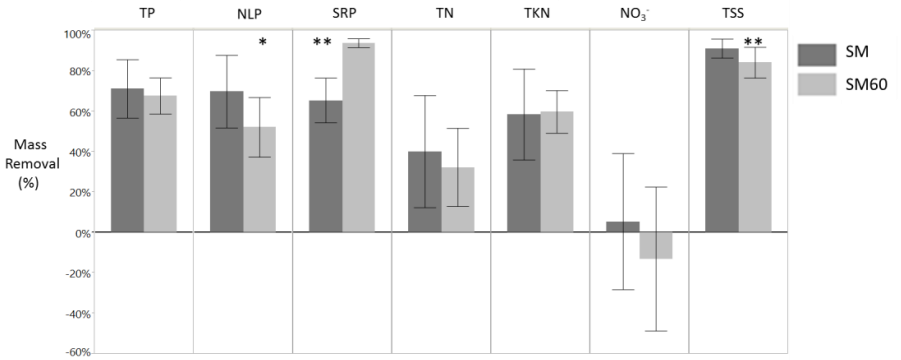

Figure 25 a, b, c, and d. Percent mass removal by treatment on an equal volume basis to 120-L (n = 6). Each error bar is 1 standard deviation from the mean. Asterisks signify a significant difference in outflow mass between treatment pairs, with ns = $p > 0.05$, * = $p \leq 0.05$, ** = $p \leq 0.01$, *** = $p \leq 0.001$, **** = $p \leq 0.0001$.

SRP export was greatest in the V1 treatment (-869%) (Figure 25). SM and SM60 reduced SRP mass loads by 66% and 94%, respectively. NLP and TKN removals were highest in V2, at 74% and 78%, respectively. TSS removal was highest in SM (91%).

5.3.4. Bioretention Sand and Compost Mixture: Pre and Post-Installation

Soil samples collected from the top 10 cm of each bioretention profile, from June 2013 to October 2014 (n = 7) (post-installation), were compared to the samples of the original (pre-installation) sand/compost mixture using Dunnett's control. SRP, NO_3^-, and NH_4^+ contents significantly decreased from the pre-installation soil media in all treatments (Figure 26).

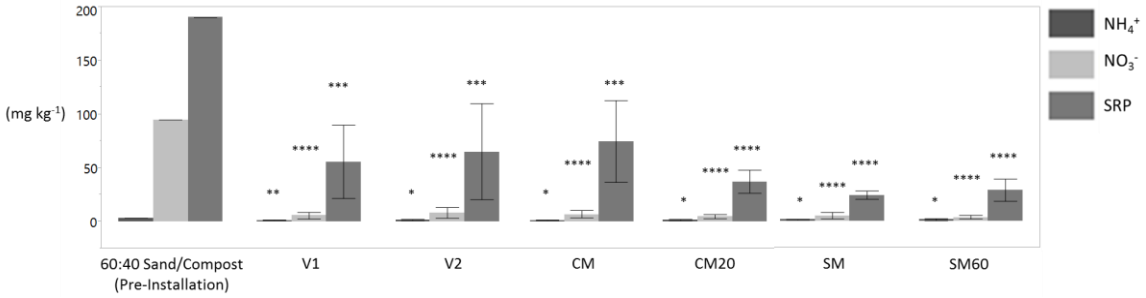

Figure 26. Comparing the soil extractable NH_4^+, NO_3^-, and SRP contents from the original pre-installation bioretention soil mix (60% sand, 40% compost) to the average after two years of installation (n = 7) using Dunnett's control. Each error bar is constructed using 1 standard deviation from the mean. CM is showing data from cell 2 only. Asterisks signify a significant decrease from the original soil media, with ns = $p > 0.05$, * = $p \leq 0.05$, ** = $p \leq 0.01$, *** = $p \leq 0.001$, **** = $p \leq 0.0001$.

There was no significant decrease in the bulk density, CEC, or organic matter content from pre to post-installation in any of the treatments (Tables 23 a, b, and c). K, Mg, and pH significantly decreased from pre to post-installation in all treatments. Soil sodium content significantly decreased in the SM and SM60 treatments. Mn significantly decreased in all treatments except SM. Sulfur content significantly decreased only in SM60.

Table 23 a, b, and c. Average characteristics of the top 10 cm of the 60:40 sand and compost mixture from June 2013 to October 2014, compared to the original pre-installation media using Dunnett's control (d) (α = 0.05). No significant differences were found in table c.

Treatment	Soil Test P (orthophosphate)				NO_3^-				NH_4^+				pH				Bulk Density		
	mg kg^{-1}				mg kg^{-1}				mg kg^{-1}				-log $[H^+]$				g cm^{-3}		
	n	Mean	±	|d|	n	Mean	±	|d|	n	Mean	±	|d|	n	Mean	±	|d|	n	Mean	±
Original	1	190	-	2.38	1	94.75	-	2.30	1	2.86	-	2.24	1	8.40	-	2.38	1	1.37	-
V1	7	55	23	<.0001	13	5.25	2.31	<0001	13	0.89	0.23	0.0041	7	7.04	0.10	<0001	10	1.34	0.09
V2	7	65	44	<.0001	13	7.83	4.59	<0001	13	1.23	0.45	0.0179	7	6.85	0.23	<0001	10	1.30	0.09
CM	7	74	38	0.0298	13	6.65	3.52	<0001	13	0.88	0.43	0.0008	7	7.16	0.16	0.0004	10	1.35	0.07
CM20	7	37	11	<.0001	13	4.43	1.89	<0001	13	1.21	0.58	0.0176	7	6.88	0.13	<0001	10	1.34	0.09
SM	7	24	4	<0001	13	5.03	3.05	<0001	13	1.16	0.45	0.0146	7	7.05	0.15	<0001	10	1.27	0.15
SM60	7	29	10	<0001	13	3.63	1.75	<0001	13	1.26	0.94	0.0219	7	6.98	0.20	<0001	10	1.44	0.10

Treatment	n	K			Mg			S			Mn			Na		
		mg kg^{-1}			mg kg^{-1}			mg kg^{-1}			mg kg^{-1}			mg kg^{-1}		
		Mean	±	|d|	Mean	±	|d|	Mean	±	|d|	Mean	±	|d|	Mean	±	|d|
Original	1	286	-	2.43	237	-	2.43	23.00	-	2.43	11.10	-	2.43	148	-	-
V1	7	29	11	<0001	73	16	<0001	15.57	3.01	NS	6.15	0.915	0.0134	76	76	NS
V2	7	37	13	<0001	75	26	<0001	15.57	4.77	NS	6.57	1.26	0.0242	56	46	NS
CM	7	35	19	<0001	89	28	0.0027	18.00	5.29	NS	6.31	1.31	0.0141	85	68	NS
CM20	7	30	10	<0001	71	21	<0001	12.57	5.29	NS	7.09	1.49	0.0481	41	29	NS
SM	7	29	11	<0001	79	18	<0001	11.86	4.49	NS	8.40	1.98	NS	33	24	NS
SM60	7	27	12	<0001	62	16	<0001	7.71	2.36	0.0378	6.57	1.82	0.0242	28	32	0.0457

Treatment	n	Ca		Al		Fe		Zn		Cu		CEC		Organic Matter	
		mg kg^{-1}		mg kg^{-1}		mg kg^{-1}		mg kg^{-1}		mg kg^{-1}		$cmol_c$ kg^{-1}		%	
		Mean	±	Mean	±	Mean	±	Mean	±	Mean	±	Mean	±	Mean	±
Original	1	711	-	9.00	-	2.70	-	1.10	-	0.20	-	6.30	-	1.10	-
V1	7	978	117	8.14	2.00	2.70	0.49	2.80	0.99	0.61	1.05	5.58	0.67	1.52	0.39
V2	7	985	162	8.36	0.556	2.71	0.65	2.94	1.68	0.96	2.06	5.66	1.01	1.79	0.64
CM	7	1,086	205	7.43	2.64	2.87	0.79	2.61	0.855	0.48	0.65	6.27	1.22	1.56	0.44
CM20	7	811	124	8.00	1.83	2.80	1.18	2.54	0.67	0.39	0.34	4.71	0.74	1.32	0.36
SM	7	873	146	6.29	1.70	3.10	0.72	3.41	1.27	0.33	0.37	5.11	0.90	1.39	0.42
SM60	7	702	153	7.29	1.11	3.06	1.53	3.13	1.91	0.61	1.08	4.11	0.92	1.18	0.26

5.3.5. Bioretention Sand and Compost Mixture: Differences between Treatments

The sand/compost mixture was tested in each cell over two years and compared between treatments. Paired t-test results indicate that V1 had significantly lower extractable soil NO_3^- ($t(12) = -2.60$, $p = 0.0117$) and NH_4^+ ($t(12) = -3.13$, $p = 0.0043$) than V2. Soil SRP was also lower in V1 than V2, but the difference was not significant. The soil pH in V1 was significantly lower than V2 ($t(6) = -2.03$, $p = 0.0446$). All other soil parameters were found to be equal between the two treatments.

Soils in the CM treatment were found to have significantly higher SRP ($t(6) = 3.29$, $p = 0.0083$), Al ($t(6) = 4.97$), Ca ($t(6) = 3.09$, $p = 0.0107$) and B ($t(6) = 2.40$, $p = 0.0266$) than in the SM treatment. CM also had significantly higher CEC ($t(6) = 2.47$, $p = 0.0013$), OM ($t(6) = 2.13$, $p = 0.0387$) and bulk density ($t(9) = 2.17$, $p = 0.0290$), than the SM. Conversely, the CM had significantly lower Zn ($t(6) = -2.88$, $p = 0.0141$), Mn ($t(6) = -4.29$, $p = 0.0026$), and Fe ($t(6) = -2.08$, $p = 0.0416$) than SM. NH_4^+ was also lower in CM than SM ($t(12) = -1.79$, $p = 0.0493$); however, soil nitrate not significantly different between the two treatments.

CM20 soils had significantly lower soil SRP ($t(6) = -3.40$, $p = 0.0073$) and NO_3^- ($t(6) = -3.05$, $p = 0.0050$) than CM; however, NH_4^+ was not significantly different between the two treatments. CM20 had significantly lower Ca ($t(6) = -4.61$, $p = 0.0018$), Mg ($t(6) = -2.46$, $p = 0.0247$), B ($t(6) = -2.27$, $p = 0.0317$) and Na ($t(6) = -2.31$, $p = 0.0302$) than CM. This likely contributed to a lower CEC ($t(6) = -4.42$, $p = 0.0020$) and pH ($t(6) = -4.52$, $p = 0.0020$) in CM20 than CM.

The soil SRP, NO_3^-, and NH_4^+ constituents were not significantly different between SM and SM60. SM60 had less soil Ca ($t(6) = -2.09$, $p = 0.0406$), Al ($t(6) = -$

2.04, p = 0.0432), Mg (t (6) = -2.30, p = 0.0370), Mn (t (6) = -2.99, p = 0.0121) and S (t (6) = -2.46, p = 0.0245) than the SM treatment. This likely contributed to a lower CEC in SM60 (t (6) = -2.10, p = 0.0400). Bulk density was found to be higher in the SM60 treatment (t (9) = 3.65, p = 0.0027).

5.3.6. Mass Balance: SRP and NO_3^-

The original sand/compost mixture was found to contain more soil test P and NO_3^- than could be removed from the media via plant uptake, resulting in a net export of labile nutrients in some cases. Upon installation, there was approximately 1,552 kg of 60:40 sand and compost mixture in each of the bioretention cells. A volume of 1.13 $m^3$of the sand-compost mixture contained an average of 294,880 mg of soil test P, 147,052 mg of NO_3^-, and 4,439 mg of NH_4^+ prior to any precipitation events. Approximately 69 inches (1.75 m) of rainfall fell on the site during the study period (NOAA, National Weather Service Forecast). Looking again at the sand-compost media two-years post installation, the average soil test P content (n = 7) in the sand/compost mixture decreased by between 66% (201 g) and 87% (257 g) across all treatments. NO_3^- decreased between 92% (135 g) and 96% (141 g). NH_4^+ decreased between 56% (2.49 g) and 69% (3.06 g).

Stormwater from the drainage area was found to contribute only 1% and 2% of the total SRP load to the outflow across all the cells, with the remainder coming from the sand/compost mixture. NO_3^- mass load from stormwater contributed between 9% and 22% of the total load, with larger loads coming from the larger watersheds, as a result of larger runoff volumes (Chapter 4). Cumulative outflow mass from each treatment was well predicted by cumulative volume, as shown in Table 21.

Of the total SRP and NO_3^- mass loads released from the combination of compost and incoming stormwater, approximately 70% was found to be removed by vegetation in V1 and 30% was released in the outflow effluent. Vegetation in V2 was found to remove approximately 80% of the SRP and NO_3^- from the compost and incoming stormwater, releasing 20% to the outflow. SRP uptake by plants was approximately 97 mg kg^{-1} in V1 and 103 mg kg^{-1} in V2. NO_3^- uptake was approximately 70 mg kg^{-1} in V1 and 81 mg kg^{-1} in V2.

The CM20 treatment was found to remove approximately 144 mg kg^{-1} of SRP and 97 mg kg^{-1} of NO_3^- during the two year period after the bioretention cells were installed. Nitrate removal from the stormwater and sand/compost mixture was approximately 98%, with approximately 43 g of nitrate removed, possibly via denitrification.

Sorbtive Media™ has a bulk density of approximately 0.72 g cm^{-3}. The SM and SM60 cells each contained approximately 204 kg of the material. The total SRP removal from the SM and SM60 cells during the two year period following installation was found to be 164 mg kg^{-1} and 160 mg kg^{-1}, respectively. Nitrate removal from the SM and SM60 cells was approximately 84 mg kg^{-1} and 53 mg kg^{-1}, respectively. The total SRP removal can be broken out into plant uptake, and sorption of SRP; and total NO_3^- removal is associated with plant uptake and enhanced NO_3^- removal, where the removal mechanism is still unknown. Notably, both SM treatments were planted with the same species mix in V1. If the plant uptake rates from V1 are applied to the SM and SM60 treatments, the media alone can be predicted to have removed approximately 104,573 mg of SRP in SM and 98,389 mg in SM60 during the study period. If the V1 plant uptake rates are applied,

110 mg of NO_3^- were removed per kg of Sorbtive Media™ in SM. In SM60, NO_3^- removal was approximately 126 mg kg^{-1}.

5.3.7. Outflow Partial Event Mean Concentrations

Average partial event mean concentration (PEMC) of the inflow and the outflow during the first two seasons of monitoring (2013 to 2014) can be found in Table 24.

Table 24 a and b. Average inflow and outflow partial event mean concentration by treatment, where n is equal to the number of storm events. All parameters are in units of µg L^{-1} except TSS (mg L^{-1}). CM contains cell 2 only.

PEMC for inflow and vegetation treatments									
Parameter	n	Inflow	±	n	V1	±	n	V2	±
TP	35	104	73	10	590	455	9	474	606
NLP	35	67	54	10	45	32	9	36	39
SRP	35	38	43	10	546	429	9	438	568
TN	35	570	361	10	888	666	9	748	805
TKN	35	380	268	10	356	228	9	270	287
NO3	35	196	166	10	547	535	9	499	553
TSS	34	23	24	10	6.0	4.05	9	6.13	6.18

PEMC for soil media and precipitation treatments												
Parameter	n	CM	±	n	CM20	±	n	SM	±	n	SM60	±
TP	4	618	461	4	183	127	4	73	55	5	53	29
NLP	4	53	36	4	18	11	4	49	48	5	49	29
SRP	4	568	431	4	164	116	4	24	6	5	4	3
TN	4	546	302	4	192	22	4	819	536	5	751	356
TKN	4	257	292	4	149	15	4	376	329	5	287	147
NO3	4	291	237	4	44	15	4	463	208	5	464	274
TSS	4	10.20	1.76	4	3.03	0.42	4	5.26	4.79	5	5.34	2.34

5.3.8. Soil Greenhouse Gas Emissions

Soil gas fluxes (CO_2, N_2O, and CH_4) were measured during season II (July 2014 to October 2014) in each of the cells (Figure 27). The minimum, mean and maximum soil gas flux from each treatment across the 11 sample events are provided in Table 25.

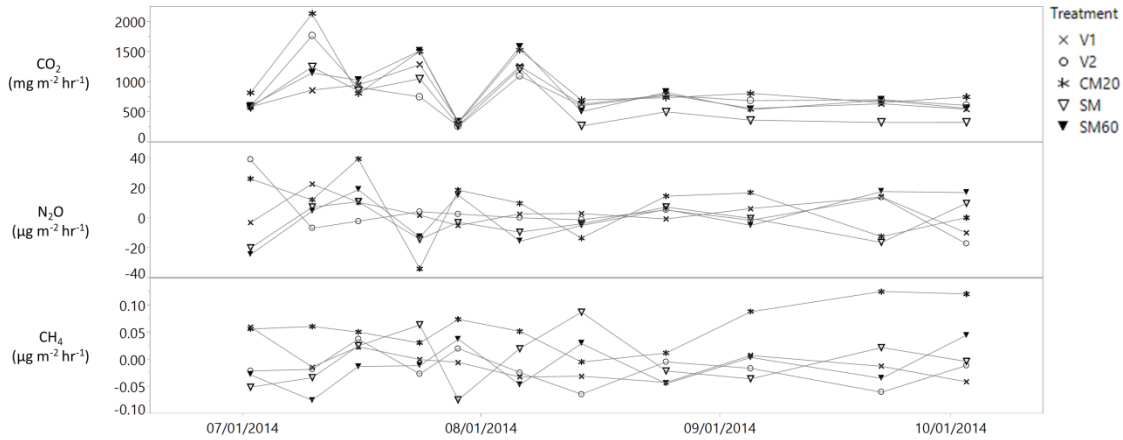

Figure 27. CO_2, N_2O, and CH_4 emissions by treatment, from June 2014 to October 2014 (n = 11, n is equal to the number of sample events).

Table 25. Summary statistics for CO_2, N_2O, and CH_4 emissions by treatment (n = 11, where n is equal to the number of sample events).

	CO_2				N_2O				CH_4			
	mg m^2 hr^{-1}				µg m^2 hr^{-1}				µg m^2 hr^{-1}			
Treatment	Min	Mean	±	Max	Min	Mean	±	Max	Min	Mean	±	Max
V1	337	768	300	1,286	-10.03	3.70	9.22	22.57	-0.0423	-0.0079	0.0306	0.0601
V2	261	797	383	1,768	-17.25	3.11	14.04	38.62	-0.0640	-0.0171	0.0297	0.0377
CM	326	778	330	1,482	-25.69	4.98	19.54	35.28	-0.0545	-0.0046	0.0480	0.1009
CM20	313	979	524	2,137	-33.94	6.90	20.54	39.09	-0.0047	0.06080	0.0408	0.1259
SM	266	638	387	1,250	-20.16	-3.06	10.97	10.69	-0.0746	-3×10^{-5}	0.0493	0.0876
SM60	335	850	419	1,584	-24.55	1.30	15.01	18.63	-0.0753	-0.0125	0.0384	0.0449

5.3.9.1. Carbon Dioxide (CO_2)

There were no other significant differences in the CO_2 emissions between treatment pairs. The CO_2 emissions across all cells and events (n = 77) were variable, ranging from a minimum of 251 mg m^{-2} hr^{-1} to a maximum of 2,650 mg m^{-2} hr^{-1}. CO_2 positively correlated with soil temperature (r_s = 0.2545, p = 0.0255), and negatively correlated with antecedent precipitation conditions (r_s = -0.5333, p<0.0001) and water filled pore space (r_s= -0.5400, p=0.0065). . CO_2 was found to be higher in SM60 than SM (t (10) = 4.17, p = 0.0019).

5.3.9.2. Nitrous Oxide (N_2O)

The bioretention soil media was found to be a small source for N_2O in all treatments except SM, which was found to be a small sink, however there were no statistically significant differences in N_2O emissions between treatments. N_2O ranged from -33.94 μg m^{-2} hr^{-1} to 65.8μg m^{-2} h^{-1} across all samples (n = 77). The average N_2O emissions by treatment ranged from 1.3 μg m^{-2} $h^{-1}$to 6.9 μg m^{-2} h^{-1} with peaks between 10.69 μg m^{-2} h^{-1} and 39.09 μg m^{-2} h^{-1}. CM20 had the highest maximum N_2O peak. The average N_2O emission from CM20 was higher than CM, but the difference was not statistically significant. N_2O was found to positively correlate with average daily air temperature (r_s = 0.7062, p = 0.0152) and Al (r_s = 0.7364, p = 0.0152), and negatively correlate with NH_4^+ (r_s = -0.3037, p = 0.0425) and Mg (r_s = -0.7295, p = 0.0166).

5.3.9.3. Methane (CH_4)

The bioretention soil was found to be a small sink for CH_4 on average for all treatments (n = 11), except CM20, which was found to be a small source. CH_4 levels across all samples (n = 77) ranged from -0.1014 μg m^{-2} h^{-1} to 0.1259 μg m^{-2} h^{-1}. CH_4 was found to be significantly higher in the CM20 treatment than its CM treatment pair (t (10) = 3.64, p = 0.0046). There were no other significant differences in CH_4 found between treatments.

5.4. Discussion

5.4.1. Hydrologic Bioretention Performance

The reductions in stormwater volume and peak flow rate were in alignment with what has been previously reported in the literature (Table 26), although inflow peak flow rates were on the low end, likely due to the smaller watershed sizes in this study.

Table 26. Infiltration rates within soil media in select bioretention cells.

Reference	Infiltration Rate
This study	Modelled Rate at Installation: 131 cm hr^{-1}
Arias et al (2001)	Actual Rate: 463 cm hr^{-1}
Brix et al. (2001)	Actual Rate: 92 cm hr^{-1}
Chen et al (2013)	Actual Rate: 1.3 cm hr^{-1}
Davis et al. (2009)	Recommends > 2.5 cm hr^{-1}
Debusk et al. (2011)	Actual Rate: 11.8 cm hr^{-1}
Dietz and Clausen (2005)	Design Rate: 10 – 13 cm hr^{-1}Actual Rate: 3.5 cm hr^{-1}
Hatt et al. (2008)	Actual Rate: 26.028 cm hr^{-1} to 232.92 cm hr^{-1} in different treatments
Hunt et al. (2006)	Actual Rate: 7.62 cm hr^{-1} – 38.1 cm hr^{-1}
Li and Davis (2008)	Actual Rate: Reduction from 43 – 164 cm hr^{-1} to 3-11 cm hr^{-1}
Lucas and Greenway (2011)	Vegetated: 27.7 cm hr^{-1} to 59.6 cm hr^{-1}
Thompson et al. (2008)	Actual Rate: 150 to 178 cm hr^{-1} (sand/compost mix)
Washington State University Pierce County Extension (2012)	Recommends > 2.54 cm hr^{-1}

Hunt et al. (2008) demonstrated peak flow reductions of greater than 95%, with inflow discharge peaks between 3.7 L s^{-1} and 50.8 L s^{-1}, and a maximum outflow peak of 0.48 L s^{-1}. DeBusk et al. (2011) found peak flow reductions greater than 99%, with inflow flow rates between 0.006 L s^{-1} and 22.4 L s^{-1}. Volume reductions were greater than 97%, with only five events producing outflow, and the maximum outflow peak flow rate was 2.09 L s^{-1} (DeBusk et al. 2011). The maximum outflow flow rate from all treatments in this research did not rise above 0.26 L s^{-1}, which was lower than outflow peaks reported by both Hunt et al. (2008) and DeBusk et al. (2011).

Hydraulic conductivities of the CM and SM were much higher than the minimum recommended 2.54 cm hr^{-1} (Davis et al. 2009; Washington State University Pierce County Extension 2012), and the conductivities reported by many others (Table 19), but were similar to infiltration rates found by Thompson et al. (2008) for sand and compost mixes (150 to 178 cm hr^{-1}) and mixtures with silt loam (87 to 141 cm hr^{-1}).

Rapid infiltration is ideal for flood control (Dietz 2007) but can be in direct competition with residence time, which is a key factor in pollutant removal (Brown and Hunt 2011).

5.4.2. Factors Affecting Nutrient and Sediment Dynamics

The export of nutrients in many of the treatments are likely directly attributable to the release of labile N and P from the sand/compost mixture during precipitation events, which was counterbalanced to some degree by uptake of nutrients from the soil pore water between storm events by plant roots. An additional fraction of outflowing nutrients originated from the potting soil that was introduced to the bioretention cells when the plants were originally transplanted from their nursery pots during construction. Because the volume of this material is minimal in comparison to the total volume of the sand/compost mixture, it is not expected to have been a major nutrient contributor.

The nutrient contents in the pre-installation sand/compost mixture were found to be comparable to those reported within the literature. For instance, the soil P content of the pre-installation sand/compost mixture (190 mg kg^{-1}) was higher than the 92 mg kg^{-1} used by Bratieres et al. (2008) (reported in Lintern et al. (2011) but similar to 138 mg kg^{-1} to 196 mg kg^{-1} range in the materials tested by Liu et al. (2014). Soil extractable NO_3^- content in this research (94.75 mg kg^{-1}) was similar to the Virginia Tech bioretention mixture (120 mg kg^{-1}) but was much lower than the TerraSolve (4,700 mg kg^{-1}) experimental bioretention media tested by Liu et al. (2014).

The starting CEC of the bioretention media used in this study was 6.30 $cmol_c$ kg^{-1}, which was typical of a sand (Sonon et al. 2014), and comparable to that used by Passeport et al. (2009) (6.2 $cmol_c$ kg^{-1}) and Hunt et al. (2006) (1.9 – 7.3 $cmol_c$ kg^{-1}). Dietz and Clausen (2005) used a higher CEC soil (16.8 $cmol_c$ kg^{-1} – 22.7 $cmol_c$ kg^{-1}), a range

that is typical of a clay loam (Sonon et al. 2014). The authors showed some of the lowest outflow TP concentrations reported (39 μg L^{-1} to 43 μg L^{-1}) (Dietz and Clausen 2006).

5.4.2.1. Vegetation Treatments, V1 and V2

The higher outflow mass from V1 of all N and P constituents, as well as sediment, were not expected, and may be attributable to root characteristics. V1 contained plants with predominantly shallow root systems, whereas V2 was dominated by *Panicum virgatum* (switchgrass), which is known for its deep, fibrous roots (Figure 21). For instance in V1, *Helenium autumnale* (Sneezeweed) and *Aquilegia Canadensis* (Columbine) have shallow, fibrous roots (Hallman 2009; The Lady Bird Johnson Wildflower Center 2016a). The *Aster novae angliae* (New England Aster) has fibrous roots which stem from short rhizomes, and reproduce vegetatively (The Lady Bird Johnson Wildflower Center 2016a; b) although we have not observed rhizomes on the New England Aster in this study. New England Aster and Sneezeweed had the largest observable above ground biomass during the majority of the growing season. The *Lobelia cardinalis* (Cardinal Flower) and *Asclepias tuberosa* (Butterfly Milkweed) have woody taproots, with the latter capable of reaching depths of greater than 6 feet (Natural Resources Conservation Service 2005; The Lady Bird Johnson Wildflower Center 2016c). The *Baptisia australis* (Blue False Indigo) is a legume that produce root nodules, which harbor nitrogen fixing *Rhizobium* bacteria (The Lady Bird Johnson Wildflower Center 2016d). The *Anemone canadensis* (Windflower) was typically the earliest to bloom and spread via rhizomes (Hilty 2015).

V2's below ground root biomass was likely dominated by *Panicum virgatum* (switchgrass), which is known for its deep, fibrous roots. For instance, Mann et al. (2013)

found that within 30 weeks of planting switchgrass, the roots had reached a depth greater than 6 feet in a non-irrigated system. The outflow mass of all constituents, both labile and non-labile, were lower from V2 , which may indicate that the deep rooted switchgrass in V2 had access to labile nutrients throughout a larger portion of the soil profile, utilizing both the small proportion of nutrients from stormwater which were held in the soil matrix between events, and the nutrients from the sand/compost media. The lower outflow NLP and TSS mass from V2 may suggest that the deep rooted switchgrass provided superior soil stability, or interception via its fine root structure. TKN was also lower in the outflow from V2, which may point to the retention of the organic N component and/or ammonium uptake. Further research including an investigation of root distributions within the soil profile of the bioretention cells is needed to confirm these hypotheses.

5.4.2.2. Soil Media Treatments, CM and SM

The higher retention of SRP in the SM treatment was in accordance with our original hypothesis and likely due to sorption of the SRP in both stormwater and the sand/compost mixture, to the Sorbtive Media™. However, the lower nitrate mass from the SM was not expected, especially given that the NO_3^- mass load to SM from stormwater is predicted to have been larger that the CM load overall due to SM having a larger drainage area (Chapter 4). The NO_3^- mass from the sand/compost mixture appears to have been predominantly removed by vegetative uptake in both the CM and SM treatments (the planting palette in V1 was the same as SM), yet if NO_3^- uptake rates from V1 are applied to SM, there is a portion of NO_3^- mass from the soil media that did not make it to the outflow, and was thus removed by other mechanisms.

Microbial denitrification is thought to be the primary nitrate removal mechanism by bioretention systems (Bratieres et al. 2008; Davis et al. 2006; Kim et al. 2003; Lucas and Greenway 2008), but typically requires an IWS zone. A small IWS zone was present in all treatments, therefore any denitrification attributable to this feature would have been observed in both CM and SM. An alternative explanation for why the NO_3^- mass from SM was lower than CM is abiotic reduction via chemodenitrification by soil cations (Fe^{2+}, Cu^{2+}) (Davidson et al. 2000; Luther et al. 1997; Pilegaard and Pilegaard 2013). The reservoir of ionic material provided by the SM layer may have contributed to some level of nitrate reduction and lower outflow mass loads. Nitrate reduction by Sorbtive Media™ or other ionic soil media components has not been previously documented in bioretention and warrants future research.

Removal of both labile and non-labile constituents in the SM treatment may have also been influenced by the lower hydraulic conductivity (K) of the SM. The lower (K) layer may have forced water to decelerate, providing conditions for larger particles to settle out and increasing retention time (Roy-Poirier 2009).

The total P sorptive capacity of the SM is estimated to be 5,850 mg of SRP per kg of Sorbtive Media™ (Imbrium Systems, personal communication, December 13, 2015), which is equivalent to approximately 1.4 x 10^6 mg of SRP (0.2832 m^3 of Sorbtive Media™ was used). At the current loading rate, the material is estimated to reach P removal capacity in approximately 27 years, although that lifespan is likely to dramatically increase once the labile nutrients from the sand/compost mixture are depleted and loading comes primarily from the stormwater. The average annual precipitation in Burlington, VT is predicted to deliver approximately 3 g of SRP to the

SM cells per year (Chapter 4), and is not likely to significantly impact the lifespan of the media when compared to the compost loading contribution.

5.4.2.3. Precipitation Treatment, CM and CM20

Enhanced SRP, NLP, NO_3^-, and TSS stormwater mass removals in CM20 were not expected, for the additional runoff and precipitation added to this treatment was predicted to increase the mobilization and transport of nutrients and sediment within the cell, increasing the mobilization of larger particulate constituents (i.e., NLP, TSS) and the solubilization of nutrients within the soil profile, resulting in higher outflow mass loads.

The additional runoff and precipitation added to CM20 may have resulted in the transport of fines and sediment to lower layers of the soil profile (Mengel and Kirkby 2001), causing a partial clogging of the underdrain at the outflow. This clogging would have inadvertently prevented larger particulates from exiting the underdrain and increased retention time, thereby enhancing pollutant removal. This hypothesis is supported by a number of ancillary measurements. For instance, the average daily VWC at the 61 cm depth (0.1266 ± 0.0379), was significantly higher than at the 5 cm depth (0.0751 ±0.0316) in CM20 ($t(252) = 26.51$, $p<0.0001$), and above field capacity (Figure 26). Sandy soils typically have a field capacity relating to a volumetric water content (VWC) of between 5% - 10% (Zotarelli et al. 2010). The electrical conductivity (EC) at the 61 cm depth was significantly higher than the 5 cm depth in CM20 ($t(252) = 32.16$, $p<0.0001$), indicating a vertical migration of ionic material within the soil media (Figure 28). A paired t-test indicated that the CM20 had a lower peak flow rate than CM ($t(5) = -3.35$, $p = 0.0204$). Further, the nitrate reduction in CM20 was particularly noteworthy, at

91% (Table 20), and likely the result of microbial denitrification, which requires some level of saturation (Lucas and Greenway 2008).

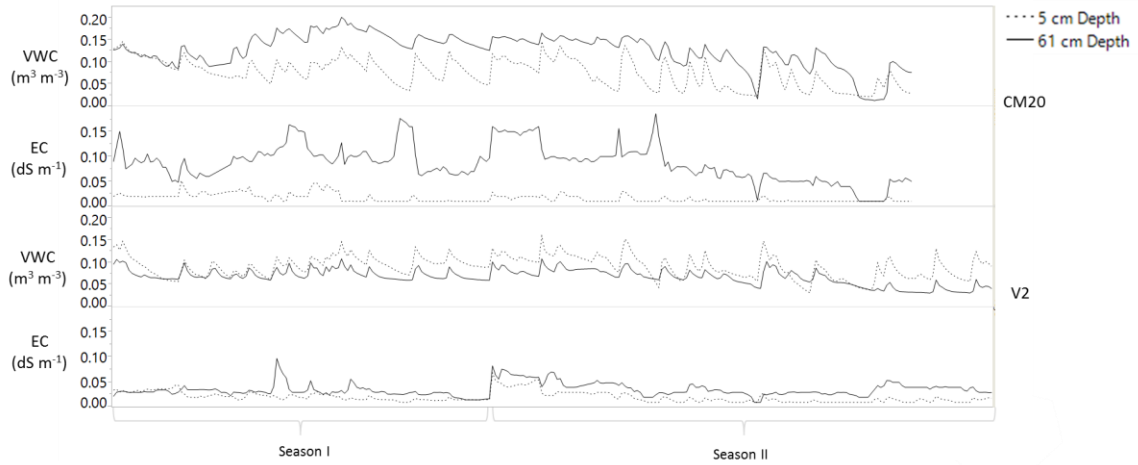

Figure 28. VWC and EC at the 5cm and 61cm depths during season I and II in CM20 and V2.

5.4.2.4. Precipitation Treatment, SM and SM60

The reduced outflow mass from the CM20 treatment which may have resulted from a partial clogging of the underdrain as a result of increased runoff and precipitation, did not appear to apply to the SM60 treatment, which had a 60% increase in precipitation and runoff added, but also contained a layer of Sorbtive Media™. SM60 was found to have greater masses of NLP and TSS in the outflow than SM (the treatments are otherwise identical). This was in accordance with our original hypothesis asserting that the larger volume of water received by SM60 would result in more pollutant export; the results were likely due to the flushing of the larger, predominantly particulate, constituents through the sand media and out into the underdrain with the additional precipitation. Interestingly, the increase in pollutant export with larger influent volumes did not hold true for the labile N and P components. The SRP mass loads in the outflow from SM60 were lower than for SM, despite the SM60 receiving more runoff an

precipitation volume and having higher inflow SRP mass loads. It is possible that the additional runoff and precipitation added to SM60 increased mixing between stormwater/compost leachate and the Sorbtive Media layer, which enhanced removal of SRP, as shown by lower SRP outflow mass from SM60 than SM.

The NO_3^- mass in the outflow between the SM and SM60 treatments was not significantly different, despite the larger NO_3^- load predicted to have entered the SM60 treatment due to its larger drainage area. Any potential chemodenitrification occurring in SM may have also been a factor in SM60. The additional precipitation to the SM60 treatment did not appear to have an effect on the solubilization and transport of NO_3^- or SRP in the soil media, for the soil nutrient contents over the course of two years following installation were not found to be statistically different. It is possible that the nutrients removed from the soil media during a precipitation event had an upper limit, which was not exceeded despite the additional volume added.

5.4.3. Outflow Partial Event Mean Concentrations

The inflow N, P, and sediment PEMC found in stormwater runoff from the paved road surface (Chapter 4) were similar to the EMC previously documented by others (Davis 2007; Geosyntec Consultants and Wright Water Engineers 2012; Hunt et al. 2006), although they were on the lower end overall. The relatively low influent concentrations of pollutants influence the calculation of percent mass removal of all the treatments; reported percent removal typically increases with increasing inflow mass load and volume reduction. When the outflow PEMC from the monitored portion of the event (i.e., not limited to the 120 liters of volume previously described) from each treatment are compared to the outflow EMC data from the literature, the cells in this study were all

comparable in their performance, despite the additional nutrients from the sand/compost mixture.

Looking at all treatments in the study, the outflow NLP PEMC was lowest from the CM20 treatment (18 μg L^{-1}) and highest from the CM treatment (cell 2 only; 53 μg L^{-1}). Both values are on low end of what has been found by others (Geosyntec Consultants and Wright Water Engineers 2008; Hunt et al. 2006; O'Neill and Davis 2011). For instance, Hunt et al. (2006), found NLP effluent to be between 40-800 μg L^{-1}.

Outflow SRP PEMC was highest from the CM treatment (cell 2 only; 568 μg L^{-1}) and lowest from SM60 (4 μg L^{-1}). Both treatment PEMC values were lower than the outflow SRP EMC found by Hunt et al. (2006) (2,200 μg L^{-1}) and Geosyntec Consultants and Wright Water Engineers (2008) (210 μg L^{-1} – 670 μg L^{-1}). Outflow SRP PEMC from the SM (24 μg L^{-1}) and SM60 (4 μg L^{-1}) treatments were much lower than most conventionally designed bioretention cells, with Bratieres et al. (2008) and Komlos et al. (2012) being exceptions. Bratieres et al. (2008) saw outflow SRP concentrations as low as 13 μg L^{-1} using a *Carex* vegetation and a sandy loam. After nine years of operation, Komlos et al. (2012) found the SRP concentrations to be as low as 30 μg L^{-1}. The soil media used by Komlos et al. (2012) was a 1:1 ratio of native material and imported sand, with SRP contents after nine years between 80 mg kg^{-1} and 160 mg kg^{-1} (Komlos and Traver 2012). The outflow SRP concentrations from SM and SM60 were lower than the 140 μg L^{-1} from iron coated sand used by Chardon et al. (2005) and similar to O'Neill and Davis (2011), (<10 μg L^{-1}), who used wastewater treatment residuals.

Outflow TKN PEMC was lowest from the CM20 treatment (149 μg L^{-1}), and highest from the SM treatment (376 μg L^{-1}). Outflow TKN values across all treatments

were much lower than the outflow TKN EMC's reported by Geosyntec Consultants and Wright Water Engineers (2008) (1,240 -1,780 μg L^{-1}) and Hunt et al. (2006) (4,900 μg L^{-1}).

Average NO_3^- was highest from V1 (547 μg L^{-1}) and similar to those reported by Geosyntec Consultants and Wright Water Engineers (2008) (410 – 790 μg L^{-1}). Average NO_3^- PEMC from V2 (227 μg L^{-1}) was similar both Hunt et al. (2006) and Dietz and Clausen (2006), who used elevated underdrains (IWS) to enhance denitrification (Table 14). CM20 exhibited strong signs of denitrification, with an average outflow nitrate PEMC of 44 μg L^{-1}. This was similar to the outflow nitrate concentrations found by Davis (2007) in a lined system (between 10 μg L^{-1} to 50 μg L^{-1}) and Lucas and Greenway (2008) (40 μg L^{-1}), who did not specifically design for saturation.

The outflow TSS PEMC was lowest from CM20 (3.03 mg L^{-1}) and highest from CM (cell 2 only,10.2 mg L^{-1}). Both were slightly lower than the outflow TSS EMCs reported by Geosyntec Consultants and Wright Water Engineers (2008) (15 to 33 mg L^{-1}) and similar to that found by Davis (2007) (4 and 64 mg L^{-1}). Overall, the outflow PEMC for TSS was low across all treatments, which further supports the consistent ability of bioretention cells to remove TSS from stormwater, even under simulated increases in precipitation due to climate change.

5.4.4. Soil Greenhouse Gas Emissions

5.4.4.1. Carbon Dioxide (CO_2)

There is little research on soil GHG emissions within bioretention cells specifically; however, soil gas emissions in other land-use setting are influenced by similar factors (e.g., soil porosity, mineral content, water content, pH, temperature). For

instance, the range of soil CO_2 emissions found in the treatments in this study (251 mg m^{-2} hr^{-1} to 2,650 mg m^{-2} hr^{-1}) were similar to Adviento-Borbe et al. (2010) who also found large variations in CO_2 flux from soils in maize field (13 mg m^{-2} hr^{-1} to 1,015 mg m^{-2} hr^{-1}). Positive correlations between CO_2 and temperature are common in all soils due to increases in microbial respiration (Mith et al. 2003). For instance, Qiu et al. (2005) found an increase CO_2 production with increasing temperature in dry lakebed soils, with a smaller range of flux values overall (170 mg m^{-2} hr^{-1} to 365 mg m^{-2} hr^{-1}).. The authors also found that leaf litter was a significant source of CO_2 overall (Qui et al. 2005). Leaf litter was purposefully removed from the anchors prior to gas sampling in this study, but may warrant further investigation in future studies.

The negative correlation between water filled pore space and CO_2 found in this research is likely the result of water within micro and macropores impeding the diffusion of CO_2 (Matson and Harris 1995; Smith et al. 2003). For instance, the 7/29/14 sampling date in Figure 27 shows a drop in CO_2, which corresponded with a 25% WFPS and was the highest WFPS measured. Qiu et al. (2005) also found that temporary submersion resulted in declining CO_2.

The addition of 20% more runoff and precipitation to CM20 did not appear to have had a significant effect on CO_2 emissions. However, the additional 60% volume in SM60, when compared to SM, may have supported a more rigorous soil microbial population (Bond-Lamberty and Thomson 2010), resulting in significantly higher CO_2 emissions from the SM60 treatment. The investigation of underground root and microbial biomass in bioretention is not well studied and warrants further research.

5.4.4.2. Nitrous Oxide (N_2O)

All treatments were found to exhibit both positive and negative N_2O fluxes, with the majority of treatments being a small source of N_2O overall. Average N_2O emissions across all treatments were between 1.3 μg m^{-2} $h^{-1}$to 6.9 μg m^{-2} h^{-1} with peaks between 10.69 μg m^{-2} h^{-1} and 39.09 μg m^{-2} h^{-1}. The emissions were similar to the ranges found in natural and urban ecosystems (Grover et al. 2013; Kaye et al. 2004). For instance, total soil N_2O fluxes of less than 4 μg m^{-2} h^{-1}, with peaks between 15 μg m^{-2} h^{-1} and 19 μg m^{-2} h^{-1} were found in grasslands and wheat fields during winter measurements (Kaye et al. 2004). Urban ecosystems have shown N_2O fluxes of 27 μg m^{-2} h^{-1} (Kaye et al. 2004). In one of the only studies that previously quantified emissions of N_2O in bioretention cells, Grover el al. (2013) found that the soil was a source of N_2O overall, with average fluxes of 13.8 μg m^{-2} h^{-1} and 65.6 μg m^{-2} h^{-1} in sandy loam, and 80% sandy loam, 10% compost, 10% hardwood mulch, respectively. The simulated rain events used by the authors resulted in WFPS as high as 70% (Grover et al. 2013).

The maximum average (7 μg m^{-2} h^{-1}) and peak (39 μg m^{-2} h^{-1}) N_2O production came from CM20. This is particularly interesting because CM20 was also found to exhibit substantial removal of nitrate mass from inflow to outflow (> 90%), and had the lowest outflow NO_3^- mass loads, which may be attributed to some level of saturation in the subsoils due to partial clogging of the underdrain. Maximum N_2O production is thought to occur when available nitrate levels are high and oxygen content in the soils are high enough for some oxidation of NH_4^+ but are not fully aerobic (Kaspar 1982). N_2O production from nitrification is thought to occur when WFPS is greater than 50% (Castellano et al. 2010; Davidson et al. 2000). In this research, the maximum WFPS

during soil gas measurements was across all treatments was 33%, indicating largely aerobic conditions, with any N_2O production likely occurring during nitrification (Castellano et al. 2010; Chapuis-Lardy et al. 2007), however these measurements were taken at the soil surface. The WFPS at the bottom of the CM20 treatment may have been much higher, as indicated by the lower NO_3^- outflow mass.

Although most soils act as a net source of N_2O emissions, uptake or consumption has also been observed (Butterbach-Bahl et al. 2013; Chapuis-Lardy et al. 2007; Conrad 1996; Schlesinger 2013). Conditions which lead to N_2O consumption are not yet fully understood (Butterbach-Bahl et al. 2013), but are thought to be influenced by soil available N, moisture, pH, and temperature (Syakila and Kroeze 2011). N_2O consumption occurs during both nitrification and denitrification reactions (Schlesinger 2013), with denitrification being the larger consumptive process overall (Chapuis-Lardy et al. 2007). Heterotrophic denitrifying bacteria utilize N_2O as an energy source and terminal electron acceptor when NO_3^- concentrations are very low and WFPS is moderate to high (Chapuis-Lardy et al. 2007; Conrad 1996). The bacteria contain nitrous oxide reductase (N_2OR), which is an enzyme that uses copper (Cu) clusters as a catalyst (Thomson et al. 2012), and allows the bacteria to reduce nitrous oxide to nitrogen gas (Butterbach-Bahl et al. 2013; Chapuis-Lardy et al. 2007). N_2O consumption typically ranges from 0.01 $\mu g\ m^{-2}\ h^{-1}$ to 10 $\mu g\ m^{-2}\ h^{-1}$ (Schlesinger 2013; Syakila and Kroeze 2011).

The SM treatment was found to consume N_2O on average over the course of the growing season (-3 $\mu g\ m^{-2}\ h^{-1}$), which is particularly interesting given the highly charged ionic material present (i.e., Sorbtive Media™) in that treatment. Abiotic reactions between NO_3^- and soil minerals (Fe^{2+}, Cu^{2+}) have been shown as a result of

chemodenitrification (Butterbach-Bahl et al. 2013; Chapuis-Lardy et al. 2007; Luther et al. 1997). It is possible that the reservoir of ionic material provided by the Sorbtive Media™ may have resulted in some abiotic reduction of NO_3^- and N_2O consumption. More research would be needed to verify this hypothesis.

5.4.4.3. Methane (CH_4)

All of the treatments were found to exhibit a very small amounts of CH_4 consumption on average (3×10^{-5} μg m^{-2} hr^{-1} to 0.0171 μg m^{-2} hr^{-1}) except for CM20, which was interestingly found to be a small source of CH_4 (0.0608 μg m^{-2} hr^{-1}). The factors contributing to production and consumption of methane in soils are complex and include organic matter, temperature, moisture, and populations of methanotrophic (consuming) and methanogenic (producing) soil microorganisms (Harriss et al. 1982; Nesbit and Breitenbeck 1992; Nisbet et al. 2014; Steudler et al. 1989).

CH_4 production occurs under anaerobic conditions in saturated soils whereas CH_4 consumption occurs in aerobic soils (Matson and Harris 1995; Smith et al. 2003). Grover et al. (2013) found CH_4 emissions in bioretention to be < 20 μg m^{-2} h^{-1}, although large peaks were observed on occasion (~200 μg m^{-2} h^{-1}). The positive CH_4 flux exhibited by CM20 is particularly interesting, for as previously described, the CM20 treatment exhibited signs of having some level of saturation present in the subsoils (e.g., showed significant nitrate mass reductions, from inflow to outflow, had the lowest NO_3^- mass from the outflow of any of the other treatments and had the highest N_2O peak).

The high oxygen diffusion capabilities of sand, low soil organic matter content and generally low soil moisture conditions likely contributed to methane oxidation/consumption in the other treatments. Grover et al. (2013) found average

methane uptake rates in bioretention soils to be 16.4 μg m^{-2} h^{-1} in cells with an IWS zone and 4.2 μg m^{-2} h^{-1} in a non-IWS cell. The high WFPS created with simulated events may have contributed to a higher initial production of CH_4, which was then oxidized in the upper soil layers (Grover et al. 2013). The consumption of CH_4 by other land-uses (e.g., rural forest, urban lawn, sub-artic tundra) has been between 10 μg m^{-2} h^{-1} and 125μg m^{-2} h^{-1}, with urban soils tending to be on the lower end of the consumption spectrum (Adamsen and King 1993; Groffman and Pouyat 2009; Kaye et al. 2004).

Another factor that may have influenced the CH_4 production/consumption was the depth to the layer most likely to be saturated. Smith et al. (2003) found that methane fluxes were negatively correlated with the depth to groundwater due to the oxidation of methane in the upper soil layers. At 50 cm below the surface, Smith et al. (2003) predicts the CH_4 flux would be < 1.6 μg m^{-2} h^{-1}, which is in accordance with our findings. Both production and consumption rates of gases in this research were extremely small in the global context, but are interesting, in that they offer insight into the processes taking place inside the bioretention cells.

5.5. Conclusions

Bioretention cells have exciting potential to mitigate the impacts of urbanization and help restore impaired waterbodies. In this research, bioretention cells were shown to consistently reduce peak flow rates and stormwater volumes, making them adept at increasing local climate change resiliency. Non-labile nutrient removal in bioretention was also considerable and found to be largely a function of physical filtration, similar to TSS.

The sand-based bioretention soil media used in this research was resilient to simulated increases in precipitation due to climate change (i.e., 20% more runoff and precipitation per bioretention cell) that are projected for the northeastern U.S., in that nutrient and sediment removal did not decrease with increased storm volumes. This phenomenon may be site-specific, however, and designs in other climates or which included other soil types, would need to be evaluated for resiliency. When subjected to much larger increases in precipitation (e.g., 60% more runoff and precipitation falling on the cell), the bioretention cells with Sorbtive Media™ showed enhanced SRP removal. NLP and TSS retention was not robust under these conditions, yet outflow concentrations were still comparable to the other treatments, and those reported in the literature.

Organic amendments such as compost are likely to contain labile nutrient contents far greater than that of incoming stormwater from a medium-traffic paved road surface. If high effluent mass loads of nutrients are to be avoided, the total available nutrient mass in the soil media needs to be less than the vegetative uptake capacity. Increased effluent nutrient loads may be temporary (a few years), but the short-term impacts of those nutrients should be assessed and minimized prior to the selection of soil media for bioretention. Sorbtive Media™ was shown to be effective at removing SRP and presents opportunities for the development of localized soil blends that can maximize phosphorus removal through sorption.

Vegetation characteristics such as root depth, texture, and architecture played a key role in the removal of both labile and non-labile nutrients from the soil profile. Deep-rooted plants provided soil stability and greater access to nutrients throughout a soil profile, contributing to enhanced labile nutrient uptake. Successful vegetative

establishment in the absence of excessive soil amendments like compost (that leach nutrients) will require plants that can tolerate low nutrient conditions, and which are tolerant of both floods and droughts. The nutrient requirements and uptake capacities of different bioretention plants are not well quantified and warrant further research.

Nitrate reduction may be achieved with extended detention in an anaerobic environment, and may be enhanced by abiotic reactions (i.e., chemodenitrification), although specific conditions conducive to maximizing denitrification efficiency (e.g., nitrate concentrations, duration, labile carbon content, soil mineral content, electron donors) need further investigation. Hybrid conditions which allow for both oxidative and reductive processes could maximize both P and N removal and warrant future research.

It appears that bioretention cells may be a small source of N_2O, but it is not likely to be significant in the greater context of global emissions. Bioretention cells may act as a sink for CH_4, if soils at the surface are aerobic; however, the inclusion of an internal water storage zone may alter CH_4 and N_2O emissions and uptake dynamics and require further investigation.

REFERENCES

Adamsen, A., and King, G. (1993). "Methane consumption in temperate and subartic forest soils: Rates, vertical zonation, and responses to water and nitrogen." *Applied and Environmental Microbiology*, 59(Feb), 485–490.

Adviento-Borbe, M. ., Kaye, J. P., Bruns, M. A., McDaniel, M. D., McCoy, M., and Harkcom, S. (2010). "Soil greenhouse gas and ammonia emissions in long-term maize-based cropping systems." *Soil Biology & Biochemistry*, 74(5), 1623–1634.

Alias, N., Liu, A., Egodawatta, P., and Goonetilleke, A. (2014). "Sectional analysis of the pollutant wash-off process based on runoff hydrograph." *Journal of Environmental Management*, 134, 63–9.

Allen Burton, G., and Pitt, R. (2002). *Stormwater effects handbook: a toolbox for watershed managers, scientists, and engineers*. Lewis Publishers, Boca Raton.

Antonio, A., and Walker, D. (2011). *Total Kjeldahl Nitrogen: Simplified with s-TKN ™*.

APHA. (1992). *Standard Methods for the Examination of Water and Wastewater*. American Public Health Association, Washington, D.C.

APHA. (2011). *Standard Methods for the Examination of Water and Wastewater*. American Public Health Association, Washington, D.C.

Arias, C., Del Bubba, M., and Brix, H. (2001). "Phosphorus removal by sands for use as media in subsurface flow constructed reed beds." *Water Research*, 35(5), 1159–68.

Basta, N., and Dayton, E. (2007). "Phosphorus chemistry and sequestration in soil." 1–23.

Blecken, G.-T., Zinger, Y., Deletić, A., Fletcher, T., Hedström, A., and Viklander, M. (2010). "Laboratory study on stormwater biofiltration: Nutrient and sediment removal in cold temperatures." *Journal of Hydrology*, 394(3-4), 507–514.

Blecken, G.-T., Zinger, Y., Deletić, A., Fletcher, T., and Viklander, M. (2009). "Influence of intermittent wetting and drying conditions on heavy metal removal by stormwater biofilters." *Water Research*, 43(18), 4590–8.

Bond-Lamberty, B., and Thomson, a. (2010). "A global database of soil respiration data." *Biogeosciences*, 7(6), 1915–1926.

Bouwman, A. (1998). "Nitrogen oxides and tropical agriculture." *Nature*, 392(April), 866–867.

Brady, N. C., and Weil, R. R. (2008). *The nature and properties of soils*. Prentice Hall, Upper Saddle River.

Bratieres, K., Fletcher, T., Deletic, A., and Zinger, Y. (2008). "Nutrient and sediment removal by stormwater biofilters: a large-scale design optimisation study." *Water Research*, 42(14), 3930–40.

Brix, H. (1994). "Functions of macrophytes in constructed wetlands." *Water Science and Technology*, 29(4), 71–78.

Brix, H. (1997). "Do macrophytes play a role in constructed treatment wetlands." *Water Science and Technology*, 35(5), 11–17.

Brix, H., Arias, C. A., and del Bubba, M. (2001). "Media selection for sustainable phosphorus removal in subsurface flow constructed wetlands." *Water Science & Technology*, 44(11-12), 47–54.

Brown, R. A., Birgand, F., and Hunt, W. F. (2013). "Analysis of consecutive events for nutrient and sediment treatment in field-monitored bioretention cells." *Water, Air, and Soil Pollution*, 224(6), 1581.

Brown, R. A., and Hunt, W. F. (2011). "Impacts of media depth on effluent water quality and hydrologic performance of undersized bioretention cells." *Journal of Irrigation and Drainage Engineering*, 137(March), 132–143.

Butterbach-Bahl, K., Baggs, E. M., Dannenmann, M., Kiese, R., and Zechmeister-boltenstern, S. (2013). "Nitrous oxide emissions from soils : how well do we understand the processes and their controls?" *Philosophical Transactions of the Royal Society Biological Sciences*, 368.

Castellano, M. J., Schmidt, J. P., Kaye, J. P., Walker, C., Graham, C. B., Lin, H., and Dell, C. J. (2010). "Hydrological and biogeochemical controls on the timing and magnitude of nitrous oxide flux across an agricultural landscape." *Global Change Biology*, 16(10), 2711–2720.

Chapuis-Lardy, L., Wrage, N., Metay, A., Chotte, J.-L., and Bernoux, M. (2007). "Soils, a sink for N2O? A review." *Global Change Biology*, 13(1), 1–17.

Chen, X., Peltier, E., Sturm, B. S. M., and Young, C. B. (2013). "Nitrogen removal and nitrifying and denitrifying bacteria quantification in a stormwater bioretention system." *Water Research*, 47(4), 1691–700.

Claassen, V., and Young, T. (2010). *Model guided specification for using compost and mulch to promote establishment of vegetation and improvement in stormwater quality*.
Clark, S., and Pitt, R. (2009). "Storm-water filter media pollutant retention under aerobic versus anaerobic conditions." *Journal of Environmental Engineering*, (May), 367–371.
Claytor, R. A., and Schueler, T. R. (1996). *Design of stormwater filtering systems*. Ellicott City.
Collins, K. A., Lawrence, T. J., Stander, E. K., Jontos, R. J., Kaushal, S. S., Newcomer, T. A., Grimm, N. B., and Cole Ekberg, M. L. (2010). "Opportunities and challenges for managing nitrogen in urban stormwater: A review and synthesis." *Ecological Engineering*, 36(11), 1507–1519.
Connor, F. M. O., Boucher, O., Gedney, N., Jones, C. D., Folberth, G. A., Coppell, R., Friedlingstein, P., Collins, W. J., Chappellaz, J., Ridley, J., and Johnson, C. E. (2010). "Possible role of wetlands, permafrost, and methane hydrates in the methane cycle under future climate change: a review." *Review of Geophysics*, 48, 1–33.
Conrad, R. (1996). "Soil microorganisms as controllers of atmospheric trace gases (H2, CO, CH4, OCS, N2O, and NO)." *Microbiological Reviews*, 60(4), 609–40.
Corbella, C., and Puigagut, J. (2013). "Improving the reliability of closed chamber methodologies for methane emissions measurement in treatment wetlands." *Water, Science, and Technology*, 69(9), 2097–2102.
Correll, D. L. (1999). "Phosphorus: A rate limiting nutrient in surface waters." *Poultry Science*, 78(5), 674–82.
Le Coustumer, S., Fletcher, T., Deletic, A., Barraud, S., and Poelsma, P. (2012). "The influence of design parameters on clogging of stormwater biofilters: A large-scale column study." *Water Research*, 6, 0–9.
Dalal, R. C., Wang, W., Robertson, G. P., and Parton, W. J. (2003). "Nitrous oxide emission from Australian agricultural lands and mitigation options: a review." *Australian Journal of Soil Research*, 41(2), 165.
Davidson, E., Keller, M., Erickson, H., Verchot, L., and Veldkamp, E. (2000). "Testing a conceptual model of soil emissions of nitrous and nitric oxides." *BioScience*, 50(8), 667–680.
Davis, A. P. (2007). "Field performance of bioretention: water quality." *Environmental Engineering Science*, 24(8), 1048–1064.
Davis, A. P. (2008). "Field performance of bioretention: hydrology impacts." *Journal of Hydrologic Engineering*, 13(2), 90–95.
Davis, A. P., Hunt, W. F., Traver, R. G., and Clar, M. (2009). "Bioretention technology: Overview of current practices and future needs." *Journal of Environmental Engineering*, 135(3), 109–117.
Davis, A. P., Shokouhian, M., Sharma, H., and Minami, C. (2001). "Laboratory study of biological retention for urban strmwater management." *Water Environment Research*, 73(1), 5–14.
Davis, A. P., Shokouhian, M., Sharma, H., and Minami, C. (2006). "Water quality improvement through bioretention media: nitrogen and phosphorus removal." *Water Environment Research*, 78(3), 284–93.
Davis, M., and Cornwell, D. (1998). *Inroduction to environmental engineering*. McGraw-Hill, Boston.
DeBusk, K., Hunt, W., and Line, D. (2011). "Bioretention outflow: does it mimic nonurban watershed interflow?" *Journal of Hydrologic Engineering*, 16(March), 274–279.
DeBusk, K., and Wynn, T. (2011). "Storm-water bioretention for runoff quality and quantity mitigation." *Journal of Environmental Engineering*, 137(September), 800–808.
Decagon Devices. (2015). *5TE: Water Content, EC and Temperature Sensor*.
Dietz, M. (2007). "Low impact development practices: a review of current research and recommendations for future directions." *Water, Air, and Soil Pollution*, 186(1-4), 351–363.
Dietz, M., and Clausen, J. (2005). "A field evaluation of rain garden flow and pollutant treatment." *Water, Air, and Soil Pollution*, 167(1-4), 123–138.
Dietz, M. E., and Clausen, J. C. (2006). "Saturation to improve pollutant retention in a rain garden." *Environmental Science & Technology*, 40(4), 1335–40.
Dlugokencky, E. J., Bruhwiler, L., White, J. W. C., Emmons, L. K., Novelli, P. C., Montzka, S. A., Masarie, K. A., Lang, P. M., Crotwell, A. M., Miller, J. B., and Gatti, L. V. (2009). "Observational constraints on recent increases in the atmospheric CH4 burden." *Geophysical Research Letters*, 36(18), n/a–n/a.
Dytham, C. (2003). *Choosing and using statistics: A biologist's guide*. Blackwell Publishing, Malden, MA.
Edwards, G. S. (1992). "Root distribution of soft-stem bulrush (Scirpus validus) in a constructed wetland." *Ecological Engineering*, 1, 239–243.

Essington, M. E. (2004). *Soil and water chemistry: An integrated approach*. CRC Press, Boca Raton.
Fassman, E., Simcock, R., and Wang, S. (2013). *Media specification for stormwater bioretention devices*.
Frumhoff, P., Mccarthy, J. J., Melillo, J. M., Moser, S. C., and Wuebbles, D. J. (2007). *Confronting climate change in the U.S. northeast*. *Northeast Climate Impacts Assessment*.
Gagnon, V., Chazarenc, F., Kõiv, M., and Brisson, J. (2012). "Effect of plant species on water quality at the outlet of a sludge treatment wetland." *Water Research*, 46(16), 5305–15.
Geosyntec Consultants, and Wright Water Engineers. (2008). *Overview of Performance by BMP Category and Common Pollutant Type*. *International Stormwater Best Management Practices (BMP) Database*.
Geosyntec Consultants, and Wright Water Engineers. (2012). *International Stormwater Best Management Practices (BMP) Database Pollutant Category Summary Statistical Addendum: TSS, Bacteria, Nutrients, and Metals*.
Geosyntec Consultants, and Wright Water Engineers. (2013). *Advanced analysis: influence of design parameters on performance*.
Gerritse, R. G. (1993). "Prediction of travel times of phosphate in soils at a disposal site for wastewater." *Water Resources*, 27(2), 263–267.
Giardina, C. P., and Ryan, M. G. (2000). "Evidence that decomposition rates of organic carbon in mineral soil do not vary with temperature." *Nature*, 404(April), 858–861.
Groenenberg, J. E., Chardon, W. J., and Koopmans, G. F. (2013). "Reducing phosphorus loading of surface water using iron-coated sand." *Journal of Environment Quality*, 42(1), 250.
Groffman, P. M., and Pouyat, R. V. (2009). "Methane uptake in urban forests and lawns." *Environmental Science & Technology*, 43(14), 5229–5235.
Del Grosso, S. J., and Parton, W. J. (2012). "Climate change increases soil nitrous oxide emissions." *New Phytologist*, 196.
Grover, S. P. P., Cohan, A., Chan, H. Sen, Livesley, S. J., Beringer, J., and Daly, E. (2013). "Occasional large emissions of nitrous oxide and methane observed in stormwater biofiltration systems." *The Science of the Total Environment*, Elsevier B.V., 465, 64–71.
Guilbert, J., Betts, A., Rizzo, D., Beckage, B., and Bomblies, A. (2015). "Characterization of increased persistence and intensity of precipitation in the northeastern United States." *Geophysical Research Letters*, 1888–1893.
Hallman, C. (2009). *Native Plants of Maryland's Coastal Plain*.
Harriss, R. C., Sebacher, D. I., and Day, F. P. (1982). "Methane flux in the Great Dismal Swamp." *Nature*, 297(5868), 673–674.
Hatt, B. E., Fletcher, T. D., and Deletic, A. (2008). "Hydraulic and pollutant removal performance of fine media stormwater filtration systems." *Environmental Science & Technology*, 42(7), 2535–41.
Herrera Environmental Consultants. (2012). *Pollutant export from bioretention soil mix*.
Higgins, I. J., Best, D. J., Hammond, R. C., and Scott, D. (1981). "Methane-oxidizing microorganisms." *Microbiological Reviews*, 45(4), 556–90.
Hilty, J. (2015). "Anemone canadensis." *Illinois Wildflowers*.
Hogan, D. M., and Walbridge, M. R. (2007). "Best management practices for nutrient and sediment retention in urban stormwater runoff." *Journal of Environment Quality*, 36(2), 386–95.
Horst, W. J., Kamh, M., Jibrin, J. M., and Chude, V. O. (2001). "Agronomic measures for increasing P availability to crops." *Plant and Soil*, 237, 211–223.
Houdeshel, D., Hultine, K., Johnson, N. C., and Pomeroy, C. (2015). "Evaluation of three vegetation treatments in bioretention gardens in a semi-arid climate." *Landscape and Urban Planning*, Elsevier B.V., 135, 62–72.
Hsieh, C., and Davis, A. P. (2003). "Multiple-event study of bioretention for treatment of urban storm water runoff." *Diffuse Pollution Conference Dublin 2003*, Dublin, 55–59.
Hsieh, C., and Davis, A. P. (2006). "Evaluation and optimization of bioretention media for treatment of urban storm water runoff." *Journal of Environmental Engineering*, 131(11), 1521–1531.
Hunt, W. F., Jarrett, A. R., Smith, J. T., and Sharkey, L. J. (2006). "Evaluating bioretention hydrology and nutrient removal at three field sites in North Carolina." *Journal of Irrigation and Drainage Engineering*, 132(6), 600–608.
Hunt, W. F., Smith, J. T., Jadlocki, S. J., Hathaway, J. M., and Eubanks, P. R. (2008). "Pollutant removal and peak flow mitigation by a bioretention cell in urban Charlotte, N.C." *Journal of Environmental Engineering*, 134(5), 403–408.

Hurley, S. E., and Forman, R. T. T. (2011). "Stormwater ponds and biofilters for large urban sites: Modeled arrangements that achieve the phosphorus reduction target for Boston's Charles River, USA." *Ecological Engineering*, 37(6), 850–863.
Hutchinson, G. L., and Livingston, G. P. (1993). "Use of chamber systems to measure trace gas fluxes." *Agricultural Ecosystem Effects on Trace Gases and Global Climate Change*.
Imbrium Systems. (2012). *A Breakthrough in Total Phosphorus Removal: The Science behind Sorbtive Media*.
Kadlec, R. H., Cuvellier, C., and Stober, T. (2010). "Performance of the Columbia, Missouri, treatment wetland." *Ecological Engineering*, Elsevier B.V., 36(5), 672–684.
Kaspar, H. F. (1982). "Denitrification in marine sediment: measurement of capacity and estimate of in situ rate." *Applied and Environmental Microbiology*, 43(3), 522–7.
Kaye, J., Burke, I., and Mosier, A. (2004). "Methane and nitrous oxide fluxes from urban soils to the atmosphere." *Ecological Applications*, 14(4), 975–981.
Keller, M., Kaplan, W. A., and Wofsy, S. C. (1986). "Emissions of N2O, CH4 and CO2 from tropical forest soils." *Journal of Geophysical Research: Atmospheres*, 91(D11), 11791–11802.
Kim, H., Seagren, E. A., Davis, A. P., and Davis, P. (2003). "Engineered bioretention for removal of nitrate from stormwater runoff." *Water Environment Federation*, 75(4), 355–367.
King, K. W., Harmel, R. D., and Fausey, N. R. (2005). "Development and sensitivity of a method to select time- and flow-paced storm event sampling intervals for headwater streams." *Journal of Soil and Water Conservation*, 60(6), 323–331.
Kirschke, S., Bousquet, P., Ciais, P., Saunois, M., Canadell, J., Dlugokencky, E., Bergamaschi, P., Bergmann, D., Blake, D., Bruhwiler, L., Cameron-Smith, P., Castaldi, S., Chevallier, F., Feng, L., Fraser, A., Heimann, M., Hodson, E., Houweling, S., Josse, B., Fraser, P., Krummel, P. B., Lamarque, J.-F., Langenfelds, R., Le Quéré, C., Naik, V., O'Doherty, S., Palmer, P., Pison, I., Plummer, D., Poulter, B., Prinn, R., Rigby, M., Ringeval, B., Santini, M., Schmidt, M., Shindell, D., Simpson, I., Spahni, R., Steele, L. P., Strode, S., Sudo, K., Szopa, S., van der Werf, G., Voulgarakis, A., van Weele, M., Weiss, R., Williams, J., and Zeng, G. (2013). "Three decades of global methane sources and sinks." *Nature Geoscience*, 6(10), 813–823.
Komlos, J., and Traver, R. G. (2012). "Long-term orthophosphate removal in a field-scale storm-water bioinfiltration rain garden." *Journal of Environmental Engineering*, 138(October), 991–998.
Kutzbach, L., Schneider, J., Sachs, T., Giebels, M., and Nyk, H. (2007). "CO2 flux determination by closed-chamber methods can be seriously biased by inappropriate application of linear regression." *Biogeosciences*, 1005–1025.
Lantzke, I. R., Heritage, a. D., Pistillo, G., and Mitchell, D. S. (1998). "Phosphorus removal rates in bucket size planted wetlands with a vertical hydraulic flow." *Water Research*, 32(4), 1280–1286.
Lefevre, G. H., Paus, K. H., Natarajan, P., Gulliver, J. S., Novak, P. J., and Hozalski, R. M. (2015). "Review of dissolved pollutants in urban storm water and their removal and fate in bioretention cells." *Journal of Environmental Engineering*, 141.
Leytem, A., and Bjorneberg, D. (2009). "Changes in soil test phosphorus and phosphorus in runoff from calcareous soils recieve manure compost, and fertilizer application with and without alum." *Soil Science*, 174.
Li, H., and Davis, A. P. (2008). "Urban particle capture in bioretention media." *Journal of Environmental Engineering*, 134(June), 409–418.
Li, H., and Davis, A. P. (2009). "Water quality improvement through reduction of pollutant loads using bioretention." *Journal of Environmental Engineering*, 135(August), 567–576.
Lintern, A., Daly, E., Duncan, H., Hatt, B. E., Fletcher, T. D., and Deletic, A. (2011). "Key design characteristics that influence the performance of stormwater biofilters." *12th International Conference on Urban Drainage, Porto Alegre, Brazil*, 11–16.
Liu, J., Sample, D., Owen, J., Li, J., and Evanylo, G. (2014). "Assessment of selected bioretention blends for nutrient retention using mesocosm experiments." *Journal of Environment Quality*.
Lucas, W. C., and Greenway, M. (2008). "Nutrient retention in vegetated and nonvegetated bioretention mesocosms." *Journal of Irrigation and Drainage Engineering*, 134(5), 613–623.
Lucas, W., and Greenway, M. (2011). "Hydraulic response and nitrogen retention in bioretention mesocosms with regulated outlets: part I - hydraulic response." *Water Environment Research*, 83(8).
Luther, G. W., Sundby, B., Lewis, B. L., Brendel, P. J., and Silverberg, N. (1997). "Interactions of manganese with the nitrogen cycle: Alternative pathways to dinitrogen." *Geochimica et*

Cosmochimica Acta, 61(19), 4043–4052.
Mann, J. J., Barney, J. N., Kyser, G. B., and DiTomaso, J. M. (2013). "Root system dynamics of Miscanthus x giganteus and Panicum virgatum in response to rainfed and irrigated conditions in California." *Bioenergy Research*, 6, 678–687.
Masterson, J., and Bannerman, R. (1994). "Impacts of stormwater runoff on urban streams in Milwaukee country, Wisconsin." *American Water Resources Association*.
Matson, P. A., and Harris, R. C. (1995). *Biogenic trace gases: Measuring emissions from soil and water*. Blackwell Science Ltd, Oxford.
McCulley, R. L., Jobbágy, E. G., Pockman, W. T., and Jackson, R. B. (2004). "Nutrient uptake as a contributing explanation for deep rooting in arid and semi-arid ecosystems." *Oecologia*, 141(4), 620–8.
Mengel, K., and Kirkby, E. (2001). *Principles of plant nutrition*. Springer Netherlands.
Le Mer, J., and Roger, P. (2001). "Production, oxidation, emission and consumption of methane by soils : A review." *European Journal of Soil Biology*, 37(2001).
Michigan Department of Environmental Quality. (2008). *Low Impact Development Manual for Michigan: A Design Guide for Implementers and Reviewers*.
Mith, K. A. S., All, T. B., Onen, F. C., Obbie, K. E. D., Assheder, J. M., and Ey, A. R. (2003). "Exchange of greenhouse gases between soil and atmosphere : interactions of soil physical factors and biological processes." *European Journal of Soil Biology*, 54(December), 779–791.
Muthanna, T. M., Viklander, M., Blecken, G., and Thorolfsson, S. T. (2007). "Snowmelt pollutant removal in bioretention areas." *Water Research*, 41(18), 4061–72.
National Research Council. (2008). *Urban Stormwater Management in the United States*.
Natural Resources Conservation Service. (2005). *Plant Guide: Cardinal Flower*.
Nesbit, S. P., and Breitenbeck, G. A. (1992). "A laboratory study of factors influencing methane uptake by soils." *Agriculture, Ecosystems and Environment*, 41, 39–54.
Nisbet, E. G., Dlugokencky, E. J., and Bousquet, P. (2014). "Atmospheric science. Methane on the rise--again." *Science*, 343(6170), 493–5.
Northeast Regional Coordinating Committee on Soil Testing. (2009). *Recommended Soil Testing Procedures for the Northeastern United States. 3rd Edition. Northeastern Regional Publication No. 493*.
Nylen, N. G., and Kiparsky, M. (2015). *Accelerating cost-effective green stormwater infrastructure: learning from local implementation*.
O'Neill, S. W., and Davis, A. P. (2011). "Water treatment residual as a bioretention amendment for phosphorus. II: Long-term column studies." *Journal of Environmental Engineering*, 138(March), 328–336.
Palmer, E. T. (2012). "Nitrate and phosphate removal through an optimized bioretention system." *Masters Thesis*, Washington State University.
Parkin, T., and Venterea, R. (2010). *USDA-ARS GRACEnet Project Protocols Chapter 3. Chamber-Based Trace Gas Flux Measurements 4*.
Passeport, E., Hunt, W. F., Line, D. E., Smith, R. A., and Brown, R. A. (2009). "Field study of the ability of two grassed bioretention cells to reduce storm-water runoff pollution." *Journal of Irrigation and Drainage Engineering*, 135(August), 505–510.
Patton, C., and Kryskalla, J. (2003). *Methods of Analysis by the U.S. Geological Survey National Water Quality Laboratory - Evaluation of alkaline persulfate digestion as an alternative to kjeldahl digestion for determination of total and dissolved nitrogen and phosphorous in water*. *U.S. Geological Survey Water-Resouces Investigations Report 03-4174*.
Pilegaard, K., and Pilegaard, K. (2013). "Processes regulating nitric oxide emissions from soils." *Philosophical Transactions of the Royal Society Biological Sciences*, 368(2).
Plaxton, W. C., and Podestá, F. E. (2006). "The functional organization and control of plant respiration." *Critical Reviews in Plant Sciences*, 25(2), 159–198.
Portmann, R. W., Daniel, J. S., and Ravishankara, A. R. (2012). "Stratospheric ozone depletion due to nitrous oxide: influences of other gases." *Philosophical transactions of the Royal Society*, 367(1593), 1256–64.
Preti, F., Dani, a., and Laio, F. (2010). "Root profile assessment by means of hydrological, pedological and above-ground vegetation information for bio-engineering purposes." *Ecological Engineering*, 36(3), 305–316.

Qiu, S., McComb, A., Bell, R., and Davis, J. (2005). "Response of soil microbial activity to temperature, moisture, and litter leaching on a wetland transect during seasonal refilling." *Wetlands Ecology and Management*, 13(2002), 43–54.
Ravishankara, A. R., Daniel, J. S., and Portmann, R. W. (2009). "Nitrous oxide (N2O): the dominant ozone-depleting substance emitted in the 21st century." *Science*, 326(5949), 123–5.
Read, J., Wevill, T., Fletcher, T., and Deletic, A. (2008). "Variation among plant species in pollutant removal from stormwater in biofiltration systems." *Water Research*, 42(4-5), 893–902.
Rochette, P., Ellert, B., Gregorich, E. G., Desjardins, R. L., Pattey, E., Lessard, R., and Johnson, B. G. (1997). "Description of a dynamic closed chamber for measuring soil respiration and its comparison with other techniques." *Canadian Journal of Soil Science*, 77(2), 195–203.
Rochette, P., and Hutchinson, G. (2005). "Measurement of soil respiration in situ : Chamber techniques." *Micrometeorology in Agricultural Systems*, 247–286.
Rosenquist, S. E., Hession, W. C., Eick, M. J., and Vaughan, D. H. (2010). "Variability in adsorptive phosphorus removal by structural stormwater best management practices." *Ecological Engineering*, Elsevier B.V., 36(5), 664–671.
Roy-Poirier, A. (2009). "Bioretention for phosphorus removal: Modelling stormwater quality improvements." *Masters Thesis*, Queen's University, Canada.
Sansalone, J. J., and Cristina, C. M. (2004). "First flush concepts for suspended and dissolved solids in small impervious watersheds." *Journal of Environmental Engineering*, 130(November), 1301–1314.
Schachtman, D. P., Schachtman, D. P., Reid, R. J., Reid, R. J., Ayling, S. M., and Ayling, S. M. (1998). "Phosphorus uptake by plants: From soil to cell." *Plant Physiology*, 116(2), 447–453.
Schenk, H. J. (2008). "The shallowest possible water extraction profile: A null model for global root distributions." *Vadose Zone Journal*, 7(3), 1119.
Schlesinger, W. H. (2013). "An estimate of the global sink for nitrous oxide in soils." *Global Change Biology*, 19(10), 2929–31.
Seelsaen, N., McLaughlan, R., Moore, S., Ball, J. E., and Stuetz, R. M. (2006). "Pollutant removal efficiency of alternative filtration media in stormwater treatment." *Water Science and Technology*, 54, 299–305.
Serna, M. D., Borras, R., Legaz, F., and Primo-Millo, E. (1992). "The influence of nitrogen concentration and ammonium /nitrate ratio on N-uptake, mineral composition and yield of citrus." *Plant and Soil*, 147(1), 13–23.
Smart, D., and Peñuelas, J. (2005). "Short-term CO2 emissions from planted soil subject to elevated CO2 and simulated precipitation." *Applied Soil Ecology*, 28, 247–257.
Smith, K. A. S., Ball, T. B., Conen, F. C., Dobbie, K. E. D., Massheder, J. M., and Rey, A. R. (2003). "Exchange of greenhouse gases between soil and atmosphere : interactions of soil physical factors and biological processes." *European Journal of Soil Science*, (December), 779–791.
Sollins, P., Homann, P., and Caldwell, B. A. (1996). "Stabilization and destabilization of soil organic matter : mechanisms and controls." 74, 65–105.
Sollins, P., Robertson, P., and Uehara, G. (1988). "Nutrient mobility in variable- and permanent-charge soils." *Biogeochemistry*, 6(3), 181–199.
Sonon, L. S., Kissel, D. E., and Saha, U. (2014). *Cation Exchange Capacity and Base Saturation*.
Spivakov, B. Y., Maryutina, T. a., and Muntau, H. (1999). "Phosphorus speciation in water and sediments." *Pure and Applied Chemistry*, 71(11), 2161–2176.
Stenstrom, M., and Kayhanian, M. (2005). *First flush phenomenon characterization*. Sacramento.
Steudler, P. A., Bowden, R. D., Melillo, J. M., and Aber, J. D. (1989). "Influence of nitrogen fertilization on methane uptake in temperate forest soils." *Nature*, 341(6240), 314–316.
Stoner, D., Penn, C., McGrath, J., and Warren, J. (2012). "Phosphorus removal with by-products in a flow-through setting." *Journal of Environment Quality*, 41, 654.
Syakila, A., and Kroeze, C. (2011). "The global nitrous oxide budget revisited." *Greenhouse Gas Measurement and Management*, 1(1), 17–26.
Tanner, C. C. (1996). "Plants for constructed wetland treatment systems - A comparison of the growth and nutrient uptake of eight emergent species." 7, 59–83.
Taylor, A., and Wong, T. (2002). *Non-structural stormwater quality best management practices - a literature review of their value and life-cycle costs*.
The Lady Bird Johnson Wildflower Center. (2016a). "Helenium autumnale." *Native Plant Database*, <https://www.wildflower.org/>.

The Lady Bird Johnson Wildflower Center. (2016b). “Aster novae angliae.” *Native Plant Database*, <https://www.wildflower.org/>.
The Lady Bird Johnson Wildflower Center. (2016c). “Asclepias tuberosa.” *Native Plant Database*, <https://www.wildflower.org/>.
The Lady Bird Johnson Wildflower Center. (2016d). “Baptisia australis.” *Native Plant Database*.
Thompson, A. M., Paul, A. C., and Balster, N. J. (2008). “Physical and hydraulic properties of engineered soil media for bioretention basins.” *American Society of Agricultural and Biological Engineers*, 51(2), 499–514.
Thomson, A. J., Giannopoulos, G., Pretty, J., Baggs, E. M., and Richardson, D. J. (2012). “Biological sources and sinks of nitrous oxide and strategies to mitigate emissions.” *Philosophical Transactions of the Royal Society Biological Sciences*, 367(1593), 1157–68.
Turner, R., and Rabalais, N. (2013). “Nitrogen and phosphorus phytoplankton growth limitation in the northern Gulf of Mexico.” *Aquatic Microbial Ecology*, 68(2), 159–169.
U.S. Bureau of Reclamation. (2001). *Water Measurement Manual*. U.S. Government Printing Office, Washington, D.C.
U.S. Climate Change Science Program and the Subcommittee on Global Change Research. (2008). *Weather and Climate Extremes in a Changing Climate*. Washington, D.C.
U.S. Environmental Protection Agency. (1997). “Load Estimation Techniques.” *National Management Measures to Control Nonpoint Pollution from Agriculture*, 225–242.
U.S. Environmental Protection Agency. (1998). *Report of the Federal Advisory Committee on the Total Maximum Daily Load (TMDL) Program*.
U.S. Environmental Protection Agency. (2008). *TMDLs to Stormwater Permits Handbook*.
U.S. Environmental Protection Agency. (2015). *Tools, Strategies and Lessons Learned from EPA Green Infrastructure Technical Assistance Projects*.
Vance, C. P., Uhde-Stone, C., and Allan, D. L. (2003). “Phosphorus acquisition and use: critical adaptations by plants for securing a nonrenewable resource.” *New Phytologist*, 157(3), 423–447.
Vermont Agency of Natural Resources. (2002). *The Vermont Stormwater Management Manual Volume I - Stormwater Treatment Standards*.
Vilain, G., Garnier, J., Decuq, C., and Lugnot, M. (2014). “Nitrous oxide production from soil experiments: denitrification prevails over nitrification.” *Nutrient Cycling in Agroecosystems*, 98(2), 169–186.
Washington State University Pierce County Extension. (2012). *Low Impact Development Technical Guidance Manual for Puget Sound*.
Weng, L., Van Riemsdijk, W. H., and Hiemstra, T. (2012). “Factors controlling phosphate interaction with iron oxides.” *Journal of Environmental Quality*, 41(3), 628–35.
Wong, T. H. F. (2006). “An Overview of Water Sensitive Urban Design Practices in Australia.” 1(1).
Zhuang, Q., Lu, Y., and Chen, M. (2012). “An inventory of global N2O emissions from the soils of natural terrestrial ecosystems.” *Atmospheric Environment*, Elsevier Ltd, 47, 66–75.
Zinger, Y., Blecken, G.-T., Fletcher, T. D., Viklander, M., and Deletić, A. (2013). “Optimising nitrogen removal in existing stormwater biofilters: Benefits and tradeoffs of a retrofitted saturated zone.” *Ecological Engineering*, 51, 75–82.
Zotarelli, L., Dukes, M., and Barreto, T. (2010). *Interpretation of Soil Moisture Content to Determine Soil Field Capacity and Avoid Over Irrigation in Sandy Soils Using Soil Moisture Measurements*.

COMPREHENSIVE BIBLIOGRAPHY

Adamsen, A., and King, G. (1993). "Methane consumption in temperate and subartic forest soils: Rates, vertical zonation, and responses to water and nitrogen." *Applied and Environmental Microbiology*, 59(Feb), 485–490.

Adviento-Borbe, M. ., Kaye, J. P., Bruns, M. A., McDaniel, M. D., McCoy, M., and Harkcom, S. (2010). "Soil greenhouse gas and ammonia emissions in long-term maize-based cropping systems." *Soil Biology & Biochemistry*, 74(5), 1623–1634.

Alias, N., Liu, A., Egodawatta, P., and Goonetilleke, A. (2014). "Sectional analysis of the pollutant wash-off process based on runoff hydrograph." *Journal of Environmental Management*, 134, 63–9.

Allen Burton, G., and Pitt, R. (2002). *Stormwater effects handbook: a toolbox for watershed managers, scientists, and engineers*. Lewis Publishers, Boca Raton.

Antonio, A., and Walker, D. (2011). *Total Kjeldahl Nitrogen: Simplified with s-TKN ™*.

APHA. (1992). *Standard Methods for the Examination of Water and Wastewater*. American Public Health Association, Washington, D.C.

APHA. (2011). *Standard Methods for the Examination of Water and Wastewater*. American Public Health Association, Washington, D.C.

Arias, C., Del Bubba, M., and Brix, H. (2001). "Phosphorus removal by sands for use as media in subsurface flow constructed reed beds." *Water Research*, 35(5), 1159–68.

Bach, P. M., McCarthy, D. T., and Deletic, A. (2010). "Redefining the stormwater first flush phenomenon." *Water Research*, 44(8), 2487–98.

Basta, N., and Dayton, E. (2007). "Phosphorus chemistry and sequestration in soil." 1–23.

Bertrand-Krajewski, J.-L., Chebbo, C., and Saget, A. (1998). "Distribution of pollutant mass vs volume in stormwater discharges and the first flush phenomenon." *Water Resources*, 32(8), 2341–2356.

Blecken, G.-T., Zinger, Y., Deletić, A., Fletcher, T., Hedström, A., and Viklander, M. (2010). "Laboratory study on stormwater biofiltration: Nutrient and sediment removal in cold temperatures." *Journal of*

Hydrology, 394(3-4), 507–514.

Blecken, G.-T., Zinger, Y., Deletić, A., Fletcher, T., and Viklander, M. (2009). "Influence of intermittent wetting and drying conditions on heavy metal removal by stormwater biofilters." *Water Research*, 43(18), 4590–8.

Bond-Lamberty, B., and Thomson, a. (2010). "A global database of soil respiration data." *Biogeosciences*, 7(6), 1915–1926.

Booth, D. (1991). "Urbanization and the natural drainage system - impacts, solutions and prognosis." *The Northwest Environmental Journal*, 7(1).

Booth, D. B., and Jackson, C. R. (1997). "Urbanization of aquatic systems: degratation thresholds, stormwater detection, and the limits of mitigation." *Journal of the American Water Resources Association*, 33(5), 1077–1090.

Bouwman, A. (1998). "Nitrogen oxides and tropical agriculture." *Nature*, 392(April), 866–867.

Brady, N. C., and Weil, R. R. (2008). *The nature and properties of soils*. Prentice Hall, Upper Saddle River.

Bratieres, K., Fletcher, T., Deletic, A., and Zinger, Y. (2008). "Nutrient and sediment removal by stormwater biofilters: a large-scale design optimisation study." *Water Research*, 42(14), 3930–40.

Brezonik, P. L., and Stadelmann, T. H. (2002). "Analysis and predictive models of stormwater runoff volumes, loads, and pollutant concentrations from watersheds in the Twin Cities metropolitan area, Minnesota, USA." *Water Research*, 36(7), 1743–57.

Brix, H. (1994). "Functions of macrophytes in constructed wetlands." *Water Science and Technology*, 29(4), 71–78.

Brix, H. (1997). "Do macrophytes play a role in constructed treatment wetlands." *Water Science and Technology*, 35(5), 11–17.

Brix, H., Arias, C. A., and del Bubba, M. (2001). "Media selection for sustainable phosphorus removal in subsurface flow constructed wetlands." *Water Science & Technology*, 44(11-12), 47–54.

Brown, R. A., Birgand, F., and Hunt, W. F. (2013). "Analysis of consecutive events for nutrient and

sediment treatment in field-monitored bioretention cells." *Water, Air, and Soil Pollution*, 224(6), 1581.

Brown, R. A., and Hunt, W. F. (2011). "Impacts of media depth on effluent water quality and hydrologic performance of undersized bioretention cells." *Journal of Irrigation and Drainage Engineering*, 137(March), 132–143.

Busnardo, M. J., Gersberg, R. M., Langis, R., Sinicrope, T. L., and Zedler, J. B. (1992). "Nitrogen and phosphorus removal by wetland mesocosms subjected to different hydroperiods." *Ecological Engineering*, 1(4), 287–307.

Butterbach-Bahl, K., Baggs, E. M., Dannenmann, M., Kiese, R., and Zechmeister-boltenstern, S. (2013). "Nitrous oxide emissions from soils : how well do we understand the processes and their controls?" *Philosophical Transactions of the Royal Society Biological Sciences*, 368.

Castellano, M. J., Schmidt, J. P., Kaye, J. P., Walker, C., Graham, C. B., Lin, H., and Dell, C. J. (2010). "Hydrological and biogeochemical controls on the timing and magnitude of nitrous oxide flux across an agricultural landscape." *Global Change Biology*, 16(10), 2711–2720.

Chapuis-Lardy, L., Wrage, N., Metay, A., Chotte, J.-L., and Bernoux, M. (2007). "Soils, a sink for N2O? A review." *Global Change Biology*, 13(1), 1–17.

Charbeneau, R. J., and Barrett, M. E. (1998). "Evaluation of methods for estimating stormwater pollutant loads." *Water Environment Research*, 70(7), 1295–1302.

Chen, X., Peltier, E., Sturm, B. S. M., and Young, C. B. (2013). "Nitrogen removal and nitrifying and denitrifying bacteria quantification in a stormwater bioretention system." *Water Research*, 47(4), 1691–700.

Claassen, V., and Young, T. (2010). *Model guided specification for using compost and mulch to promote establishment of vegetation and improvement in stormwater quality*.

Clark, S., and Pitt, R. (2009). "Storm-water filter media pollutant retention under aerobic versus anaerobic conditions." *Journal of Environmental Engineering*, (May), 367–371.

Claytor, R. A., and Schueler, T. R. (1996). *Design of stormwater filtering systems*. Ellicott City.

Collins, K. A., Lawrence, T. J., Stander, E. K., Jontos, R. J., Kaushal, S. S., Newcomer, T. A., Grimm, N. B., and Cole Ekberg, M. L. (2010). "Opportunities and challenges for managing nitrogen in urban stormwater: A review and synthesis." *Ecological Engineering*, 36(11), 1507–1519.

Connor, F. M. O., Boucher, O., Gedney, N., Jones, C. D., Folberth, G. A., Coppell, R., Friedlingstein, P., Collins, W. J., Chappellaz, J., Ridley, J., and Johnson, C. E. (2010). "Possible role of wetlands, permafrost, and methane hydrates in the methane cycle under future climate change: a review." *Review of Geophysics*, 48, 1–33.

Conrad, R. (1996). "Soil microorganisms as controllers of atmospheric trace gases (H2, CO, CH4, OCS, N2O, and NO)." *Microbiological Reviews*, 60(4), 609–40.

Corbella, C., and Puigagut, J. (2013). "Improving the reliability of closed chamber methodologies for methane emissions measurement in treatment wetlands." *Water, Science, and Technology*, 69(9), 2097–2102.

Correll, D. L. (1999). "Phosphorus: A rate limiting nutrient in surface waters." *Poultry Science*, 78(5), 674–82.

Le Coustumer, S., Fletcher, T., Deletic, A., Barraud, S., and Poelsma, P. (2012). "The influence of design parameters on clogging of stormwater biofilters: A large-scale column study." *Water Research*, 6, 0–9.

Dalal, R. C., Wang, W., Robertson, G. P., and Parton, W. J. (2003). "Nitrous oxide emission from Australian agricultural lands and mitigation options: a review." *Australian Journal of Soil Research*, 41(2), 165.

Davidson, E., Keller, M., Erickson, H., Verchot, L., and Veldkamp, E. (2000). "Testing a conceptual model of soil emissions of nitrous and nitric oxides." *BioScience*, 50(8), 667–680.

Davis, A. P. (2007). "Field performance of bioretention: water quality." *Environmental Engineering Science*, 24(8), 1048–1064.

Davis, A. P. (2008). "Field performance of bioretention: hydrology impacts." *Journal of Hydrologic Engineering*, 13(2), 90–95.

Davis, A. P., Hunt, W. F., Traver, R. G., and Clar, M. (2009). "Bioretention technology: Overview of current practices and future needs." *Journal of Environmental Engineering*, 135(3), 109–117.

Davis, A. P., Shokouhian, M., Sharma, H., and Minami, C. (2001). "Laboratory study of biological retention for urban strmwater management." *Water Environment Research*, 73(1), 5–14.

Davis, A. P., Shokouhian, M., Sharma, H., and Minami, C. (2006). "Water quality improvement through bioretention media: nitrogen and phosphorus removal." *Water Environment Research*, 78(3), 284–93.

Davis, M., and Cornwell, D. (1998). *Inroduction to environmental engineering*. McGraw-Hill, Boston.

DeBusk, K., Hunt, W., and Line, D. (2011). "Bioretention outflow: does it mimic nonurban watershed interflow?" *Journal of Hydrologic Engineering*, 16(March), 274–279.

DeBusk, K., and Wynn, T. (2011). "Storm-water bioretention for runoff quality and quantity mitigation." *Journal of Environmental Engineering*, 137(September), 800–808.

Decagon Devices. (2015). *5TE: Water Content, EC and Temperature Sensor*.

Deletic, A. (1998). "The first flush load of urban surface runoff." *Water Research*, 32(8), 2462–2470.

Dietz, M. (2007). "Low impact development practices: a review of current research and recommendations for future directions." *Water, Air, and Soil Pollution*, 186(1-4), 351–363.

Dietz, M., and Clausen, J. (2005). "A field evaluation of rain garden flow and pollutant treatment." *Water, Air, and Soil Pollution*, 167(1-4), 123–138.

Dietz, M. E., and Clausen, J. C. (2006). "Saturation to improve pollutant retention in a rain garden." *Environmental Science & Technology*, 40(4), 1335–40.

Dillon, K. S., and Chanton, J. P. (2005). "Nutrient transformations between rainfall and stormwater runoff in an urbanized coastal environment: Sarasota Bay, Florida." *Limnology and Oceanography*, 50(1), 62–69.

Dlugokencky, E. J., Bruhwiler, L., White, J. W. C., Emmons, L. K., Novelli, P. C., Montzka, S. A., Masarie, K. A., Lang, P. M., Crotwell, A. M., Miller, J. B., and Gatti, L. V. (2009). "Observational constraints on recent increases in the atmospheric CH4 burden." *Geophysical Research Letters*, 36(18), n/a–n/a.

Dodds, W. K., Bouska, W. W., Eitzmann, J. L., Pilger, T. J., Pitts, K. L., Riley, A. J., Schloesser, J. T., and Thornbrugh, D. J. (2009). "Eutrophication of U.S. freshwaters: analysis of potential economic damages." *Environmental Science & Technology*, 43(1), 12–19.

Dytham, C. (2003). *Choosing and using statistics: A biologist's guide*. Blackwell Publishing, Malden, MA.

Edwards, G. S. (1992). "Root distribution of soft-stem bulrush (Scirpus validus) in a constructed wetland." *Ecological Engineering*, 1, 239–243.

Eger, C. (2012). "Nutrient retention in roadside retrofit rain gardens." Ohio State University.

Egodawatta, P., Thomas, E., and Goonetilleke, A. (2007). "Mathematical interpretation of pollutant wash-off from urban road surfaces using simulated rainfall." *Water Research*, 41(13), 3025–31.

Essington, M. E. (2004). *Soil and water chemistry: An integrated approach*. CRC Press, Boca Raton.

Fassman, E., Simcock, R., and Wang, S. (2013). *Media specification for stormwater bioretention devices*.

Francey, M. (2010). "Characterising Urban Pollutant Loads." *Masters Thesis*, Monash University.

Freeze, A. R., and Cherry, J. A. (1979). *Groundwater*. Prentice-Hall International, Englewood Cliffs, NJ.

Frumhoff, P., Mccarthy, J. J., Melillo, J. M., Moser, S. C., and Wuebbles, D. J. (2007). *Confronting climate change in the U.S. northeast*. *Northeast Climate Impacts Assessment*.

Gagnon, V., Chazarenc, F., Kõiv, M., and Brisson, J. (2012). "Effect of plant species on water quality at the outlet of a sludge treatment wetland." *Water Research*, 46(16), 5305–15.

Galster, J. C., Pazzaglia, F. J., Hargreaves, B. R., Morris, D. P., Peters, S. C., and Weisman, R. N. (2006). "Effects of urbanization on watershed hydrology: The scaling of discharge with drainage area." *Geology* , 34 (9), 713–716.

Geosyntec Consultants, and Wright Water Engineers. (2008). *Overview of Performance by BMP Category and Common Pollutant Type*. *International Stormwater Best Management Practices (BMP) Database*.

Geosyntec Consultants, and Wright Water Engineers. (2012). *International Stormwater Best Management Practices (BMP) Database Pollutant Category Summary Statistical Addendum: TSS, Bacteria,*

Nutrients, and Metals.

Geosyntec Consultants, and Wright Water Engineers. (2013). *Advanced analysis: influence of design parameters on performance*.

Gerritse, R. G. (1993). "Prediction of travel times of phosphate in soils at a disposal site for wastewater." *Water Resources*, 27(2), 263–267.

Giardina, C. P., and Ryan, M. G. (2000). "Evidence that decomposition rates of organic carbon in mineral soil do not vary with temperature." *Nature*, 404(April), 858–861.

Gillian, G., Hoodenboom, A., Carlson, S., Ford, S., Nash, J., Palchak, E., Pears, S., Underwood, K., and Baker, D. (2014). *Considering Vermont's Future in a Changing Climate: The First Vermont Climate Assessment*.

Glysson, G. D., Gray, J. R., and Conge, L. M. (2000). *Adjustment of total suspended solids data for use in sediment studies*. *Building Partnerships*, American Society of Civil Engineers, Reston, VA.

Groenenberg, J. E., Chardon, W. J., and Koopmans, G. F. (2013). "Reducing phosphorus loading of surface water using iron-coated sand." *Journal of Environment Quality*, 42(1), 250.

Groffman, P. M., and Pouyat, R. V. (2009). "Methane uptake in urban forests and lawns." *Environmental Science & Technology*, 43(14), 5229–5235.

Del Grosso, S. J., and Parton, W. J. (2012). "Climate change increases soil nitrous oxide emissions." *New Phytologist*, 196.

Grover, S. P. P., Cohan, A., Chan, H. Sen, Livesley, S. J., Beringer, J., and Daly, E. (2013). "Occasional large emissions of nitrous oxide and methane observed in stormwater biofiltration systems." *The Science of the Total Environment*, Elsevier B.V., 465, 64–71.

Guilbert, J., Betts, A., Rizzo, D., Beckage, B., and Bomblies, A. (2015). "Characterization of increased persistence and intensity of precipitation in the northeastern United States." *Geophysical Research Letters*, 1888–1893.

Gupta, K., and Saul, A. (1996). "Specific relationships for the first flush load in combined sewer flows." *Water Resources*, 1354(95), 1244–1252.

Hallman, C. (2009). *Native Plants of Maryland's Coastal Plain*.

Harmel, D., King, K., Wolfe, J., and Torbert, A. (2002). "Minimum flow considerations for automated storm sampling on small watersheds." *The Texas Journal of Science*, 54(2), 177–178.

Harmel, R. D., King, K. W., and Slade, R. M. (2003). "Automated storm water sampling on small watersheds." *Applied Engineering in Agriculture*, 19(6), 667–674.

Harriss, R. C., Sebacher, D. I., and Day, F. P. (1982). "Methane flux in the Great Dismal Swamp." *Nature*, 297(5868), 673–674.

Hathaway, J. M., Tucker, R. S., Spooner, J. M., and Hunt, W. F. (2012). "A traditional analysis of the first flush effects for nutrients in stormwater runoff from two small urban catchments." *Water, Air, and Soil Pollution*, 223(9), 5903–5915.

Hatt, B. E., Fletcher, T. D., and Deletic, A. (2008). "Hydraulic and pollutant removal performance of fine media stormwater filtration systems." *Environmental Science & Technology*, 42(7), 2535–41.

Havens, K. E., James, R. T., East, T. L., and Smith, V. H. (2003). "N:P ratios, light limitation, and cyanobacterial dominance in a subtropical lake impacted by non-point source nutrient pollution." *Environmental Pollution*, 122(3), 379–90.

Heiniger, R. W., McBride, R. G., and Clay, D. E. (2003). "Using soil electrical conductivity to improve nutrient management." *Agronomy Journal*, 95, 508–519.

Henderson, C., Greenway, M., and Phillips, I. (2007). "Removal of dissolved nitrogen, phosphorus and carbon from stormwater by biofiltration mesocosms." *Water Science & Technology*, 55(4), 183.

Herngren, L. F. (2005). "Build-up and wash-off process kinetics of PAHs and heavy metals on paved surfaces using simulated rainfall." *Masters Thesis*, Queensland University of Technology.

Herrera Environmental Consultants. (2012). *Pollutant export from bioretention soil mix*.

Higgins, I. J., Best, D. J., Hammond, R. C., and Scott, D. (1981). "Methane-oxidizing microorganisms." *Microbiological Reviews*, 45(4), 556–90.

Hilty, J. (2015). "Anemone canadensis." *Illinois Wildflowers*.

Hogan, D. M., and Walbridge, M. R. (2007). "Best management practices for nutrient and sediment retention in urban stormwater runoff." *Journal of Environment Quality*, 36(2), 386–95.

Hornberger, G., Raffensperger, J., Wiberg, P., and Eschleman, K. (1998). *Elements of physical hydrology*. The Johns Hopkins University Press, Baltimore.

Horst, W. J., Kamh, M., Jibrin, J. M., and Chude, V. O. (2001). "Agronomic measures for increasing P availability to crops." *Plant and Soil*, 237, 211–223.

Houdeshel, D., Hultine, K., Johnson, N. C., and Pomeroy, C. (2015). "Evaluation of three vegetation treatments in bioretention gardens in a semi-arid climate." *Landscape and Urban Planning*, Elsevier B.V., 135, 62–72.

Hsieh, C., and Davis, A. P. (2003). "Multiple-event study of bioretention for treatment of urban storm water runoff." *Diffuse Pollution Conference Dublin 2003*, Dublin, 55–59.

Hsieh, C., and Davis, A. P. (2006). "Evaluation and optimization of bioretention media for treatment of urban storm water runoff." *Journal of Environmental Engineering*, 131(11), 1521–1531.

Hunt, W. F. (2003). "Pollutant removal evaluation and hydraulic characterization for bioretention stormwater treatment devices." *Doctoral Dissertation*, Pennsylvania State University.

Hunt, W. F., Jarrett, A. R., Smith, J. T., and Sharkey, L. J. (2006). "Evaluating bioretention hydrology and nutrient removal at three field sites in North Carolina." *Journal of Irrigation and Drainage Engineering*, 132(6), 600–608.

Hunt, W. F., Smith, J. T., Jadlocki, S. J., Hathaway, J. M., and Eubanks, P. R. (2008). "Pollutant removal and peak flow mitigation by a bioretention cell in urban Charlotte, N.C." *Journal of Environmental Engineering*, 134(5), 403–408.

Hurley, S. E., and Forman, R. T. T. (2011). "Stormwater ponds and biofilters for large urban sites: Modeled arrangements that achieve the phosphorus reduction target for Boston's Charles River, USA." *Ecological Engineering*, 37(6), 850–863.

Hutchinson, G. L., and Livingston, G. P. (1993). "Use of chamber systems to measure trace gas fluxes." *Agricultural Ecosystem Effects on Trace Gases and Global Climate Change*.

Imbrium Systems. (2012). *A Breakthrough in Total Phosphorus Removal: The Science behind Sorbtive Media*.

Jones, D. L. (1998). "Organic acids in the rhizosphere: A critical review." *Plant and Soil*, 205, 25–44.

Jones, D. L., Healey, J. R., Willett, V. B., Farrar, J. F., and Hodge, A. (2005). "Dissolved organic nitrogen uptake by plants - An important N uptake pathway?" *Soil Biology and Biochemistry*, 37, 413–423.

Kadlec, R. H., Cuvellier, C., and Stober, T. (2010). "Performance of the Columbia, Missouri, treatment wetland." *Ecological Engineering*, Elsevier B.V., 36(5), 672–684.

Kang, J.-H., Kayhanian, M., and Stenstrom, M. K. (2006). "Implications of a kinematic wave model for first flush treatment design." *Water Research*, 40(20), 3820–30.

Kang, J.-H., Kayhanian, M., and Stenstrom, M. K. (2008). "Predicting the existence of stormwater first flush from the time of concentration." *Water Research*, 42(1-2), 220–8.

Kaspar, H. F. (1982). "Denitrification in marine sediment: measurement of capacity and estimate of in situ rate." *Applied and Environmental Microbiology*, 43(3), 522–7.

Kaye, J., Burke, I., and Mosier, A. (2004). "Methane and nitrous oxide fluxes from urban soils to the atmosphere." *Ecological Applications*, 14(4), 975–981.

Kayhanian, M., Suverkropp, C., Ruby, a., and Tsay, K. (2007). "Characterization and prediction of highway runoff constituent event mean concentration." *Journal of Environmental Management*, 85, 279–295.

Keller, M., Kaplan, W. A., and Wofsy, S. C. (1986). "Emissions of N2O, CH4 and CO2 from tropical forest soils." *Journal of Geophysical Research: Atmospheres*, 91(D11), 11791–11802.

Kim, H., Seagren, E. A., Davis, A. P., and Davis, P. (2003). "Engineered bioretention for removal of nitrate from stormwater runoff." *Water Environment Federation*, 75(4), 355–367.

King, K. W., Harmel, R. D., and Fausey, N. R. (2005). "Development and sensitivity of a method to select time- and flow-paced storm event sampling intervals for headwater streams." *Journal of Soil and Water Conservation*, 60(6), 323–331.

Kirschke, S., Bousquet, P., Ciais, P., Saunois, M., Canadell, J., Dlugokencky, E., Bergamaschi, P.,

Bergmann, D., Blake, D., Bruhwiler, L., Cameron-Smith, P., Castaldi, S., Chevallier, F., Feng, L., Fraser, A., Heimann, M., Hodson, E., Houweling, S., Josse, B., Fraser, P., Krummel, P. B., Lamarque, J.-F., Langenfelds, R., Le Quéré, C., Naik, V., O'Doherty, S., Palmer, P., Pison, I., Plummer, D., Poulter, B., Prinn, R., Rigby, M., Ringeval, B., Santini, M., Schmidt, M., Shindell, D., Simpson, I., Spahni, R., Steele, L. P., Strode, S., Sudo, K., Szopa, S., van der Werf, G., Voulgarakis, A., van Weele, M., Weiss, R., Williams, J., and Zeng, G. (2013). "Three decades of global methane sources and sinks." *Nature Geoscience*, 6(10), 813–823.

Komlos, J., and Traver, R. G. (2012). "Long-term orthophosphate removal in a field-scale storm-water bioinfiltration rain garden." *Journal of Environmental Engineering*, 138(October), 991–998.

Kosmerl, P. (2012). "Water balance of right of way retrofit gardens." Ohio State University.

Kutzbach, L., Schneider, J., Sachs, T., Giebels, M., and Nyk, H. (2007). "CO2 flux determination by closed-chamber methods can be seriously biased by inappropriate application of linear regression." *Biogeosciences*, 1005–1025.

Lantzke, I. R., Heritage, a. D., Pistillo, G., and Mitchell, D. S. (1998). "Phosphorus removal rates in bucket size planted wetlands with a vertical hydraulic flow." *Water Research*, 32(4), 1280–1286.

Law, N. L., Fraley-McNeal, L., Cappiella, K., and Pitt, R. (2008). *Monitoring to demonstrate environmental results: guidance to develop local stormwater monitoring studies using six example study designs*. Ellicott City.

LeBoutillier, D. W., Kells, J. a., and Putz, G. J. (2000). "Prediction of pollutant load in stormwater runoff from an urban residential area." *Canadian Water Resources Journal*, 25(April 2015), 343–359.

Lee, H., Lau, S.-L., Kayhanian, M., and Stenstrom, M. K. (2004). "Seasonal first flush phenomenon of urban stormwater discharges." *Water Research*, 38(19), 4153–63.

Lee, J. H., and Bang, K. W. (2000). "Characterization of urban stormwater runoff." *Water Resources*, 34(6), 1773–1780.

Lee, J. H., Bang, K. W., Ketchum, L. H., Choe, J. S., and Yu, M. J. (2002). "First flush analysis of urban storm runoff." *The Science of the Total Environment*, 293(1-3), 163–75.

Lefevre, G. H., Paus, K. H., Natarajan, P., Gulliver, J. S., Novak, P. J., and Hozalski, R. M. (2015). "Review of dissolved pollutants in urban storm water and their removal and fate in bioretention cells." *Journal of Environmental Engineering*, 141.

Lenth, J., Rheaume, A., and Tackett, T. (2008). "Lessons learned from monitoring bioretention swales in west Seattle's high point neighborhood." *Low Impact Development for Urban Ecosystem and Habitat Protection*.

Leytem, A., and Bjorneberg, D. (2009). "Changes in soil test phosphorus and phosphorus in runoff from calcareous soils recieve manure compost, and fertilizer application with and without alum." *Soil Science*, 174.

Li, H., and Davis, A. P. (2008). "Urban particle capture in bioretention media." *Journal of Environmental Engineering*, 134(June), 409–418.

Li, H., and Davis, A. P. (2009). "Water quality improvement through reduction of pollutant loads using bioretention." *Journal of Environmental Engineering*, 135(August), 567–576.

Lintern, A., Daly, E., Duncan, H., Hatt, B. E., Fletcher, T. D., and Deletic, A. (2011). "Key design characteristics that influence the performance of stormwater biofilters." *12th International Conference on Urban Drainage, Porto Alegre, Brazil*, 11–16.

Liu, J., Sample, D., Owen, J., Li, J., and Evanylo, G. (2014). "Assessment of selected bioretention blends for nutrient retention using mesocosm experiments." *Journal of Environment Quality*.

Livesley, S. J., Dougherty, B. J., Smith, A. J., Navaud, D., Wylie, L. J., and Arndt, S. K. (2010). "Soil-atmosphere exchange of carbon dioxide, methane and nitrous oxide in urban garden systems: impact of irrigation, fertiliser and mulch." *Urban Ecosystems*, 13, 273–293.

Lucas, W. C., and Greenway, M. (2008). "Nutrient retention in vegetated and nonvegetated bioretention mesocosms." *Journal of Irrigation and Drainage Engineering*, 134(5), 613–623.

Lucas, W., and Greenway, M. (2011). "Hydraulic response and nitrogen retention in bioretention mesocosms with regulated outlets: part I - hydraulic response." *Water Environment Research*, 83(8).

Luther, G. W., Sundby, B., Lewis, B. L., Brendel, P. J., and Silverberg, N. (1997). "Interactions of

manganese with the nitrogen cycle: Alternative pathways to dinitrogen." *Geochimica et Cosmochimica Acta*, 61(19), 4043–4052.

Maestre, A., and Pitt, R. (2004). *Nonparametric Statistical Tests Comparing First Flush and Composite Samples from the National Stormwater Quality Database*. *Stormwater and Urban Water Systems Modeling*.

Mangangka, I. R., Liu, A., Egodawatta, P., and Goonetilleke, A. (2014). "Performance characterisation of a stormwater treatment bioretention basin." *Journal of Environmental Management*, Elsevier Ltd, 150C, 173–178.

Mann, J. J., Barney, J. N., Kyser, G. B., and DiTomaso, J. M. (2013). "Root system dynamics of Miscanthus x giganteus and Panicum virgatum in response to rainfed and irrigated conditions in California." *Bioenergy Research*, 6, 678–687.

Marsalek, J., Karamouz, M., Goldenfum, J., and Chocat, B. (2006). *Urban water cycle processes and interactions*. Paris.

Masterson, J., and Bannerman, R. (1994). "Impacts of stormwater runoff on urban streams in Milwaukee country, Wisconsin." *American Water Resources Association*.

Matson, P. A., and Harris, R. C. (1995). *Biogenic trace gases: Measuring emissions from soil and water*. Blackwell Science Ltd, Oxford.

McCulley, R. L., Jobbágy, E. G., Pockman, W. T., and Jackson, R. B. (2004). "Nutrient uptake as a contributing explanation for deep rooting in arid and semi-arid ecosystems." *Oecologia*, 141(4), 620–8.

Van Meeteren, M. M., Tietema, A., and Westerveld, J. W. (2007). "Regulation of microbial carbon, nitrogen, and phosphorus transformations by temperature and moisture during decomposition of Calluna vulgaris litter." *Biology and Fertility of Soils*, 44, 103–112.

Mengel, K., and Kirkby, E. (2001). *Principles of plant nutrition*. Springer Netherlands.

Mengis, M., Gachter, R., and Wehrli, B. (1997). "Sources and sinks of nitrous oxide (N2O) in deep lakes." *Biogeochemistry*, 38, 281–301.

Le Mer, J., and Roger, P. (2001). "Production, oxidation, emission and consumption of methane by soils : A review." *European Journal of Soil Biology*, 37(2001).

Michigan Department of Environmental Quality. (2008). *Low Impact Development Manual for Michigan: A Design Guide for Implementers and Reviewers*.

Miguntanna, N. P., Liu, A., Egodawatta, P., and Goonetilleke, A. (2013). "Characterizing nutrients wash-off for effective urban stormwater treatment design." *Journal of Environmental Management*, 120, 61–7.

Mith, K. A. S., All, T. B., Onen, F. C., Obbie, K. E. D., Assheder, J. M., and Ey, A. R. (2003). "Exchange of greenhouse gases between soil and atmosphere : interactions of soil physical factors and biological processes." *European Journal of Soil Biology*, 54(December), 779–791.

Muthanna, T. M., Viklander, M., Blecken, G., and Thorolfsson, S. T. (2007). "Snowmelt pollutant removal in bioretention areas." *Water Research*, 41(18), 4061–72.

National Research Council. (2008). *Urban Stormwater Management in the United States*.

Natural Resources Conservation Service. (1986). *Urban Hydrology for Small Watersheds TR-55*. *Urban Hydrology for Small Watersheds TR-55*.

Natural Resources Conservation Service. (2005). *Plant Guide: Cardinal Flower*.

Nesbit, S. P., and Breitenbeck, G. A. (1992). "A laboratory study of factors influencing methane uptake by soils." *Agriculture, Ecosystems and Environment*, 41, 39–54.

Nisbet, E. G., Dlugokencky, E. J., and Bousquet, P. (2014). "Atmospheric science. Methane on the rise--again." *Science*, 343(6170), 493–5.

Northeast Regional Coordinating Committee on Soil Testing. (2009). *Recommended Soil Testing Procedures for the Northeastern United States. 3rd Edition. Northeastern Regional Publication No. 493*.

Nylen, N. G., and Kiparsky, M. (2015). *Accelerating cost-effective green stormwater infrastructure: learning from local implementation*.

O'Neill, S. W., and Davis, A. P. (2011). "Water treatment residual as a bioretention amendment for

phosphorus. II: Long-term column studies." *Journal of Environmental Engineering*, 138(March), 328–336.

Paerl, H. W. (2006). "Assessing and managing nutrient-enhanced eutrophication in estuarine and coastal waters : Interactive effects of human and climatic perturbations." *Ecological Engineering*, 26, 40–54.

Palmer, E. T. (2012). "Nitrate and phosphate removal through an optimized bioretention system." *Masters Thesis*, Washington State University.

Parkin, T., and Venterea, R. (2010). *USDA-ARS GRACEnet Project Protocols Chapter 3. Chamber-Based Trace Gas Flux Measurements 4*.

Passeport, E., Hunt, W. F., Line, D. E., Smith, R. A., and Brown, R. A. (2009). "Field study of the ability of two grassed bioretention cells to reduce storm-water runoff pollution." *Journal of Irrigation and Drainage Engineering*, 135(August), 505–510.

Patton, C., and Kryskalla, J. (2003). *Methods of Analysis by the U.S. Geological Survey National Water Quality Laboratory - Evaluation of alkaline persulfate digestion as an alternative to kjeldahl digestion for determination of total and dissolved nitrogen and phosphorous in water*. *U.S. Geological Survey Water-Resouces Investigations Report 03-4174*.

Paus, K. H., Morgan, J., Gulliver, J. S., Leiknes, T., and Hozalski, R. M. (2013). "Assessment of the hydraulic and toxic metal removal capacities of bioretention cells after 2 to 8 years of service." *Water, Air, & Soil Pollution*, 225(1), 1803.

Pearce, A. R., Rizzo, D. M., Watzin, M. C., and Druschel, G. K. (2013). "Unraveling Associations between Cyanobacteria Blooms and In-Lake Environmental Conditions in Missisquoi Bay, Lake Champlain, USA, Using a Modi fi ed Self-Organizing Map."

Peñuelas, J., Poulter, B., Sardans, J., Ciais, P., van der Velde, M., Bopp, L., Boucher, O., Godderis, Y., Hinsinger, P., Llusia, J., Nardin, E., Vicca, S., Obersteiner, M., and Janssens, I. (2013). "Human-induced nitrogen-phosphorus imbalances alter natural and managed ecosystems across the globe." *Nature Communications*, 4, 2934.

Pilegaard, K., and Pilegaard, K. (2013). "Processes regulating nitric oxide emissions from soils."

Philosophical Transactions of the Royal Society Biological Sciences, 368(2).

Plaxton, W. C., and Podestá, F. E. (2006). "The functional organization and control of plant respiration." *Critical Reviews in Plant Sciences*, 25(2), 159–198.

Portmann, R. W., Daniel, J. S., and Ravishankara, A. R. (2012). "Stratospheric ozone depletion due to nitrous oxide: influences of other gases." *Philosophical transactions of the Royal Society*, 367(1593), 1256–64.

Preti, F., Dani, a., and Laio, F. (2010). "Root profile assessment by means of hydrological, pedological and above-ground vegetation information for bio-engineering purposes." *Ecological Engineering*, 36(3), 305–316.

Qiu, S., McComb, A., Bell, R., and Davis, J. (2005). "Response of soil microbial activity to temperature, moisture, and litter leaching on a wetland transect during seasonal refilling." *Wetlands Ecology and Management*, 13(2002), 43–54.

Ravishankara, A. R., Daniel, J. S., and Portmann, R. W. (2009). "Nitrous oxide (N2O): the dominant ozone-depleting substance emitted in the 21st century." *Science*, 326(5949), 123–5.

Read, J., Wevill, T., Fletcher, T., and Deletic, A. (2008). "Variation among plant species in pollutant removal from stormwater in biofiltration systems." *Water Research*, 42(4-5), 893–902.

Rhoderick, G. C., and Dorko, W. D. (2004). "Standards development of global warming gas species: methane, nitrous oxide, trichlorofluoromethane, and dichlorodifluoromethane." *Environmental Science & Technology*, 38(9), 2685–92.

Ringler, S. (2007). "First Flush Characterization of Storm Water Runoff."

Rochette, P., Ellert, B., Gregorich, E. G., Desjardins, R. L., Pattey, E., Lessard, R., and Johnson, B. G. (1997). "Description of a dynamic closed chamber for measuring soil respiration and its comparison with other techniques." *Canadian Journal of Soil Science*, 77(2), 195–203.

Rochette, P., and Hutchinson, G. (2005). "Measurement of soil respiration in situ : Chamber techniques." *Micrometeorology in Agricultural Systems*, 247–286.

Rönner, U., and Sörensson, F. (1985). "Denitrification rates in the low-oxygen waters of the stratified baltic

proper." *Applied and Environmental Microbiology*, 50(4), 801–806.

Roseen, R., Ballestero, T., Houle, J., Avellaneda, P., Briggs, J., Fowler, G., and Wildey, R. (2009). "Seasonal performance variations for storm-water management systems in cold climate conditions." *Journal of Environmental Engineering*, 135(March).

Rosenberg, E. a., Keys, P. W., Booth, D. B., Hartley, D., Burkey, J., Steinemann, A. C., and Lettenmaier, D. P. (2010). "Precipitation extremes and the impacts of climate change on stormwater infrastructure in Washington State." *Climatic Change*, 102(1-2), 319–349.

Rosenquist, S. E., Hession, W. C., Eick, M. J., and Vaughan, D. H. (2010). "Variability in adsorptive phosphorus removal by structural stormwater best management practices." *Ecological Engineering*, Elsevier B.V., 36(5), 664–671.

Roy-Poirier, A. (2009). "Bioretention for phosphorus removal: Modelling stormwater quality improvements." *Masters Thesis*, Queen's University, Canada.

Sansalone, J. J., and Cristina, C. M. (2004). "First flush concepts for suspended and dissolved solids in small impervious watersheds." *Journal of Environmental Engineering*, 130(November), 1301–1314.

Schachtman, D. P., Schachtman, D. P., Reid, R. J., Reid, R. J., Ayling, S. M., and Ayling, S. M. (1998). "Phosphorus uptake by plants: From soil to cell." *Plant Physiology*, 116(2), 447–453.

Schenk, H. J. (2008). "The shallowest possible water extraction profile: A null model for global root distributions." *Vadose Zone Journal*, 7(3), 1119.

Schlesinger, W. H. (2013). "An estimate of the global sink for nitrous oxide in soils." *Global Change Biology*, 19(10), 2929–31.

Seelsaen, N., McLaughlan, R., Moore, S., Ball, J. E., and Stuetz, R. M. (2006). "Pollutant removal efficiency of alternative filtration media in stormwater treatment." *Water Science and Technology*, 54, 299–305.

Senbayram, M., Chen, R., Budai, A., Bakken, L., and Dittert, K. (2012). "Agriculture , Ecosystems and Environment N 2 O emission and the N 2 O /(N 2 O + N 2) product ratio of denitrification as controlled by available carbon substrates and nitrate concentrations." *Agriculture, Ecosystems and*

Environment, Elsevier B.V., 147, 4–12.

Serna, M. D., Borras, R., Legaz, F., and Primo-Millo, E. (1992). "The influence of nitrogen concentration and ammonium /nitrate ratio on N-uptake, mineral composition and yield of citrus." *Plant and Soil*, 147(1), 13–23.

Sinsabaugh, R. L., Gallo, M. E., Waldrop, M. P., and Zak, D. R. (2005). "Extracellular enzyme activities and soil organic matter dynamics for northern hardwood forests receiving simulated nitrogen deposition." *Biogeochemistry*, 75, 201–215.

Smart, D., and Peñuelas, J. (2005). "Short-term CO2 emissions from planted soil subject to elevated CO2 and simulated precipitation." *Applied Soil Ecology*, 28, 247–257.

Smith, K. a, Mosier, A. R., Crutzen, P. J., and Winiwarter, W. (2012). "The role of N2O derived from crop-based biofuels, and from agriculture in general, in Earth's climate." *Philosophical transactions of the Royal Society of London. Series B, Biological sciences*, 367(1593), 1169–74.

Smith, K. A. S., Ball, T. B., Conen, F. C., Dobbie, K. E. D., Massheder, J. M., and Rey, A. R. (2003). "Exchange of greenhouse gases between soil and atmosphere : interactions of soil physical factors and biological processes." *European Journal of Soil Science*, (December), 779–791.

Smith, V. H., Tilman, G. D., and Nekola, J. C. (1999). "Eutrophication: impacts of excess nutrient inputs on freshwater, marine, and terrestrial ecosystems." *Environmental Pollution*, 100(1-3), 179–96.

Soller, J., Stephenson, J., Olivieri, K., Downing, J., and Olivieri, A. W. (2005). "Evaluation of seasonal scale first flush pollutant loading and implications for urban runoff management." *Journal of Environmental Management*, 76(4), 309–18.

Sollins, P., Homann, P., and Caldwell, B. (1996). "Stabilization and destabilization of soil organic matter: mechanisms and controls." *Geoderma*, 74(1-2), 65–105.

Sollins, P., Homann, P., and Caldwell, B. A. (1996). "Stabilization and destabilization of soil organic matter : mechanisms and controls." 74, 65–105.

Sollins, P., Robertson, P., and Uehara, G. (1988). "Nutrient mobility in variable- and permanent-charge soils." *Biogeochemistry*, 6(3), 181–199.

Sonon, L. S., Kissel, D. E., and Saha, U. (2014). *Cation Exchange Capacity and Base Saturation*.

Spivakov, B. Y., Maryutina, T. a., and Muntau, H. (1999). "Phosphorus speciation in water and sediments." *Pure and Applied Chemistry*, 71(11), 2161–2176.

Stander, E. K., and Borst, M. (2010). "Hydraulic test of a bioretention media carbon amendment." *Journal of Hydrologic Engineering*, 15(June), 531–436.

Stenstrom, M., and Kayhanian, M. (2005). *First flush phenomenon characterization*. Sacramento.

Steudler, P. A., Bowden, R. D., Melillo, J. M., and Aber, J. D. (1989). "Influence of nitrogen fertilization on methane uptake in temperate forest soils." *Nature*, 341(6240), 314–316.

Stone, R. M. (2013). "Evaluation and optimization of bioretention design for nitrogen and phosphorus removal." *Masters Thesis*, University of New Hampshire.

Stoner, D., Penn, C., McGrath, J., and Warren, J. (2012). "Phosphorus removal with by-products in a flow-through setting." *Journal of Environment Quality*, 41, 654.

Syakila, A., and Kroeze, C. (2011). "The global nitrous oxide budget revisited." *Greenhouse Gas Measurement and Management*, 1(1), 17–26.

Tanner, C. C. (1996). "Plants for constructed wetland treatment systems - A comparison of the growth and nutrient uptake of eight emergent species." 7, 59–83.

Taylor, A., and Wong, T. (2002). *Non-structural stormwater quality best management practices - a literature review of their value and life-cycle costs*.

Taylor, G. D., Fletcher, T. D., Wong, T. H. F., Breen, P. F., and Duncan, H. P. (2005). "Nitrogen composition in urban runoff-implications for stormwater management." *Water Research*, 39(10), 1982–9.

Teledyne ISCO. (2012). *720 Submerged Probe Flow Module*.

The Lady Bird Johnson Wildflower Center. (2016a). "Helenium autumnale." *Native Plant Database*, <https://www.wildflower.org/>.

The Lady Bird Johnson Wildflower Center. (2016b). "Aster novae angliae." *Native Plant Database*,

<https://www.wildflower.org/>.

The Lady Bird Johnson Wildflower Center. (2016c). "Asclepias tuberosa." *Native Plant Database*, <https://www.wildflower.org/>.

The Lady Bird Johnson Wildflower Center. (2016d). "Baptisia australis." *Native Plant Database*.

The United Nations. (2015). *World Water Development Report*.

Thompson, A. M., Paul, A. C., and Balster, N. J. (2008). "Physical and hydraulic properties of engineered soil media for bioretention basins." *American Society of Agricultural and Biological Engineers*, 51(2), 499–514.

Thomson, A. J., Giannopoulos, G., Pretty, J., Baggs, E. M., and Richardson, D. J. (2012). "Biological sources and sinks of nitrous oxide and strategies to mitigate emissions." *Philosophical Transactions of the Royal Society Biological Sciences*, 367(1593), 1157–68.

Turner, R., and Rabalais, N. (2013). "Nitrogen and phosphorus phytoplankton growth limitation in the northern Gulf of Mexico." *Aquatic Microbial Ecology*, 68(2), 159–169.

U.S. Bureau of Reclamation. (2001). *Water Measurement Manual*. U.S. Government Printing Office, Washington, D.C.

U.S. Climate Change Science Program and the Subcommittee on Global Change Research. (2008). *Weather and Climate Extremes in a Changing Climate*. Washington, D.C.

U.S. Environmental Protection Agency. (1997). "Load Estimation Techniques." *National Management Measures to Control Nonpoint Pollution from Agriculture*, 225–242.

U.S. Environmental Protection Agency. (1998). *Report of the Federal Advisory Committee on the Total Maximum Daily Load (TMDL) Program*.

U.S. Environmental Protection Agency. (2008). *TMDLs to Stormwater Permits Handbook*.

U.S. Environmental Protection Agency. (2015). *Tools, Strategies and Lessons Learned from EPA Green Infrastructure Technical Assistance Projects*.

USDA Natural Resources Conservation Service. (2011). *Soil Quality Indicators: Soil Electrical*

Conductivity.

Vance, C. P., Uhde-Stone, C., and Allan, D. L. (2003). "Phosphorus acquisition and use: critical adaptations by plants for securing a nonrenewable resource." *New Phytologist*, 157(3), 423–447.

Vaze, J., and Chiew, F. (2003a). "Study of pollutant washoff from small impervious experimental plots." *Water Resources Research*, 39(6).

Vaze, J., and Chiew, F. (2003b). "Comparative evaluation of urban storm water quality models." *Water Resources Research*, 39(10), 1–10.

Verchot, L. V, Davidson, E. A., Cattfinio, J. H., Ackerman, T. M. I. L., Erickson, H. E., and Keller, M. (1999). "Land use change and biogeochemical controls of nitrogen oxide emissions from soils in eastern Amazonia." *Global Biogeochemical Cycles*, 13(1), 31–46.

Vermont Agency of Natural Resources. (2002a). *The Vermont Stormwater Management Manual Volume I - Stormwater Treatment Standards*.

Vermont Agency of Natural Resources. (2002b). *The Vermont Stormwater Management Manual Volume II – Technical Guidance*.

Vilain, G., Garnier, J., Decuq, C., and Lugnot, M. (2014). "Nitrous oxide production from soil experiments: denitrification prevails over nitrification." *Nutrient Cycling in Agroecosystems*, 98(2), 169–186.

Washington State University Pierce County Extension. (2012). *Low Impact Development Technical Guidance Manual for Puget Sound*.

Waters, D., Watt, E., Marsalek, J., and Anderson, B. (2003). "Adaptation of a storm drainage system to accomodate increased rainfall resulting from climate change." *Journal of Environmental Planning and Management*, 46(5), 755–770.

Wemple, B., Shanley, J., Denner, J., Ross, D., and Mills, K. (2007). "Hydrology and water quality in two mountain basins of the northeastern US : assessing baseline conditions and effects of ski area development." *Hydrologic Processes*, 21, 1639–1650.

Weng, L., Van Riemsdijk, W. H., and Hiemstra, T. (2012). "Factors controlling phosphate interaction with iron oxides." *Journal of Environmental Quality*, 41(3), 628–35.

Whitman, W., Bowen, T., and Boone, D. (2006). "The Methanogenic Bacteria." *The Prokaryotes SE - 9*, M. Dworkin, S. Falkow, E. Rosenberg, K.-H. Schleifer, and E. Stackebrandt, eds., Springer New York, 165–207.

Wong, T. H. F. (2006). "An Overview of Water Sensitive Urban Design Practices in Australia." 1(1).

Young, E. O., and Ross, D. S. (2001). "Phosphate release from seasonally flooded soils: A laboratory microcosm study." *Journal of Environmental Quality*, 30(1), 91–101.

Zhuang, Q., Lu, Y., and Chen, M. (2012). "An inventory of global N2O emissions from the soils of natural terrestrial ecosystems." *Atmospheric Environment*, Elsevier Ltd, 47, 66–75.

Zinger, Y., Blecken, G.-T., Fletcher, T. D., Viklander, M., and Deletić, A. (2013). "Optimising nitrogen removal in existing stormwater biofilters: Benefits and tradeoffs of a retrofitted saturated zone." *Ecological Engineering*, 51, 75–82.

Zotarelli, L., Dukes, M., and Barreto, T. (2010). *Interpretation of Soil Moisture Content to Determine Soil Field Capacity and Avoid Over Irrigation in Sandy Soils Using Soil Moisture Measurements*.

APPENDIX

Table 27. Watershed (drainage area) size and liner length by cell.

Cell	Area liner strip (m^2)	Watershed Areas (m^2)	Total Watershed Area (m^2)	Surface Area to Watershed Area Ratio (SA = 3.72 m^2)
1	6.89	40.32	47.21	0.08
2	3.72	33.17	36.88	0.10
3	16.64	120.12	136.77	0.03
4	19.20	64.10	83.31	0.04
5	4.45	62.62	67.07	0.06
6	4.75	53.51	58.27	0.06
7	4.94	29.73	34.67	0.11
8	5.55	61.13	66.68	0.06

Table 28. Inflow weir discharge equations, with (Q) = discharge (cfs), (H) = height (ft).

$Q1 = 7.3858 * H^{2.7088}$
$Q2 = 3.5975 * H^{2.4424}$
$Q3 = 4.3192 * H^{2.5137}$
$Q4 = 4.8798 * H^{2.5761}$
$Q5 = 3.8256 * H^{2.4750}$
$Q6 = 4.8967 * H^{2.5735}$
$Q7 = 4.1210 * H^{2.4923}$
$Q8 = 5.3260 * H^{2.6022}$

Table 29. ASTM guidelines for a 90^o weir and actual dimensions of study weirs.

ASTM Recommendation	4.57 < H < 60.96 (cm)	P > 9.14 (cm)	B > 731.5 (cm)	H/P < 1.2	H/B < 0.4
Weir	H (cm)	P (cm)	B (cm)	H/P	H/B
1	7.62	5.59	20.35	1.36	0.37
2	7.62	5.51	20.40	1.38	0.37
3	7.62	5.59	20.72	1.36	0.37
4	7.62	5.41	20.65	1.41	0.37
5	7.62	5.50	20.60	1.39	0.37
6	7.62	5.70	20.90	1.34	0.36
7	7.62	5.75	19.95	1.33	0.38
8	7.62	5.60	20.50	1.36	0.37
Average	7.62	5.58	20.51	1.37	0.37

Table 30. Time needed to monitor the inflow hydrograph.

Watershed	Drainage Area (ft^2)	Peak Flow Q = CiA (cfs)	Time of Concentration (min)	Rainfall Intensity (in/hr)	Time (min)	Time * Multiplier (min)
1	434	0.0262	5.69	3.07	18.52	37.03
2	357	0.0216	4.73	3.32	17.12	34.24
3	1293	0.0782	8.27	2.75	20.67	41.34
4	690	0.0417	6.75	2.89	19.67	39.34
5	790	0.0408	5.74	3.07	18.52	37.03
6	608	0.0348	6.26	3.07	18.52	37.03
7	320	0.0194	4.93	3.32	17.12	34.24
8	658	0.0398	6.33	3.07	18.52	37.03

Table 31. Inflow cumulative volume, antecedent conditions, and mass per m^2 of paved drainage area, where n is the number of samples.

Watershed Event	n	Precip	Cumulative Volume	ADD	Max Air Temp	APC	Q max	TP	NLP	SRP	TN	TKN	NO3	TSS
		inches	L	Days	^oF	inches	L s^{-1}	µg m^{-2}	µg m^{-2}	µg m^{-2}	µg m^{-2}	µg m^{-2}	µg m^{-2}	mg m^{-2}
1	5	0.45	542	0	86	0.13	1.4118	938	686	252	3,737	3,136	638	388.67
2	8	0.44	383	0	86	0.13	0.8688	542	312	230	2,912	2,197	848	235.29
3	3	0.33	311	0	87	0.12	2.5515	774	414	360	3,326	2,687	638	275.67
4	3	0.93	817	0	87	0.12	1.7403	2,043	1,006	1,036	11,636	9,612	2,024	716.15
5	3	0.01	23	6	81	0.22	0.0719	21	15	6	72	36	35	9.92
6	16	0.13	192	1	76	0.29	0.1372	114	82	41	1,390	446	944	18.17
7	4	0.04	78	0	80	0.28	0.3042	93	64	29	404	201	203	32.43
8	10	0.09	318	0	71	0.2	0.7968	219	95	124	672	471	201	98.26
9	22	0.34	504	0	66	0.52	0.6710	1,137	1,059	78	5,314	4,068	1,245	863.14
10	21	0.07	156	0	66	0.52	0.3042	172	121	51	721	645	76	14.87
11	11	0.15	248	0	66	0.52	0.5466	488	444	45	439	364	75	116.27
12	6	0.14	485	3	89	0.04	1.5967	791	657	133	4,047	3,563	484	197.60
13	2	0.01	27	3	89	0.04	0.1307	104	68	36	543	323	221	14.19
14	4	0.19	329	3	89	0.04	0.6057	718	705	13	3,055	2,736	319	275.38
15	19	0.49	732	3	89	0.04	1.2813	2,334	2,260	74	12,717	11,286	1,431	1,011.11
16	6	0.001	13	4	73	0.03	0.0268	11	6	6	82	64	18	0.96
17	23	0.13	195	4	73	0.03	0.1082	300	260	40	1,213	914	300	115.94
18	23	0.22	324	2	86	0.5	0.3244	233	162	71	5,786	4,450	1,336	89.87
19	4	0.01	35	0	71	0.05	0.0834	22	19	3	109	94	15	0.67
20	9	0.07	99	0	71	0.05	0.1533	276	265	10	1,710	1,232	478	23.40
21	19	0.26	888	0	86	0.03	1.3602	466	243	223	1,935	1,171	763	126.86
22	2	0.01	15	0	86	0.03	0.0715	11	10	1	213	74	139	2.37
23	20	0.61	898	0	86	0.03	1.1627	963	776	187	5,609	4,056	1,552	442.97
24	16	0.10	164	0	88	0.03	0.3811	252	196	56	902	732	304	78.50
25	22	0.25	297	0	70	1.06	0.2389	184	97	87	975	418	557	8.75
26	21	0.66	617	0	70	1.06	0.8078	599	342	257	4,878	2,555	2,323	24.31
27	21	0.78	686	2	74	1.61	0.8382	707	370	384	12,979	9,480	3,499	253.88
28	11	0.07	79	0	73	0.01	0.0143	84	17	67	371	73	315	4.25
29	20	0.07	62	0	73	0.01	0.0513	88	14	74	937	303	634	18.48
30	18	0.03	58	0	73	0.01	0.0304	27	6	21	204	132	78	5.39
31	6	0.11	134	0	89	0.01	0.7008	837	277	561	3,061	2,033	1,028	141.38
32	21	0.20	178	0	89	0.01	0.6292	1,055	311	743	3,837	2,414	1,423	89.42
33	18	0.07	88	3	79	0.45	0.1809	298	103	195	1,498	680	818	17.83
34	24	0.29	257	3	79	0.45	0.2889	406	181	225	2,901	1,504	1,397	69.34
35	22	0.87	765	11	59	0.02	0.4763	1,225	161	1,064	10,786	4,747	6,039	.

Table 32. Inflow partial event mean concentration by watershed event, where n is the number of samples.

Watershed Event	n	Cell	Date	TP PEMC	NLP PEMC	SRP PEMC	TN PEMC	TKN PEMC	NO3 PEMC	TSS PEMC
1	5	1	06/23/2013	81.74	59.81	21.93	325.66	273.26	55.61	33.82
2	8	7	06/23/2013	49.03	28.20	20.82	263.45	198.76	76.68	21.21
3	3	2	07/04/2013	91.75	49.05	42.70	394.23	318.56	75.67	32.68
4	3	7	07/04/2013	86.66	42.70	43.96	493.59	407.74	85.85	23.24
5	3	5	09/02/2013	60.62	42.67	17.94	209.19	106.28	102.92	3.10
6	16	6	09/10/2013	34.65	24.84	12.49	421.56	135.35	286.21	5.49
7	4	4	10/07/2013	98.71	67.89	30.82	429.16	213.58	215.58	34.80
8	10	3	11/01/2013	94.25	40.86	53.40	289.42	202.74	86.68	44.27
9	22	6	05/17/2014	131.38	122.32	9.06	614.00	470.11	143.88	99.61
10	21	4	05/17/2014	92.14	64.86	27.28	385.65	344.97	40.68	7.96
11	11	5	05/17/2014	132.06	120.01	12.05	118.69	98.36	20.33	31.39
12	6	3	06/03/2014	222.77	185.19	37.57	1,140.11	1,003.85	136.27	55.64
13	2	4	06/03/2014	324.48	211.88	112.60	1,698.83	1,009.18	689.65	4.93
14	4	5	06/03/2014	146.27	143.60	2.67	622.02	557.14	64.88	56.70
15	19	6	06/03/2014	185.88	179.97	5.91	1,012.58	898.67	113.91	80.51
16	6	3	06/11/2014	122.05	63.03	59.02	876.47	687.45	189.02	1.32
17	23	6	06/11/2014	89.53	77.59	11.94	362.28	272.77	89.51	34.54
18	23	6	06/17/2014	41.79	29.11	12.68	1,039.81	799.74	240.08	18.54
19	4	3	06/25/2014	86.23	74.42	11.80	431.73	373.83	57.90	2.65
20	9	6	06/25/2014	162.18	156.10	6.08	1,005.56	724.70	280.86	13.76
21	19	3	07/03/2014	71.79	37.47	34.31	297.91	180.34	117.57	19.54
22	2	4	07/03/2014	61.22	55.06	6.16	1,151.44	400.33	751.11	12.81
23	20	6	07/03/2014	62.48	50.35	12.14	363.77	263.10	100.67	28.50
24	16	5	07/08/2014	103.01	79.97	33.25	368.49	298.80	231.33	5.72
25	22	1	07/28/2014	29.20	15.36	13.83	154.85	66.40	88.46	1.39
26	21	2	07/28/2014	35.81	20.46	15.35	291.47	152.66	138.81	1.45
27	21	7	07/31/2014	35.78	18.74	19.41	656.42	479.46	176.95	12.67
28	11	1	08/13/2014	50.09	9.94	40.15	220.63	43.33	187.57	2.53
29	20	7	08/13/2014	49.13	7.75	41.37	525.13	169.78	355.35	1.36
30	18	8	08/13/2014	30.92	7.46	24.75	235.28	152.69	90.37	6.21
31	6	1	09/02/2014	294.50	97.26	197.24	1,076.36	714.76	361.59	49.72
32	21	7	09/02/2014	224.92	68.07	156.84	805.82	510.02	295.80	17.38
33	18	1	09/06/2014	158.33	54.88	103.45	794.72	360.86	433.86	9.46
34	24	7	09/06/2014	54.69	24.37	30.32	391.13	202.82	188.31	9.35
35	22	7	10/04/2014	55.52	7.30	48.22	488.92	215.17	273.75	.

Table 33. Average inflow and outflow outflow cumulative mass from 0 – 120 L per treatment. All units in µg except TSS (mg), where inflow n is the number of storm events and outflow n is equal to the number of samples.

	Vol	n	Inflow	±	n	V1	±	n	V2	±	n	CM	±	n	CM20	±	n	SM	±	n	SM60	±
TP	20	14	2,470	637	43	9,712	3,843	33	5,776	2,889	27	12,921	4,021	14	5,885	4,120	27	1,314	749	13	849	363
	40	14	3,852	793	16	27,750	7,201	34	8,655	5,881	2	37,746	8,043	10	11,287	5,756	2	1,436	755	26	1,719	593
	60	12	10,160	1,238	12	30,342	28,374	17	15,000	11,669	3	38,063	46,799	9	14,337	10,192	3	2,659	797	8	3,083	1,392
	80	11	14,063	1,423	9	39,873	38,561	17	21,253	17,431	4	51,726	62,873	10	17,700	12,714	4	3,209	1,250	5	4,557	1,645
	100	12	21,801	1,916	21	52,576	48,421	11	30,727	22,861	13	62,241	75,209	9	20,369	15,514	13	3,524	1,809	5	5,184	2,623
	120	7	28,053	2,325	6	104,665	76,691	8	56,092	48,748	3	139,313	111,734	3	28,096	15,706	3	3,935	1,858	5	6,261	3,246
NLP	20	14	1,566	373	43	784	347	33	483	371	27	1,011	355	14	659	444	27	899	603	13	766	347
	40	14	2,306	507	16	1,967	700	34	952	641	2	2,563	711	10	1,188	614	2	1,056	628	26	1,602	622
	60	12	7,119	771	12	2,531	2,491	17	1,459	1,034	3	2,976	3,663	9	1,458	978	3	1,845	733	8	2,886	1,420
	80	11	9,392	865	9	3,758	3,291	17	2,118	1,711	4	4,097	4,957	10	1,747	1,161	4	1,922	1,241	5	4,287	1,594
	100	12	15,460	1,128	21	4,698	4,174	11	2,704	1,969	13	4,522	6,108	9	1,981	1,405	13	1,930	1,666	5	4,978	2,460
	120	7	18,154	1,288	6	8,664	6,595	8	4,697	3,756	3	10,030	8,661	3	2,812	1,609	3	2,138	1,761	5	5,961	3,076
SRP	20	14	904	265	43	8,928	3,609	33	5,294	2,775	27	11,910	3,700	14	5,226	3,695	27	415	170	13	83	33
	40	14	1,558	286	16	25,783	6,861	34	7,703	5,259	2	35,183	7,401	10	10,099	5,192	2	694	181	26	117	61
	60	12	3,069	469	12	28,224	26,185	17	13,541	10,655	3	35,913	43,252	9	12,879	9,232	3	1,129	239	8	197	99
	80	11	4,717	560	9	36,528	35,307	17	19,433	15,746	4	48,455	57,986	10	15,954	11,565	4	1,602	273	5	271	143
	100	12	7,484	790	21	48,291	44,283	11	28,320	20,910	13	58,545	69,168	9	18,388	14,114	13	1,909	418	5	335	186
	120	7	11,597	1,038	6	96,414	70,131	8	51,693	45,001	3	130,109	103,142	3	25,284	14,505	3	2,112	473	5	429	248
TN	20	14	15,039	3,830	43	14,216	8,313	33	9,844	7,833	27	10,910	3,578	14	4,382	2,137	27	15,471	8,653	13	13,751	5,486
	40	14	25,694	4,605	16	35,296	15,085	34	12,624	12,266	2	22,982	7,156	10	8,494	2,513	2	20,333	13,972	26	21,900	6,909
	60	12	59,370	6,117	12	38,951	27,408	17	21,827	20,089	3	23,434	30,785	9	12,134	2,521	3	32,962	16,649	8	36,955	17,685
	80	11	74,658	7,060	9	44,707	35,135	17	28,510	23,694	4	32,608	40,394	10	16,398	2,755	4	37,173	30,123	5	48,958	23,435
	100	12	115,802	9,002	21	58,318	39,558	11	34,746	39,036	13	42,534	48,919	9	19,963	3,203	13	44,748	34,449	5	61,372	27,131
	120	7	147,942	9,948	6	89,734	63,765	8	52,718	46,108	3	88,528	69,883	3	22,261	3,280	3	50,019	39,046	5	76,501	33,228
TKN	20	14	8,869	1,939	43	6,094	3,414	33	2,662	1,157	27	5,525	3,049	14	3,875	2,055	27	7,268	4,198	13	3,560	1,585
	40	14	16,223	1,961	16	11,652	5,922	34	4,822	2,185	2	6,726	6,099	10	7,658	2,431	2	8,139	4,656	26	7,398	2,778
	60	12	40,193	3,500	12	13,121	8,581	17	8,256	4,758	3	6,827	10,366	9	10,638	2,743	3	11,409	7,012	8	16,190	6,189
	80	11	48,620	3,584	9	13,952	10,283	17	10,719	6,019	4	8,096	11,842	10	13,941	3,312	4	16,161	13,440	5	21,310	7,709
	100	12	81,799	5,343	21	17,377	11,305	11	12,606	10,926	13	8,813	13,437	9	16,710	4,128	13	22,988	15,774	5	26,656	9,511
	120	7	105,248	5,512	6	25,915	16,961	8	17,679	13,990	3	17,644	17,075	3	18,911	4,551	3	24,977	17,911	5	33,394	11,794
NO3	20	14	6,302	1,958	43	8,124	5,835	33	7,183	6,952	27	5,385	2,029	14	506	238	27	8,203	5,258	13	10,191	4,685
	40	14	9,738	2,771	16	25,135	11,305	34	8,532	11,031	2	18,658	4,058	10	865	279	2	12,193	9,507	26	14,502	6,706
	60	12	19,434	2,853	12	27,263	21,411	17	14,300	16,711	3	19,010	23,427	9	1,645	355	3	21,553	9,661	8	20,765	12,170
	80	11	26,648	3,780	9	32,430	28,138	17	18,952	20,071	4	26,915	31,556	10	2,607	652	4	22,095	16,716	5	27,647	16,170
	100	12	38,105	3,896	21	44,795	33,151	11	23,302	30,459	13	36,124	38,475	9	3,402	857	13	27,210	18,577	5	34,716	17,852
	120	7	47,555	4,741	6	68,954	54,152	8	36,202	34,432	3	73,286	55,814	3	3,574	1,087	3	30,492	20,154	5	43,107	21,667
TSS	20	13	773	120	41	165	70	24	77	39	26	244	83	9	71	31	20	125	59	12	207	115
	40	12	1,247	161	13	477	132	28	178	108	2	776	165	6	155	34	3	174	61	26	286	147
	60	12	3,686	181	9	808	192	14	349	231	2	1,334	269	5	186	50	3	179	75	8	449	212
	80	10	4,530	266	4	917	261	8	492	391	2	1,494	372	7	250	57	3	231	148	5	529	280
	100	11	6,774	280	8	946	311	8	590	409	2	1,512	372	6	292	61	15	474	329	5	670	306
	120	6	7,903	439	6	1,080	348	8	868	596	2	1,588	390	3	323	80	7	528	409	5	775	320

Table 34. Outflow PEMC by date and cell, where n is the number of samples.

	Outflow PEMC									
	Date	Cell	n	TP	NLP	SRP	TN	TKN	NO_3^-	TSS
				$\mu g\ L^{-1}$	$\mu g\ L^{-1}$	$\mu g\ L^{-1}$	$\mu g\ L^{-1}$	$\mu g\ L^{-1}$	$\mu g\ L^{-1}$	$mg\ L^{-1}$
1	06/23/2013	7	12	556.21	42.27	513.94	1,816.23	580.39	1,235.84	16.44
2	07/04/2013	7	9	1,957.91	133.09	1,824.82	1,759.4	669.71	1,279.71	14.65
3	08/01/2013	8	5	729.18	44.21	684.98	1,873.68	692.58	1,181.1	0.32
4	09/02/2013	6	8	791.8	23.6	768.19	2,475.37	605.95	1,869.96	1.71
5	10/07/2013	2	22	1,143.09	84.6	1,072.25	728.85	122.76	614.52	11.47
6	10/07/2013	3	25	33.55	27.82	5.73	738.15	101.67	636.48	6.16
7	11/01/2013	4	22	44.88	23.04	21.84	404.26	96.67	307.59	0.61
8	05/17/2014	3	24	58.98	50.6	8.39	1,340.77	487.31	853.46	1.29
9	05/17/2014	4	16	66.87	42.14	24.73	1,009.67	379.8	629.88	3.21
10	05/17/2014	6	22	1,475.76	103.25	1,372.51	1,352.27	502.08	908.9	4.98
11	06/03/2014	3	5	91.18	88.17	3.01	726.11	368.86	357.25	5.8
12	06/03/2014	4	9	151.5	118.85	32.65	1,491.25	837.36	653.89	11.81
13	06/03/2014	6	9	419.45	32.1	387.35	1,243.9	604.51	639.39	9.22
14	06/18/2014	6	2	206.45	29.98	176.47	406.37	312.75	93.62	1.91
15	06/25/2014	3	22	66.38	64.24	2.35	416.26	217.16	199.1	7.33
16	06/25/2014	6	23	175.72	22.39	153.33	589.93	218.73	371.2	1.47
17	07/03/2014	3	6	17.23	15.09	2.15	534.9	262.29	272.61	6.12
18	07/03/2014	4	16	28.49	10.98	17.5	370.25	190.67	260.31	5.42
19	07/03/2014	6	19	359.84	30.96	328.89	631.07	288.75	427.13	3.73
20	07/08/2014	8	2	446.4	12.59	433.82	342.98	93.32	249.66	6.52
21	07/28/2014	8	21	170.48	21.78	148.7	202.68	52.76	149.92	2.55
22	07/31/2014	1	19	365.71	33.41	332.3	219.64	196.2	26.78	2.56
23	07/31/2014	2	9	763.12	77.21	685.91	790.45	675.8	114.66	8.2
24	08/13/2014	1	24	111.11	12.03	99.08	172.4	131.59	40.81	3.17
25	08/13/2014	7	23	86.46	10.13	76.33	105.84	27.19	78.65	1.36
26	08/13/2014	8	27	182.75	38.14	144.61	292.47	156.24	136.24	5.3
27	09/06/2014	1	4	168.79	18.66	150.12	175.29	111.37	63.92	3.36
28	09/06/2014	2	16	520.97	44.31	476.66	541.73	217.62	324.11	10.94
29	09/06/2014	7	25	88.03	13.58	74.45	184.35	66.56	117.8	1.86
30	10/04/2014	1	19	84.74	8.39	76.35	200.95	157.24	43.71	.
31	10/04/2014	2	14	43.16	4.81	38.36	121.94	10.78	111.16	.
32	10/04/2014	7	22	45.96	6.17	39.79	150.26	90.87	59.39	.